A biocatalytic approach for the synthesis of known antitubercular and antischistosomal compounds

Kabelo M. Zimba

A dissertation submitted to the Faculty of Science, University of the Witwatersrand, in fulfilment of the requirements of the Degree of Master of Science.

Johannesburg, 2025

Declaration

I declare that the dissertation presented herein is my own work. It was carried out under the supervision of **Professor Moira Bode**, and co-supervision of **Professor Dean Brady** and **Dr Jenny-Lee Panayides**. It is submitted for the degree of Master of Science at the University of the Witwatersrand, Johannesburg. No prior submission of this work for any degree or examination or to any other University exists.

K.M Zimba

Kabelo M. Zimba

June 2025

Abstract

The aim of this project was to develop greener synthetic approaches for producing intermediates of two important therapeutics: the anti-schistosomal drug praziquantel (PZQ) and the anti-tubercular drug isoniazid (INH). These routes were designed to be compatible with biocatalytic methods, particularly lipase- and nitrile hydratase-mediated transformations, which offer more environmentally benign alternatives to traditional chemical processes.

For PZQ, five different synthetic strategies were explored to access the key tetrahydroisoquinoline intermediate. The first method employed a Ugi multicomponent reaction using imines, acids, and isocyanides to produce carboxamides: 2-benzoyl-N-cyclohexyl-1,2,3,4-tetrahydroisoquinoline-1 carboxamide and 2-benzoyl-*N*-(*tert*-butyl)-1,2,3,4-tetrahydroisoquinoline-1 carboxamide. Of these, only 2-benzoyl-*N*-(*tert*-butyl)-1,2,3,4-tetrahydroisoquinoline-1 carboxamide underwent successful acid hydrolysis to form the desired tetrahydroisoquinoline-1-carboxylic acid. Attempts to convert this acid to its ester form yielded poor results. The second approach involved partial hydrogenation of isoquinoline-1-carboxylic acid using heterogeneous catalysis, followed by esterification. While moderate yields of the hydrogenated acid were achieved, esterification remained inefficient. The third approach reversed this sequence, carrying out esterification on the fully aromatic isoquinoline1-carboxylicacid before hydrogenation. The ester formed in good yield, but hydrogenation occurred at the aromatic ring rather than the intended site, giving undesired products.

The fourth strategy took a more fundamental approach by building the isoquinoline scaffold from simpler precursors using the Bischler-Napieralski reaction. Although initial steps provided the required precursors in modest yields, only ethyl 2-((3,4-dimethoxyphenethyl)amino)-2-oxoacetate cyclised successfully to form the ethyl 6,7-dimethoxy-3,4-dihydroisoquinoline-1-carboxylate, and subsequent reduction attempts were unsuccessful. These outcomes informed a fifth strategy that integrated successful steps from previous approaches. Starting with the partially tetrahydroisoquinoline-1-carboxylic acid, the amine was protected using a Boc group to enable efficient esterification. Subsequent deprotection gave the desired PZQ, methyl 1,2,3,4-tetrahydroisoquinoline-1-carboxylate intermediate in moderate yield, representing a key breakthrough in the synthetic route.

With several PZQ intermediates in hand, enzyme-catalysed hydrolysis was investigated. Four ester derivatives were tested using lipases, including Novozyme 435. These were ethyl

isoquinoline-1-carboxylate, ethyl 1,2,3,4-tetrahydroisoquinoline-1-carboxylate, 2-*tert*-butyl 1-methyl 3,4-dihydroisoquinoline-1,2(1*H*) dicarboxylate and methyl 1,2,3,4-tetrahydroisoquinoline-1-carboxylate. Only one intermediate - ethyl isoquinoline-1-carboxylate - underwent successful hydrolysis to the corresponding acid. Control reactions confirmed that the transformation was enzyme-specific. While the saturated analogues were unreactive under these conditions, this result indicates that, with the right enzyme or optimized conditions, selective enzymatic hydrolysis of PZQ intermediates is feasible.

In the case of isoniazid, a nitrile hydratase-catalysed conversion of 4-pyridinecarbonitrile to its corresponding amide intermediate was successfully carried out. The reaction afforded the desired product in good yield, while avoiding over-hydrolysis to the carboxylic acid, a common limitation of conventional methods. This represents a more selective and efficient route to an important INH precursor.

Together, these findings demonstrate the potential of integrating biocatalysis with carefully designed chemical synthesis to produce key pharmaceutical intermediates using greener, more sustainable processes. Further research into enzyme selection, reaction conditions, and continuous flow systems may unlock even more efficient and scalable methods for industrial application.

Acknowledgements

I want to express my deepest thanks to **Professor Moira Bode** for her consistent guidance throughout the years. Our association commenced during my third year of study when she assigned me to her Ph.D. student, **Dr. Charles Changunda**. His mentorship, facilitated by Professor Moira, has allowed me to appreciate the elegance of organic chemistry. Meeting **Prof. Moira** has been a truly enriching experience, and her mentorship has proven to be incredibly valuable. I am forever thankful for the knowledge she has shared, especially her meticulous attention to detail, which I hope has become a part of my own approach.
I would like to express my appreciation to **Prof. Dean Brady and Dr. Jenny-Lee Panayides** for their collaborative co-supervision of this project. Your suggestions and recommendations have been truly valuable.

I also want to extend my gratitude to:

- The **University of the Witwatersrand** and the **School of Chemistry** for providing this significant opportunity, valuable resources, and an environment conducive to research.
- **Prof. Amanda Rousseau, Prof. Charles de Koning, Prof. Jo Micheal, Dr. Memory Zimuwandeyi, Dr Songeziwe Ntsimango, Nompumelelo Mathebula, Edward Chavalala** and the entire **Organic Chemistry Group** for generously sharing their research expertise and contributing to the success of this project.
- My research colleagues with whom I could openly discuss challenges without feeling embarrased as a researcher. I had an amazing time with them, and I am truly thankful.

I will forever appreciate the financial support received from the **Council of Scientific and Industrial Research (CSIR)** and the **Wits School of Chemistry**.
Lastly, I would like to express my gratitude to my family for their financial and emotional support. Special thanks to go to my mother**, Ntombifuthi Zimba, my cousins Prudence Zimba, Sifiso Zimba, my paternal grandmother Manzi Moagi**, and my Uncle **Thomas Moagi** for their unwavering support. To my friends who kept me sane for the duration of these studies, particularly **Thabani Sithebe, Sibusiso Dlamini,** and **Tshepo Maphathe**- thank you immensely!

List of abbreviations and formulae

AcK	Acetate Kinase
BOC	*tert*-butyloxycarbonyl
DABCO	1,4-diazabicyclo[2.2.2]octane
DIPE	Diisopropylether
DCM	Dichloromethane
DMAP	4-Dimethylaminopyridine
DNA	Deoxyribonucleic acid
EKR	Enymatic kinetic resolution
EMB	Ethambutol
HIV	Human Immunodeficiency virus
HPLC-MS	High-performance liquid chromatography-mass spectrometry
HSQC	Heteronuclear single quantum coherence
IBX	Iodoxybenzoic acid
INH	Isoniazid
IR	Infrared
MCRs	Multicomponent reaction
MDR-TB	Multidrug resistant tuberculosis
MIC	minimum inhibitory concentration
MTPA	α-methoxy-α-(trifluoromthyl)phenylacetic acid
NBS	*N*-bromosuccinimide
NHase	Nitrile hydratase
OXA	Oxamniquine
PC	Preventative chemotherapy

PZA	Pyrazinamide
PZQ	Praziquantel
RIF	Rifampicin
RNA	Ribonucleic acid
SAC	School-aged children
TB	Tuberculosis
TLC	Thin layer chromatography
WHO	World Health Organization
XDR-TB	Extensively drug resistant tuberculosis
4CR	Four-component reaction
^{13}C NMR	Carbon nuclear magnetic resonance
^{1}H NMR	Proton nuclear magnetic resonance

Contents

Chapter 1: Introduction

1.1 Schistosomiasis

Schistosomiasis, also known as bilharzia , the second most lethal tropical parasitic disease after malaria,[1,2] is caused by trematode worms of the genus *Schistosoma*.[3] Only five species of the genus *Schistosoma* infect humans: *S. haematobium, S. mansoni, S. japonicum, S. intercalatum and S. mekongi*.[4–6] Morbidity associated with schistosomiasis can present as acute or chronic; acute schistosomiasis is observed in tourists or immigrants who travel to the endemic areas,[7] whereas chronic schistosomiasis is common in permanent dwellers.[8,9] Given the number of schistosome species humans are susceptible to, there are two major forms of schistosomiasis that pose the greatest threat, and these are urogenital and intestinal schistosomiasis.[9] Other manifestations of schistosomiasis exist and are dependent on the type of species involved. For example, *S. mansoni* causes intestinal damage whilst *S. haematobium* causes damage to pelvic organs.[10] The debilitating effects of schistosomiasis are mostly felt in poor communities, particularly in children, causing an array of afflictions such as nutritional deficiencies, haematuria, dysuria, kidney failure and growth retardation.[11]

1.1.1 Global and Regional Prevalence

The endemic areas of schistosomiasis are in tropical and subtropical regions of Saharan and sub-Saharan Africa, South America, the Middle East, and Asia (Fig. 1).[9] In the past decade, beginning from 2009 to 2019, the global annual estimate of schistosomiasis infections has stood at over 200 million, where 90% of these cases are from Africa.

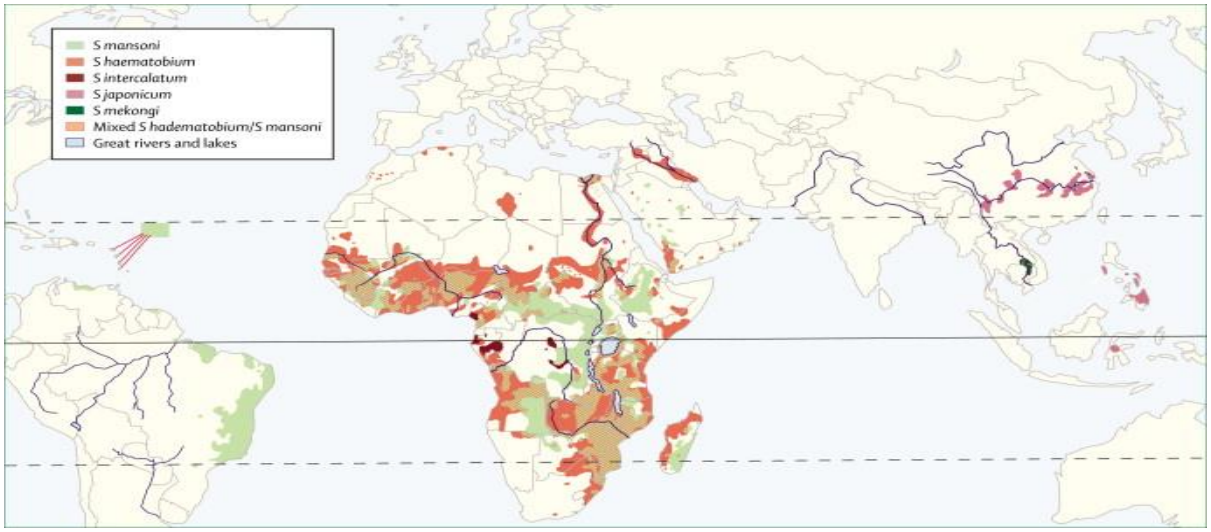

Figure 1: Global distribution of human schistosomiasis transmissions.[9]

Some schistosome species are only found in specific parts of the world.[10,12] For instance, the most common and widespread schistosome species, *S. mansoni* and *S. haematobium* are most prevalent in sub-Saharan Africa, India, the Middle East, South America, and the Caribbean. The other two schistosome species *S. mekongi* and *S. japonicum* only occur in Asia, while *S. intercalatum* occurs in Central and West Africa.[13,14]

In 2017, Africa accounted for 79% of countries that required preventative chemotherapy. The number of infected Africans stood at about 108 million, representing 90% of the global burden of schistosomiasis cases. This value may have been understated, given that some African countries did not submit their schistosomiasis statistics to the World Health Organization at the time of the compilation of the 2017 WHO report on schistosomiasis.[15]

In South Africa, an estimated 6 million people are currently infected with schistosomiasis, the majority of whom are women and children.[16] The presence of this disease in South Africa was reported as far back as the 1900's and recent studies conducted in the early 2000's show that schistosomiasis is still endemic in South Africa, particularly in the Eastern Cape, KwaZulu Natal, Limpopo, Mpumalanga, and the North-West Province (Fig. 2).[17]

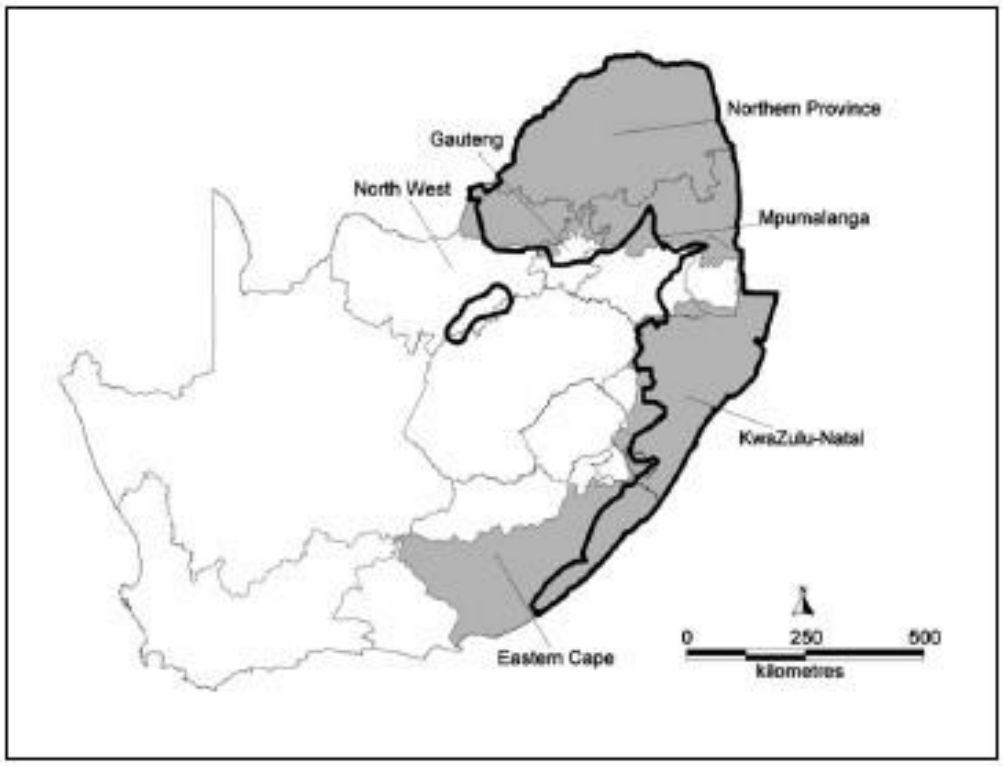

Figure 2: Distribution of human schistosomiasis transmissions in South Africa, as mapped in 1938 (shaded area) and in 1980 (area within the solid black line)[17]

1.1.2 Key Challenges

The uninterrupted focus on HIV, TB and malaria have led to the neglect of other life-threatening diseases. Indeed, the notoriety of the 'big three' had eroded whatever attention was left for equally debilitating ailments nature had in store for humanity.[18] Efforts to curb the 'big three' were commendable and still are, however, we now see that they are myopic, given that they have led to the total disregard of Neglected Tropical Diseases - helminthic, protozoan, bacterial, and viral diseases whose effects are felt by people in the bottom billion who are the poorest in the world.[19] Simply put, schistosomiasis is a disease of poverty; the commonality between the nations that harbour the worst schistosomiasis cases is the fact that they all suffer from extreme poverty.[8]

A closer look at the factors that exacerbate the prevalence of schistosomiasis reveals a synergy between poverty and limited access to safe and clean water. People in poverty-stricken areas often experience poor sanitary conditions, they bathe and swim in dams and rivers, they cross rivers barefooted to and from school, and they use unprotected water sources to water vegetation. All these activities are associated with significantly higher rates of infection.[4,20]

The current chemotherapeutic drug administered to schistosomiasis patients is praziquantel (PZQ) **1** (Fig. 3).[21–24] Its discovery and synthesis were hailed as an important discovery, since it exhibited a rapid reduction in morbidity, particularly in sub-Saharan Africa where morbidity control was a major problem when contrasted with other endemic continents.[2] Despite its success in other continents like Asia and Latin America, where the disease has been controlled or even eradicated, it remains cumbersome to effectively use in Africa. African countries still experience limited access to the wonder drug, consequently failing to keep the disease under control.[25]

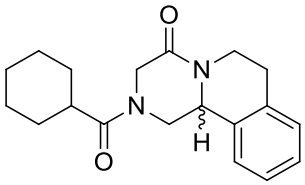

(rac)-Praziquantel **1**

Figure 3: Chemical structure of praziquantel.

In 2013, about 260 million people required praziquantel as a means of preventative chemotherapy (PC), and 90% of them lived in sub-Saharan Africa. Only about 12% of those people received treatment,[26] which deductively means a significant portion of Africa was still

burdened with the disease. To make matters worse, school-aged children (SAC) were the worst hit portion of the population, representing about 55% of all people requiring preventative chemotherapy globally in 2017.[15] In 2014, the number of people who received preventative chemotherapy rose to 21% and 28% in 2015. Between 2015 and 2017 the global coverage of PC for schistosomiasis had risen to about 45% which is gradual and much needed progress. Efforts to control schistosomiasis, particularly in SAC has been phenomenal, with PC reaching a global coverage of 67% in 2020, albeit that the ambitious target of 75% coverage set by WHO has not yet been achieved.[14]

Big 'Pharma' companies have, over the years, played a pivotal role in the control of schistosomiasis through PZQ donations and offering low-cost solutions to endemic countries.[27] In South Africa, the praziquantel administered to schistosomiasis patients is procured from Bayer, packaged as Biltricide®. The price tag on this drug is about USD 4.49 per tablet, dwarfing any practical efforts towards mass treatment programmes.[17] At this rate, it is unaffordable and undermines the objectives of the reaching 75% coverage set by WHO. Generic forms of praziquantel that are cheap, effective and are of great quality have been around for more than two decades, moreover, they are WHO-accredited and some African countries like Nigeria, Uganda and Zambia dispense them free of charge in their respective countries.[28] For effective control of schistosomiasis in South Africa, there is an urgent need to register generic forms of praziquantel and to effectively initiate conversations with Pharmaceutical companies that donate praziquantel to endemic areas.

Currently, PZQ is the only drug available for the treatment and prevention of schistosomiasis.[21–24] Like many drugs, it does have its shortcomings; it lacks activity against juvenile schistosomes, often leading to suboptimal results in mass preventative chemotherapy campaigns.[5,22] Secondly, administering the drug as a racemic mixture has been reported to contribute to side effects and patient compliance problems since the inactive *S* enantiomer contributes to the large size of the pill.[29,30] Lastly, monotherapies pose a great risk of drug resistance and praziquantel is no exception. African countries like Egypt, Senegal, and Kenya have reported praziquantel resistance.[23,24,31] This should be a stern warning for the immediate need of an enantiopure praziquantel drug and alternative schistosomiasis drugs.

1.1.3 Schistosomiasis life cycle

Schistosomes have a sophisticated life cycle that is kept in perpetuity by a fresh water snail intermediate host and a mammalian definitive host (Fig. 4).[32] Schistosome eggs produced in

the mammalian definitive host are excreted either through urine or faecal matter into the environment (Stage **1**, Fig. 4).[9,22,32] Once the eggs are in contact with fresh water, they release miracidia, whose motility help them locate the intermediate host (Stage **2**, Fig. 4). The intermediate hosts are infected by specific worms, for instance *S. intercalatum* and *S. haematobium* only infect the *Balinus* snail intermediate species, whilst *S. mansoni* is known to only infect the *Biomphalaria* snail species (Stage **3**, Fig. 4). Within the intermediate snails, the singular miracidium transforms into a sporocyst and undergoes asexual reproduction to produce cercariae (Stage **4**, Fig. 4). The release of cercariae from the snails is stimulated by sunlight and temperature, thus coinciding with human daytime activities, thereby increasing the chances of human infection.

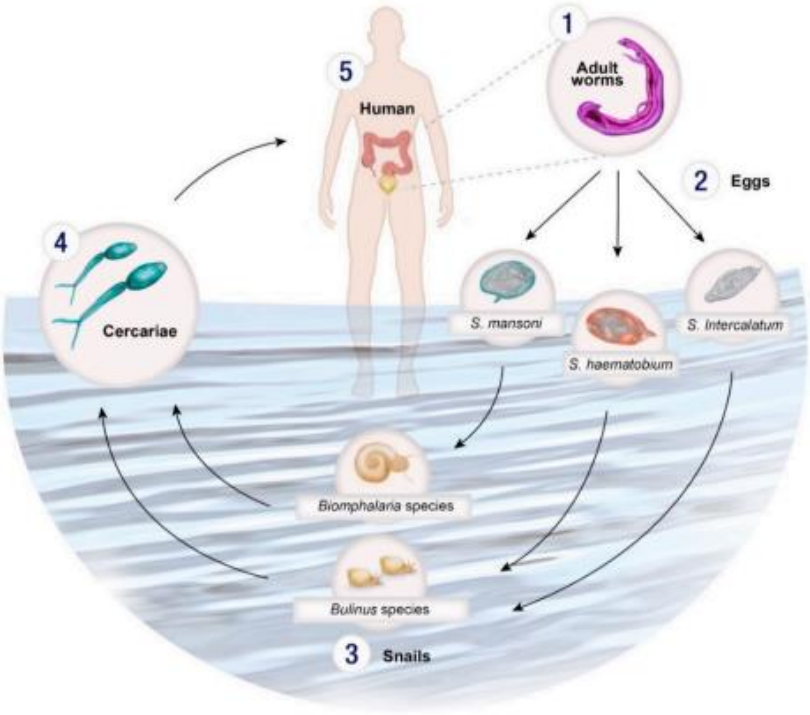

Figure 4: Schistosomiasis lifecycle.[32]

Human infection is a consequence of epidermal penetration of cercariae during contact with infested freshwater bodies (Stage **5**, Fig. 4). Once lodged inside the skin, the cercariae become schistosomula and enter the circulatory system through the capillaries and the lymphatic system. They then migrate to the portal venous system, lungs, heart, and liver where the juvenile schistosomes mature into adult worms. Upon completion of the maturation stage, the adult flukes vacate the liver and make their way to the mesenteric vessels of the bladder or bowel, where they pair up and mate. The migration either to the bladder or bowel determines

the type of ailment that will befall the victim, for instance *S. mansoni* and *S. intercalatum* attack the mesenteric vessels of the bowel, causing intestinal schistosomiasis, whereas *S. haematobium* targets the bladder and causes urogenital schistosomiasis. The eggs produced from the mating flukes are distributed by the blood circulation throughout the body where they become lodged in tissues, where they trigger an inflammatory response, resulting in acute or chronic diseases. Only a proportion of the eggs are excreted through urine or faeces, leaving the rest to perpetuate the diseases in their human hosts for years to come.

1.1.4 Treatment methods

Treating schistosomiasis has proved to be a challenging endeavour, which we can attribute to the daunting task of disentangling the complex interplay between the definitive host, the intermediate hosts, and the aqueous media through which the two meet one another. To interrupt the transmission, one can either engage in population control of molluscs or approach the problem using preventative chemotherapy. The former strategy has been explored, where the population of infective molluscs was controlled using a chemical called niclosamide.[33] Niclosamide has been the molluscicide of choice for over 40 years, owing to its effectiveness and lower toxicity to both humans and the environment,[33] however the cost of treating sites that are infested with molluscs is unaffordable for developing countries.[33,34] Preventative chemotherapy, however, has exhibited much success in controlling schistosomiasis for several years. Indeed, chemotherapy has stood the test of time. It is for this reason that most global efforts have been directed towards preventative chemotherapy, in the pursuit of eradicating schistosomiasis. Preventative chemotherapy, together with stringent sanitary techniques, has been shown to be a winning strategy.

1.1.5 Praziquantel (PZQ) and Oxamniquine (OXA)

The history of schistosomiasis drug therapy stretches as far back as the beginning of the 20th century, where drugs like organoantimony derivatives **2**, organophosphorous **3**, and aryl isothiocyanate compounds **4** were the mainstream drugs used to treat helminthic infections like schistosomiasis (Fig. 5).[22] The organoantimony drugs were discontinued, in light of fatal side effects, and the requirement of intravenous and intramuscular administration which has been reported to be painful.[22] Organophosphorous derivatives like 2,2-dichlorovinyl-dimethylphosphate **3** had a successful tenure, exhibiting exceptional cure rates of 90-95%. The drug showed minimal toxicity and was substantially tolerated. It was withdrawn from the market because it required multiple doses, which led to compliance issues and resistance. Aryl

isothiocyanate compounds exhibited broad-spectrum efficacy, with activity observed after a single dose. They were discontinued because of high liver toxicity.

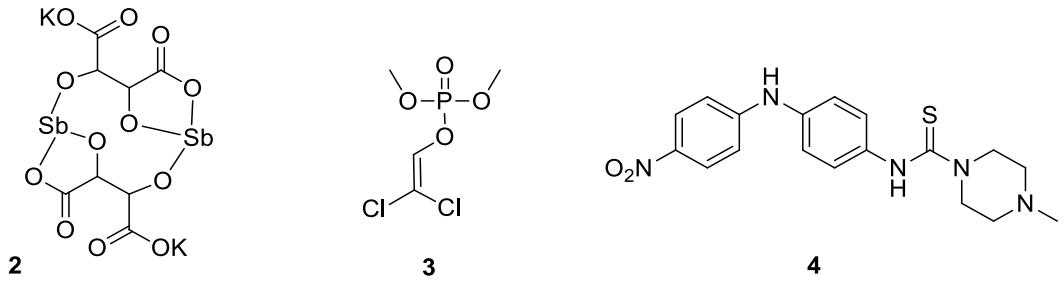

Figure 5: Relinquished schistosomiasis drugs.

In light of the relinquished aforementioned drug therapies, PZQ (**1**) and OXA (**5**) found prominence, mainly because of their safety profile and good cure rates of between 60-90% (Fig. 6).[2,21,22,30] PZQ offered broad-spectrum efficacy, exhibiting activity against all forms of adult schistosome species. OXA was widely used in Brazil as an effective anti-schistosome drug that exhibited low toxicity when tested across a host of various schistosome species.[21]

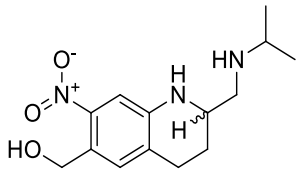

(rac)-oxamniquine **5**

Figure 6: Oxamniquine.

OXA use was discontinued because of an emergence of drug resistance and side effects.[21] The other problem with OXA was that it was only effective against *S. mansoni*. This, coupled with the comparatively cheap cost of PZQ, has made PZQ the drug of choice.[2]

1.1.5.1 Drug resistance and side effects

Despite the disappointing performance of OXA, since it is only efficacious against *S. mansoni*, the literature is awash with evidence that strongly suggests that there are some strains of *S. mansoni* that are resistant to OXA.[21,22,35] *S. mansoni* has been shown to have an elevated ability to resist therapeutic doses of the schistosomicide in question, and to find out why, the elucidation of its mechanism of action provides us with the answers.

Oxamniquine is a pro-drug, whose hydroxymethyl group is sulfated to convert it to its active form.[22,36] The sulfation is achieved by the sulfotransferase enzyme that is only present in *S.*

mansoni (SmSULT-OR). [22,36] The active form of the drug is then released from the fluke's enzyme and subsequently alkylates the fluke's DNA and various vital proteins. This permanent covalent bond between the flukes' DNA and the now active OXA drug disrupts important metabolic functions necessary for survival and kills the parasite (Scheme 1). [22,36]

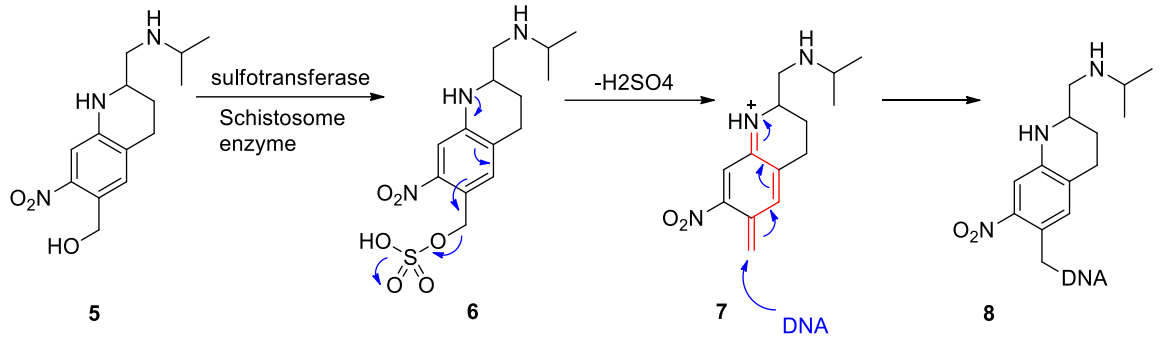

Scheme 1: Mechanism of action of OXA.

With the help of genetics, molecular biology, and biochemistry, it can be shown that OXA resistance is attributed to a single recessive gene that codes for the sulfotransferase enzyme.[21,36] The onset of drug resistance to OXA is triggered by the absence of this drug-activating enzyme. Biochemical techniques have been exploited even further to rationalize the lack of broad-spectrum efficacy of OXA, since it is ineffective against other schistosome forms. Phylogenetic analysis has been reported to have revealed similarities between sulfotransferases of *S. mansoni* with those of *S. haematobium* and *S. japonicum*. X-ray studies reveal that the catalytic mechanism is the same, however, the subtle variations in the distribution of amino acids in the active sites of these three enzymes have proven to impact the compound's binding ability negatively.[36]

1.1.5.2 Discontinuation of Oxamniquine (OXA)

The decline of oxamniquine (**5**) use, particularly in Brazil,[21] where it was exclusively used, has led to the inevitable use of monotherapy[2,24,28] to stave off schistosomiasis. OXA was a first-line treatment drug in Brazil until the 1990's,[35] when it was substituted by PZQ, since PZQ had become increasingly cheaper to produce[2] and was active against all schistosomiasis strains.[23] More reasons to replace OXA came from the emerging threat of resistance and the concern that it was only active against *S. mansoni*.[21]

1.1.5.3 Administration of Praziquantel (PZQ) as a racemate

Praziquantel (**1**), known structurally as 2-(cyclohexanecarbonyl)-2,3,6,7-tetrahydro-1*H*-pyrazino[2,1-*a*]isoquinolin-4(11b*H*)-one has an asymmetric centre at position 11b, which then

makes it chiral.[37] It exhibits a much higher pharmacological activity than OXA. The WHO recommended dosage of PZQ is between 40-60 mg.kg^{-1}.[14] PZQ is given to patients as a racemic mixture, largely because of cost effectiveness; it is synthetically cheaper to make *rac*-PZQ than it is to make enantioenriched PZQ (Fig. 7).[2]

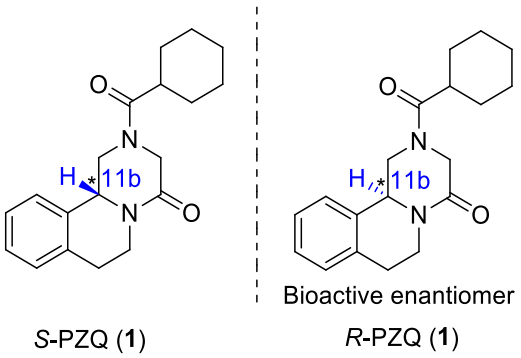

Figure 7: Non-superimposable mirror images of PZQ.

1.1.6 Synthesis of PZQ

The discovery and development of PZQ by Merck and Bayer in the early 1970's[38] came as a much-needed tool for the alleviation of the global burden of schistosome infections. They used a petrochemical product, isoquinoline **9**, as a starting material (Scheme 2).[39] This discovery was important simply because it had unveiled a direct route of synthesis. The total synthesis of praziquantel meant that the compound could be made on an industrial scale, thereby meeting the global demand for PZQ.

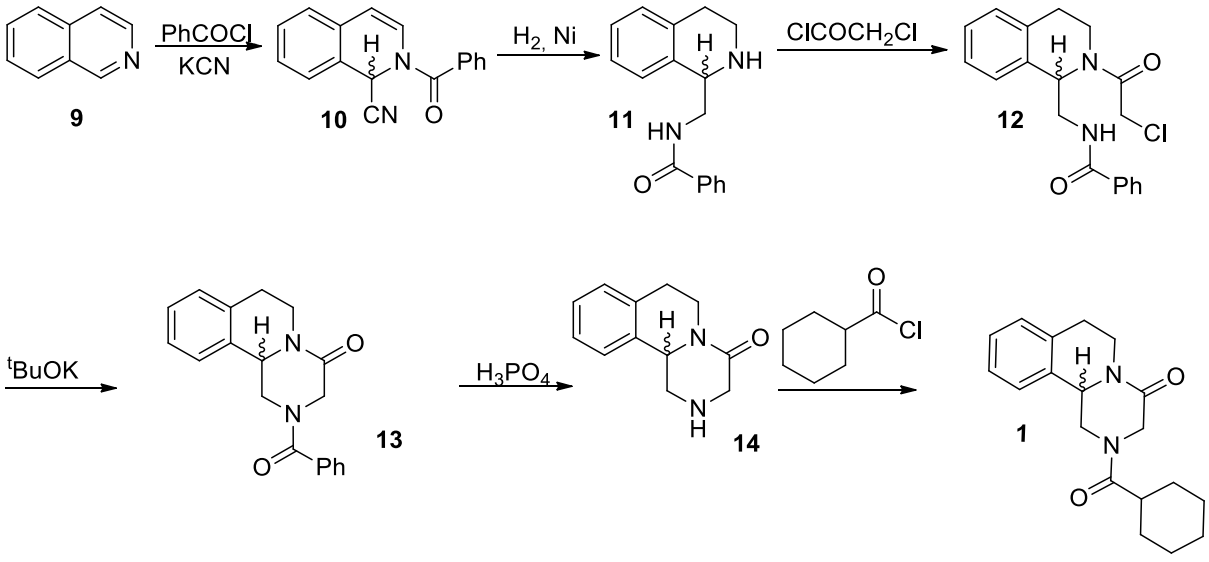

Scheme 2: Total synthesis of PZQ

To this day, this classical reaction is still widely used to make PZQ on an industrial scale, owing to the relatively low-cost and easily accessible starting materials. This six-step reaction sequence, shown in Scheme 2, begins with a Reissert reaction of isoquinoline with KCN and benzoyl chloride to give 2-benzoyl-1,2-dihydroisoquinoline-1-carbonitrile **10** in excellent yields.[39] The obtained Reissert compound is hydrogenated catalytically under high pressure to give *N*-((1,2,3,4-tetrahydroisoquinolin-1-yl)methyl)benzamide **11**. What follows is *N*-acylation using chloroacetyl chloride to afford *N*-((2-(2-chloroacetyl)-1,2,3,4-tetrahydroisoquinolin-1-yl)methyl)benzamide **12**. Treating **12** with potassium *tert*-butoxide, a strong base, gives 2-benzoyl-3-chloro-2,3,6,7-tetrahydro-1*H*-pyrazino[2,1-*a*]isoquinolin-4(11b*H*)-one **13**. The hydrolysis of the exocyclic benzamide using phosphoric acid gives **14**, which is subsequently acylated with cyclohexane carbonyl chloride to give praziquantel **1**.

This protocol involves the use of cyanide in excess, which is highly toxic. One of the companies in China that still makes PZQ using this method reported that one of the major pollutants in their effluent water is cyanide and other organic by-products.[40] Nevertheless, the discovery inevitably sparked ingenious ways to obtain the compound using alternative methods. Indeed, appreciable results from these endeavours have led to the existence of a multitude of methods that can be used to fabricate praziquantel.[37,38,41]

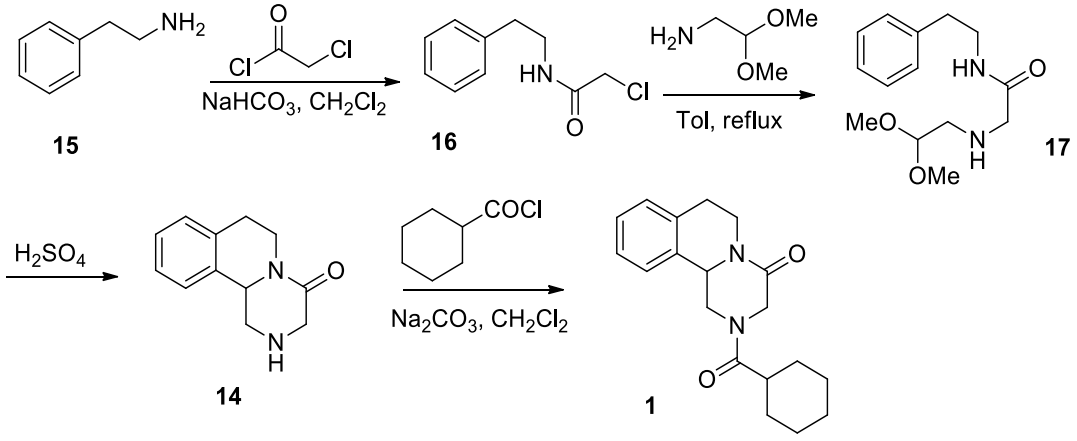

Scheme 3: The Shin Poong PZQ synthesis.

In the early 1980's, Shin Poong, a company based in Korea, devised a strategy of producing PZQ at a lower cost than was the current cost at the time.[42] By 1993, they had surpassed competing companies and had become the largest producer of PZQ globally. Their strategy involves treating phenethylamine **15** with chloroacetyl chloride to give the corresponding acetamide **16** (Scheme 3).[43] What follows is an amino alkylation reaction with amino

acetaldehyde dimethyl acetal to give **17**. Cyclisation to **14** is achieved when **17** is treated with concentrated sulfuric acid. Acylation of **14** with cyclohexane carbonyl chloride yields PZQ **1**.

Kim and co-workers reported another strategy that involved the reaction of 2-(cyclohexanecarboxamido)acetic acid **18** with ethyl chloroformate, and 2,2-diethoxy-*N*-phenethylethanamine to yield the amido compound **19** (Scheme 4).[42] Treatment of **19** with methanesulfonic acid in dichloromethane led to cyclisation, affording PZQ **1**.

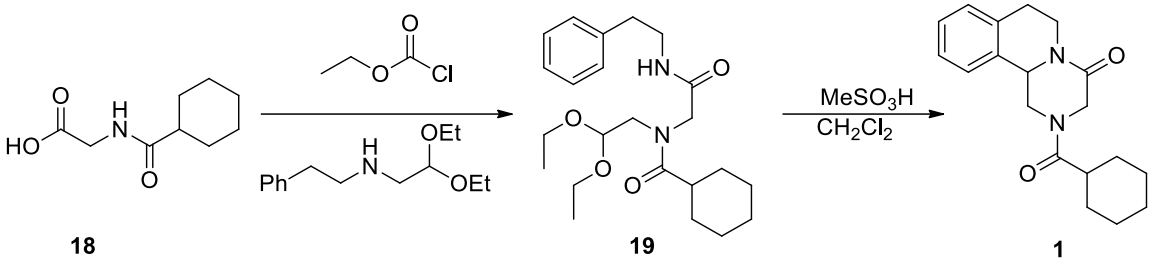

Scheme 4: Synthesis of PZQ through *N*-acyliminium cyclization.

Another ingenious way to get to PZQ has been reported to take place using the Diels-Alder reaction (Scheme 5).[42] The reaction method involves the catalytic hydrogenation of bicyclooctatriene carbonitrile **20**, followed by a condensation reaction with chloroacetamide to yield **21**. Adding methoxymethyldiamide via acetoxymethyldiamide and cyclohexane carboxylic acid gives **22**. Finally, treating **22** with methanol and potassium chromate gives PZQ **1**, via the reactive intermediate **23** that undergoes an internal Diels-Alder reaction.

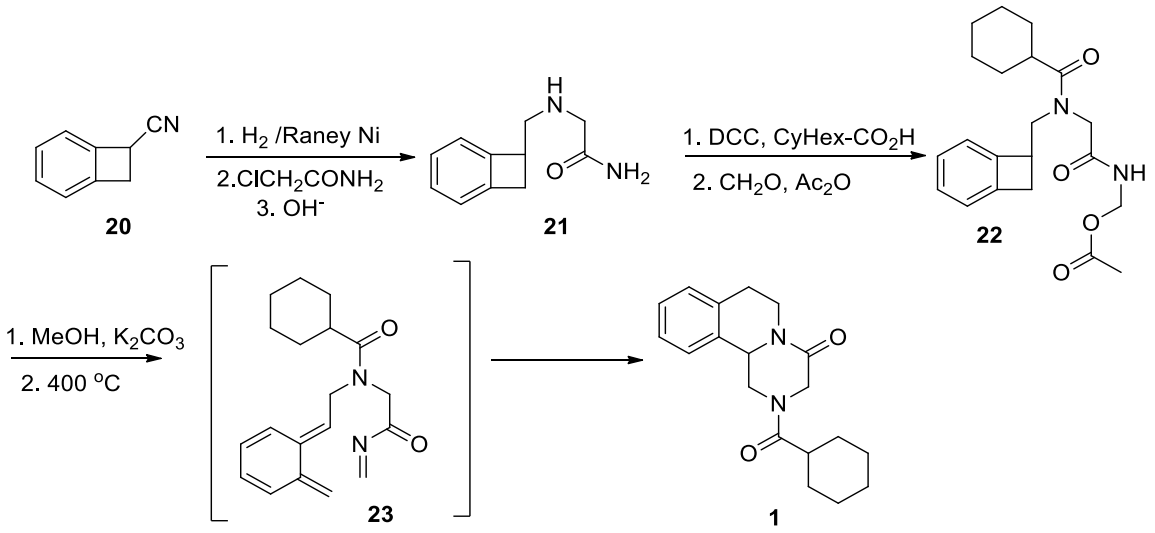

Scheme 5: An intramolecular hetero- Diels-Alder intramolecular approach to the synthesis of PZQ.

The Ugi four-component reaction (4CR) offers the shortest known synthesis of PZQ (Scheme 6).[42] This reaction involves a one-pot reaction between phenylethylisocyanide **24**, cyclohexane carboxylic acid **25**, aminoacetaldehyde dimethyl acetal **26**, and acetaldehyde **27** to give the Ugi product **28** in a quantitative yield. The Pictet-Spengler reaction under strongly acidic conditions affords PZQ **1** in about 70% overall yield.

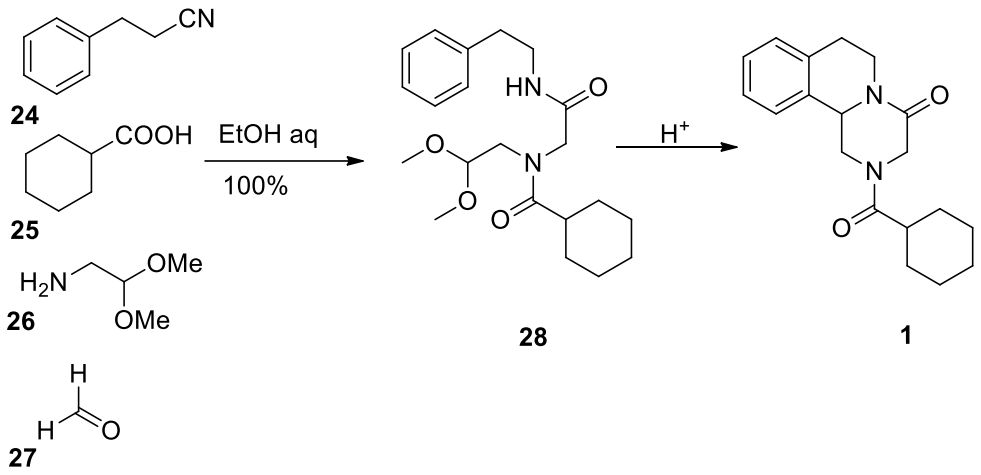

Scheme 6: Multicomponent Ugi reaction to afford PZQ in 2 steps.

The existence of PZQ for over 40 years has prompted additional studies, and we now know that from its racemic mixture, only one isomer is vital for its activity.[30] It is important to note that PZQ is still produced industrially as a racemic mixture, owing to the difficulty of devising an industrially sound method for the asymmetric synthesis of PZQ. The use of *rac*-PZQ has been reported to offer partial therapeutic effects when compared to the administration of enantiopure PZQ, and this is a consequence of the side effects that result from the inactive isomer. Only the *R*-isomer is active, and the *S*-isomer is believed to be responsible for the side effects, and the bitter taste. Removing the *S*-isomer would reduce the pill size, reduce the side effects, and improve patient compliance, particularly for children who suffer the most from schistosomiasis.

1.1.6.1 Enantioselective/ Asymmetric synthesis of PZQ

PZQ has existed for many years, yet very little has been done to invent ingenious ways to make it as the *R* enantiomer. Since its conception, the scientific community has contributed several methods to make praziquantel in its racemic form. [37,38,41] The enantiomeric fabrication of PZQ has gained little traction, and the only notable contribution is largely experimental and industrially unfeasible.[30]

Two notable contributions to the enantioselective synthesis of PZQ have been described.[42] The first method made use of an enantiopure Anderson's reagent [(1*S*,2*R*,5*S*)-methyl-(*R*)-*p*-toluenesulfinate] **29**, which was reacted with compound **30**, resulting in enantiopure compound **31** (Scheme 7).[42] The induced stereochemistry from this reaction is achieved via a Pictet-Spengler reaction, using a Lewis acid at -78°C. The first step is achieved in excellent yields (88%) and diastereoselectivity (93:7). The deprotection of the cyclic amine gave **32**, which was reacted with hydrazine monohydrate in ethanol to give the diamine **33**. The amidation of the primary amine using cyclohexane carbonyl chloride affords **34**, whose cyclisation to **1** is achieved when it is reacted with chloroacetyl chloride. The overall synthesis has a discouragingly low yield of 12%.

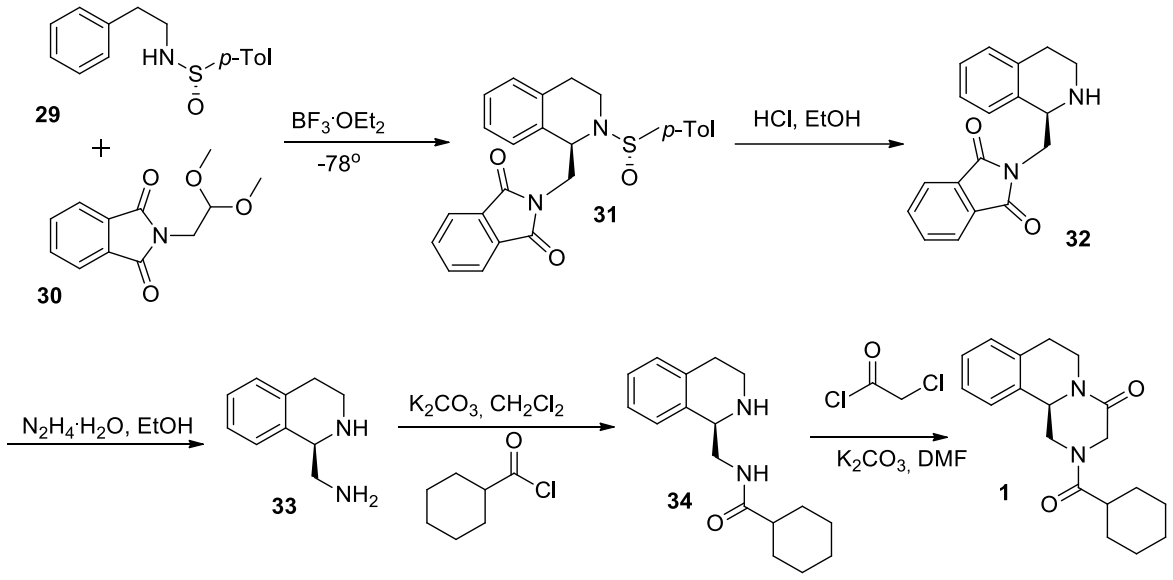

Scheme 7: The stereoselective synthesis of PZQ **1**.

Roszkowski and co-workers managed to double the yield to 22% when they used a prochiral dihydroisoquinoline derivative **36**, derived from phenethylamine **15** and dioxoisoindoline **35**, to make the corresponding tetrahydroisoquinoline **37** (Scheme 8).[37]

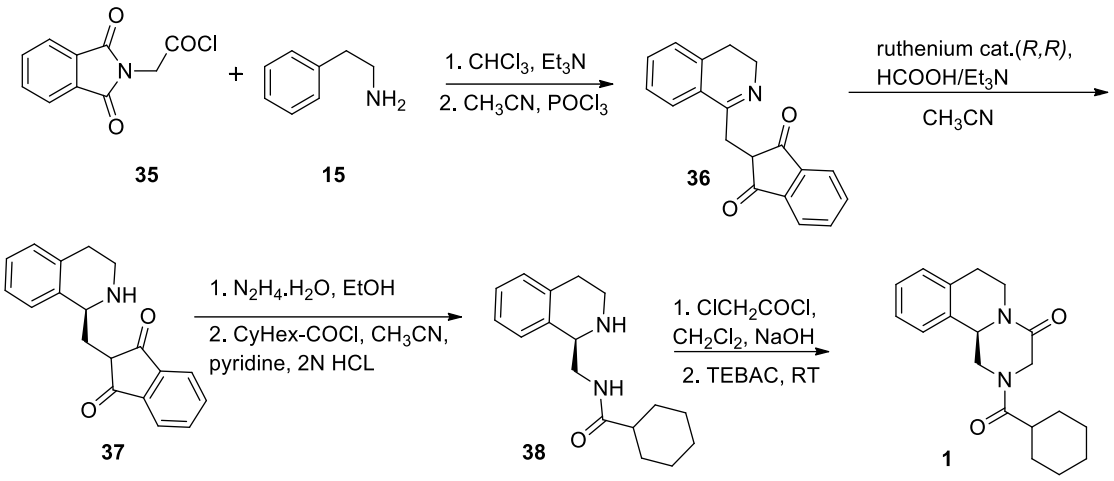

Scheme 8: The stereoselective synthesis of PZQ **1** reported by Roszkowski.

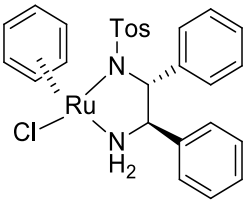

ruthenium catalyst.
(*R,R*)

Figure 8. Chiral ruthenium catalyst.

The authors disclosed that this key step takes place via an asymmetric transfer hydrogenation reaction facilitated by a chiral ruthenium catalyst (*R,R*) shown in Fig. 8, otherwise referred to as the Noyori protocol. Reacting **37** with hydrazine monohydrate, followed by cyclohexane carbonyl chloride gives **38**. Cyclisation to **1** is achieved when chloroacetyl chloride is reacted with **38**. The enantiomeric excess is reported to be 62%. The absolute stereochemistry of the chiral hydrogen was elucidated by X-ray structure analysis of the (*S*)-Mosher acid amide derivative.

Lastly, the chirality of Mosher's reagents has also been exploited to induce chirality in some compounds. A notable contribution to the stereoselective synthesis of PZQ comes from Laurent and co-workers.[42] They were able to covalently bond [α-methoxy-α-(trifluoromethyl)phenylacetic acid (MTPA)] (Mosher's acid) to praziquanamine **14** (Scheme 9).[44] The resulting diastereoisomers could be separated using column chromatography to obtain enantiopure **39** in near quantitative yields of 50%. The removal of Mosher's acid proved to be difficult, requiring strong acid conditions and long reaction times (Scheme 9).[44]

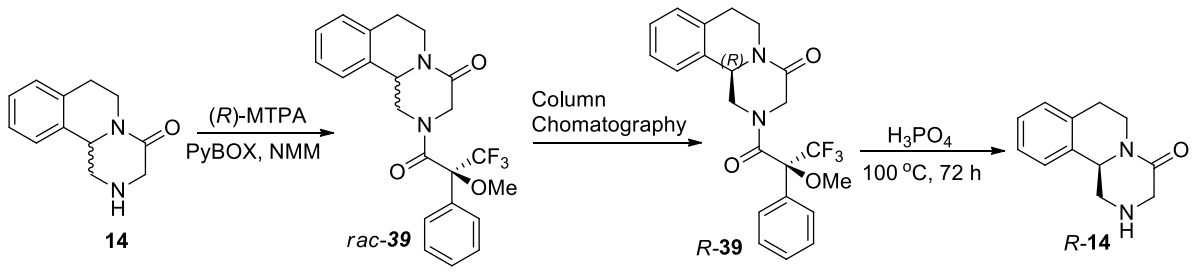

Scheme 9: Chiral synthesis of praziquanamine using Mosher's Acid as a resolving agent.

To make enantiopure PZQ is not merely for interest's sake or a an academic exercise for synthetic chemists; it is of vital importance given what we know about the pharmacodynamic activity of the active isomer. Current science offers four methods to achieve enantioenriched PZQ. The first is enantioselective synthesis, which usually makes use of chiral catalysts and/or chiral substrates on a prochiral PZQ intermediate [30] (Scheme 7, 8). The second one is chromatographic separation, which uses a chiral stationary phase to retard one enantiomer (Scheme 9).[30] The third one is stereoablation, where the stereocentre is destroyed and reconstructed selectively. The last option is resolution. Part of the reason why these methods have not been given considerable attention is because the methods lack the potential for industrial production of enantiopure PZQ.

It is undeniable that the methods discussed thus far have brought humankind ever closer to solving the problem of schistosomiasis, and this is seen through the skilful application of various synthetic methods of fabricating PZQ. In the quest of synthesizing praziquantel, it must have been important for the preceding researchers to understand its fundamental building blocks. In our pursuit to reveal methods of obtaining enantiopure PZQ, it was equally important to understand which building blocks were vital for a successful synthesis of PZQ. This led us to the isoquinoline core. A brief look at the methods of synthesizing praziquantel discussed in section **1.1.6** and **1.1.6.1** reveals that the isoquinoline scaffold was central in every method, and it would be remiss not to give the reader some background on the isoquinoline core and various ways to fabricate it. In essence, the isoquinoline scaffold can be thought of as a PZQ intermediate, which in turn, gives importance to the understanding of its chemistry. It is also important to mention that knowledge on the isoquinoline scaffold has been pivotal, particularly for the synthesis of PZQ intermediates in this project, as will be shown later in Chapter 2.

1.1.7 The isoquinoline core: a key PZQ intermediate

The isoquinoline skeleton is among the most important classes of alkaloids in chemistry and biology. It is reported that plants produce over 3000 tetrahydroisoquinoline alkaloids, with the

inclusion of opioids such as morphine and codeine.[45] This is a clear indication that tetrahydroisoquinolines play a pivotal role in plant biochemistry and by extension, in animal biochemistry. In fact, this skeleton has been successfully applied to a wide range of human chemotherapies.[45] The ubiquity of isoquinolines has also been reported to pervade the human brain, where they occur naturally as derivatives of 1,2,3,4-tetrahydroisoquinoline-1-carboxylic acid. One particular example that has been brought to the fore by researchers is the naturally occurring (-)-salsolinol-1-carboxylic acid **40** shown in Figure 8, which is merely a 6,7-dihydroxy-1-methyl-substituted tetrahydroisoquinoline-1-carboxylic acid.[46]

Whilst nature has exhibited a remarkable ability to stitch together complex compounds from just four elements (C, H, O, N), humans too have shown appreciable aptitude for the fabrication of life-saving therapies. Apart from praziquantel **1**, which has already been discussed, other examples of drugs containing the isoquinoline core include noscapine **41** and quinapril **42** (Fig. 9). [46,47]

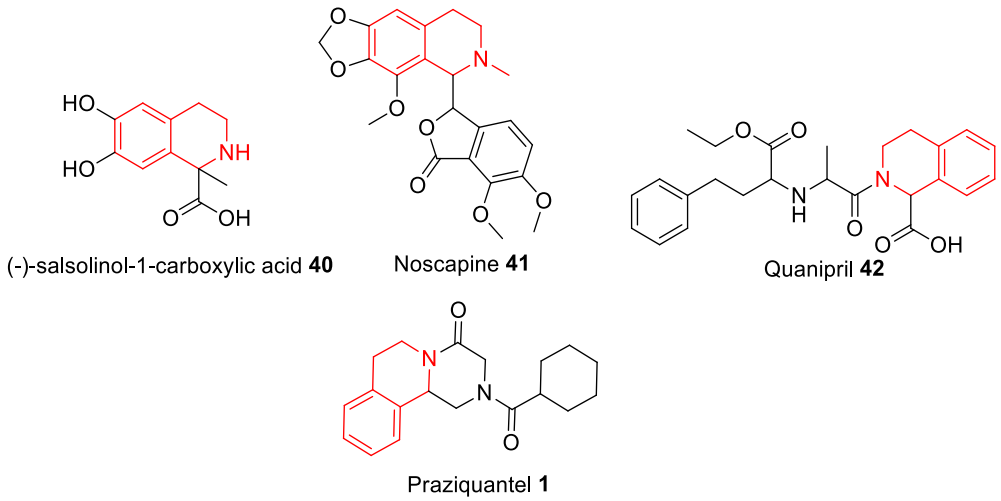

Figure 9: Biologically active compounds based on the tetrahydoisoquinoline skeleton.[46,47]

The methods used by nature to make compounds are often complex and difficult to reproduce on a large scale and this has inspired the discovery and invention of methods humans can perform with reproducible efficacy. Some of these methods used for the synthesis of isoquinolines include the Ugi multicomponent reaction, the Pictet-Spengler reaction, the Bichler-Napieralski reaction, and non-eponymous reactions like a combination of conventional chemical transformations. These are briefly discussed in the next section.

1.1.8 Methods for the synthesis of isoquinolines

Section 1.1.6 gave a brief overview of the total synthesis of praziquantel using various preparatory methods. However, the synthesis of isoquinolines as intermediates of PZQ has not been described thus far and this section seeks to close this gap. Recent advances in spectroscopic methods, chromatographic techniques and the preparation of new catalysts and reagents have seen the proliferation of new synthetic methods.[48] Amidst the crystallization of new ideas, the classical methods have stood the test of time and have become a reference point for the basic understanding of isoquinoline chemistry. A brief revisitation of the literature on isoquinolines reveals that, classically, they have been prepared using the Bischler-Napieralski and the Pictet-Spengler reaction. [48] Discussed herein, is the exploitation of the Ugi, the Pictet-Spengler and the Bichler-Napieralski reactions respectively, in the pursuit of accessing functionalized tetrahydroisoquinoline scaffolds.

1.1.8.1 Multicomponent reactions: The Ugi reaction

Multicomponent reactions (MCR) are generally revered in drug research for their applicability. What makes them particularly attractive is the fact that they are usually one-pot reactions and can be achieved under mild conditions.[49] To date, many MCRs have been exploited to synthesize elaborate chemical scaffolds, however, special attention has been given to the eponymous Mannich, Passerini, Ugi, Hantzch, and Biginelli MCRs, owing to the importance of their corresponding compounds.[50]. Among these reactions, the Ugi reaction emerged as the most suitable for the purpose of our study.

The Ugi MCR, first disclosed in 1959 by Ivar Ugi, has garnered considerable attention, owing to its synthetic applications. The reaction offers a gateway to structurally diverse products, given the number of ways each starting material can be altered.[50] Classically, the Ugi four component reaction is thought to take form as outlined in Scheme 10. Mechanistically, the reaction begins with reaction of an amine with a ketone or aldehyde to form the corresponding imine, followed by reaction of the imine with an acid and an isocyanide to give an imidate intermediate. This then undergoes a Mumm rearrangement to form the final α-acylaminocarboxamide product.[50]

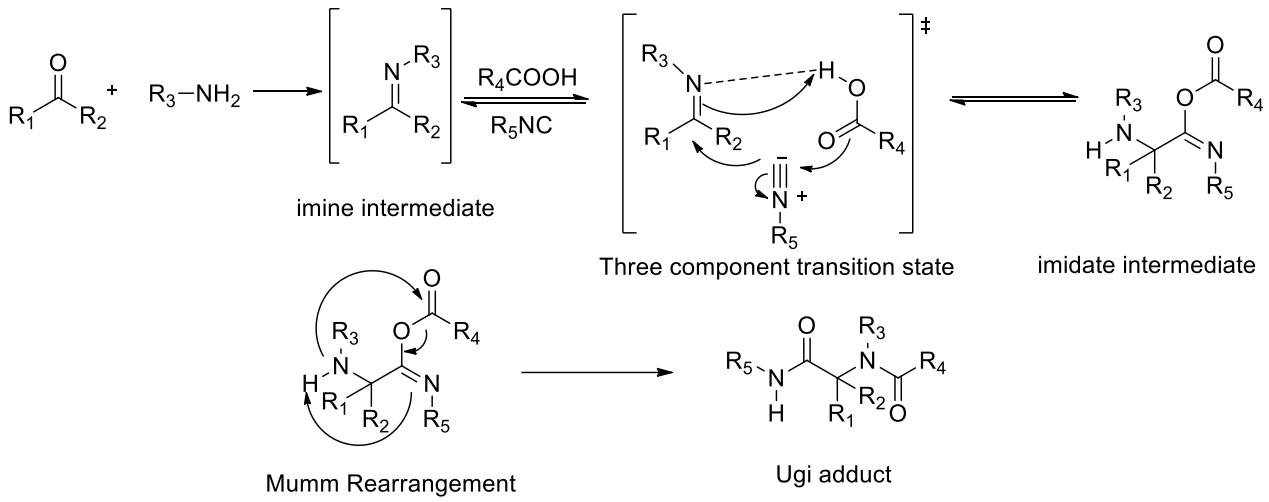

Scheme 10: Mechanistic insights into the generally accepted Ugi-MCR.[50]

Despite the lack of universal agreement as to how exactly the Ugi-MCR reaction proceeds, this has not stopped researchers from fabricating useful organic compounds using the Ugi-MCR. In fact, the Ugi reaction has been utilized to synthesize vital heterocycles, which have found importance in everyday life. For example, lidocaine is a topical pain relief product that is prepared using the Ugi-MCR. Paraformaldehyde **43**, diethylamine **44**, and 2.6-dimethylphenyl isocyanide **45** are reacted together in methanol and acetic acid at room temperature to yield lidocaine **46** shown in Scheme 11. Altering the amine from **44** to **47** gives bupivacaine **48** shown in Scheme 12, another local anaesthetic, via an intramolecular imine formation shown in Scheme 13.[51]

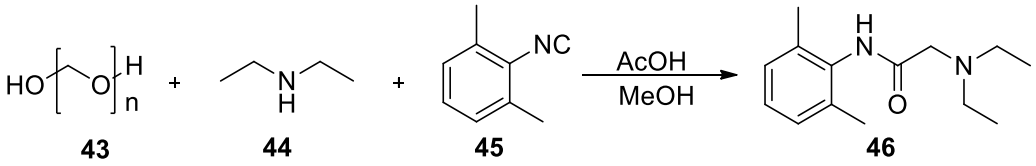

Scheme 11: The synthesis of Lidocaine **46** using the Ugi-MCR.

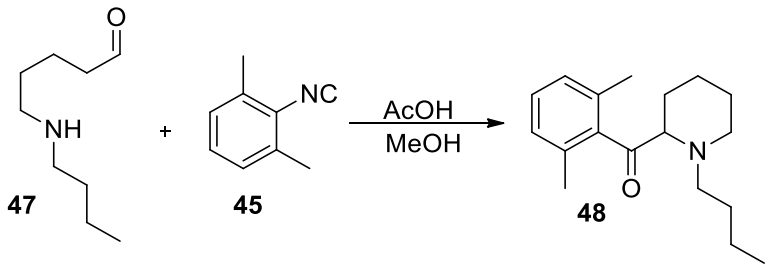

Scheme 12: The synthesis of bupivacaine **48** using the Ugi-MCR.

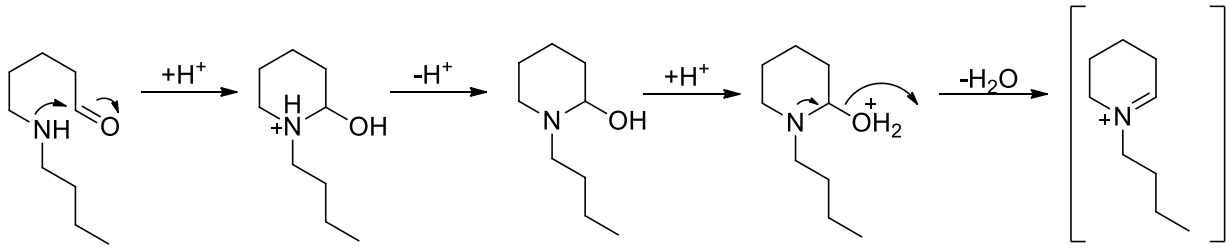

Scheme 13: Ugi-type Intramolecular imine formation of bupivacaine **48** intermediate.

1.1.8.2 The Pictet-Spengler reaction and the Bichler-Napieralski reaction

Aromatic functionalisation chemistry has also been exploited to offer synthetic methods that eventually lead to the formation of tetrahydroisoquinoline derivatives. These methods include the Pictet-Spengler reaction and the Bischler–Napieralski reaction.[52] The former reaction is an eponymous reaction carried out for the first time in 1911 by Amé Pictet and Theodor Spengler in their laboratory at the University of Geneva. They noticed that tetrahydroisoquinoline **49** and tetrahydroindole **51** form readily when β-amine **15** and tryptamine **50** are heated in the presence of an acid and an aldehyde (Scheme 14). Pictet was already on a quest to form alkaloids under mild conditions long before he co-discovered the cycloaddition reaction of β-arylamines and aldehydes in the presence of acids. His work suggested a deliberate intent for the creation of new science, and today the reaction is still used for the synthesis of a vast number of heterocycles.

The Bischler–Napieralski reaction predates the Pictet-Spengler, reported in 1893, and was the first of its kind to fabricate 3,4-dihydroisoquinoline derivatives from the condensation of β-arylethylamides or β-arylethylcarbamates using readily available condensing agents like phosphorus oxychloride ($POCl_3$), phosphorus pentoxide (P_2O_5) or zinc chloride ($ZnCl_2$) as shown in Scheme 15. In fact, Amé and Theodore cited Bischler and Napieralski when they first reported their alkaloid-forming cyclisation reaction. Both these reaction methodologies contributed immensely to the science of heterocyclic compounds, particularly the isoquinoline scaffolds, which have already been demonstrated to exhibit vital therapeutic and physiological importance.[49,53]

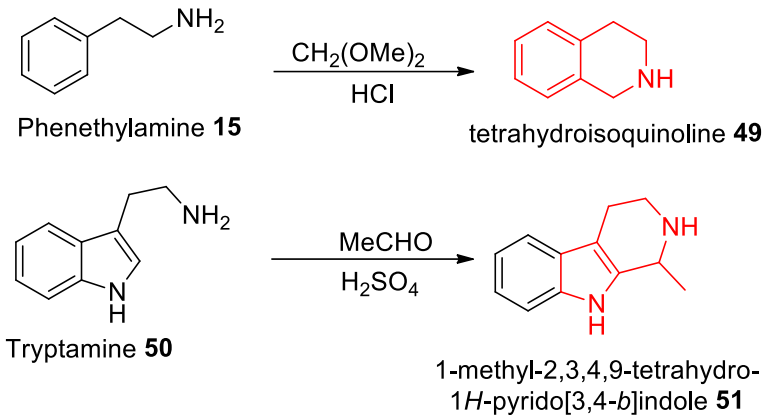

Scheme 14: Two heterocyclic scaffolds prepared from phenethylamine and tryptamine using Pictet-Spengler conditions.

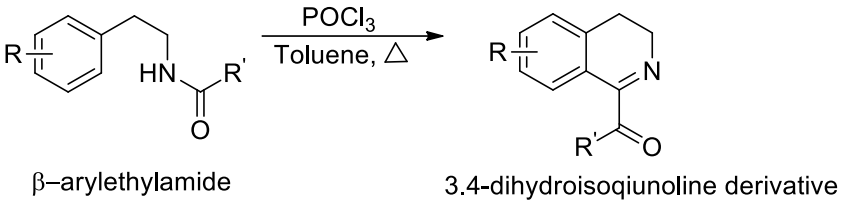

Scheme 15: Bischler–Napieralski reaction for the preparation of 3,4-dihydroisoquinoline derivatives

Studies of both mechanisms show that these reactions are ring-closing reactions, where for both reactions, a β-aryethylamine is condensed with a carbonyl compound. What forms next dictates the type of the reaction that results; the Bischler-Napieralski is preceded by the formation of an amide derivative, whilst the Pictet-Spengler reaction is preceded by the formation of a secondary amine.

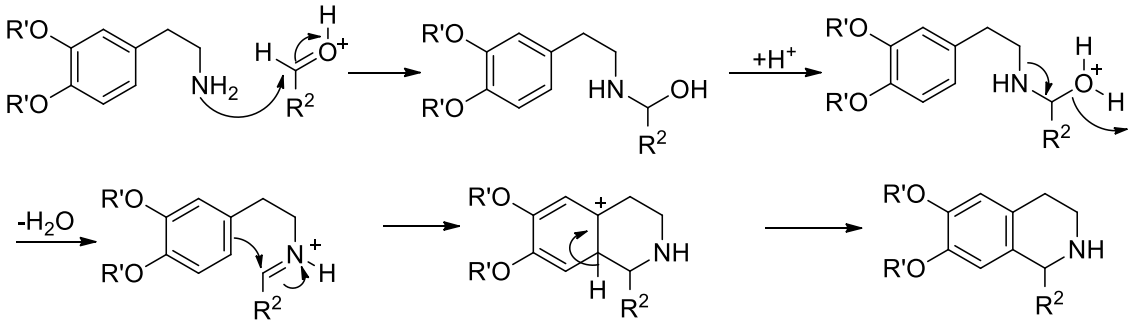

Scheme 16: Pictet Spengler reaction mechanism.

For the final step, which is the cyclisation, the Pictet-Spengler reaction exhibits a self-propagating mechanism, where the collapse of the nitrogen lone pairs into the α-position expels water, forming an imine intermediate that is attacked by the phenyl ring. The restoration of the

aromaticity is through the deprotonation of the proton nestled between the phenyl ring and the newly formed bond, which in turn forms the desired isoquinoline (Scheme 16). On the contrary, the Bichler-Napieralski reaction requires a condensing agent. Phosphoryl oxides and oxychlorides are famous for this transformation; movement of a lone pair from the nitrogen atom causes the empty orbital in phosphorus to accept a lone pair from a carbonyl oxygen to form a phosphorus-oxygen bond, releasing a chloride ion. The chloride ion deprotonates the newly formed iminium ion. The resulting ion is attacked by the nucleophilic phenyl ring, and the aromaticity is restored through the abstraction of a ring proton to form HCl, thereby forming a dihydroisoquinoline derivative (Scheme 17).

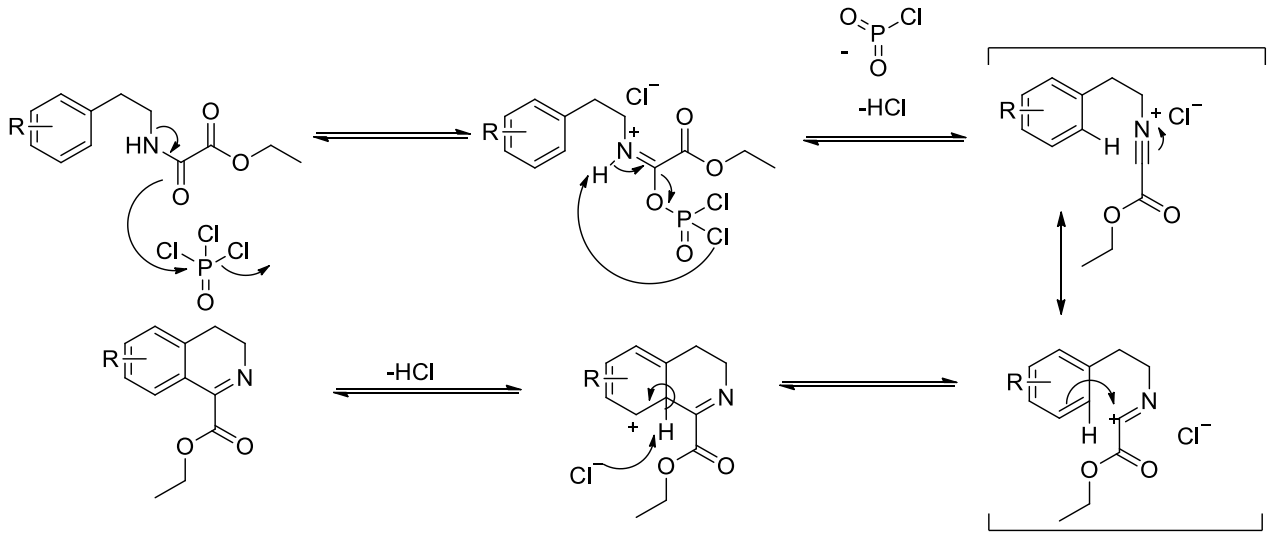

Scheme 17: Bischler-Napieralski reaction mechanism.

1.2 Tuberculosis

Tuberculosis (TB), a transmissible disease dating as far back as the neolithic period, is caused by *Mycobacterium tuberculosis.*[54–56] Its effects were somewhat negligible, until the industrial revolution, where overcrowded human settlements fostered its spread.[54] Currently, it is ranked 13th among the global causes of death, and it is the leading cause of death from just a single infectious agent.[56] Tuberculosis was a mystery until the early 1880's when Dr Robert Koch shared with the scientific community his discovery of the bacillus that was causing the disease.[56] Since then, the quest for knowledge pertaining to TB has not ceased. We now know that the *M. tuberculosis* complex is comprised of about 9 species in the genus *Mycobacterium* of the family Mycobacteriaceae, and order Actinomycetales.[54] It is these species that cause a multitude of human and zoonotic ailments. For instance, *Mycobacterium africanum* is largely confined to West Africa,[57] whilst *Mycobacterium canetti* has very little global footprint but has garnered some notoriety in Eastern Africa.[54,58] *M. bovis* is zoonotic in nature and jumps

from cattle to human hosts when the latter hosts consume unprocessed animal products. Other known zoonotic species are *M. microti, M. pinnipedi* and *M. caprae*.[54]

1.2.1 Global and Regional Prevalence

It is estimated that about a quarter of the world's population has TB, which translates to about 2 billion people, most of whom also live in abject poverty.[56,59]

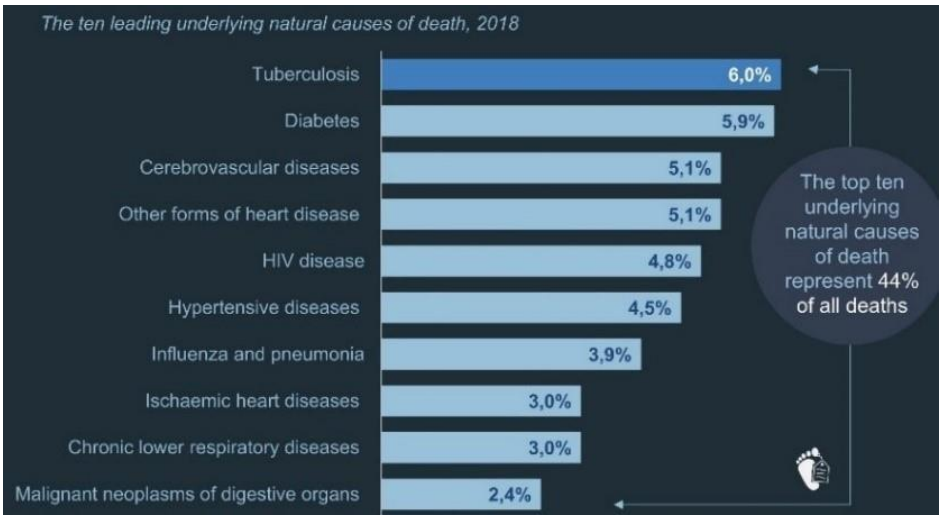

Figure 10: Causes of Mortality in South Africa in 2018.[60]

This is gravely concerning, given the vastly diverse and modern tools available to suppress TB. In the year 2020 alone, about 10 million people were infected with TB and among these 1.1 million of them were children, 3.3 million were women and 5.6 million were men.[3]

In 2020, Africa's TB burden, against the global burden, stood at 25% and a total of 44% of mortalities.[56] This may be perceived as a relatively small number; however, it is vital to note that of the 8 countries that accounted for two-thirds of the global incidence cases in 2020, two of them are housed in Africa and one of them is South Africa. To make TB even harder to combat, immunocompromising ailments like HIV lower the barrier of entry for TB in patients who have had the least amount of exposure to the bacilli.[61]

The 2020 World Health Organization TB report listed South Africa among the 30 high TB burden countries that account for 86% of all global TB incident cases.[56] From this list of 30 countries, only 8 countries account for the vast majority of incident cases, representing about two thirds of the global total cases. Of these 8 countries, South Africa, after Nigeria, represents a large portion of African incidence cases. This agrees with what has been reported locally; the 2018 Statistics South Africa report (Stats SA) ranked TB as the leading cause of death from 2016 through 2018 (Fig. 10).[60]

1.2.2 Key Challenges

The synergy between poverty and global diseases is arguably the most daunting challenge that world experts have had to solve. To this day, poverty and disease have persisted in their everlasting symbiosis; tuberculosis is often referred to as "the disease of the poor".[62,63] With that said, the hurdles that impede the eradication of TB become intuitive. The obvious issue pertaining to combating TB is unequal access to healthcare. TB is curable, however, unequal access to healthcare does not only have detrimental effects on the dispensary of life-saving medicines, but it also shines light on the inadequacies of social awareness.[64,65] A well-established education programme would equip people with the required knowledge needed to avoid contracting tuberculosis and to refrain from interrupting TB treatment. It comes as no surprise that developing countries are the worst hit countries, whilst developed countries are cushioned by good healthcare programmes, where TB cases are only prevalent in rural pockets.[66]

The current TB treatment has demonstrated tremendous success in its bactericidal activity. This success has, in part, been diminished by the accompanying long duration of chemotherapy required for a full recovery.[63,67] The duration of the treatment is thought to be a result of having TB bacteria existing as subpopulations of organisms whose growth is occurring at different rates; at any given moment, the bacteria present in the host spans the spectrum from metabolically latent to actively proliferating bacteria.[63] This physiological phenomenon explains the heterogeneity of TB drugs; they work on killing different subpopulations in a non-concerted manner; isoniazid is known to kill actively replicating bacilli whilst rifampicin can inhibit RNA synthesis in both replicating and non-replicating bacilli.[68] Pyrazinamide, on the other hand, is reported to disrupt cell membrane metabolic reactions. The combined effect of these drugs has successfully shortened the duration of the treatment from 18-24 months to 6-9 months. This becomes a success story, only if medical practitioners manage to keep patients compliant until the completion of the treatment and no resistance to drugs arises midway through the treatment.

The unfortunate news is that patients do default, which, in one way, inevitably leads to drug resistance when they are put back on the medication,[69] in the pursuit of containing the resurgence of TB. On the 1st of September, in the year 2006, the first case in the world of a new tuberculosis strain that was extensively resistant to TB drugs (XRD-TB) was announced by WHO to have been found in KwaZulu-Natal, which happens to be the epicentre of HIV/AIDS

in South Africa (Fig. 11).[70] This finding not only threatened healthy South Africans, but it also brought immeasurable worry to individuals who were living with HIV/AIDS.[17]

Figure 11: Map of KwaZulu-Natal in South Africa, where the first XDR-TB strain was found.[70]

The challenges of tuberculosis are not a distant observation, in fact, South Africa is familiar with the debilitating effects of tuberculosis and HIV.[70–72] The Big Pharma industry has shown very little inclination for producing new TB therapies,[63] and as a result, the best the developing nations can do is to either invest in the development of novel TB drugs or locally develop the current ones that have long been off patent, with vital changes that lower their production costs.

1.2.3 Tuberculosis infection

Infection is usually a consequence of inhalation of tubercle bacilli (Fig. 12).[54,55,73,74] People who are infected with pulmonary tuberculosis create an aerosol of saliva when they sing, talk and cough.

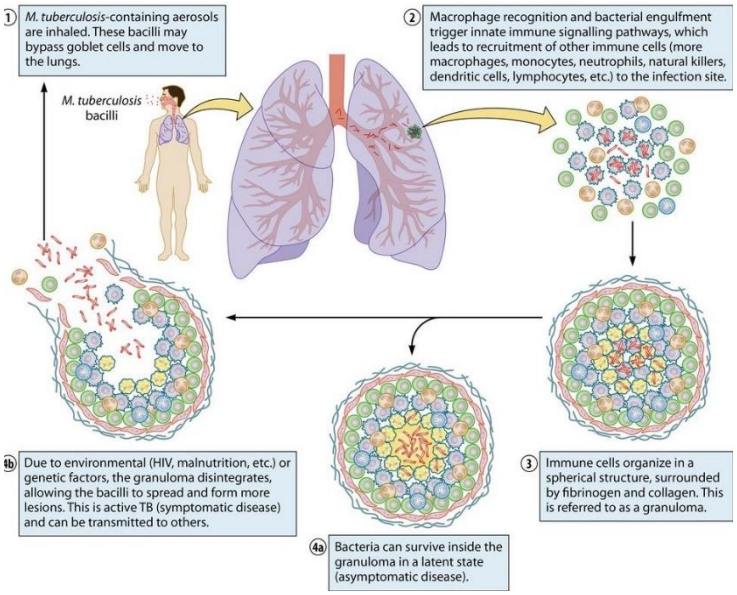

Figure 12: Pathogenesis of *Mycobacterium tuberculosis*.[74]

The droplets released into the atmosphere encapsulate tubercle bacilli and are inhaled into the terminal air spaces of the lungs of a healthy individual, where they multiply. The first immune response of the invasion is through the alveolar macrophages, which ingest and kill the bacteria. The extent to which the initial immune response can fight off the invasion is dependent on the microbicidal capacity of the phagocytes of the host, and the severity of the TB bacteria. The bacilli that have managed to evade the immune response replicate and disrupt the alveolar macrophage response mounted by the host.

This alveolar macrophage disruption triggers a second immune response by the host. To fight back, the host deploys blood lymphocytes and monocytes to the infected lungs, where they differentiate into secondary macrophages which again engulf the mycobacteria, but do not destroy them. At this point, mycobacteria strive and grow with little tissue damage, which causes an accumulation of blood-borne secondary macrophages. The host develops T-cell immunity at about 2-3 weeks of infection, triggering a rapid multiplication of antigen-specific T-lymphocytes within the ingested tubercles, which signals the secondary macrophages to destroy intracellular mycobacteria. This halts bacterial growth and causes bacterial death. The debris left behind by bacterial death inhibits bacterial extracellular proliferation, thus preserving existing bacilli and thereby introducing what is termed bacterial latency. In this latent stage, *Mycobacterium* can remain dormant for a duration ranging from months to decades. For people living with immunosuppressing ailments like HIV/AIDS, TB is known to spill tubercle-invaded cells into the bloodstream, thereby infecting other organs.[75] Other

conditions that favour TB activation from its latent form are chronic renal failure, malnutrition, chemotherapy, malignancy, drug addiction, and smoking.

1.2.4 Treatment methods

Tuberculosis chemotherapy has remained relatively unchanged for some time. The current anti-tuberculosis regimen includes pyrazinamide (PZA) **52**, isoniazid (INH) **53**, ethambutol (EMB) **54** and rifampicin (RIF) **55** (Fig. 13).[76] This four-drug regimen called Rifafour is administered first as a combination of INH, PZA, EMB and RIF for two months, followed by INH and RIF for four months.[76]

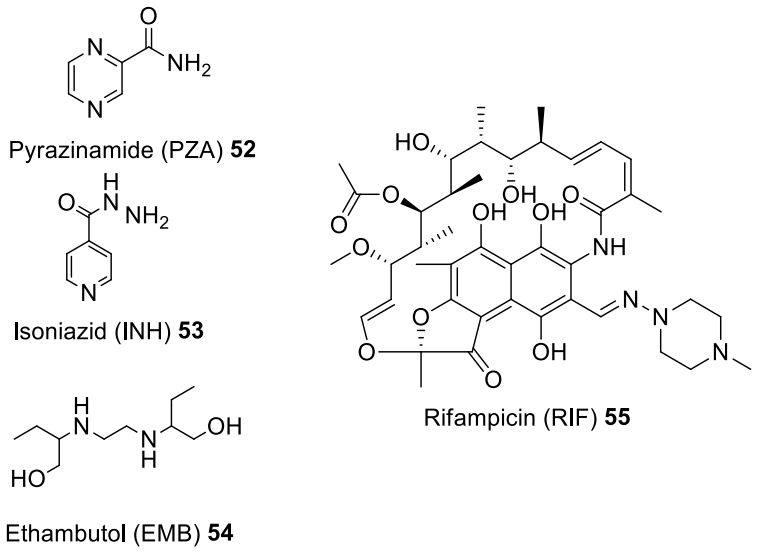

Figure 13: Chemical structures of PZA, INH, RIF, and EMB.

Tuberculosis is treated by means of combinational chemotherapy, where multiple drugs are administered.[67] This form of therapy increases the efficacy and reduces the chances of the emergence of resistant bacilli strains. The combinatorial nature of TB drugs is exemplified by the modes of action each of them exhibit.[63] Broadly speaking, TB drugs can be classed as inhibitors of bacterial protein synthesis, inhibitors of electron transport across the bacterial membrane, inhibitors of cell wall synthesis and inhibitors of nucleic acid synthesis (Fig. 14).[63]

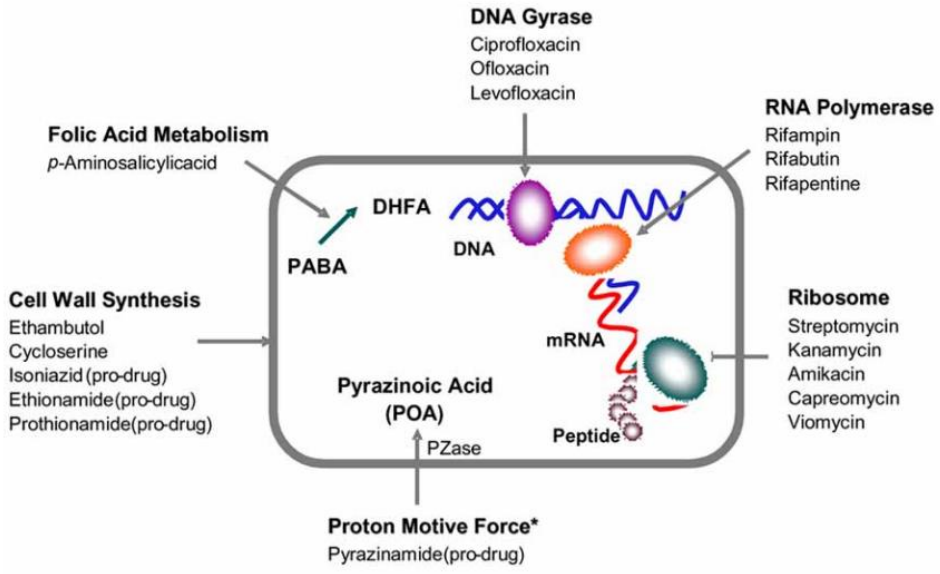

Figure 14: A diagrammatic illustration of sites of action for the available anti-tuberculosis drugs.[63]

The emergence of MDR-TB (strains that are resistant to at least isoniazid and rifampicin)[77] and XDR-TB (strains that are resistant to isoniazid, rifampicin, fluoroquinolones, and at least one injectable drug like capreomycin, kanamycin, or amikacin)[77] have threatened the prospects of achieving worldwide eradication of tuberculosis. However, the current TB chemotherapy has not become obsolete. In fact, the current TB regimen is still being reported to be highly effective under strictly regulated programmes, whose cure rates have been reported to exceed 90%.[63] Alongside the development of novel TB drugs, the improvement of the current TB drugs should be treated with the same vigour and enthusiasm.

1.2.4.1 Isoniazid (INH)

Isoniazid is an important first-line bactericidal drug that kills actively proliferating mycobacteria. It has a minimum inhibitory concentration (MIC) of 0.02 μg mL^{-1}, and also exhibits activity against other members of the genus mycobacterium such as *M. bovis* and *M. kansasii*.[78] Suffice to say INH has indeed stood the test of time, given that its existence has been reported as far back as the 1950s.[78] Today, the modern synthetic chemist is furnished with innumerable ways to fabricate INH, otherwise referred to as isonicotinic acid hydrazine **53**. Of the many ways to arrive at INH, the most prevalent ones can be grouped into three major strategies; one can either start from isonicotinic acid **56** (Scheme 18), 4-pyridinecarbonitrile **57** (Scheme 19), or isonicotinates **58-63** (Scheme 20).[78]

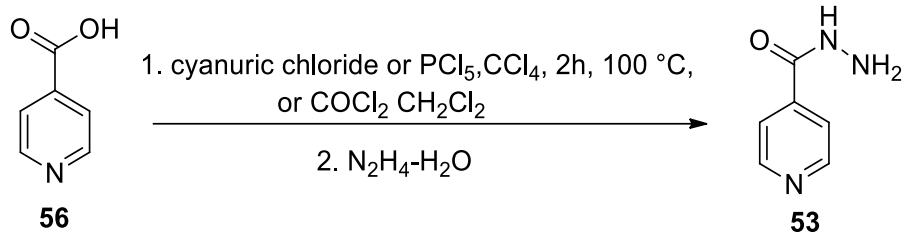

56 **53**

Scheme 18: Synthesis of INH **53** from isonicotinic acid **56**.

The conversion of isonicotinic acid **56** to isoniazid **53** is a facile conversion that involves the chlorination of the carbonyl functional group to form an acyl halide, which is then reacted with hydrazine monohydrate to give the desired isonicotinic acid hydrazine **41** (Scheme 18). Various chlorinating reagents can be used to achieve this transformation.[78]

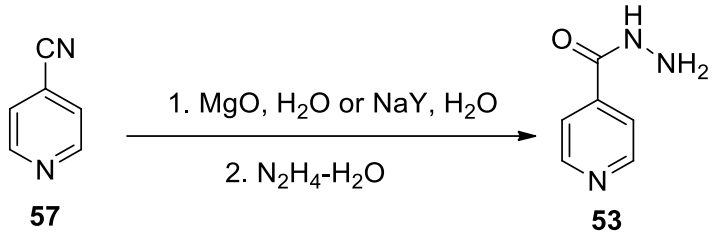

57 **53**

Scheme 19: Synthesis of INH **53** from 4-pyridinecarbonitrile **57**.

4-Pyridinecarbonitrile **57** can be converted to INH **53** first by hydrolysis in the presence of alkaline catalysts such as NaOH or MgO, followed by reaction with hydrazine monohydrate (Scheme 19).

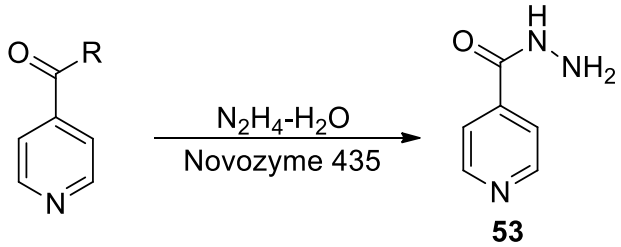

53

58.R= OC_2H_5, **59**.R=OCH_3, **60**.R=OC_4H_9, **61**.R=Im, **62**.R=NH_2, **63**.R=OCOOEt

Scheme 20: Synthesis of Isoniazid **53** from isonicotinate (**58-63**).

The use of synthetic zeolites has also been reported to catalyse the hydrolysis of 4-pyridinecarbonitrile.[78]. Isonicotinates **58-63** can be converted to INH **53** in the presence of Novozyme 435, yielding **53** in moderate to good yields (Scheme 20). Interestingly, this strategy uses a lipase catalysed hydrazinolysis. The use of biocatalysts in this strategy has encouraged and inspired some of the work presented in this dissertation.[78]

1.3 Biocatalysis

Chemical reactions that occur on their own accord, without any chemical or physical intervention are said to be spontaneous.[79] A classic example is the melting of ice into water at temperatures above zero degrees centigrade.[79,80] For many years, it has been established that the spontaneity of chemical reactions is not a universally intrinsic characteristic; some chemical reactions must be 'activated' to afford the conversion of one chemical species to another.[81] This activation can be in the form of applying heat, altering the concentrations of the reacting species, increasing the pressure if the reacting species are gases, increasing the surface area so there can be more sites of interaction, and controlling the orientation of reacting species to effect good collisions. All of these can be thought of as increasing the rate of a reaction and can, in principle, be applied to both spontaneous and non-spontaneous reactions.[79] The application of these physical techniques has been shown to improve the rate at which reactions occur, however, it could still be difficult to overcome the energy barrier required for the formation of a new species, and this is where *catalysis* finds purpose and significance.[82]

Catalysts are substances that lower the energy barrier that must be overcome for a successful chemical conversion of one substance into another.[79,81] Thermodynamically, this energy is expressed in terms of free energy change. The interaction of the reacting species with the catalyst forms an activated transition complex, which exists at a significantly lower energy state, thereby delivering the desired product at a fraction of the required energy in the absence of the catalyst (Fig. 15).[79,81]

The fact that the catalyst can facilitate the transformation without being used up or altered explains how it is able to catalyse reactions in perpetuity.[79] In principle, there should exist a system where a reaction could be catalysed indefinitely and unimpeded, since the catalyst retains its activity and its structural integrity. We now know that such a perfect system would violate the second law of thermodynamics that deals with entropy, since everything in the universe tends to disorder.[79] Practically, a catalyst is subject to structural changes as a consequence of the conditions it is subject to, and this cascades to its stability and its ability to retain its activity.[83]

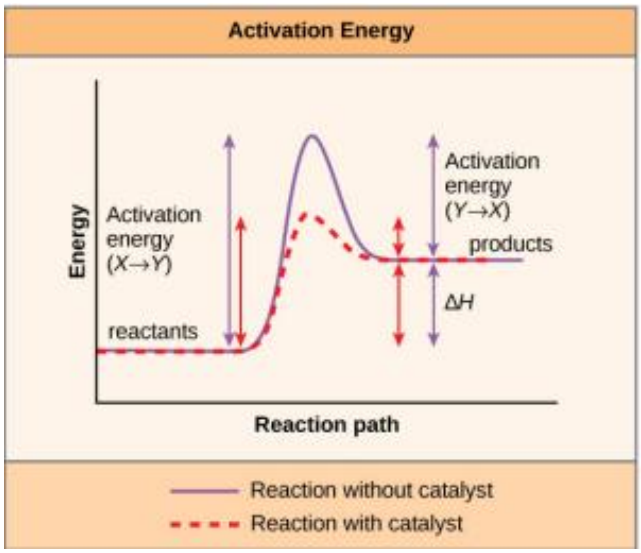

Figure 15: A diagram illustrating the mechanism of catalysis.[81,84]

Catalysis has played a pivotal role in the fabrication of useful compounds, both in academia and in industry.[85] Recently, there has been a growing interest in *biocatalysis*, owing to its advantages such as its high activity under moderate conditions, high specificity, biodegradability, high turnover numbers and its general environmental benignity.[86] Biocatalysts are generally sought after for their remarkable propensity of catalysing stereoselective reactions that afford products with excellent enantiopurity. Moreover, the use of enzyme catalysis allows for the omission of protection and deprotection reaction steps that are common in conventional syntheses.[87,88] The benefits of biocatalytic reactions, economically and environmentally, have made them an attractive additional tool for the modern synthetic chemist.

Enzymes have shown a remarkable ability to catalyse diverse chemical reactions, the vast majority of which are very complex to replicate in a laboratory setting.[86] An enzyme, whose primary protein structure contains 100 amino acid residues would have 20^{100} possible permutations. With that said, it is generally presumed that there is an enzyme that is able to catalyse any chemical reaction known to humankind.[81] Indeed, we have now arrived in the era where chemical reactions can be performed under total enzymatic synthetic conditions; Huffman and co-workers from Merck have managed to develop a total enzymatic synthesis of islatravir, which is an HIV drug. The enzymatic synthesis is devised to make use of five important enzymatic steps shown in red (Scheme 21).[89]

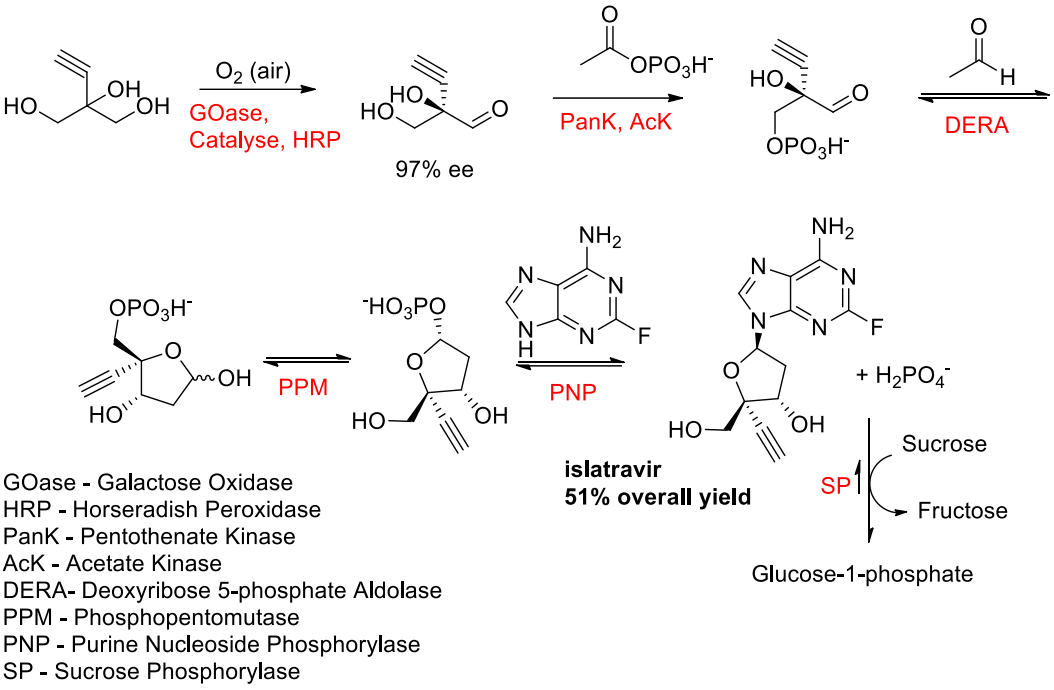

Scheme 21: Total enzymatic synthesis of islatravir.

1.3.1 Lipases

Lipases (EC 3.1.1.3) are ester hydrolase enzymes that facilitate the hydrolysis of long-chain acylglycerides.[90,91] Their popularity in organic synthesis is not only limited to their environmental friendliness, nor their economic benefits. What makes them a valuable tool in synthetic chemistry is their remarkable ability to exhibit chemo-, stereo- and regio-selectivity.[90,91] Secondly, they can be sourced from microorganisms like fungi and bacteria, which can be genetically modified to produce large quantities of lipases. Thirdly, many of the lipases known have already been structurally elucidated using X-ray crystallographic techniques, which in turn means scientists are in a better position to understand the modes of action when lipases are involved.

Lastly, lipases do not require co-factors to function and there have been no reports where lipases catalyse unwanted side reactions.[90] With that said, it comes as no surprise that lipases are the most widely used biocatalysts in organic synthetic chemistry, particularly in industry, where they continue to be exploited in industrial processes that deal with detergents, baking, paper, leather processing and hard surface cleaning.[91] The structure of lipases is such that they contain a lipophilic active site that is protected by a helical oligopeptide unit. The active site is reported to only open up when it is in close proximity with a hydrophobic substance.[91] This movement of the active site exposes the lipid-like substance to an active site that is

characterized by a triad (serine, histidine, and aspartate) of amino acid residues which are responsible for much of the catalysis that takes place inside the active site (Fig. 16). [92]

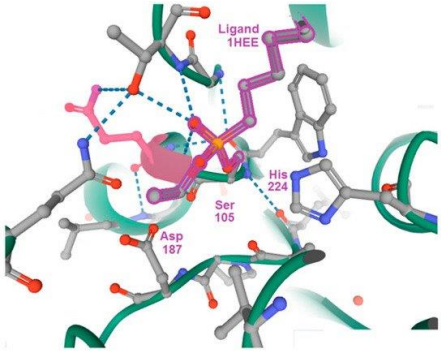

Figure 16: Active site of a lipase enzyme, showing a bound lipophilic substance.[92]

In synthetic chemistry, lipases are mostly used to catalyse the hydrolysis of carboxylic acid esters or the acylation of carboxylic acids and amines in organic solvents.[90,91] Many researchers have exploited lipases and have furnished interested readers with interesting findings. Liljeblad and co-workers have shown the resolution of racemic methyl indole-2-carboxylate **64** using *C. antarctica* lipase A (Scheme 22).[93] They were able to *N*-acylate **64**, affording enantiopure **65** in an excellent enantiomeric ratio of more than 200 (E>200). They also discovered that in the absence of the methyl ester, the acylation proved to be prohibitively slow.[93] The methyl ester could presumably be enhancing the binding interactions at the active site.

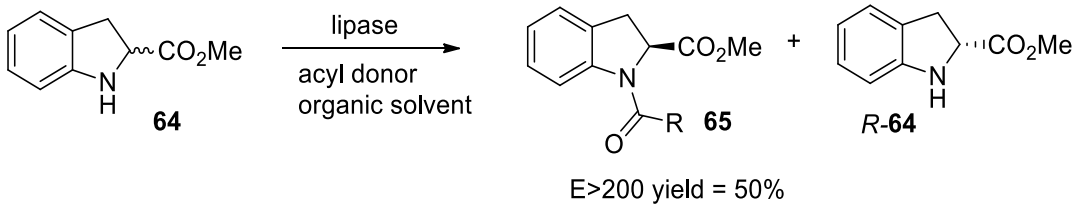

Scheme 22: EKR of methyl indole-2- carboxylate **64** achieved by Liljeblad and co-workers using CAL A lipase.

Sanchez and co-workers have reported a lipase mediated hydrolysis of methyl 1,2,3,4-tetrahydroisoquinoline-3-carboxylate **65**, where they demonstrated that an animal-based lipase could also be used to hydrolyse methyl esters to the corresponding carboxylic acids (Scheme 23).[94] In this way, they were able to prepare an enantio-enriched tetrahydroisoquinoline -3-carboxylic acid **66** and the now enantiopure **65**.

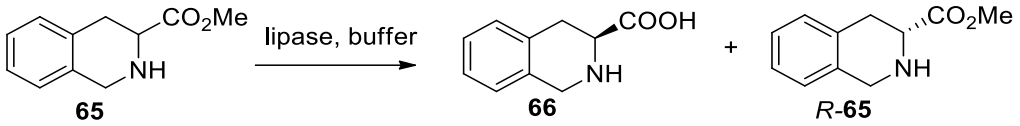

Scheme 23: Hydrolysis of methyl 1,2,3,4-tetrahydroisoquinoline-3-carboxylate **65** animal-based lipase.

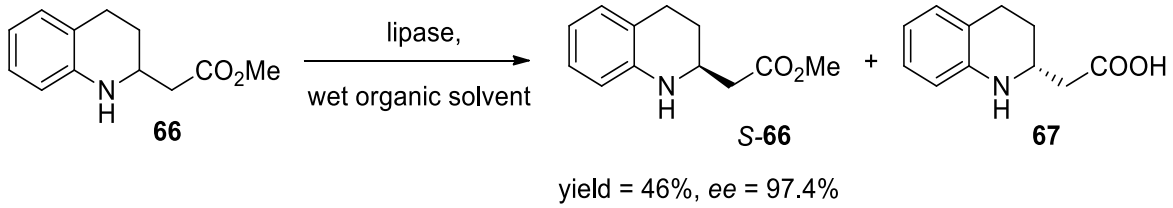

Scheme 24: Enzymatic kinetic resolution of **66**, achieved using Novozyme 435 lipase.

Another lipase-mediated hydrolysis of a methyl ester has been demonstrated by Katayama and co-workers when they hydrolysed tetrahydroquinoline derivative **66** using Novozyme 435 lipase as their preferred biocatalyst (Scheme 24).[95] This biocatalytic reaction afforded the now enantiopure methyl ester *S*-**66** with a yield of 46%, enantiomeric excess of 97.4% and an enantiomeric ratio of greater than 100 (E>100).

1.3.2 Nitrile Hydratase

As is already established, the number of enzymes one could obtain by arranging the 20 amino acids in various permutations is astounding to say the least. The number of enzymes nature is able to tailor with impeccable precision is endless, and from this list, we have also taken a keen interest in one class of enzymes called Nitrile Hydratases (NHase). Nitrile hydratases are metalloenzymes that play a key role in the assimilation of nitrile-bearing compounds by microorganisms.[96] They do this by hydrating the nitrile moiety to the corresponding carboxamide (Scheme 2 5, **A**).[96,97]

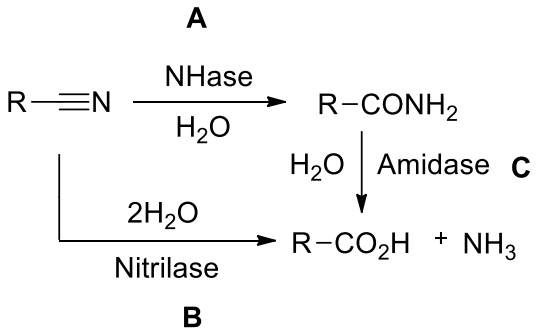

Scheme 25: Enzyme catalysed hydration of nitrile-bearing compounds.

Since the successful application of NHase in conversion of acrylonitrile **68** to acrylamide **69** (Scheme 26)[98] on an industrial scale, there has been a growing interest in the use NHase, particularly in hydration of various nitrile-bearing compounds.[97]

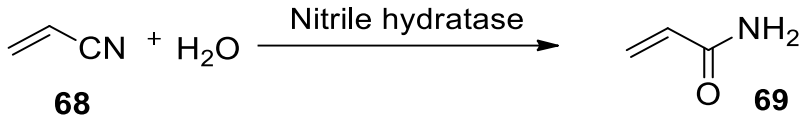

Scheme 26: Industrial production of acrylamide from acrylonitrile using biocatalysis.

NHases are water soluble metalloenzymes that contain a non-heme Fe (III) or a non-corrin Co (III) ion at the enzyme catalytic site. Both the Co NHase and the Fe NHase have been shown to exhibit an aptitude for hydrating aliphatic nitrile compounds, however, Co NHases have been shown to possess an additional advantage of hydrating aromatic nitrile compounds.[99] NHases are usually isolated from their parent whole cell *Rhodococcus rhodochrous* J1, in an attempt to control the hydration since there are three enzymes that are involved in nitrile hydrolysis found within cells.[99] Nitrile-bearing compounds can be hydrolysed in a two-step fashion by NHases using one water molecule to afford the corresponding amide, which is then followed by another hydrolysis reaction facilitated by amidases, again using one water molecule, yielding the corresponding carboxylic acid and ammonia (Scheme 25 **A** + **C**). Nitrilases on the other hand, can hydrolyse nitriles in one step using 2 water molecules affording the expected carboxylic acid together with an ammonia molecule (Scheme 25, **B**).[96]

It is important to note that the hydrolysis of nitrile-bearing compounds using conventional synthetic chemistry is a facile reaction. Nitriles can be converted to their carboxamide analogues using the classic acid or base catalysed hydrolysis method.

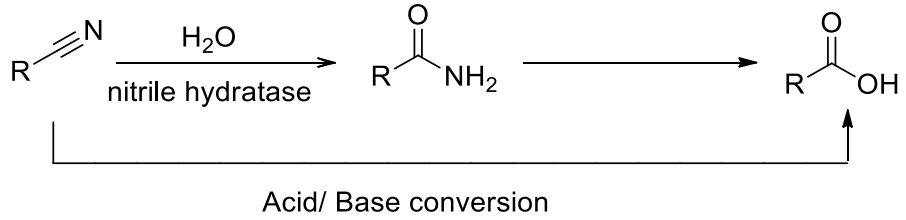

Scheme 27: Acid/base catalysed hydrolysis of nitriles contrasted with NHase catalysed hydrolysis.

However, the gravitation towards biocatalysis, particularly the use of NHase enzymes stems from the fact that it is difficult to control the reaction under acid/base conditions since nitriles

easily convert to the carboxylic acid, which becomes a problem if the desired product is the carboxamide (Scheme 27).[99] Because Nitrile hydratases can be isolated from their whole cell parent and have demonstrated a remarkable ability to hydrate nitriles only to the amide derivative under much milder conditions, they have easily become the catalyst of choice for the hydrolysis of nitrile-bearing compounds to amides.

1.4 Project aims and objectives

The continued prevalence and persistence of schistosomiasis and tuberculosis has necessitated a continual effort to wage a war against these ailments, through the design of new chemotherapies and the improvement of the methods for the preparation of existing ones. As already discussed thus far, existing methods have been reported to make use of toxic starting materials and harsh reaction conditions [40] and the vast majority of the methods, if not all, produce PZQ as a racemate, where one isomer is associated with side effects and contributes to patient non-compliance.[30] The same can be said about isoniazid, whose method of synthesis industrially, remains largely reliant on classical alkali and alkaline metal catalysts such as NaOH or MgO at elevated temperatures, rendering the synthetic method hazardous, energy intensive and expensive.[100]

The aim of this study was to develop greener routes towards the efficient synthesis of existing anti-tubercular and anti-schistosomal compounds. With the use of biocatalysts, the broader research is anticipated to reveal methods of obtaining enantiopure praziquantel (PZQ) and a new biocatalytic route of obtaining isoniazid (INH). To achieve the said goals, it is necessary to synthesize PZQ and INH intermediates that are amenable to lipase and nitrile hydratase enzyme reactions, respectively.

1.4.1 Planned synthetic approaches: PZQ intermediate

Based on the literature discussed in section **1.3.1** on the use of lipases for chemical transformations, it is understood that the substrates amenable to lipase reactions are usually esters, amines, and carboxylic acids. Depending on the conditions, the transformations under the influence of lipases would then be tailored to form esters, carboxylic acids, amines, and amides in their enantiopure form, as shown in Schemes 22, 23, and 24. The approach taken in choosing the best way to prepare the desired intermediates was informed by the importance of having functional groups that were compatible with lipase chemistry. It is the inclusion of these functional groups that dictated the type of intermediates that ought to be prepared.

What followed next involved retrosynthesis of PZQ (**1**), in pursuit of identifying intermediates that would be amenable to enzyme resolution. [101]Looking at the retrosynthetic scheme presented in Scheme 28, we found that the best place to start from was the isoquinoline core, particularly alkyl 1,2,3,4-tetrahydroisoquinoline-1-carboxylates **71** and **72**. These compounds contain two functional groups that are amenable to lipase enzyme reactions, and the prospects of success have been demonstrated by Sanchez *et al.*[94] and Katayama *et al.*[95] when they used lipases for the resolution of closely related isoquinoline **65** and quinoline **66** scaffolds shown in Schemes 23 and 24.

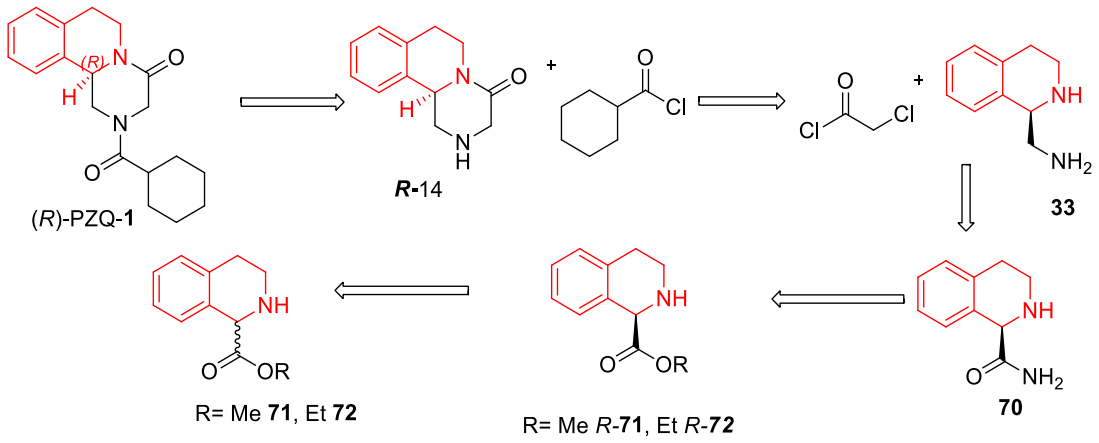

Scheme 28: Retrosynthetic analysis of praziquantel (PZQ).

1.4.1.1 First synthetic strategy

The idea behind the first strategy was centred around finding a reaction protocol that would lead to fewer reaction steps, less waste, mild conditions and allowed for ease of set-up. The Ugi multicomponent reaction fits the reaction profile that was sought after, particularly for the facile synthesis of tetrahydroisoquinoline scaffolds.

Generally, the reaction requires a combination of four reactants in one pot, dissolved in a solvent, and stirred at ambient temperature overnight. It is possible to reduce the reaction to three reactants; effectively, if the imine is pre-generated, it represents two components in one, and this makes it possible to achieve the Ugi reaction using only three components. What would follow next would be the extraction and purification using chromatographic techniques. In this strategy, two Ugi-MCR reactions would be set-up. The first one would comprise of a one pot reaction between tetrahydroisoquinoline **49**, benzoic acid **73**, and cyclohexyl isocyanide **74a**. The second one would be set up under the same conditions, only that the isocyanide source will be *tert*-butyl isocyanide **74b**. Following the successful synthesis of the Ugi products **76a-b**, a hydrolysis reaction giving tetrahydroisoquinoline-1-carboxylic acid **77** would be

necessary, followed by an esterification reaction to obtain the desired racemic ester analogues **71** and **72** (Scheme 29).

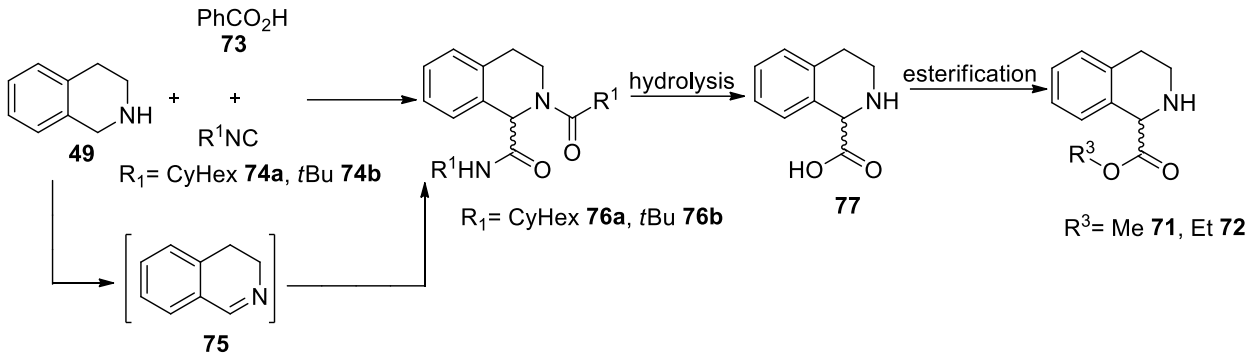

Scheme 29: Envisaged first synthetic strategy for accessing tetrahydroisoquinolines.

1.4.1.2 Second and third synthetic strategy

The conception of the second and third synthetic strategies required careful consideration of other methods that could be exploited to fabricate PZQ intermediates. The answers came from disassembling the structure in question in various positions and trying to put it back together again using retrosynthetic techniques. Using this technique on the PZQ intermediate has presented some interesting insight; a closer look at the retrosynthetic scheme shown below (Scheme 30), reveals that another method of arriving at the said intermediates **71,** and **72** involves the hydrogenation of a commercially available isoquinoline-1-carboxylic acid **78** to the partially saturated analogue **77**.

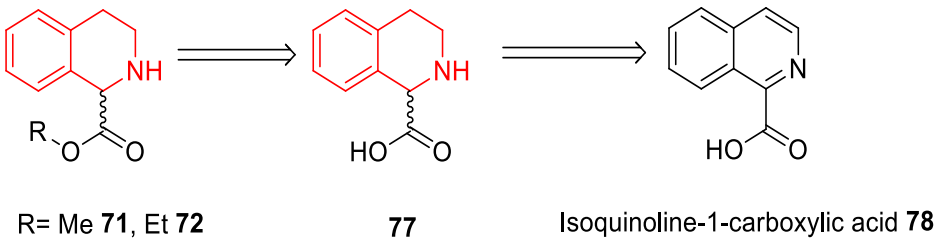

Scheme 30: Retrosynthesis of PZQ intermediate.

For this transformation, two variations are possible. One is to begin with the partial hydrogenation of isoquinoline-1-carboxylic acid **78**, followed by an esterification reaction of the resulting zwitterion **77**. The second variant begins with the esterification of isoquinoline-1-carboxylic acid, followed by hydrogenation of the esterified compound.

1.4.1.3 Fourth strategy

With the use of the Bischler–Napieralski reaction, it is possible to access tetrahydroisoquinoline scaffolds using commercially available starting materials. The following reactions would be set up to produce 3,4 dihydroisoquinoline derivatives **82a-c**, which would be partially hydrogenated and demethylated to unlock hydroxy tetrahydrosioquinoline carboxylates **84a-c**. This alternative route may prove to be beneficial because it may circumvent the need of the esterification reactions described in the first three strategies. Phenethylamine analogues **79a-c** would be reacted with diethyl oxalate **80** to yield corresponding phenethyl amide derivatives **81a-c**. The rationale behind choosing phenethylamines with methoxy groups was informed by the evidence from literature that suggests that the cyclisation reaction occurs more readily when there are electron rich substituents on the ring.[101] These resulting compounds would then be subjected to Bischler-Napieralski reaction conditions to afford **82a-c**, followed by a partial hydrogenation reaction to give **83a-c**. Finally, to see what effects a hydroxy functional group would have on the behaviour of the tetrahydroisoquinoline scaffolds when subjected to lipase enzymes, a demethylation reaction to yield the intermediates **84a-c,** which are effectively hydroxy analogues of the desired intermediate **72**, would be attempted.

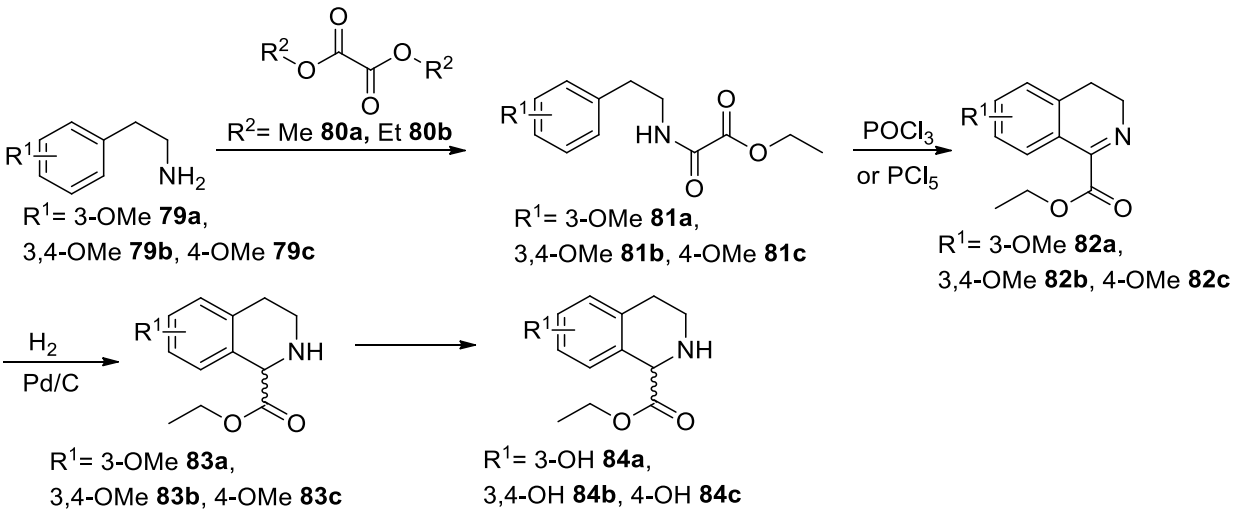

Scheme 31: Bichler- Napieralski reaction used in the fourth synthetic strategy.

1.4.2 Biocatalytic synthesis of isoniazid.

As already mentioned, isoniazid plays a pivotal role in the control and eradication of tuberculosis from its human host. The use of enzymes for the synthesis of INH has not been well covered in literature, particularly the use of nitrile hydratase as an enzyme of choice. There

is adequate literature precedent on the use of nitrile hydratase for the hydrolysis of cyanide bearing compounds to their corresponding amides. [96,97]

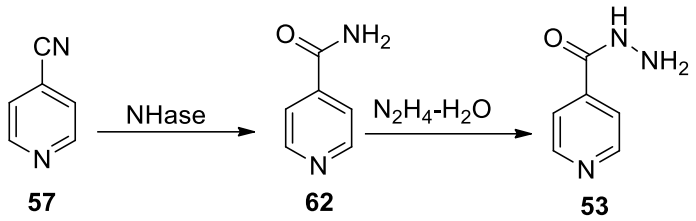

57 **62** **53**

Scheme 32 : Proposed biocatalyic synthetisis of Isoniazid **53**.

Because 4-cyanopyriddine **57** can be used as an INH starting material and it contains a cyanide group, we hypothesized that it could be amenable to nitrile hydratase hydrolysis. Therefore, the proposed reaction is detailed in Scheme 32, where nitrile hydratase would hydrolyse the cyanide group of **57** to its amide analogue **62**, followed by the use of hydrazine hydrate to obtain INH **53**.

Chapter 2: Results and discussion

The project was aimed at developing green routes for the efficient synthesis of known anti-schistosomal and anti-TB compounds. As such, it was envisaged that this body of work should reveal methods of preparing isoniazid (INH) and enantiopure praziquantel (*R*-PZQ) using enzyme catalysis as a key step. To achieve the said goals, it was necessary to synthesize PZQ and INH intermediates. The intermediate synthesis was of vital importance since it formed the basis of the biocatalysis performed in this project. As will be shown herein, the PZQ intermediates were subjected to lipase enzymes. The choice of the enzyme class used was based on the versatility of lipase enzymes and what has been reported in the literature. The same logic was adopted for the INH intermediate when choosing the enzyme class to utilize for this synthesis.

2.1 Towards the synthesis of PZQ

As previously mentioned in section **1.4.1**, the synthesis of enantiopure PZQ was designed and constructed such that it incorporated enzyme catalysis, which will play a pivotal role in selectively hydrolysing and/or acylating one enantiomer over the other. However, the synthesis of the intermediates precedes the enzyme reactions. The required intermediates were accessed using the synthetic strategies discussed below.

2.1.1 First synthetic strategy

Various synthetic strategies were applied towards the synthesis of alkyl 1,2,3,4-tetrahydroisoquinoline-1-carboxylate intermediates **71** and **72** for the final synthesis of the *R*-enantiomer of praziquantel. The strategies chosen were those that made use of synthetic protocols that were as green as possible, to align with the overall aim of the project. The first practical choice adopted was drawn from the multicomponent reactions. The overwhelming interest in MCRs stretches beyond the fact that their reactions are generally green; the interest also stems from the importance of the synthesized products, which have been shown to exhibit bio-active properties such as anti-bacterial, antioxidant, anti-microbial, anti-HIV, and anti-inflammatory activities.[102] It is for these reasons that MCRs were chosen and these reactions have become a vital tool in the arsenal of the organic chemist.

This type of reaction finds precedent in Ngouansavanh *et al.* [103], when they prepared tetrahydroisoquinoline carboxamides **76a-b** using benzoic acid **73**, tetrahydroisoquinoline **49**, and isocyanides **74a-b**. As mentioned in section **1.4.1.1,** to reduce the reaction to three

components, an imine would be required, and in this instance, Ngouansavanh and co-workers cleverly formed the imine **75** *in-situ* using iodoxybenzoic acid **86,** as shown in *Scheme 33*.

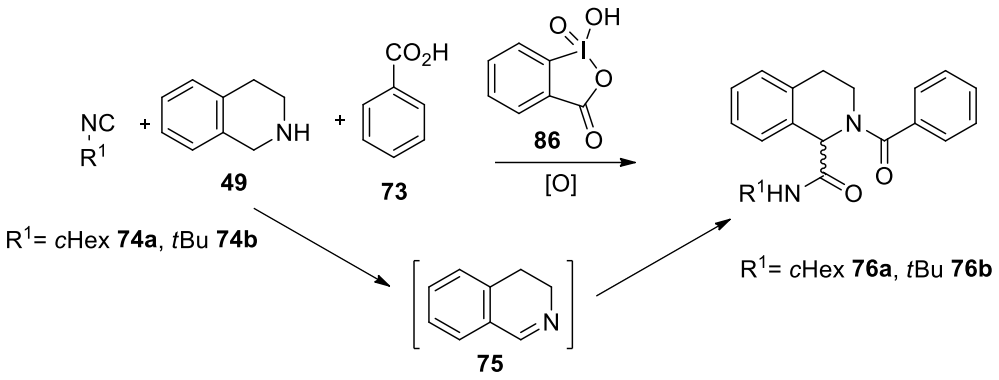

Scheme 33: One-pot Ugi reaction via oxidation of cyclic amine reported by Ngouansavanh *et al.* [103]

Notable from the mechanistic studies of the Ugi-4CR and Ngouansavanh and co-workers' work, is the revelation that the reaction goes through an imine intermediate, as shown in Scheme 10 (Section 1.1.8.1), and Scheme 33. With this insight, it was envisaged that it should be possible to obtain the tetrahydroisoquinolines from an imine**,** a carboxylic acid, and an isocyanide in a 3-component Ugi reaction. This important piece of mechanistic knowledge has also inspired ways to further optimise the Ugi-MCR via an *in-situ* oxidation of cyclic amines to form the corresponding imines using mild oxidants.[103] Equipped with this knowledge, now one is presented with two feasible routes towards the formation of Ugi products. The importance of understanding how the Ugi reaction works, and the conditions thereof, finds relevance in this project in that tetrahydroisoquinolines form a class of compounds that can be prepared using the Ugi protocol. This means that, using the Ugi reaction, we would be able to access tetrahydroisoquinolines **76a-b** from reagents **49**, **73,** and **74a-b** shown in Scheme 29 (Section 1.4.1.1), which are typical Ugi starting materials.

During the course of this research, we have learned that to readily access the Ugi products that are of interest to us, we needed to pre-form the imine **75**. The amine **49** starting material for this transformation was available in our labs, and therefore we required an oxidant. The choice of the oxidant used was informed by Ngouansavanh *et al.* when they reported the use of iodoxybenzoic acid (IBX) **86** as a mild oxidant for the *in-situ* oxidative Ugi-type multicomponent reactions.[103]

Prior to the Ugi-MCR setup, the IBX **86** was prepared by slowly adding potassium bromate to a rigorously stirred solution of 2-iodobenzoic acid **85** in sulfuric acid (Scheme 34).[104] Upon completion of the reaction, the product **85** recovered was a white crystalline compound in 65% yield. The white crystalline solid **86** was characterized using ^{1}H NMR spectroscopy. The analysis of the ^{1}H NMR spectrum of the synthesized IBX **86** showed four peaks in the aromatic region between 8.15-7.82 ppm, integrating for a total of 4 protons with typical aromatic coupling constants of 7-8 Hz, which was expected since IBX has 4 aromatic protons.

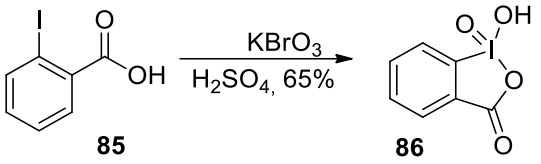

Scheme 34: Iodoxybenzoic acid synthesis conditions.

The ^{13}C NMR spectrum had 7 signals, 6 of which were of aromatic nature, ranging from 147.0 ppm to 125.5 ppm. The signal at 168.0 ppm was that of the carbonyl carbon. Similar NMR spectra were obtained by Fallis *et al.* [104] when they synthesised **85**; their aromatic ^{1}H signals ranged from 8.15 to 7.84 ppm. Their carbon spectrum had 6 aromatic signals ranging from 146.6 to 125.0 ppm and the carbonyl signal appeared at 167.5 ppm. These spectral similarities confirmed the successful synthesis of **86**.

[104]Following the successful synthesis of IBX **86**, the first one pot Ugi-type reaction was set up. The choice of starting materials for the synthesis of the Ugi products finds precedent in Ngouansavanh and co-workers when they synthesized a series of carboxamides, including **76a** and **76b** in quantitative yields using iodoxybenzoic acid **86,** tetrahydroisoquinoline **49,** benzoic acid **73** and either cyclohexyl isocyanide **74a** or *tert*-butyl isocyanide **74b** in THF (Scheme 33).[103] The successful formation of the carboxamides meant they were able to perform the oxidation of **49** to **75** *in situ* and it was from this success that the project drew inspiration to synthesize the first class of tetrahydroisoquinoline derivatives.

The Ugi reaction conditions were replicated using the same set of reagents as reported by Ngouansavanh *et al.* [103] Two separate reactions were set up using iodoxybenzoic acid (IBX) **86** as the amine oxidant, the cyclic amine 1,2,3,4-tetrahydroisoquinoline **49**, benzoic acid **73**, and cyclohexyl isocyanide **74a** in one vessel and *tert*-butyl isocyanide **74b** in another reaction vessel to obtain carboxamides **76a** and **76b** respectively.

However, the results obtained did not point to the successful formation of the desired Ugi products (Scheme 35). The ^{1}H NMR spectral data did not match what was expected for the products since the required signals were missing. This meant that the IBX mediated synthesis of both **76a** and **76b** did not yield the expected results. This could have been a consequence of the dismal solubility of IBX in DMF. Moreover, the handling and storage of IBX posed a risk; IBX is moisture sensitive and explosive under impact or temperatures above 200 °C.[104]

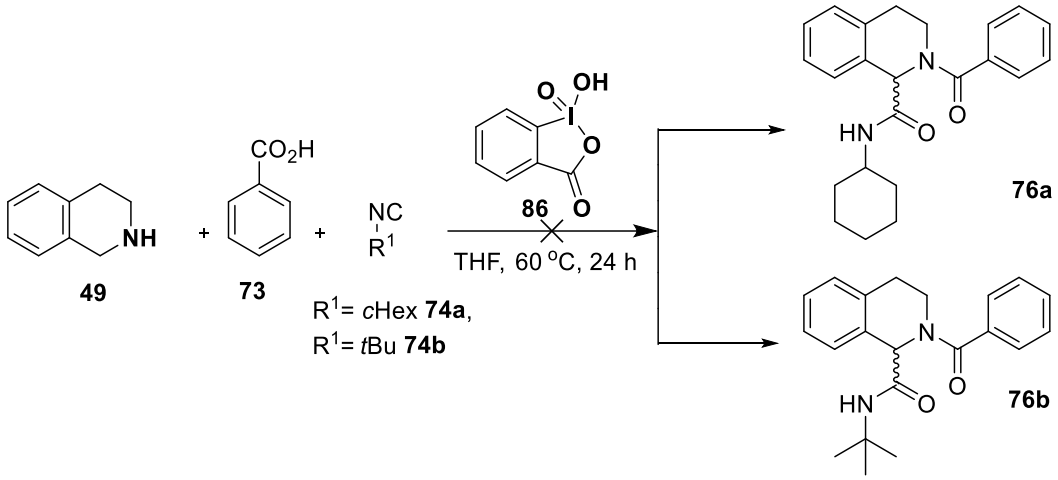

Scheme 35: Unsuccessful one-pot Ugi reaction via oxidation of cyclic amine.

Contrary to what Ngouansavanh and co-workers did, the alternative option explored was to prepare the required imine *ex situ*. 1,2-Dihydroisoquinoline **75** was obtained through the oxidation of 1,2,3,4- tetrahydroisoquinoline **49** using *N*-bromosuccinimide (NBS) **87** and sodium hydroxide in dichloromethane, at room temperature for 30 minutes, giving the target compound over 70% yield (Scheme 36). This method was adopted from Shi *et al* when they prepared **75** in 92% yield.[105]

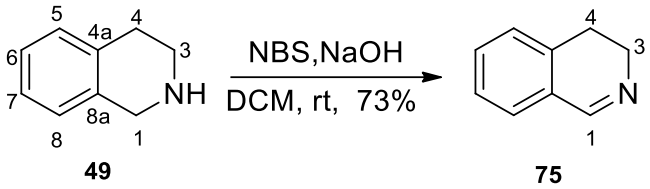

Scheme 36: Oxidation of a cyclic amine to yield the corresponding imine.

Very little knowledge exists in literature as to how exactly NBS **87** oxidises the cyclic amine **49.** A feasible postulation for the formation of **75** is that the reaction begins with the homolytic cleavage of the N-Br bond of NBS **87**, forming a Br radical. The formed radical from the

succinimide moiety is stabilized through two resonance structures shown in Scheme 37, which aids in initiating the homolysis of the N-Br bond.

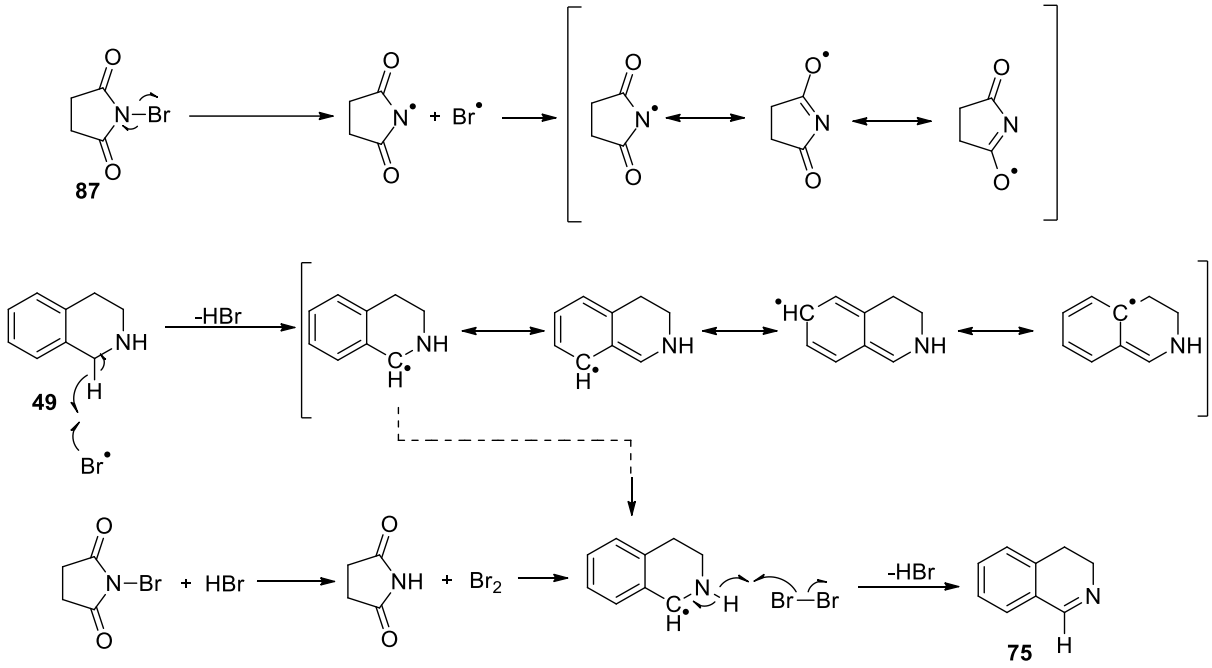

Scheme 37: Proposed mechanism for the oxidation of the cyclic amine to the corresponding imine **75**.

The Br radical goes on to extract an benzylic hydrogen atom in the α-position relative to the N atom, thereby forming another radical that is stabilized by the tetrahydroisoquinoline benzene ring. HBr is formed through the allylic hydrogen extraction, which later reacts with NBS, forming small amounts of Br_2. The formed Br_2 extracts the amine hydrogen, thereby forming a new bond between the amine and the α-carbon (C-1), qualifying the newly formed compound as an imine **75**. This postulation finds precedent in literature, particularly in the work of Potter *et al.*[106] when they managed to form tetrahydroquinoline amide substituted phenyl pyrazoles using NBS as an oxidant. The resulting solution matured to a brown colour, indicating either the formation of hydrobromic acid or the evolution of bromine gas. This was suggestive of the decomposition of *N*-bromosuccinimide as the reaction progressed to form the desired imine.

Looking at the stacked NMR spectra presented below, the starting material, tetrahydroisoquinoline **49**, shown in the red ^{1}H NMR spectrum had all the typical textbook aromatic and aliphatic peaks. What was notable was the peak at about 4 ppm (Fig. 30). This peak integrated for two protons and was a singlet by virtue of having no neighbouring protons. This peak played a pivotal role in giving experimental evidence that supported the theory that predicted the protons at position 1 (H-1) should be more deshielded than those at position 3

(H-3), even though they are both in the α-position relative to the nitrogen atom. Protons with increased electron density tend to be more shielded, appearing upfield. The opposite is true for deshielded protons, as they tend to appear downfield.

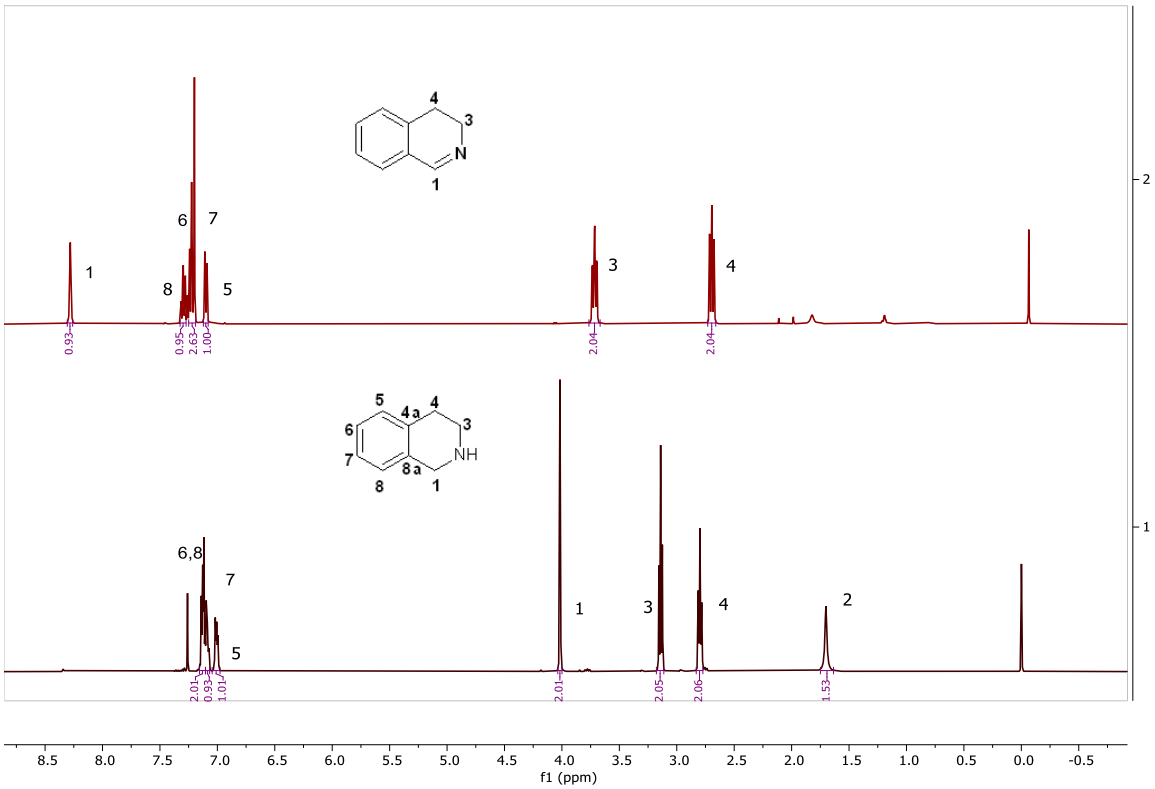

Figure 30: Stacked ^{1}H NMR spectra of cyclic amine **49** below and the corresponding imine **75** above.

The deshielding effect observed for the protons at C-1 relative to C-3 was a consequence of C-1 protons being nestled between two electron-withdrawing groups, namely the nitrogen atom and the phenyl ring. Additionally, the resulting radical at position 1 is at a benzylic position, which is afforded additional stability through delocalisation of the electron charge onto the phenyl ring. It is this hydrogen at C-1 that gets pulled from the amine **49** by the Br radical to form the imine **75**. The ^{1}H NMR peak appearing at about 4 ppm was also used to track changes in the oxidation reaction since it should disappear on conversion to the imine and be replaced by a far more deshielded proton peak, signalling an imine proton that usually appears in the region of aldehyde proton signals. Indeed, the expected signal was observed at about 8.2 ppm (H-1), thus representing the successful formation of the desired imine **75** shown in the blue ^{1}H NMR spectrum (Fig. 30). Lastly, the imine signal from the ^{13}C NMR spectrum appeared at 160.4 ppm. The NMR data discussed here shared similarities to that reported by Pena-Lopez *et al.*[107]: the proton peak at 8.28 ppm shown in the red spectrum in Fig. 30 corresponded to

their peak that appeared at 8.34 ppm. The imine signal from their ^{13}C NMR spectrum appeared at 160.5 ppm. From the IR spectrum, the imine (C=N) IR stretch appeared at 1625 cm^{-1}, thus confirming the successful formation of imine **75**.

Following the successful oxidation of tetrahydroisoquinoline **49** to 1,2 dihydroisoquinoline **75**, this compound was reacted together with benzoic acid **73** and either cyclohexyl isocyanide **74a** or *tert*-butyl isocyanide **74b** in methanol at room temperature overnight,[108] yielding carboxamide **76a** and **76b** in 78% and 83% yield, respectively (Scheme 38). The two carboxamides were characterized using NMR and IR spectroscopy. NMR analyses of both **76a** and **76b** point to the successful formation of the desired carboxamides; the *tert*-butyl carboxamide **76b** ^{1}H NMR spectrum had a characteristic peak at 1.39 ppm, appearing as a singlet and integrating for nine protons, which was expected since the 3 methyl groups of the *tert*-butyl moiety are in the same chemical environment.

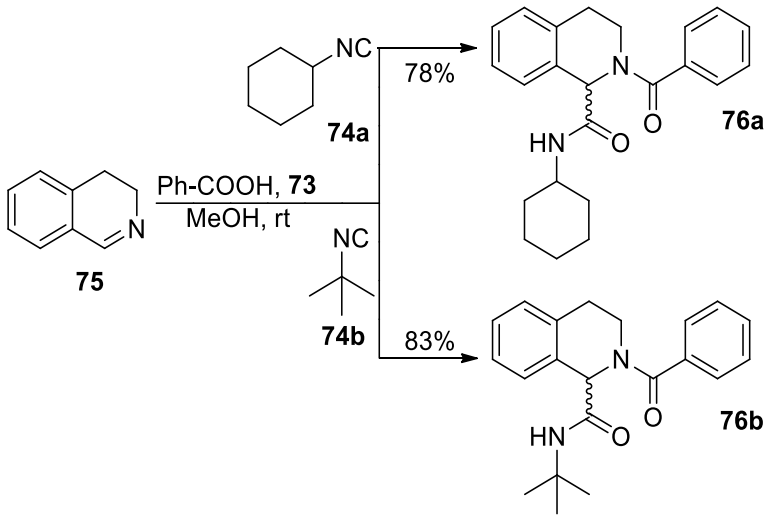

Scheme 38: Successful Ugi reaction.

The ^{13}C NMR spectrum had the expected two new carbonyl carbon signals at 171.5 ppm and 169.5 ppm assigned to the two amide functional groups. Another notable signal from the *tert*-butyl carboxamide **76b** was the ^{1}H NMR singlet signal at 5.96 ppm, which is the proton attached to the stereogenic centre. This spectrum replaced the imine proton (Fig. 30, blue spectrum signal 7), which confirmed the formation of a new species or rather a new covalent bond between the isocyanide moiety and the isoquinoline core.

From the IR spectrum, the amide (N-H) stretch was found at 3321 cm^{-1}, which substantiated the successful grafting of *tert*-butyl isocyanide **74b** onto the imine 3,4-dihydroisoquinoline **75**. Similar NMR signals were observed from the work reported by Ngouansavanh *et al.*[103]; the

signals at 1.39 ppm corresponding to the *tert*-butyl moiety corresponded to theirs that appeared at 1.38 ppm. Their proton attached to the stereogenic centre appeared at 5.97 ppm and their carbonyl carbon signals appeared at 171.4 and 169.5 ppm.

The cyclohexyl carboxamide **76a** ^{1}H NMR spectrum also had a characteristic signal at 6.01 ppm, which suggested that the imine had been consumed to form the desired carboxamide. The aliphatic region contained distorted signals, and this was attributed to the fact that the cyclic alkyl protons are rotationally restricted, therefore positioned at axial and equatorial positions (Scheme 39), appearing in the range between 1.9-1.1 ppm. What was also observed is that the axial and equatorial positions were effectively different chemical environments, which ultimately gave each rotationally restricted proton their own chemical signals. [101] This observation was confirmed with Heteronuclear Single Quantum Coherence (HSQC) which is a 2-dimensional NMR technique that is used to determine the correlation between carbon-proton single bonds. Looking at the HSQC spectrum shown in Fig. 31, particularly in the range between 2.00 ppm and 1.15 ppm, there were two cyclohexyl proton signals (at 1.92 and 1.25 ppm) that shared one cyclohexyl carbon signal at 32.9 ppm. Ordinarily, these two proton nuclei would appear as one ^{1}H NMR signal corresponding to one ^{13}C NMR signal, however, the rotational restriction causes each proton nucleus to have its own unique chemical environment.

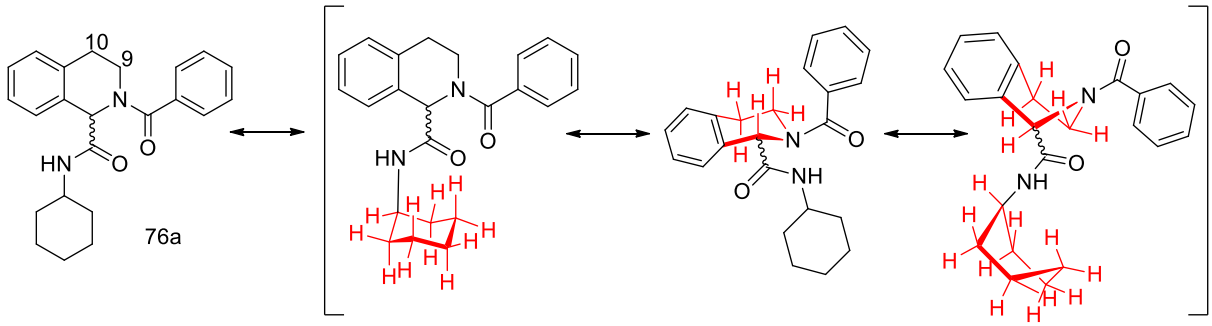

Scheme 39: Possible structural conformations of cyclohexyl carboxamide **76a**.

The two aliphatic proton signals **9** and **10** shown in Scheme 39 were shifted by 1-2 ppm downfield, appearing 2.8-3.8ppm, and this was a consequence of the neighbouring cyclic amide functional group and the phenyl ring pulling the electron density away from aliphatic sites. What was also observed was the new amide carbon signals at 171.8 ppm and 169.5 ppm. The IR frequencies generated from **76a** had the expected amide (N-H) stretch of 3292 cm^{-1}, and the carbonyl (C=O) stretch of 1650 cm^{-1}.

The data under discussion here shared similarities to that discussed by Ngouansavanh *et al.*[103]; their ^{1}H NMR cyclohexyl peaks appeared between 1.94-1.22 ppm. Their proton attached to the

stereogenic centre appeared at 6.01 ppm and their carbonyl carbon signals appeared at 172.2 and 169.2 ppm.

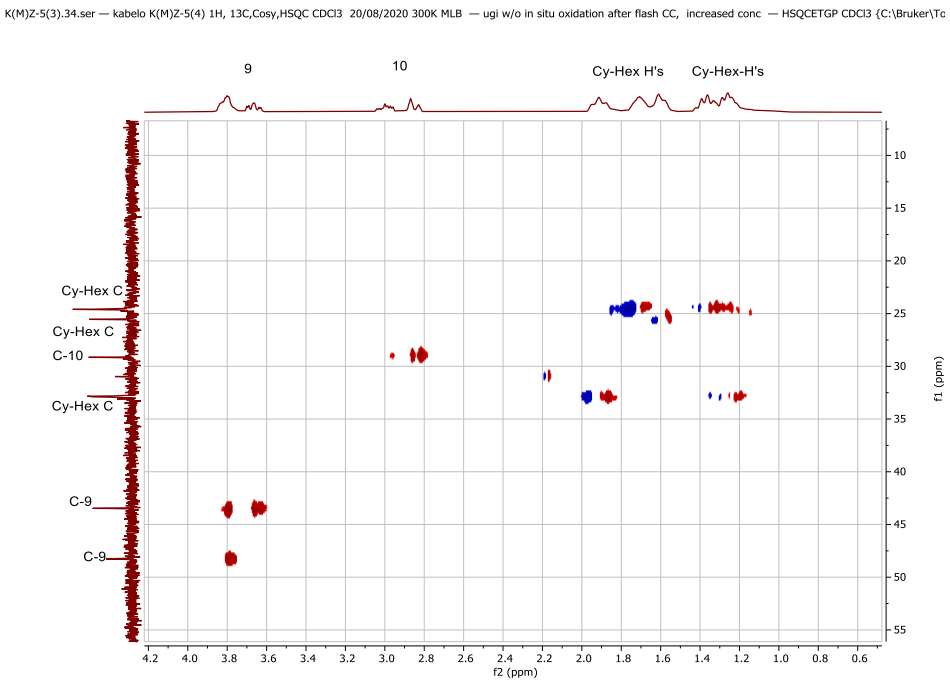

Figure 31: The aliphatic range of the HSQC spectrum of **76a**.

The preparation of the PZQ intermediate using the preceding synthetic strategy required the hydrolysis of the carboxamides formed from the Ugi reaction. The hydrolysis would then cleave both amides generated from the carboxylic acid and the isocyanide moieties. This meant that the resulting fragments of the hydrolysis reaction should be stable enough to exist on their own, thus increasing the likelihood of a successful hydrolysis. It is this realization that informed the type of isocyanides and alcohol used. The hydrolysis of amides under acid conditions results in carboxylic acids and ammonium/amine salts (Scheme 40).[109] The ease of hydrolysis is dependent on the type of amines and carboxylic acids that results from the hydrolysis; the more stable they are the more likely the hydrolysis will favour the forward reaction. This means that acids with additional stability either from mesomeric or inductive electronic factors will favour the forward reaction of hydrolysis. The same can be said about the resulting amines; those that possess additional stability by virtue of being conjoined to functional groups that offer chemical stability such as alkyl groups or unsaturated carbons with delocalisable electrons will favour the forward reaction of hydrolysis.[109]

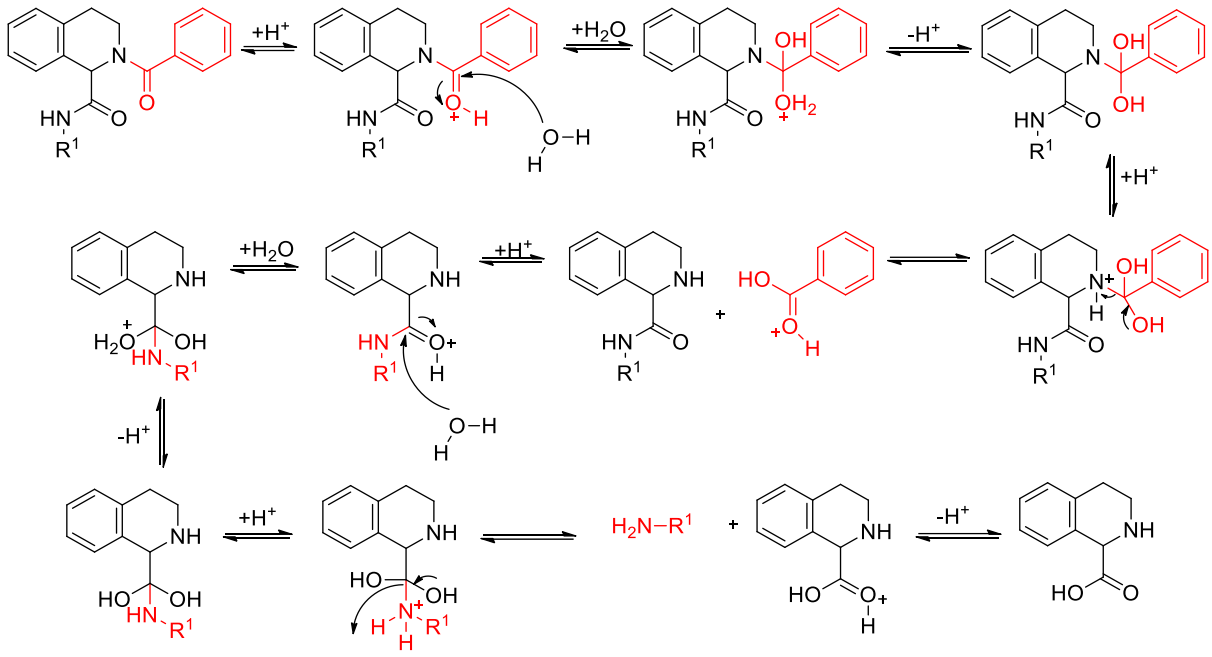

Scheme 40: Hydrolysis of 2 amide bonds from an Ugi-3C carboxamide

With this in mind, it becomes intuitive that when one sets up an Ugi reaction, one would synthesize Ugi adducts with isocyanides and acids whose hydrolysis leads to stable amines and acids upon cleavage with water. In theory, amines with 3 alkyl groups should have the best stability, followed by 2 alkyl groups, then 1 alkyl group. Similarly, α-unsaturated acids would be afforded more stability through conjugation when contrasted with α-alkylated acids which would only be stabilised inductively. This was the rationale for choosing cyclohexyl isocyanide **74a**, *tert*-butyl isocyanide **74b** and benzoic acid **73** as Ugi starting materials.

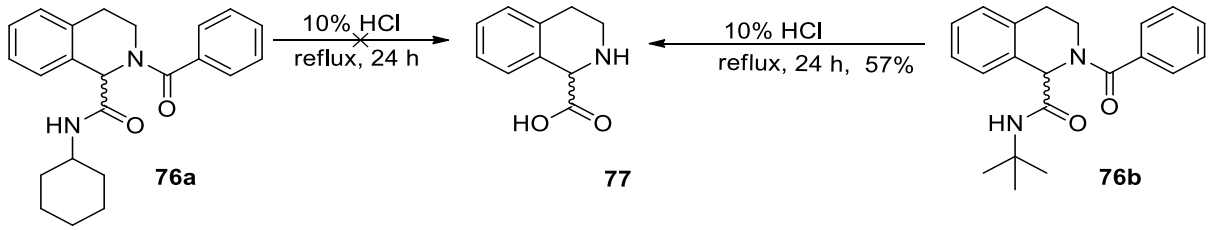

Scheme 41: Hydrolysis of Ugi products **76a** and **76b**.

The hydrolysis reaction of the Ugi products **76a** and **76b** was attempted using 10% hydrochloric acid under reflux for 24 hours (Scheme 41).[108] ^{1}H and ^{13}C NMR analyses of the hydrolysis reaction products revealed that only the *tert*-butyl carboxamide **76b** hydrolysed to the corresponding 1,2,3,4-tetrahydroisoquinoline-1-carboxylic acid **77**, in 57% conversion. The ^{1}H NMR spectrum contained 4 aromatic signals ranging from 7.38 ppm to 7.15 ppm. The 2 CH_2 signals appeared at 3.52-3.28 ppm and 2.95 ppm integrating for 2 protons each. Because

the spectrum was run in D_2O, the OH proton most likely exchanged with deuterium hence it did not appear in the spectrum. The ^{13}C NMR spectrum had 6 aromatic carbon signals between 131.7-126.9 ppm and the carbonyl peak appeared at 171.9 ppm. The work published by Schuster *et al.*[108] on the synthesis of 1,2,3,4-tetrahydroisoquinoline-1-carboxylic acid derivatives via Ugi reactions formed the basis from which the hydrolysis of **76a** and **76b** were attempted. One of their hydrolysis products that they were able to isolate included **77** whose proton and carbon spectra are used in this work for spectral comparison. Upon inspection of their hydrolysis product, it was observed that their aromatic protons appeared between 7.28-7.55 ppm. The 2 -CH_2 appeared at 3.10 ppm and 3.50-3.66 ppm integrating for two protons each. The reason for the slight variations relative to what was obtained for **77** was that they isolated the compound as a hydrochloride salt. The ^{13}C NMR spectrum had 6 aromatic signals between 132.2-126.6 ppm which share close similarity to those obtained from **77**. Their carbonyl peak appeared at 170.7 ppm while that of **77** was at 171.9 ppm. This slight difference is also attributed to the nature of **77** since it was not isolated as a hydrochloride salt.

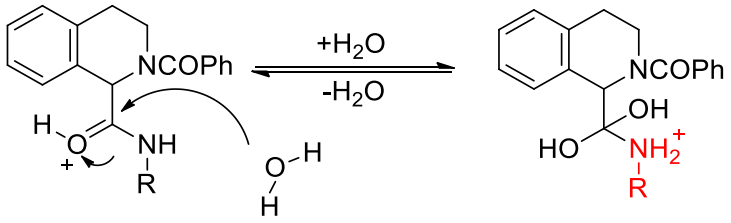

Where R= *tert*-butyl or CyHex

Scheme 42: Mechanistic insight into the hydrolysis of Ugi reaction products.

The preferential hydrolysis of the *tert*-butylcarboxamide **76b** over cyclohexylcarboxamide **76a** under the same set of conditions can be rationalized by looking at the relative stability of the ammonium ions that are formed during the hydrolysis (Scheme 42). Alkyl groups are known to be electron donating;[110] thus, the *tert*-butyl ammonium ion had the added advantage of being inductively stabilized by 3 methyl groups whose carbon is attached to the nitrogen shown in red whilst the cyclohexyl ammonium ion was only inductively stabilized by 2 CH_2 groups of the carbon attached to the nitrogen and extending to the cyclohexyl moiety as shown in Scheme 43.

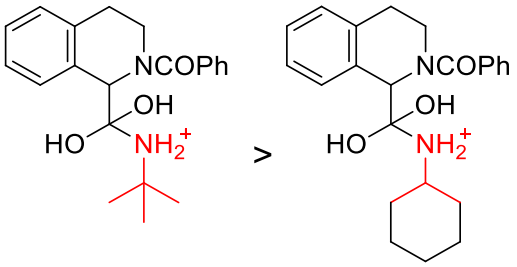

Scheme 43: Chemical stability of ammonium ions formed during amide hydrolysis.

Following the hydrolysis of the *tert*-butylcarboxamide analogue **76b**, we were one step closer to realising the desired PZQ intermediates **71** and **72**. The esterification of compound **77** to either a methyl ester analogue **71** or ethyl ester analogue **72** would mean that the compounds would now be amenable to enzymatic hydrolysis, and so emphasizing the importance of a successful preparation of the ester analogues.

The esterification of the now hydrolysed Ugi compound **77** was important for the project, given that it would later be the subject of enzymatic hydrolysis. The esterification reaction of **77** has previously been demonstrated by Paal *et al.* using thionyl chloride.[111] The reaction is believed to proceed through an *in-situ* formation of hydrochloric acid from thionyl chloride and ethanol, which then catalyses the formation of the ester **72** shown in Scheme 44. In our hands the reaction was successful, however the yields were disappointingly low, only reaching a maximum of 17% (Scheme 45).

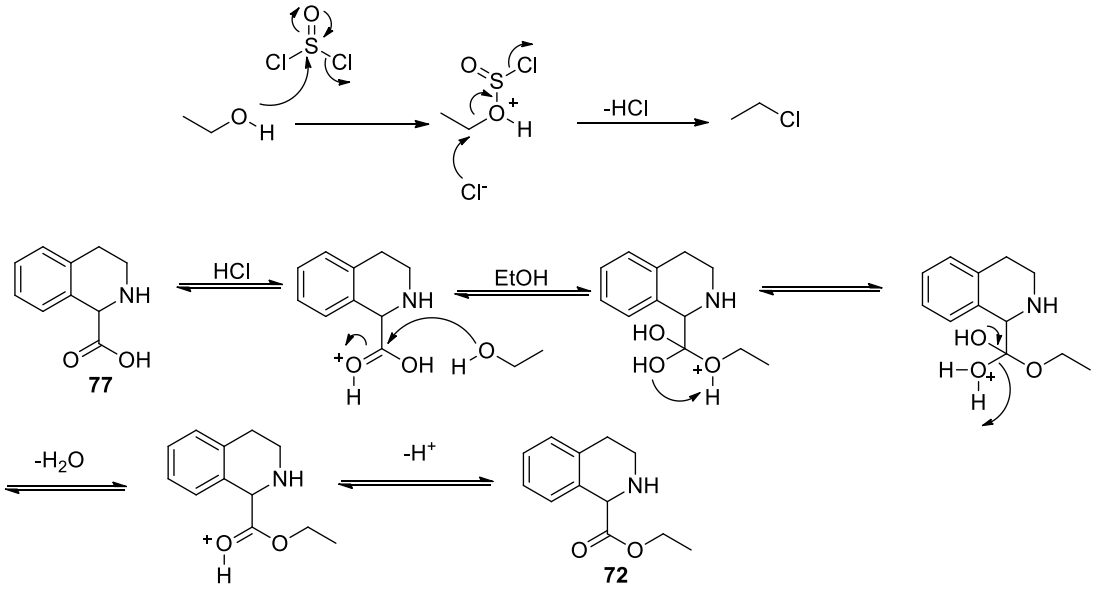

Scheme 44: Reaction mechanism for the esterification of **72**

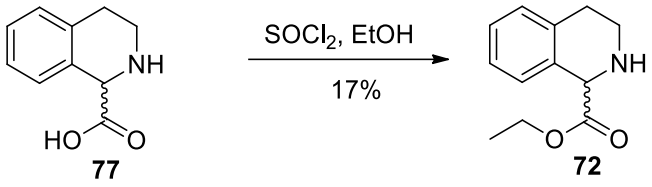

Scheme 45: Esterification of acid **77** using thionyl chloride in ethanol

The low yields recovered from the esterification reaction presented an impediment to the progress of the project. It is unclear what could have contributed to the diminished yield; however, the only explanation was that there could have been side reactions that were in competition with the desired reaction. Possible side reactions that could have taken place include the decomposition of thionyl chloride in the presence of water (**A**), the reaction of thionyl chloride with the cyclic amine instead of the carboxylic acid (**B**), or the *in-situ* hydrolysis of the newly formed ester (**C**) (Scheme 46).

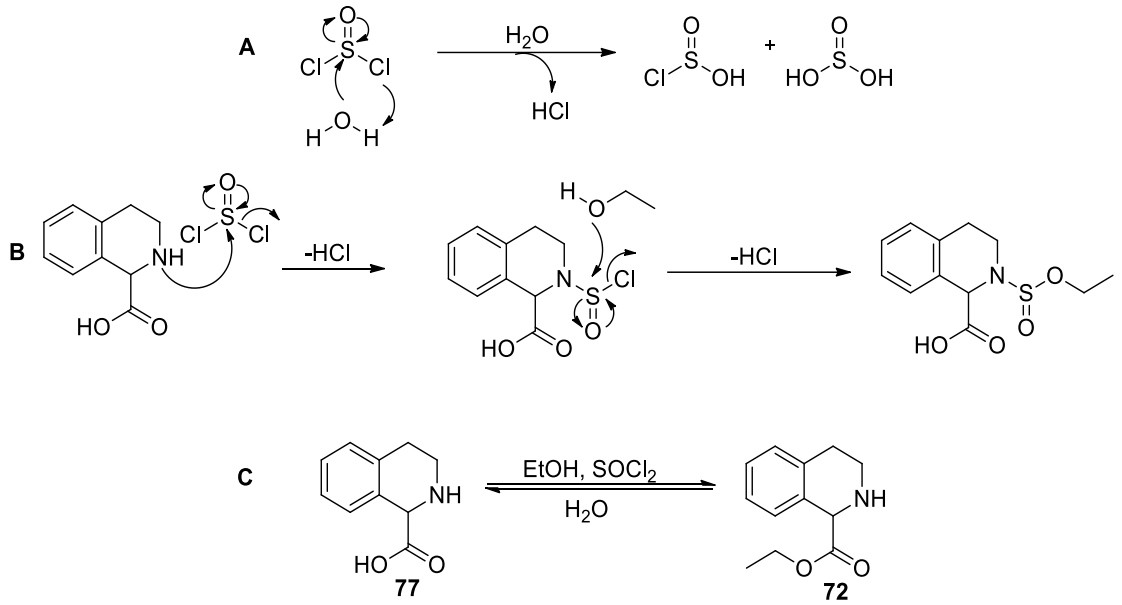

Scheme 46: Possible side reactions that are in competition with the desired esterification reaction.

A close inspection of the side reactions hypothesized in Scheme 46 revealed that the first two side reactions generate HCl *in situ***.** As such, the reaction should have still proceeded since HCl is a well-known acid catalyst for the esterification of carboxylic acids to acid esters; the acid proton makes OH into a better leaving group.[112] However, the yield generated from all attempts did not exceed 17%. The ^{1}H NMR spectrum of **72** contained 4 aromatic protons between 7.36-7.10 ppm and the 2 CH_2 signals appeared between 3.37-3.01 ppm and 2.90-2.72

ppm each integrating for 2 protons. The two signals that prove the successful synthesis of the ester are the two signals at 4.21-4.14 ppm and 1.30 ppm representing the CH_2 and CH_3 respectively, of the ethyl ester moiety. The amine peak appeared as a singlet at 2.14 ppm. The ^{13}C NMR spectrum had six aromatic proton signals between 135.5-125.8 ppm. The ethyl moiety was represented by two carbon signals at 40.9 ppm for CH_2 and 14.20 for CH_3. The carbonyl signal appeared at 173.1 ppm. For comparative purposes, reference to Forro *et al.*[113] provided spectral data of **72** since it also formed part of their study. Their ^1H NMR spectrum contained 4 aromatic signals between 7.35-7.11ppm which were very similar to those obtained for **72.** The ester CH_3 appeared between 1.28-1.31ppm and the CH_2 at 4.24-4.19 ppm which were also very similar to those of **72**. Lastly, their amine peak appeared at 2.0-2.2 ppm and the value obtained for **72** fell within this range.

An alternative explanation for the low yield could be attributed to the zwitterionic nature of the compound to be esterified. Tetrahydroisoquinoline carboxylic acid **77** has a free base and carboxylic acid. This means that in acidic media, the amine would be protonated (Scheme 47). To make things worse, the carbonyl oxygen is weakly basic when contrasted with the free base.[101] This means the protons are predominantly drawn to the nitrogen atom more than they are attracted by the carbonyl oxygen. Once the amine is protonated, it prevents the protonation of the oxygen, owing to the proximity of two positive charges that would result, thus existing in the same vicinity and de-stabilising the resulting compound. When the amine is protonated, the carbonyl carbon does not get activated enough for the nucleophilic attack by the alcohol. This action impedes the esterification reaction as there is a competition for the acidic protons.

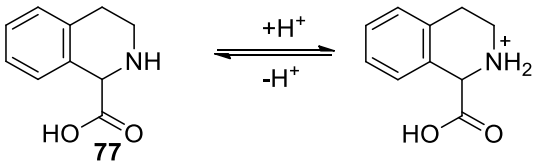

Scheme 47: Competition for acidic proton between free base and carbonyl carbon.

This synthetic strategy was a convenient strategy in that the chemistry has been around for some time, as such it has been sufficiently studied and is well understood. This has made it possible to manipulate and optimize the conditions. One example was the important migration from using IBX *in-situ* to using NBS *ex-situ*, which gave the desired outcome. What was most important was that the chemistry worked, reproducibly. However, the major concern was that the reaction was not atom economical; the nature of the Ugi reaction is such that the resulting compound combines 3 or 4 reactants into one molecule, and any subsequent reaction that seeks

to break the newly formed bonds undermines the whole point of forming these new bonds in the first place. Moreover, the hydrolysed Ugi product bore a free amine and an acid, giving problems associated with transforming zwitterionic species.

2.1.2 Second synthetic strategy

The elegance of synthetic chemistry finds expression in arriving at a desired chemical structure using various strategies. What keeps organic chemists glued to chemical structures is the endless possibilities and multiple chemical conditions that can be exploited to arrive at a particular chemical scaffold. As such, it is always important to go back and examine the chemical scaffolds one may be working on, in the hope of discovering new ways of altering them towards the desired scaffold. The first strategy showed promise and achievability, albeit in low yields and poor atom economy. To circumvent the problems encountered in the first strategy, a second strategy was devised such that it should improve atom economy and chemical yield.

Significant advances made on the hydrogenation of isoquinolines have been minute, however, brilliant examples do exist. In fact, the hydrogenation of isoquinolines is a subject explored mostly in patents and has very little prevalence in open-source literature. What makes the hydrogenation of isoquinolines even more difficult is chirality that is introduced when the pyridine moiety bearing substituents is hydrogenated. Thus, it became important to control the stereochemistry of the resulting tetrahydro derivative. Currently, the asymmetric hydrogenation of isoquinolines reported by Zhou *et al.* is the only such example that exists.[114] They discovered that the addition of chloroformates as activating reagents allowed for the partial hydrolysis of quinolines and isoquinolines using an Iridium complex catalyst $[Ir(COD)Cl]_2$/ (*S*)-SegPhos (**L2**) (Scheme 48).

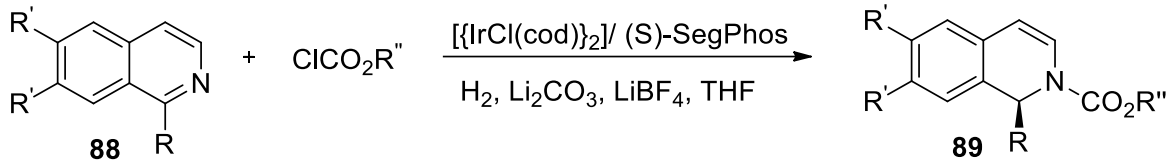

Scheme 48: Partial hydrogenation of isoquinoline derivatives using an Iridium complex.

Even though it was effective, it only managed to hydrogenate isoquinoline derivatives **88** to their dihydroisoquinoline derivatives **89** and required the conditions to be optimized in order to obtain the tetrahydro derivatives **92** and **93** through a reduction reaction using $LiAlH_4$ in THF (Scheme 49).[115]

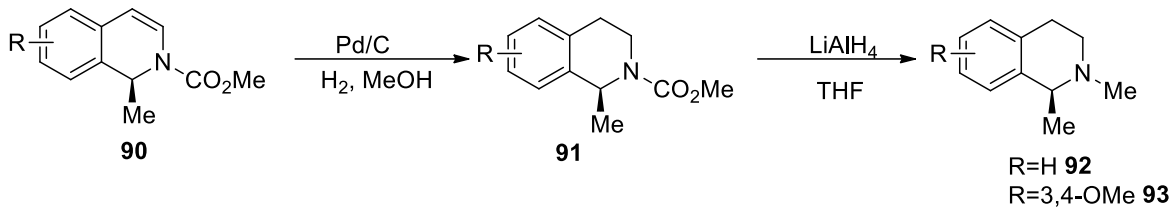

Scheme 49: Optimization of isoquinoline hydrogenation to achieve tetrahydroisoquinoline derivatives.

Given the challenges associated with the asymmetric hydrogenation of isoquinoline to tetrahydroisoquinoline, alternative methods to unlocking the tetrahydro scaffold were sought and feasible methods were explored in this study. Apart from an asymmetric hydrogenation reaction that leads to an enantio-enriched product, it should be theoretically possible to first hydrogenate the pyridine moiety of the isoquinoline scaffold **94** to the racemate **95** and then resolve to the respective enantiomers **96**(*S*) and **96**(*R*) shown in Scheme 49.

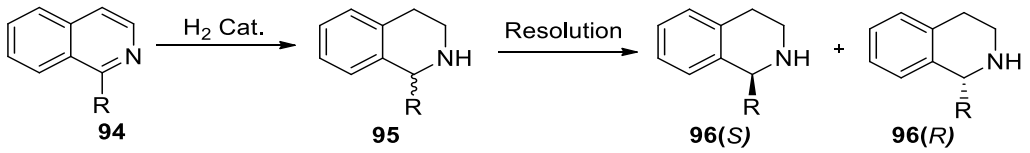

Scheme 49: Symmetric synthesis of tetrahydroisoquinoline derivatives.

Our first attempt towards this transformation involved the use of Pd/C as a catalyst of choice, as this catalyst is famously known for its universality in hydrogenation reactions.[116] Isoquinoline-1-carboxylic acid **78** and 20% Pd/C (wt%) were dissolved in acetic acid and stirred under 7 bars of hydrogen atmosphere, at room temperature for 24 hours (Scheme 50). The resulting mixture was filtered, and the solvent was removed under low pressure. The resulting solid was analysed by ^{1}H NMR spectroscopy and the spectrum obtained did not match that of the expected product **77**, instead, it matched that of the starting material. [116]

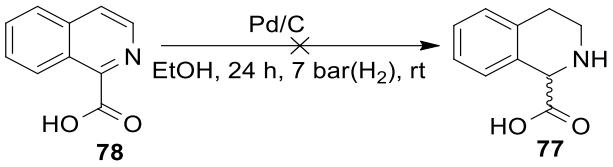

Scheme 50: Attempted hydrogenation of isoquinoline carboxylic acid **78** to **77** using Pd/C.

Looking at the existing literature on the hydrogenation of isoquinoline carboxylic acid, no literature on the hydrogenation of **78** using Pd/C was found. Interestingly, nitrogen-containing compounds have been reported to poison Pd/C, and this may have been the reason why this

transformation had no precedent in literature and the reaction did not yield the desired compound **77**.[115]

The only catalyst in literature, patent literature in particular, that was shown to demonstrate the ability to effect the transformation in question was Pt(IV) oxide (Adam's Catalyst), whose catalytic mechanism is largely enigmatic and unexplored. The only piece of information about Adam's catalyst reported in literature was that, on reduction with hydrogen, the dark-brown catalyst in question becomes highly dispersible black Pt(0), which presumably provided a substantially large surface area for the successful hydrogenation of inert heterocyclic hydrocarbons.[117] Albeit very little knowledge about PtO_2 being reported, the commercially available catalyst was purchased and tested.

As already mentioned, the choice of PtO_2 as the preferred catalyst was based on the difficulty observed when using Pd/C under the same conditions. Moreover, there was no literature on the hydrogenation of **78** using Pd/C. On the contrary, the use PtO_2 as the catalyst particularly suited for this transformation found precedent in literature and patents.[111,118–120] Several variations to catalyst load and pressure were attempted in pursuit of improving the yield of **77** and are shown in Table 1 below.

Table 1: Variation of reaction conditions tested for the hydrogenation of **78** to PZQ intermediate **77**.

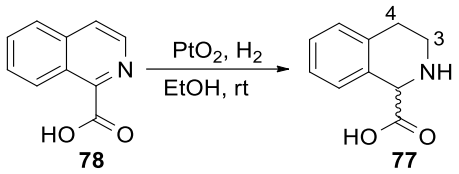

78 **77**

Entry	PtO_2 (wt%)	Reaction time (h)	Pressure (Bar)	Yield (%)
1	7	20	7	53
2	10	24	7	55
3	66	18	7	61

From the set of conditions illustrated in Table 1, it was evident that the Pt-based catalyst exhibited a modest ability to catalyse the hydrogenation of isoquinoline carboxylic acid **78**, giving the corresponding tetrahydroisoquinoline carboxylic acid **77** in moderate yields. What was observed was that varying the weight percentage of the catalyst relative to the reagent had an effect on the percentage yield, albeit very small. Looking at entry 2, it is evident that

increasing the catalyst load and reaction time did improve the yield, but only very slightly. However, there was reason to believe that the optimum catalyst load was about 10-15% (wt%) and this was informed by the fact that even at 66% of catalyst load, the percentage yield did not improve in the same proportion (entry 3). The data generated from the hydrogenation reactions essentially suggested that the optimum time was between 18-24 hours and the optimum catalyst load should be between 10-15%. Previous studies had shown that acetic acid was the best solvent for transformations using Pt catalysts,[121–123] either by dissolving the surface bound alkali metals, thereby accelerating the hydrogenation reactions or by preventing the deactivation of the catalyst by the product. It is for this reason that the solvent effects were not investigated in this section. Experimental data that supported the successful synthesis of **77** in this section was obtained using NMR spectroscopic techniques; both the ^{1}H and ^{13}C NMR spectra resembled those discussed in the first synthetic strategy. Despite all the attempts, only a maximum yield of 61% was obtained and the reason for this had been traced back to the preferential solubility of tetrahydoisoquinoline in methanol and water.

During the work-up, the hydrogenation product **77** was separated from the catalyst through filtration and the acetic acid was removed under reduced pressure. What remained in the round bottom flask was a beige/ brownish solid material that was triturated in methanol or water and the solvent removed by filtration to obtain a white solid, which was shown to be the product using NMR spectroscopic techniques. The methanol or water filtrate was a brown solution that, when left overnight, evaporated to leave behind a light-brown solid. The light- brown solid contained some of the product and impurities when analysed by NMR spectroscopy. This finding led to the realization that some of the product remained in solution during the trituration process, as a consequence of solubility. A solubility test revealed that compound **77** had a high affinity for polar protic solvents like methanol and water, so much that its recovery from the reaction matrix composed of water or methanol required multiple extractions. The ^{1}H NMR analysis revealed elaborately resolved peaks with coupling constants consistent with theoretical expectations; the aliphatic protons of **77** experienced rotational restrictions, and so they were largely equatorial, axial or held in pseudo axial and pseudo equatorial, and this was seen in the coupling patterns, appearing as multiplets rather than triplets since there were only 2 neighbouring protons (Fig. 32). The typical coupling constants between two rotationally restricted CH_2's is 10-16 Hz for geminal protons and 6-8 Hz for vicinal protons.

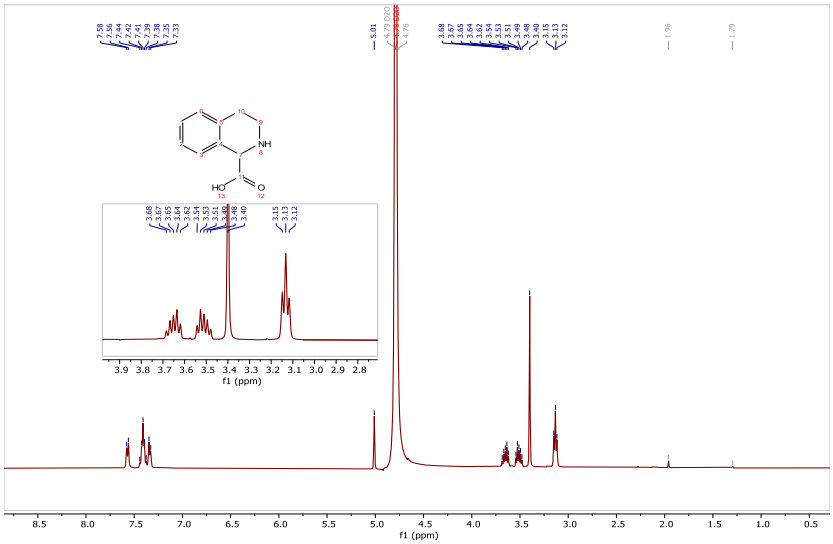

Figure 32: ^{1}H NMR spectrum of tetrahydroisoquinoline-1-carboxylic acid.

[101] Indeed, two coupling constants for signal 9 of 6.2 Hz and 12.5 Hz were observed, which are believed to be typical of a vicinal coupling constant between signal 9 and 10 and a geminal coupling constant between the two signal 9 protons respectively. This phenomenon of geminal and vicinal coupling exhibited by signal 9 manifested itself as two sets of multiplets , as seen at 3.5 ppm in the proton spectrum shown in Figure 32. The IR frequencies of **77** typically included the carbonyl (C=O) stretch at 1606 cm^{-1}, the aliphatic (C-H) stretches in the range of 2953-2869 cm^{-1} and the alkene (=C-H) stretch at 3057 cm^{-1}.

The esterification of **77** was performed using thionyl chloride and ethanol (Scheme 51).[111] Again, the yield of ester **72** obtained was also disappointingly low, reaching a maximum of 17%. ^{1}H and ^{13}C NMR spectral data for **72** matched that discussed earlier when this compound was synthesised using the first synthetic strategy. The possible reason for the low yield has already been provided in the first synthetic strategy section. An alternative method to esterify compound **72** using the Steglich esterification method shown in Scheme 52 was also explored. Tetrahydroisoquinoline-1-carboxylic acid **77** was dissolved in dry dichloromethane, followed by the addition of DMAP and ethanol. The resulting mixture was cooled to 0 °C and DCC was then added and stirred for five minutes. The resulting mixture was allowed to warm to 20 °C and the reaction mixture was stirred for 3 hours.[124] The product extracted from the reaction matrix was analysed using TLC and ^{1}H NMR spectroscopy and it was found that the product did not point to the successful formation of the desired ester **72**.

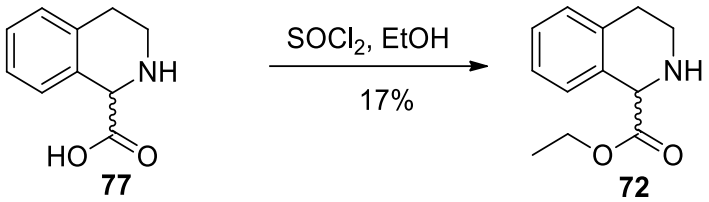

Scheme 51: Esterification of acid **80** using thionyl chloride in ethanol.

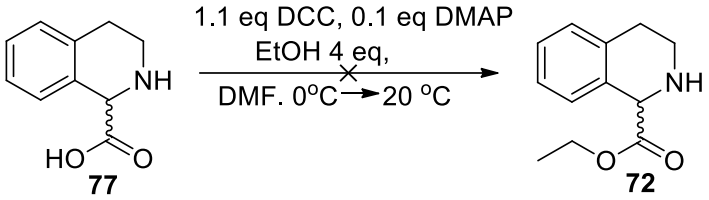

Scheme 52: Attempted Steglich esterification reaction for the synthesis of tetrahydroisoquinoline carboxylic ester.

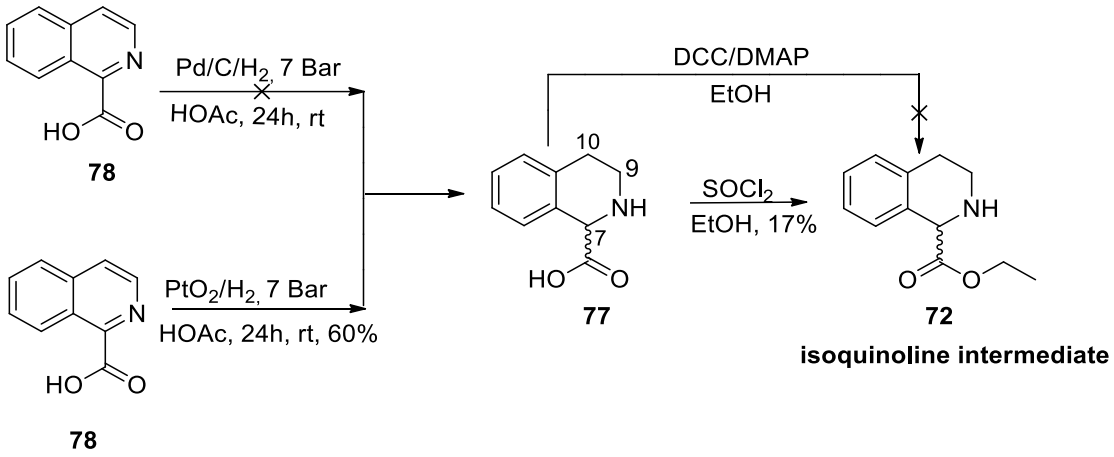

Scheme 53: Preparation of PZQ intermediate in 2 reaction steps.

The second synthetic strategy presented advantages of ease of reaction and reproducibility (Scheme 53). It also provided a much shorter route to get to tetrahydroisoquinoline carboxylic acid **77** when contrasted with the Ugi reaction. The problem associated with this reaction involved the extraction of the compound to a quantity that exceeded 60% while achieving good purity. Another problem was that once the acid **77** had been formed, the esterification reaction conditions were exactly the same as those used on the Ugi hydrolysed compound, therefore the chances of obtaining a significantly different outcome were very low.

2.1.3 Third synthetic strategy

From the preceding two synthetic strategies, it was clear that esterifying tetrahydroisoquinoline-1-carboxylic acid **77** was a challenge. Literature offers many examples

of the esterification of the 3-carboxylic acid moiety,[125,126] but not many for the 1-carboxylic acid moiety. As previously mentioned in section **2.1.1**, it was theorised that the reason for problems with the esterification involved the difficulty of esterifying a carboxylic acid moiety of a molecule that also carried a free base. Again, considering the difficulties encountered in the last two strategies, it is safe to assume that esterifying a molecule that also bears a free base was a not an easy feat to achieve. Therefore, it was decided to explore methods where the base was masked in order to increase the likelihood of the esterification reaction. This method has precedent, albeit predominantly in patent literature.[127]

Indeed, it was found that the esterification of acids whose free base moiety had been masked either in the form of an imine or an amide offered a gateway to the corresponding esters in moderate to good yields.[128] Instead of beginning with the regioselective hydrogenation of **78**, it could be first esterified, followed by the hydrogenation of the pyridine ring of **97** to yield the much-anticipated ester **72** (Scheme 54).

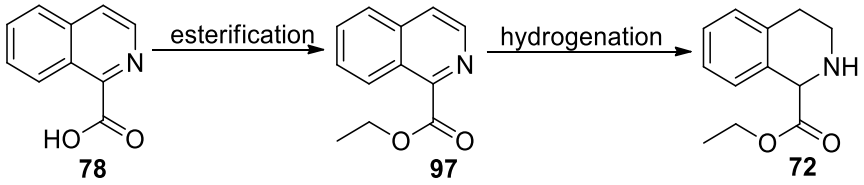

Scheme 54: Proposed esterification of isoquinoline-1-carboxlic acid **78**, followed by regioselective hydrogenation of **97** to yield **72**.

The esterification reaction to obtain **97** was performed by dissolving **78** in absolute ethanol and adding thionyl chloride dropwise over a period of 5 minutes. The resulting solution was refluxed for 4 hours, and ethanol was removed by distillation. This was followed by a workup and purification by column chromatography to obtain ester **97** in 75% yield as shown in Scheme 55.[128] The successful formation of **97** was confirmed by NMR spectroscopy. The ester contained only two aliphatic signals, one belonging to the methyl signal, at 1.44 ppm and the CH_2 signal at 4.55 ppm, which were both from the ester moiety. The aromatic signals that were more downfield were those from the heterocyclic ring since the nitrogen atom has more polarizing power. Indeed, two aromatic signals at 8.73 and 8.59 ppm, each integrating for one proton belonging to the pyridine ring were observed. The homocyclic ring signals appeared more upfield between 7.82-7.65 ppm. The ^{13}C NMR spectrum had the characteristic carbonyl carbon peak at about 166.0 ppm and the two aliphatic carbon signals at 62.1 ppm for the OCH_2 carbon and 14.34 ppm for the methyl carbon. The data generated from FT-IR was also

suggestive of the successful formation of **97**. The carbonyl (C=O) stretch was identified at 1716 cm^{-1}, the alkene (=C-H) stretch at 3056 cm^{-1}, and the aliphatic (-C-H) stretch at 2928 cm^{-1}. Platte *et al.*[129] were only able to synthesise **97** in 67% yield, and the NMR spectrum generated from the compound had peaks that were slightly different from those obtained in this study and the reason for this is attributed to the fact that they ran their NMR experiments using deuterated DMSO as their preferred NMR solvent while this project made use of $CDCl_3$.

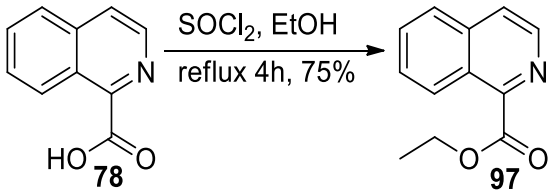

Scheme 55: Esterification of isoquinoline-1-carboxlic acid **96**

Nonetheless, the two peaks corresponding to the 2 pyridine protons signals from compound **97** synthesised by Platte and co-workers appeared at 8.59 ppm and 8.42 ppm whilst ours appeared at 8.73 and 8.59 ppm. Their phenyl ring proton signals appeared between 8.09-7.78 ppm. The two signals from the ethyl moiety were 4.48ppm for OCH_2- and 1.39 ppm for CH_3. In contrast, we observed signals at 4.58 ppm and 1.51 ppm for OCH_2 and CH_3 respectively. These values are slightly different because different NMR solvents were used to obtain the spectra under discussion. The same could be said about the ^{13}C NMR spectrum obtained by Platte and co-workers: their C=O carbon signal appeared at 165.8 ppm, whilst ours appeared at 166.0 ppm. Their ethyl moiety had the carbon peak of the OCH_2 appearing at 61.0 ppm and for CH_3 appearing at 13.8 while we observed these signals at 62.1 ppm and 14.3 ppm, respectively.

The successful formation of ester **97** prompted us to attempt the regioselective hydrogenation of this newly formed isoquinoline ester to afford the tetrahydroisoquinoline ester **72**. The hydrogenation of **97** was initially carried out by dissolving the ester in ethanol: acetic acid solution 10:1, followed by the addition of 10 wt% of Pd/C. The resulting solution was hydrogenated at 1 atm overnight (Scheme 56). NMR analysis of the compound obtained revealed that the desired hydrogenation had not taken place, however, there was strong NMR evidence that suggested that the hydrogenation reaction instead took place at the phenyl ring, leaving the pyridine ring intact and affording undesired compound **98** (Scheme 56).

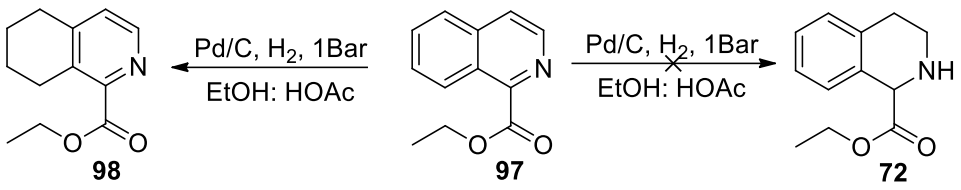

Scheme 56: Hydrogenation of ethyl isoquinoline-1-carboxylate **97** to **72**.

^{1}H and ^{13}C NMR analysis of the generated compound from the hydrogenation reaction strongly suggested the formation of **98**: the ^{1}H NMR spectrum contained two aromatic signals at 8.36 ppm and 7.11ppm, both of which integrated for one proton and appeared as doublets. These are the pyridine protons at the α-position and β-position relative to the N atom. What followed next was the upfield signal appearing at 4.44 ppm as a quartet, integrating for 2 protons and this signal belonged to the OCH_2 protons of the ester moiety. Further upfield were two signals appearing at 3.01 ppm and 2.81 ppm, integrating for 2 protons each, representing two CH_2 groups of the cyclohexyl ring conjoined to the pyridine ring. The last two CH_2 signals of the cyclohexyl ring appeared as one signal integrating for 4 protons and appearing as a doublet of quartets at 1.82 ppm. Finally, the ester CH_3 signal appeared as a triplet at 1.43 ppm integrating for 3 protons. From the ^{13}C NMR spectrum, the C=O signal appeared at 166.7 ppm. All five of the expected pyridine carbon signals were accounted for and appeared between 148.4-126.4 ppm. The aliphatic region of the ^{13}C NMR spectrum was expected to have 6 signals, and these were all accounted for; the OCH_2 carbon signal appeared at 61.5 ppm and the 4 signals from the cyclohexyl moiety appeared between 29.5-21.7 ppm and lastly the CH_3 signal appeared at 14.3 ppm.

The work presented by Boger *et al.*[130] gave credibility to the NMR assignments made for **98** since it was their intention to synthesise **98**. The NMR data found from the work of Boger and co-workers confirmed that indeed we had unintentionally made **98**; their work only presented ^{1}H NMR spectroscopic data, nonetheless the data they presented was enough to make a comparison to that generated from this work. Two proton signals at 8.35 ppm and 7.09 ppm integrating for 1 proton each and appearing as doublets were obtained, which were very similar in the NMR spectra to what we obtained for **98**. At 4.43 ppm, appeared a quartet integrating for 2 protons, which must have been from the ethyl ester moiety, which corresponded to ours at 4.44 ppm. Between 3.10-2.60 ppm appeared one multiplet signal which integrated for 4 protons of the cyclohexyl moiety whilst ours appeared at 3.01 and 2.81 ppm integrating for two protons each. The remaining 2 CH_2 groups appeared at 1.80-1.60 ppm whilst ours appeared as one signal at 1.82 ppm integrating for 4 protons.

What was attempted next was the use of PtO_2 as the catalyst. The pressure was varied between 1-5 bars and catalyst loading was tested between 10-20 wt% in ethanol: acetic acid. The reaction was stirred for a duration of between 4-24 hours. The analysed reaction material resulting from reactions of varying conditions proved to be the starting material. Failure to obtain compound **72** prompted the use of Rh/C catalyst since there was precedent of its use in literature, particularly for this transformation.[131]

Table 2: Variation of reaction conditions tested for the hydrogenation of **97** to PZQ intermediate.

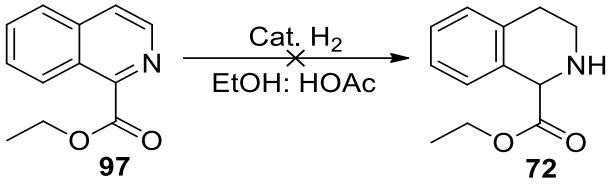

Entry	PtO_2 or Rh/C (% wt)	Reaction time (h)	Pressure (bar)
1	10	4	2
2	20	24	2
3	10	24	4.5
4	10	24	7

The hydrogenation reaction using the expensive Rh/C catalyst was also set up under the same conditions as PtO_2 and analytical data did not point to the successful formation of **72**, instead, only the starting material was recovered.

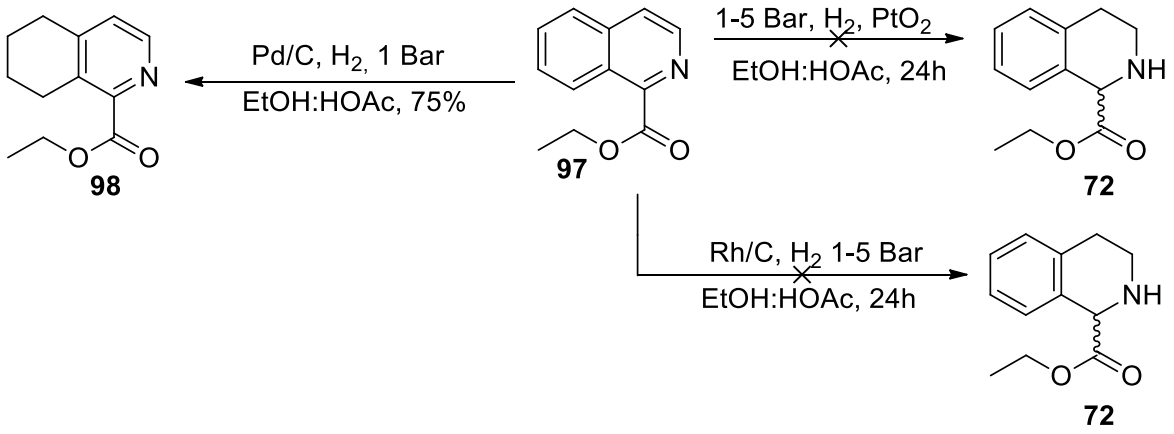

Scheme 57: Failed hydrogenation of **97** using Rh/C, Pd/C and PtO_2.

This strategy offered fewer reaction steps to get to the final intermediate. It also presented the esterification product **97** in a good yield. It however failed when it came to the hydrogenation of ethyl isoquinoline-1-carboxyliate as shown in Scheme 57. Use of Rh/C or PtO_2 returned only starting material while the use of Pd/C hydrogenated the phenyl ring, thus generating an unwanted product **98**.

2.1.4 Fourth synthetic strategy

Having tried several synthetic strategies to prepare the desired PZQ intermediate, the progress made was disappointing, with the successful synthesis of the PZQ intermediate **72** yielding only 17% in two of the proposed strategies presented (1st and 2nd strategy). The third strategy did not offer a practical solution either, instead it presented difficulty in the hydrogenation reaction step, generating an unwanted product and showing no positive results, even when using expensive catalysts like rhodium. As a result, the direction of the project veered towards alternative strategies that have been reported for the synthesis of isoquinoline derivatives. Our interest was piqued by the well-established class of synthetic chemistry called aromatic functionalisation chemistry.[132]

2.1.4.1 Pictet-Spengler Reaction

The initial plan was to make use of the Pictet-Spengler protocol to prepare the isoquinoline scaffold, which could be further functionalized. Initially, 3-methoxyphenethylamine **99** and glyoxylic acid monohydrate **100** were reacted together in absolute methanol at 5 °C as shown in Scheme 58, and the reaction was allowed to warm to room temperature.[133] After 6 hours, the reaction was analysed by TLC. From the spots that were visualised, there was no experimental evidence that suggested the formation of the new species **101**. On the contrary, the generated TLC spots bore resemblance to those of the starting materials.

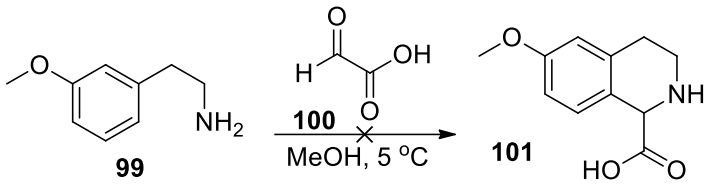

Scheme 58: Failed Pictet-Spengler cyclisation reaction.

Next, it was envisaged that perhaps converting the methoxy group to the hydroxyl group would make the phenyl ring a bit more electron rich, thereby increasing the chances of electrophilic aromatic substitution. For such a transformation, a demethylation of 3-methoxyphenethylamine **99** to 3-hydroxyphenethylamine **102** would be required, as shown in

Scheme 60. To begin, the demethylation was attempted using boron tribromide (BBr_3) in dichloromethane at -78°C (Scheme 59).[134] The reaction was allowed to warm to room temperature and was stirred for the next 20 hours.

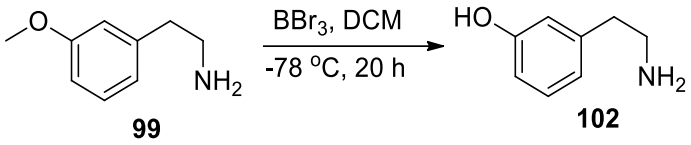

99 **102**

Scheme 59: Demethylation of 3-methoxyphenethylamine to 3-hydroxyphenethylamine.

The ^1H NMR analysis of the reaction product suggested a successful demethylation. The ^1H NMR spectrum had two aromatic signals at 7.18 ppm and 6.74 ppm for one proton and three protons respectively. The ethyl moiety appeared as two distinct signals appearing as triplets, each integrating for two protons at 3.18 ppm and 2.91 ppm respectively. The acidic protons from the hydroxide and the amine functional groups did not appear in the spectrum due to proton exchange with the deuterium enriched deuterated methanol NMR solvent. The spectrum in question was devoid of the methoxy group, which pointed to the successful demethylation of **99**. Despite attempts at acquiring the ^{13}C NMR spectrum, the acquisition of the ^{13}C NMR spectrum became a challenge given the small size of the sample collected. From the ^{13}H NMR spectrum, it became clear that the product could be successfully demethylated, however, the isolation of the product presented with challenges of separating it from the boronic salts and adducts that were formed during the reaction. Zhao *et al*[135] have demonstrated the synthesis of **102** in 99% by refluxing **99** in 48% HBr for 12 hours, followed by cooling and concentrating in *vacuo.* The ^1H NMR spectrum they generated looked identical to that obtained for **102** using BBr_3 as the reagent. Their aromatic signals appeared at 7.15 ppm and 6.74-6.70 ppm, integrating for one proton and three protons respectively. The two proton peaks from the ethyl moiety were reported to appear at 3.16 ppm and 2.89 ppm, both appearing as triplets and integrating for two protons each. The ^1H NMR provided by Zhao and co-workers proves the successful demethylation of **99**.

Faced with this challenge of isolating **102** from the reaction medium, sodium ethyl sulphide (NaEtS) was then used as an alternative reagent for conversion of **99** to **102**, with the aim of improving product recovery from the reaction matrix (Scheme 60). ^1H NMR analysis of a sample extracted from the reaction mixture did not suggest the formation of the desired product.

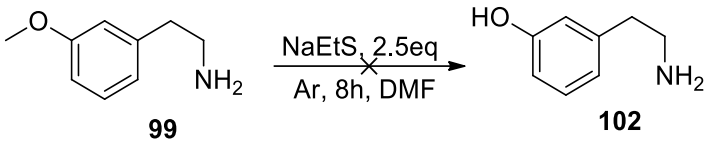

99 **102**

Scheme 60: Attempted demethylation of 3-methoxyphenethylamine to 3-hydroxyphenethylamine.

The final attempt towards the recovery of the newly formed 3-hydroxyphenethylamine **102** made use of a continuous extraction apparatus shown in Figure 33. Effectively, this apparatus is designed to extract the desired compound from a reaction matrix whose complexity makes it difficult to work with using conventional chromatographic techniques. Conceptually, a solvent in which the desired compound dissolves is chosen and is heated from a round bottom flask and distilled into the extractor containing the reaction matrix.

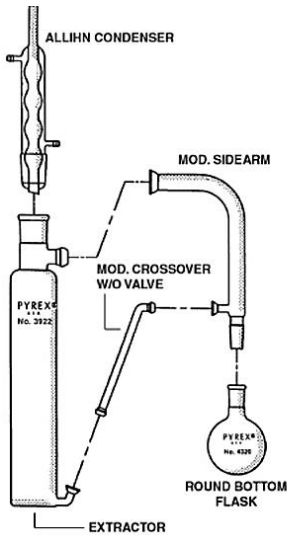

Figure 33: Continuous extraction apparatus.

The apparatus is designed such that it can collect the extractor solvent either from the top if the extraction solvent is less dense than the reaction solvent matrix or the bottom if the reaction matrix solvent is less dense than the extraction solvent. For the purpose of this study, dichloromethane was chosen, owing to its dissolution prowess, particularly towards polar organic compounds. DCM was heated from a round bottom flask and allowed to enter the extractor chamber via a sidearm. Upon entering the extractor, it was condensed into the aqueous reaction matrix. Because DCM is denser than water, it sank to the bottom, collected into the round bottom flask via a cross over valve, and was continuously distilled to perpetually extract the desired compound. This process was left to run overnight, and the extractor solvent

was distilled out under high vacuum in pursuit of concentrating the now extracted compound. The residue was analysed using TLC and ^{1}H NMR; the generated data did not suggest the successful extraction of the desired compound.

At this point, it was clear that the attempts to prepare the phenethylamine intermediate, preceding the Picted-Spengler reaction had failed. This led to the decision to abandon this approach.

2.1.4.2 Bischler-Napieralski Reaction: Amide preparation

The second attempt at making tetrahydroisoquinoline derivatives using aromatic functionilsation chemistry was conducted using the Bischler–Napieralski method. Looking at the structure of the desired PZQ intermediate **72**, it was important that the reagents used would lead to the desired scaffold with the fewest number of reaction steps. In terms of the phenethylamines, which are responsible for the construction of the isoquinoline backbone, three were selected for testing. For the source of the carbonyl functional group, which ultimately attaches to the C-1 carbon positioned α relative to the nitrogen atom and gives the compound its racemic character, diethyl oxalate was found to be ideal choice. The choice of diethyl oxalate was attractive because it meant the final dihydroisoquinoline compound would have an ester group on the C-1 atom, which would later play a vital role in the enzymatic resolution work. Interestingly, similar reagents were used by Zalán *et al.*[136] to prepare various tetrahydroisoquinoline analogues. Borrowing some learnings from Zalán and co-workers, it became interesting to know if other oxalates would facilitate the formation of the desired amides. To test this notion, a model reaction was conducted, where dimethyl oxalate **80a**, which we had readily available in our laboratory, was reacted with 4-methoxyphenethylamine **79c** at 140 °C for 6 hours as shown in Scheme 61.

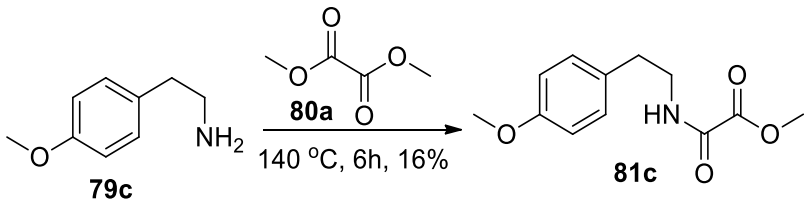

Scheme 61: Reaction of 4-methoxyphenethylamine and dimethyl oxalate to yield the corresponding amide.

^{1}H NMR analysis suggested the successful formation of the desired compound **81c**. The aromatic signals appeared at 7.12 and 6.86 ppm, integrating for 2 protons each, appearing as

two doublets, alluding to the symmetry associated with *para*-disubstituted phenyl rings. The methoxy group attached to the phenyl ring appeared at 3.80 ppm and the methyl ester at 3.89 ppm, both integrating for 3 protons, respectively. The two -CH_2- protons appeared at 3.58 and 2.82 ppm as a quartet and a triplet respectively. Lastly, the amide NH signal appeared at about 7.12 ppm, overlapping with the aromatic peaks at 7.12 ppm since this doublet peak integrated for 3 protons. The ^{13}C NMR spectrum had the typical 4 aromatic carbon signals instead of 6, owing to the symmetry in the compound. The two quaternary carbons appeared at 156.2 ppm and 130.0 ppm, respectively, whilst the 2 CH carbons appeared at 129.6 ppm and 114.2 ppm. The methoxy carbon appeared at 53.6 ppm while the methyl ester CH_3 carbon appeared at 55.3 ppm. The two –CH_2- carbon signals nestled between the phenyl ring and the amide functional group appeared at 41.2 ppm and 34.2 ppm. The presence of the two carbonyl carbon signals confirmed the successful formation of **81c**, appearing at 161.2 ppm and 158.5 ppm. We found no experimental data from the literature that we could use for comparative purposes between what we found and what had been done previously. However, it is important that to note that the reaction shown in Scheme 62 served as a good model reaction, which shone light on the type of NMR spectra to be expected for this type of compound.

Despite the overall success of the synthesis of **81c**, the yield obtained was disappointingly low, seeing that it was only recovered in 16%. The reason for this poor yield was only revealed when a second compound eluted from the column upon purification. Scrutiny of the proton NMR spectrum of the second compound pointed to the fact that it was neither the starting material, nor was it the product. The unknown compound was missing one methyl group, and we initially thought the methyl group must have been cleaved from the ester moiety through hydrolysis, leaving the carboxylic acid. However, based on the identity of the side-products isolated from subsequent reactions on related substrates, we now suspect that a *bis*-amide **103** was formed instead (Scheme 62). The ^{1}H NMR spectrum of **103** had the amide NH peak at 7.46 ppm, integrating for one proton, and two aromatic signals appeared at 7.11 ppm and 6.85 ppm, integrating for 2 protons each, appearing as two doublets. The methoxy group attached to the phenyl ring appeared at 3.79 ppm and the two -CH_2- protons appeared at 3.53 ppm and 2.79 ppm as a quartet and a triplet respectively. The quartet might result from coupling with the neighbouring -CH_2- as well as to the NH, with the coupling constants being of similar value, giving the appearance of a quartet.

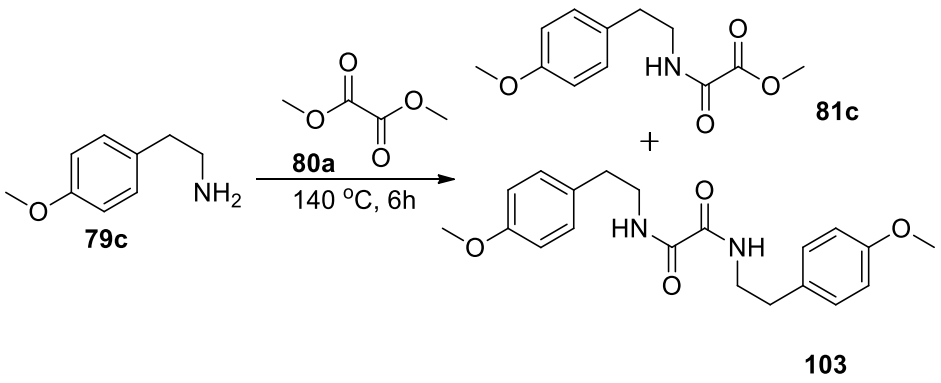

Scheme 62: Emergence of unexpected *bis*-amide **103** from the reaction to prepare oxoacetate **81c**.

The small amount of ester **81c**, isolated from the preceding reaction was then used in the Bichler-Napieralski reaction, where it was refluxed in phosphorus oxychloride and 96% ethanol (Scheme 63). The reaction was then monitored using TLC. Over a period of 24 hours, the TLC analysis did not suggest the formation of a new species **104**.

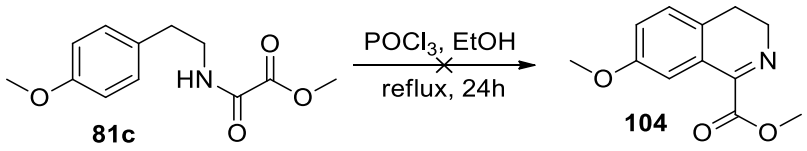

Scheme 63: Unsuccessful Bichler-Napieralski cyclisation reaction.

Looking at the mechanism of the reaction shown in Scheme 17, it is evident that the reaction is enhanced by *para*-directors since the site of cyclisation occurs *para* relative to the phenyl substitution, and it is for this reason that we considered that the methoxy group *para* to the ethylamine alkyl group could have been deactivating the centre of cyclisation. The use of dimethyl oxalate and *p*-phenethylamine as a model reaction offered some valuable insights. It was now understood that the formation of the amide was a facile reaction, however it was susceptible to the formation of a *bis*-amide side product. Secondly, it is worth noting that the position of the methoxy group on the phenyl ring might have an effect on the cyclisation that would follow. The mitigation strategy used to exclusively form the desired compounds involved the introduction of a bulkier ester moiety like an ethyl group. To increase the chances of cyclisation, the only phenethylamines used were those that have methoxy groups positioned such that they may activate the cyclisation reaction.

To test out the theory, the next step involved alternating from dimethyl oxalate **80a** to diethyl oxalate **80b** as the carbonyl donor. The phenethylamines used were 3-methoxyphenethylamine **79a** and 3,4-dimethoxyphenethylamine **79b** as shown in Scheme 64.

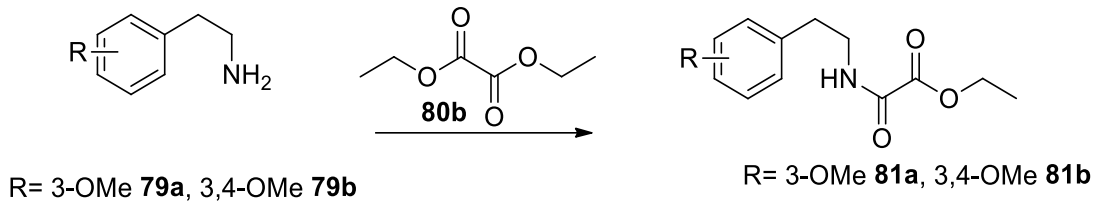

Scheme 64: Amide formation using diethyl oxalate **80b** to form new oxoacetates **81a-b**.

Reagent 3-methoxyphenethylamine **79a** was mixed with diethyl oxalate **80b** and heated to 140 °C for 6 hours to afford the oxoacetate **81a** (Scheme 65). [113,136] After purification of compound **81a** through column chromatography, it was obtained in 33% yield. despite the observed success in the formation of **81a**, alternating to diethyl oxalate **80b** from dimethyl oxalate **80a** did not solve the problem of forming a *bis*-amide encountered from the reaction highlighted in Scheme 62.

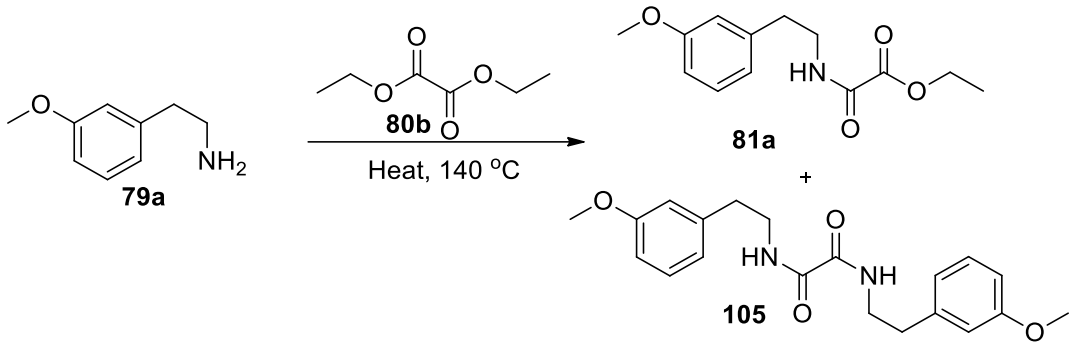

Scheme 65: Amide formation using diethyl oxalate **80b** to form new oxoacetate **81a** and *bis*-amide side product **105**.

The purification of **81a** using column chromatography was followed by a secondary elution of a compound that we struggled to identify at first. The analysis of the ^{1}H NMR spectrum of **105** was somewhat challenging at first because the spectrum did not bear any resemblance to the starting material nor the expected product; what was distinct from the ^{1}H NMR spectrum of the starting material **79a** was the proton signal that represented the amine protons. This signal disappeared on conversion to the unknown product and was replaced by an amide proton peak. Now, product **105** had neither the amine protons nor the ester moiety, and so it was concluded that it was neither the starting material nor the product, or even a mixture of both. After much

deliberation with colleagues and senior chemists, a closer look at the ^{1}H and ^{13}C NMR spectra revealed that diethyl oxalate **80b** had reacted with 2 moles of 3-methoxyphenethylamine **79a** to form a *bis*-amide **105.**

Looking at the ^{1}H NMR spectrum of **81a**, the amide NH peak appeared at 7.11 ppm as a singlet. The aromatic protons appeared at 7.17 ppm as a multiplet, integrating for 1 proton, 6.72 ppm as a multiplet, integrating for 2 protons and 6.67 ppm appearing as a singlet and integrating for 1 proton. The -OCH_2- signal appeared at 4.26 ppm as a quartet, integrating for 2 protons. The methoxy group appeared at 3.73 ppm as a singlet and integrating for 3 protons, followed by the two -CH_2- signals between the phenyl group and the amide group at 3.53 ppm and 2.77 ppm, each integrating for 2 protons. Lastly, the ester -CH_3 appeared at 1.30 ppm as a triplet, integrating for 3 protons. The ^{13}C NMR spectrum had all the characteristic peaks expected from the aromatic region and the aliphatic region; the 6 signals between 156.6-112.2 ppm were those of the aromatic region. The ester -OCH_2- peak appeared at 63.2 ppm and the methoxy peak at 55.21 ppm. The two -CH_2- signals appeared at 40.9 ppm and 35.3 ppm. Lastly, the -CH_3 signal appeared at 14.0 ppm. Most notably, were the two new carbonyl peaks at 160.7 ppm and 159.9 ppm, which also signified the successful preparation of **81a**.

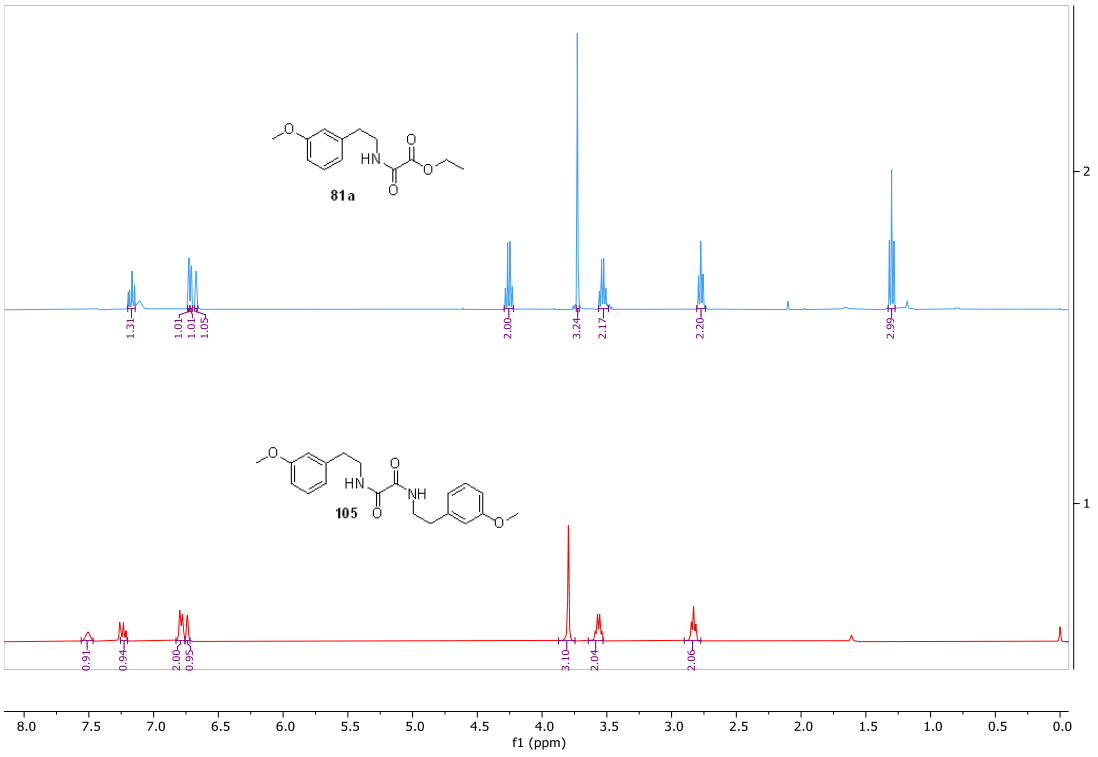

Figure 34: Stacked proton NMR spectra of **81a** and **105**.

Looking at the ^{1}H NMR spectrum of the second compound eluted, as mentioned above, it became evident that a *bis*-amide side product **105** had been generated. From the proton spectrum, the amide NH peak appeared at 7.51 ppm as a singlet. Three aromatic signals collectively integrating for 4 protons were observed between 7.23 ppm and 6.74 ppm, which were slightly upfield when contrasted with those obtained for **81a**. What followed then was the methoxy group at 3.80 ppm. Next, came the two $-CH_2-$ signals of the protons attached to the carbons next to the phenyl group and the amide functional group, appearing at 3.56 ppm and 2.83 ppm. What was missing from the spectrum was the $–OCH_2-$ and $-CH_3$ proton signals, which alluded to the hypothesis that a *bis*-amide product has been formed. Looking at Fig. 34, the spectrum in blue is that of **81a** and the one in red is that of **105**. From the stacked proton NMR spectra shown, it was evident that **105** was missing two signals, which were those of the ester $-OCH_2-$ and $-CH_3$ signals.

The ^{13}C NMR spectrum of **105** had 3 aliphatic signals, one belonging to the methoxy group, appearing at 55.2 ppm and the other two were those of the 2 $-CH_2-$ carbons, appearing at 40.8 ppm and 35.5 ppm. From this region, the presence of the ethyl ester would have been signified by the presence of its $-OCH_2-$ and $-CH_3$ carbon signals. The absence of these signals confirmed what was observed from the ^{1}H NMR spectrum about the cleavage of the ester from **81a**. The 4 CH carbons appeared at 129.8 ppm, 121.0 ppm, 114.4 ppm and 112.14 ppm. The carbons that are not attached to protons appeared at 140.1 ppm and 159.7 ppm. The signal at 159.9 ppm was that of the carbonyl signal. Because the *bis*-amide compound has a C2 axis of symmetry, we observed one signal for each pair of chemically equivalent carbon atoms, and this is the reason why there is only one carbonyl signal instead of two, and the same is true for the rest of the signals. There was very little success in locating previous work in literature that reported on the experimental data of compounds **81a** and **105**, with the exception of patents, where experimental data is seldom reported.

3,4-Methoxyphenethylamine **79b** was mixed with 3 mole equivalents of diethyl oxalate **80b** and heated to 140 °C for 6 hours to afford the oxoacetate **81b** (Scheme 66).[113,136] The same purification process was used for the isolation of **81b**, where again two compounds were eluted from the chromatographic column. The compound identities were determined using nuclear magnetic resonance spectroscopic techniques. The first compound eluted was **81b** in 41% yield. The second compound that was eluted displayed a similar ^{1}H and ^{13}C spectrum to those seen for compound **105**, where the ethyl ester moiety is missing from both spectra and the one carbonyl carbon signal is also missing from the carbon spectrum. In essence, both 1-D and 2-

D NMR spectra pointed to the formation of the *bis*-amide **106**, whose axis of symmetry allows it to be indistinguishably superposed. When that happens, the NMR instrument can only "see" one half of the structure, and this is what made the structure elucidation challenging initially.

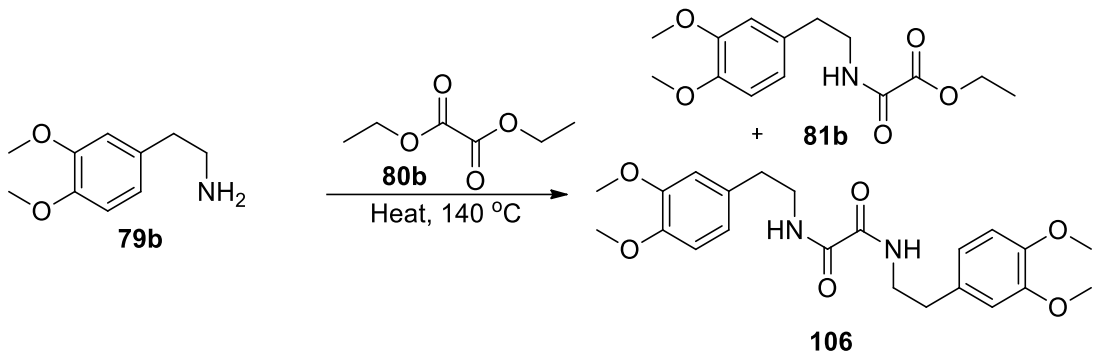

Scheme 66: Formation of **81b** and side-product **106** from **79b** using diethyl oxalate **80b**.

[114,137]^{1}H NMR spectroscopy of compound **81b** showed the amide NH peak at 7.13 ppm integrating for one proton, and 2 aromatic proton signals at 6.82 ppm and 6.73 ppm, integrating for one proton and two protons, respectively. The -OCH_2- signal appeared at 4.33 ppm as a quartet, integrating for 2 protons. Next were the 2 methoxy groups at 3.88ppm and 3.87 ppm, collectively integrating for 6 protons. The two -CH_2- proton signals appeared at 3.59 ppm and 2.82 ppm, each integrating for 2 protons. Lastly, the ethyl ester -CH_3 protons signal appeared at 1.38 ppm as a triplet, integrating for 3 protons. Looking at the ^{13}C NMR spectrum, the aromatic region had the 6 expected signals, 3 of which were CH carbon signals, appearing at 120.6 ppm, 111.9 ppm and 111.5 ppm. The 3 quaternary carbons appeared at 149.2 ppm, 147.9 ppm and 130.6 ppm. The ester -OCH_2- signal appeared at 63.2 ppm whilst the two methoxy groups attached to the phenyl ring appeared at 56.0 ppm and 55.9 ppm. The two -CH_2- carbon signals appeared at 41.1 ppm and 34.9 ppm. Lastly, the -CH_3 signal appeared at 14.0 ppm. Lastly, the two carbonyl carbons appeared at 160.7 ppm and 156.5 ppm. Zalán *et al*[136] prepared **81b** in 81% yield, which was almost double the yield obtained in this study, even though the exact reaction conditions were used. What differed was that Zalán and co-workers were able to obtain **81b** through crystallisation whilst the compound **81b** prepared in this study was obtained through purification using column chromatography. Nonetheless, the ^{1}H NMR data obtained by Zalán and coworkers for **81b** had the exact signals to those obtained in this study, with the exception of the two aromatic protons appearing at 6.73 ppm, where they reported to be in a range of 6.70-6.76 ppm. No ^{13}C NMR data was reported by Zalán and co-

workers, however, the ^{1}H NMR data they reported was sufficient to draw the required comparison in order to make informed conclusions.

The ^{1}H NMR spectrum of **106** was observed to have a similar pattern to that of **81b** only that the ester moiety was absent, rendering the compound a *bis*-amide. The amide NH peak appeared at 7.13 ppm, integrating as a triplet, and the 3 aromatic protons appeared as a multiplet at 6.72 ppm. The two methoxy groups appeared at 3.67 ppm and 3.64 ppm, integrating for 3 protons each. The two -CH_2- signals appeared at 3.07 ppm and 2.83 ppm, both integrating for 2 protons each. The spectrum was missing the ethyl ester moiety, which was a phenomenon also observed in the synthesis of **81a** and **105**.

Presented in Table 3 are the compounds synthesized and their respective side product *bis*-amide analogues. The percentage yields are also tabulated. From the data, it became evident how influential the groups attached to the phenyl groups were to the overall reactivity of the phenethylamines. The *meta* and disubstituted methoxy-phenethylamines had percentage yields that were 2-fold bigger than that of the *para*-substituted compound. The reason for this is unclear since the formation of the oxoacetates **105**, **106** and **103** did not involve the phenyl group. The lack of proximity of the phenyl group to the site of amidation makes it improbable for the methoxy groups attached to the phenyl ring to influence the reactivity of the respective reactions. The importance of having the methoxy groups *para* to the site of cyclisation was solely to aid the ring closure reaction and it was unexpected that the yields of the amidation reaction were affected by the substitution pattern on the phenyl ring.

Table 3: Amidation of phenethylamines **79a-c**, to yield oxoacetates **81a-c**.

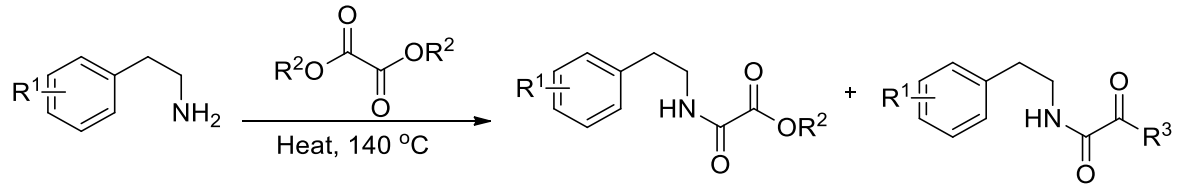

As already mentioned, the isolation of both oxoacetates **81a** and **81b** were accompanied by unexpected compounds, which were analysed using NMR spectroscopy and confirmed to be **105** and **106**. The formation of these undesired *bis*-amides explained why the oxoacetates were isolated in yields not exceeding 50%. Synthetically speaking, the formation of the *bis*-amide

side products points to the addition of the respective phenethylamine derivatives on both sides of diethyl oxalate **80b**, as shown in Scheme 67.

Entry	R^1 group	R^2 group	Percentage yield	Side Product R^3
1	3-OMe **79a**	Ethyl, **81a**	33%	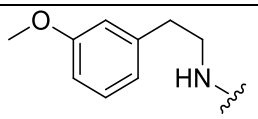 **105**
2	3,4-OMe **79b**	Ethyl, **81b**	41%	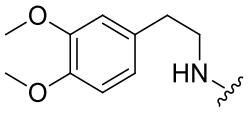 **106**
3	4-OMe **79c**	Methyl, **81c**	16%	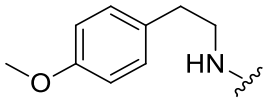 **103**

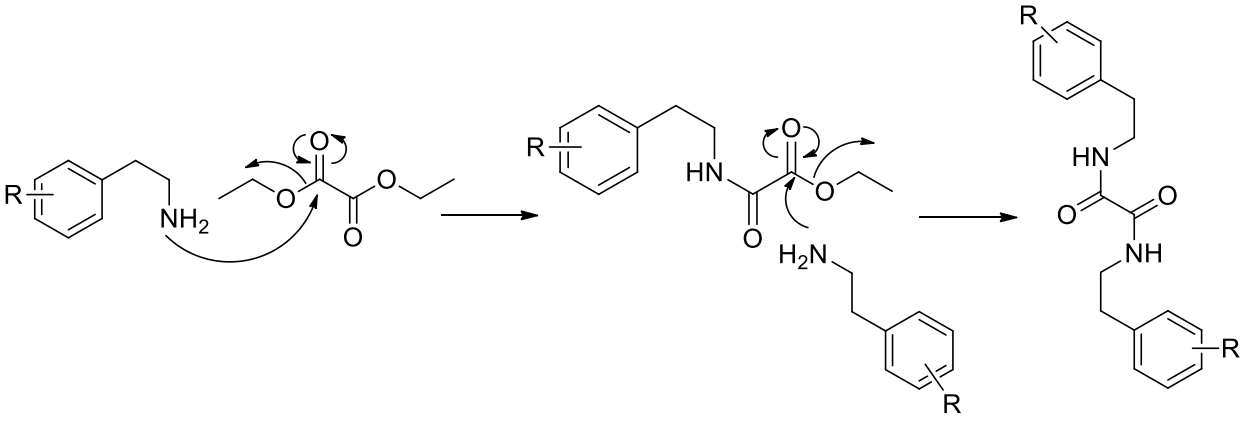

Scheme 67: *Bis*-amidation of phenethylamines **79a-c** to yield *bis*-amides **103**, **105** and **106**.

The discovery of unintended formation of the *bis*-amide products was made later in the study, which meant we could not go back and explore ways to exclusively form the intended amide products. In retrospect, to avoid the double addition, one would have to try the reaction at room temperature, as opposed to reflux conditions. Another possible solution would be to halve the mole ratios of the phenethylamines and distil out the excess diethyl oxalate **80b**. Lastly, perhaps *tert*-butyl oxalate would provide the necessary bulk required to hinder a double addition.

2.1.4.3 Bischler-Napieralski Reaction: Cyclisation reactions

The Bischler–Napieralski reactions for the cyclisation of **81a** and **82b** were set up. This reaction is effectively a cyclisation reaction, facilitated by phosphoryl chloride species (Scheme 17).[52] For the cyclisation reactions, **81a** and **81b** were dissolved in a toluene: ethanol 10:1 mixture, followed by the addition of freshly distilled $POCl_3$.[113,136] The resulting mixtures were stirred overnight and refluxed for 3 hours. The cyclisation reaction of **81a** afford **107** shown in Scheme 68 did not work, instead what was recovered was starting material. However, the cyclisation reaction **81b** with $POCl_3$ yielded compound **108** in 50% as a beige-brown crystalline product shown in Scheme 69.

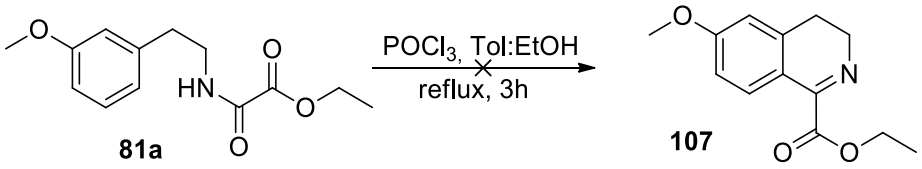

Scheme 68: Failed Bischler-Napieralski isoquinoline synthesis.

The successful formation of **108** was confirmed by ^1H and ^{13}C NMR spectroscopy. The expected result was the disappearance of one aromatic proton, as a consequence of the fusion between the ethylamide moiety with the 3,4-methoxyphenyl ring. Indeed, 2 aromatic protons instead of 3 were observed from the proton NMR spectrum of **108** at 7.38 ppm and 6.69 ppm, integrating for one proton each and appearing as singlets. Next, was the ethyl signal -OCH_2- proton peak at 4.42 ppm, integrating for 2 protons and appearing as a quartet. The two methoxy groups appeared at 3.92 ppm and 3.89 ppm as singlets and the two –CH_2- signals appeared as two multiplets at 3.85 ppm and 2.69 ppm, both integrating for 2 protons.

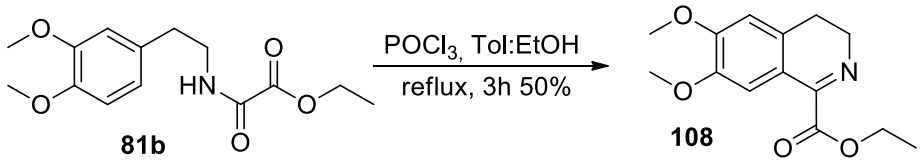

Scheme 69: Successful Bischler-Napieralski isoquinoline synthesis.

Lastly, the ethyl ester –CH_3 appeared at 1.43 ppm. From the ^{13}C NMR spectrum, the carbonyl peak appeared at 164.9 ppm and the imide peak at 158.6 ppm. The 6 aromatic carbons appeared between 151.6-110.1 ppm, and the ethyl –OCH_2- carbon signal appeared at 61.92 ppm. The 2 methoxy groups appeared at 56.1 ppm and 56.0 ppm whilst the two –CH_2- carbon signals appeared at 47.7 ppm and 25.2 ppm. Lastly, the ethyl –CH_3 peak appeared at 14.2 ppm. The

infrared spectrum shows the imide (C=N) stretching frequency at 1616 cm^{-1} and the carbonyl (C=O) stretching frequency at 1714 cm^{-1}. Zalán *et al*[136] prepared **108** without purification in 61% yield, and the generated ^{1}H NMR looks very similar to that obtained in this study. Again, no ^{13}C NMR data was reported, however, ^{1}H NMR data was sufficient to make a comparison. They reported that the two aromatic protons appeared at 7.39 ppm and 6.70 ppm, both integrating for 1 proton each and appearing as singlets. The ethyl ester -OCH_2- protons appeared at 4.43 ppm as a quartet and the 2 methoxy groups appeared at 3.93 ppm and 3.90 ppm. The two –CH_2- signals appeared as two multiplets at 3.83-3.89 ppm and 2.67-2.74 ppm, both integrating for 2 protons. Lastly, the ethyl ester -CH_3 they reported appeared at 1.44 ppm.

Having a closer look at the Birchler- Napieralski reactants **81a** and **81b**, one would expect both these reactants to cyclise and form the expected products. Because methoxy groups are electron donating (*ortho* and *para* directors),[101] it was anticipated that the methoxy groups in **81a** and **81b** that are *para* to the site of cyclisation would activate the site and facilitate the formation of Bischler–Napieralski products. For reasons unknown to us, the only product formed was **108**, as shown in Scheme 69.

Something interesting happened when we attempted the cyclization of **105** to form **109** using the Bischler–Napieralski conditions. What formed was the oxoacetate **81a** as shown in Scheme 70. The obtained results suggest the cleavage of the *bis*-amide using ethanol, thereby returning the ester **81a**. Despite the unexpected result, the formation of the ester **81a** from what was initially planned to be a ring-closing reaction of the *bis*-amide analogue **105** meant that the unusable acid had acquired synthetic value as a starting material for the Bischler–Napieralski reaction.

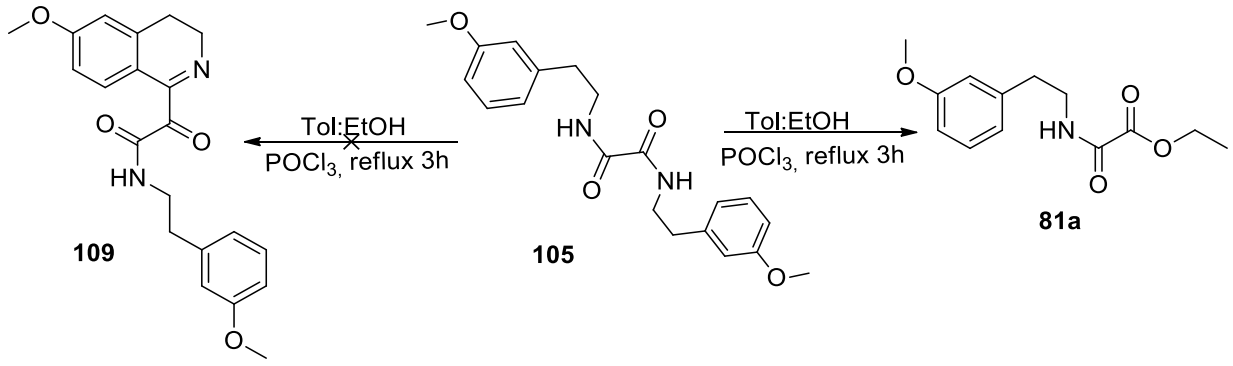

Scheme 70: Unexpected esterification of **105** using Bischler-Napieralski conditions.

^{1}H NMR data obtained pointed to the serendipitous formation of **81a**; the amide peak appeared at 7.15 ppm and the 3 aromatic peaks appeared at 7.24 as a multiplet integrating for 1 proton,

6.79 ppm as a multiplet integrating for 2 protons and 6.74 ppm integrating for 1 proton. Next was the ethyl -OCH_2- proton peak at 4.33 ppm, followed by the methoxy group at 3.80 ppm, integrating for 3 protons and appearing as singlet. The 2 -CH_2- signals appeared at 3.61 ppm and 2.85 ppm, integrating for two protons each and appearing as a quartet and a triplet respectively. Lastly, the ethyl -CH_3 appeared at 1.38 ppm.

The hydrogenation of the Bischler–Napieralski product **108** to afford **110** was set up using Pd/C as the catalyst, under various positive pressures of H_2 gas to increase the chances of the reduction reaction. This method found precedent in Zalán *et al*[136] when they hydrogenated **108** in EtOH using Pt/C at atmospheric pressure. ^{1}H NMR analysis of the reaction material extracted from the reaction matrix revealed peaks that resembled that of the starting material, alluding to the failure to form **110** as shown in Scheme 71. This may have been due to the difference in catalyst choice, which may have affected the successful formation of **110**. In as much as hydrogenation catalysts work the same way, what was observed in this study was that all the transformations that required hydrogenation almost always involved expensive catalysts like PtO_2, Rh/C and now the formation of **110** required the expensive Pt/C catalyst which was not available to test.

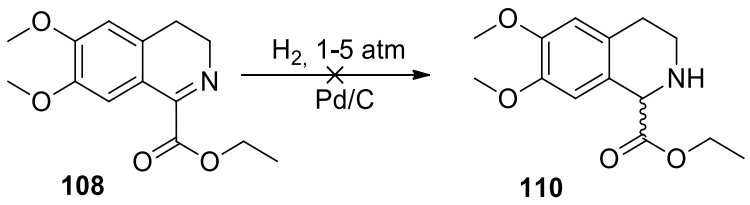

Scheme 71: Attempted hydrogenation of Birchler-Napieralski product.[111]

2.1.5 Fifth synthetic strategy

Despite the overall failure of devising a synthetic strategy that produced the required PZQ intermediate in appreciable yields, it has been demonstrated that it was indeed possible to obtain the intermediate, as is evidenced from analytical data of compound **72**. It is also important to mention that the four attempts were of vital importance to our study, whose failures have revealed valuable lessons. We now understand that it is rather cumbersome to esterify tetrahydroisoquinoline-1-carboxylic acid **77**, owing to the nature of its heterocyclic structure, existing as a zwitterion in acidic and basic media. It has also been equally fruitless to try and hydrogenate **97**, although there was some success in the preceding esterification reaction of **78** to **97**. From these challenges, it became immediately intuitive to protect the free

amine, and to attempt the esterification again. This could then be followed by the de-protection to expose the much-anticipated PZQ intermediate.

The sequence began with the hydrogenation of the relatively cheap isoquinoline acid **78** to **77**, which has already been discussed in section **2.1.2**. The reaction that followed then was of pivotal importance because it sought to protect the cyclic amine, thus masking it from taking part in the reactions that would ensue. The protection reaction of compound **77** was under the employ of di-*tert*-butyl dicarbonate (Boc_2O),[127] which proved to be a vital step in the synthesis of the PZQ intermediate, availing **111** in 89% yield for the next steps. The successful protection of the free amine **77** to obtain **111** shown in Scheme 72 was confirmed by NMR spectroscopy.

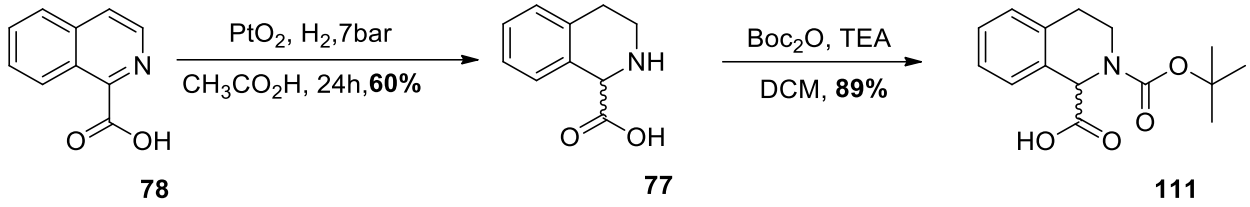

Scheme 72: Partial hydrogenation of **78**, followed by the Boc protection of cyclic amine **77**.

The ^{1}H NMR spectrum of **111** had the expected 3 methyl groups from the Boc moiety, appearing as two peaks at about 1.46 ppm. What was also observed was the splitting of the chiral proton peak into two signals in the same ratio as the two Boc peaks, appearing at about 5.50 ppm. The two -CH_2- signals appeared as 2 sets of multiplets at 3.71 ppm and 2.87 ppm. The aromatic protons collectively integrated for 4 protons, appearing as multiplets at 7.47 ppm, 7.23 ppm and 7.15 ppm.

The ^{13}C NMR spectrum of **111** revealed a splitting of all the signals, ranging from the aliphatic through to the aromatic and the carbonyl region. In an attempt to account for the splitting of the NMR signals, it is important to revert to the structure in question and interrogate the movement of electrons within the compound itself. It is well established that there is restricted rotation about the C-N bond, and this leads to the existence of rotamers, which can exist as *cis* and *trans* isomers. As a result of donation of electron density from nitrogen to the carbonyl group, the C-N bond has partial double-bond character, as shown in Scheme 74. The resulting rotamers are long-lived enough to be detected by the NMR instrument, leading to the splitting of NMR signals.[101]

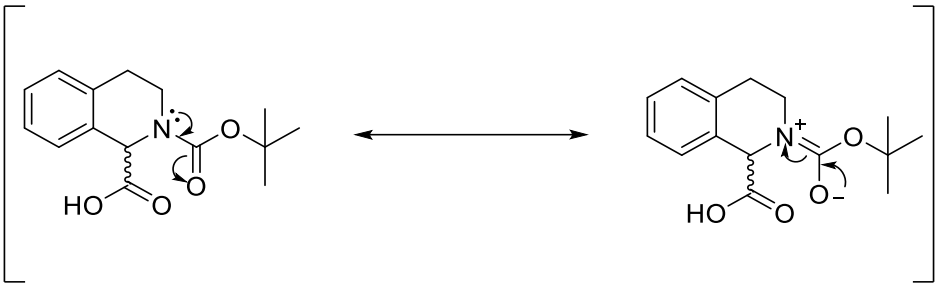

Scheme 74: Resonance forms for compound **111** showing reasons for restricted rotation about the C-N bond.

Looking at the ^{13}C NMR spectrum of **111**, all the signals were split into two. The 3 methyl groups appeared as split in two between 29.8-28.3 ppm, whilst the two -CH_2- signals appeared at 40.4 ppm and 58.0 ppm. The stereogenic carbon appeared at 81.1 and 80.95 ppm, followed by 6 aromatic signals that appeared between 126.6 ppm and 130.3 ppm. Lastly, the two carbonyl carbon signals appeared at 179.2-180.5 ppm and 159.2-158.1 ppm. Ho *et al.*[137] prepared **111** in 84%, which was slightly less than what we obtained, owing to differing synthetic methods. Looking at the ^{1}H NMR data they reported, their Boc protons appeared at 1.44 ppm, whilst the two –CH_2- signals appeared at 2.87 ppm and 3.45 ppm as multiplets. The proton attached to the stereogenic carbon appeard at 5.53 ppm as a doublet, and the aromatic protons appeared at 7.53ppm as a multiplet. The carboxylic acid proton appeared at 9.45 ppm. All these peaks shared similarities to those we obtained for **111**. The ^{13}C NMR peaks reported by Ho and workers also shared similarities to those obtained when we prepared **111**. What is noteworthy is that they also observed split signals, as was observed from our ^{13}C NMR spectrum; the Boc carbon signals appeared at 28.3-28.7 ppm, whilst the two –CH_2- signals appeared at 39.9-41.0 ppm for one signal and 57.6-58.7 ppm for the other. The stereogenic carbon signals appeared between 80.9-81.3 ppm whilst the aromatic carbons appeared between 126.6-135.8 ppm. Lastly, the two carbonyl signals appeared at 155.0-155.5 ppm and 176.2-176.8 ppm.

Following the successful protection of the amine group, the next step was to execute the esterification reaction of the carboxylic acid moiety. Making use the of the esterification conditions already explored in the first and second strategy ran the risk of hydrolysing the Boc protecting group of compound **111**. Therefore, an alternative reaction that would furnish us with the ester without cleaving the protecting group was sought. Among the options considered for the required synthetic transformation, patent literature provided a simple, yet elegant solution. The answer was the methylation of the carboxylic acid under mild oxidant conditions.

Indeed, this newly devised strategy proved profoundly prudent, availing methyl 1,2,3,4-tetrahydroisoquinoline-1-carboxylic acid **112** in 64% yield as shown in Scheme 74. The first clue that alluded to the successful formation of the ester analogue was observed from a TLC plate that was developed in 30% Ethyl acetate: Hexane; the R_f value of the newly formed compound was 0.63 and the R_f value of **111** was 0.33 and this pointed to the masking of the hydroxy group that had previously interacted strongly with the TLC plate. [138]

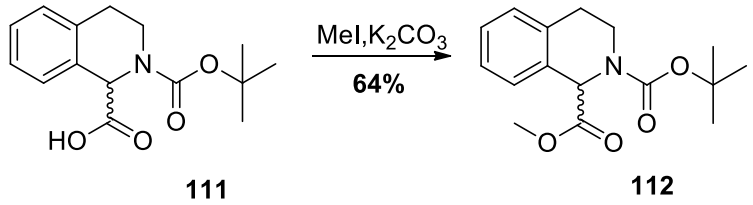

111 **112**

Scheme 74: Esterification of Boc protected tetrahydroisoqionoline-1-carboxylic acid **111**.

The ^{1}H NMR spectrum of compound **112** showed the expected aromatic signals, integrating for 4 protons: at 7.51-7.44 ppm as a multiplet integrating for 1 proton, 7.25-7.19 ppm as a 2 proton multiplet and 7.16 ppm as a singlet integrating for one proton. The proton attached to the stereogenic centre was also split into two distinct signals at 5.60 ppm and 5.43 ppm, collectively integrating for 1 proton. The two alkyl signals of the two -CH_2- groups nestled between the phenyl ring and the nitrogen atom appeared at 3.84-3.74 ppm as a 2 proton multiplet and 3.01-2.90 ppm and 2.90-2.80 ppm as multiplets, integrating for one proton each. The methyl ester protons appeared at 3.71 ppm as a singlet, integrating for 3 protons and the Boc protons appeared as a split signal at 1.48 ppm, integrating for 9 protons.

The ^{13}C NMR spectrum of **112** showed all the expected signals, which were also all split, alluding to the rotamers that still exists in the molecule. The aromatic region had the expected six 6 signals representing the phenyl carbon signals between 135.7 ppm and 126.5 ppm. The aliphatic region had the carbon signals of the newly formed methyl ester at 52.4 ppm, and the 2 carbon signals of the Boc group at 28.8 ppm and 28.4 ppm. The 2 signals of the two -CH_2- carbons attached between the phenyl ring and the nitrogen atom appeared at 58.2 ppm and 40.3 ppm. Lastly, the two carbonyl signals appeared at 171.6 ppm and 155.1 ppm. You *et al.*[139] successfully prepared **112** in 68% yield, however, they did not disclose the carbon NMR spectrum. Nonetheless, looking at the ^{1}H NMR spectrum they reported, it became evident that we were also successful in preparing compound **112**; their aromatic protons appeared at 7.60-7.43 ppm and 7.33-7.11 ppm, collectively integrating for 4 protons. The proton attached to the stereogenic centre appeared at 5.72-5.33ppm, which was within the value that we obtained.

The two alkyl signals of the two -CH_2- groups between the phenyl ring and the nitrogen atom appeared at 3.94-3.76 ppm and 3.10-2.76 ppm. The methyl ester appeared at 3.71 ppm. Their Boc group appeared between 1.69-1.37 ppm, integrating for 9 protons.

The final and most pivotal step to the overall success of the project hinged upon the successful deprotection of the methylated Boc-protected tetrahyroisoquinoline. Following the successful methylation, the crucial deprotection reaction was set up using three methods to increase the prospects of success. The first method explored involved the deprotection of **112** in a mixture of dioxane and water in a 1:10 ratio and refluxed overnight (Scheme 75). [140] The reaction mixture was extracted with ethyl acetate and dried with brine. ^{1}H NMR analysis of the resulting crude material did not point to the successful conversion of **112** to **71**, instead, the ^{1}H NMR peaks generated contained peaks of the starting material.

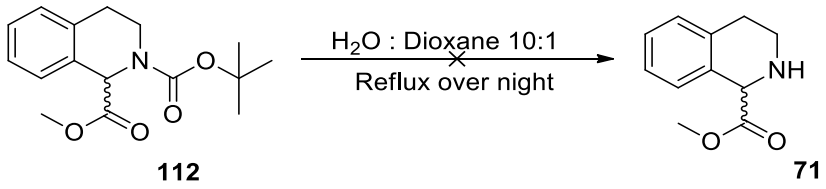

Scheme 75: Unsuccessful deprotection of **112** using water and dioxane.

As previously mentioned, this synthetic strategy made use of 3 routes. The second route attempted involved the dissolution of compound **112** in chloroform, followed by the addition of trifluoroacetic acid,[140] as shown in Scheme 76. The resulting mixture was stirred overnight at room temperature, followed by work up, extraction, and purification using column chromatography.

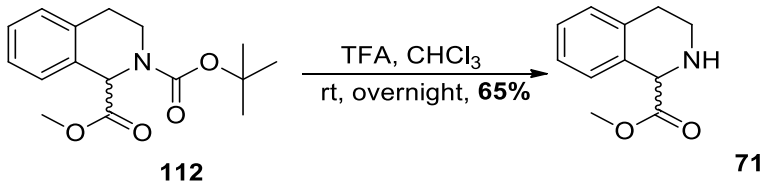

Scheme 76: Deprotection of **112** using TFA in chloroform.

From the ^{1}H NMR data generated, the most notable observation made was the disappearance of the proton NMR signals representing the Boc group shown in Fig. 35. The CH_3 signal representing the methyl ester group was left untouched, since it was also present in the spectrum, integrating for 3 protons. This observation alluded to the selectivity of the reaction, exhibiting an ability to discriminate between the Boc group and the ester group, seeing that

they are both susceptible to hydrolysis. The 4 aromatic proton signals appeared as a doublet at 7.37 ppm, integrating for one proton and a multiplet at 7.19 ppm, integrating for three protons. The proton attached to the stereogenic centre appeared at 5.31 ppm. The two -CH_2- proton signals attached to the carbon atoms between the phenyl group and the nitrogen atom appeared at 3.47 ppm and 2.96 ppm as multiplets, integrating for two protons each. The methyl ester protons appeared at 3.69 ppm as a singlet, integrating for 3 protons. The ^{13}C NMR spectrum had all the expected signals; what was notable was the absence of signal splitting, which meant the Boc group, where restricted rotation about the C-N bond is observed, had been removed. This meant that rotamers were no longer present. The carbon signals observed from the spectrum were the expected aromatic signals; 6 aromatic signals appeared between 131.8-124.9 ppm. The 2 aliphatic carbons of the saturated heterocyclic ring appeared at 39.85 ppm and 24.30 ppm. The methyl ester carbon appeared at 54.1 ppm and the stereogenic carbon at 56.10 ppm. Lastly, the carbonyl carbon appeared at 168.4 ppm.

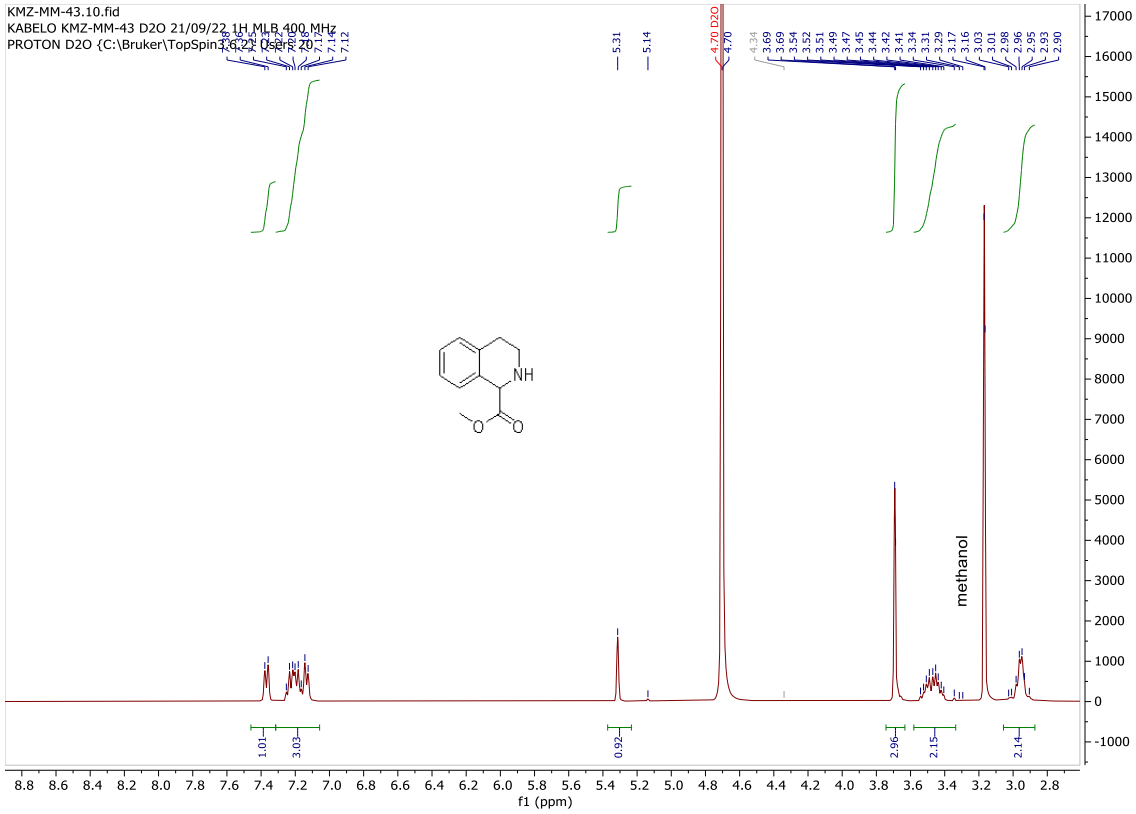

Figure 35: ^{1}H NMR spectrum of **71**.

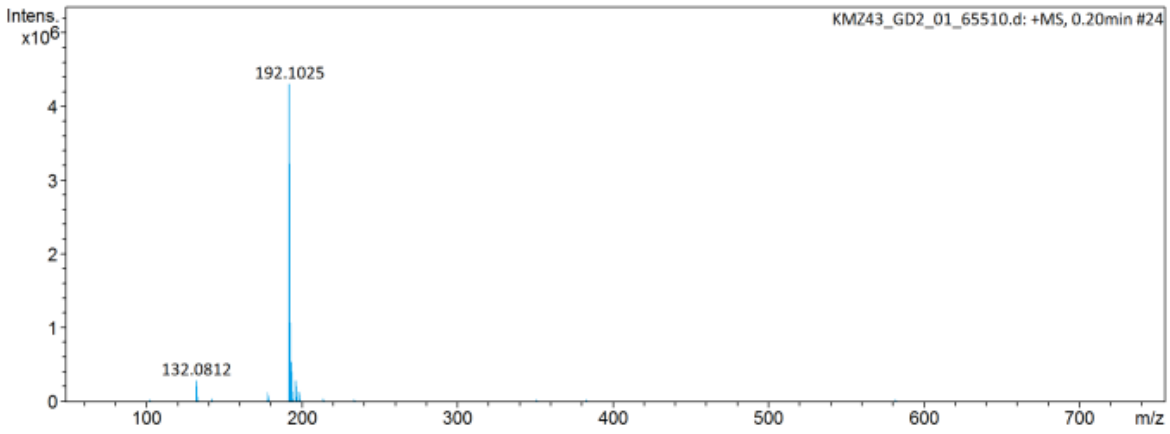

Figure 36: HPLC-MS (m/z) spectrum of compound **71.**

The successful preparation of this compound meant that we could finally proceed to enzyme reactions, which were a primary goal of this project. Prior to that, a step further was taken to confirm the successful formation of **71**. The expected molecular mass of **71** ($C_{11}H_{14}NO_2$) is 192.1025 g/mol and using HPLC-MS (m/z), the experimentally found molecular mass was 192.1025 $[M + H]^+$, as shown in Fig. 36.

The last route made use of a solution made from dioxane and 4 M HCl to convert compound **112** to the desired PQZ intermediate **71**. [140,141] A mixture of **112** in a 4 M solution of HCl in dioxane was stirred overnight (Scheme 77). The solvent was removed under reduced pressure to give **71** as a beige-brown solid. A close inspection of the ^1H NMR spectra generated from compound **71** revealed that the Boc group had been removed, as shown in Fig. 37.

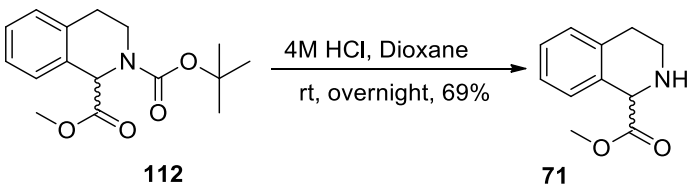

Scheme 77: Deprotection of **112** using HCl in dioxane.

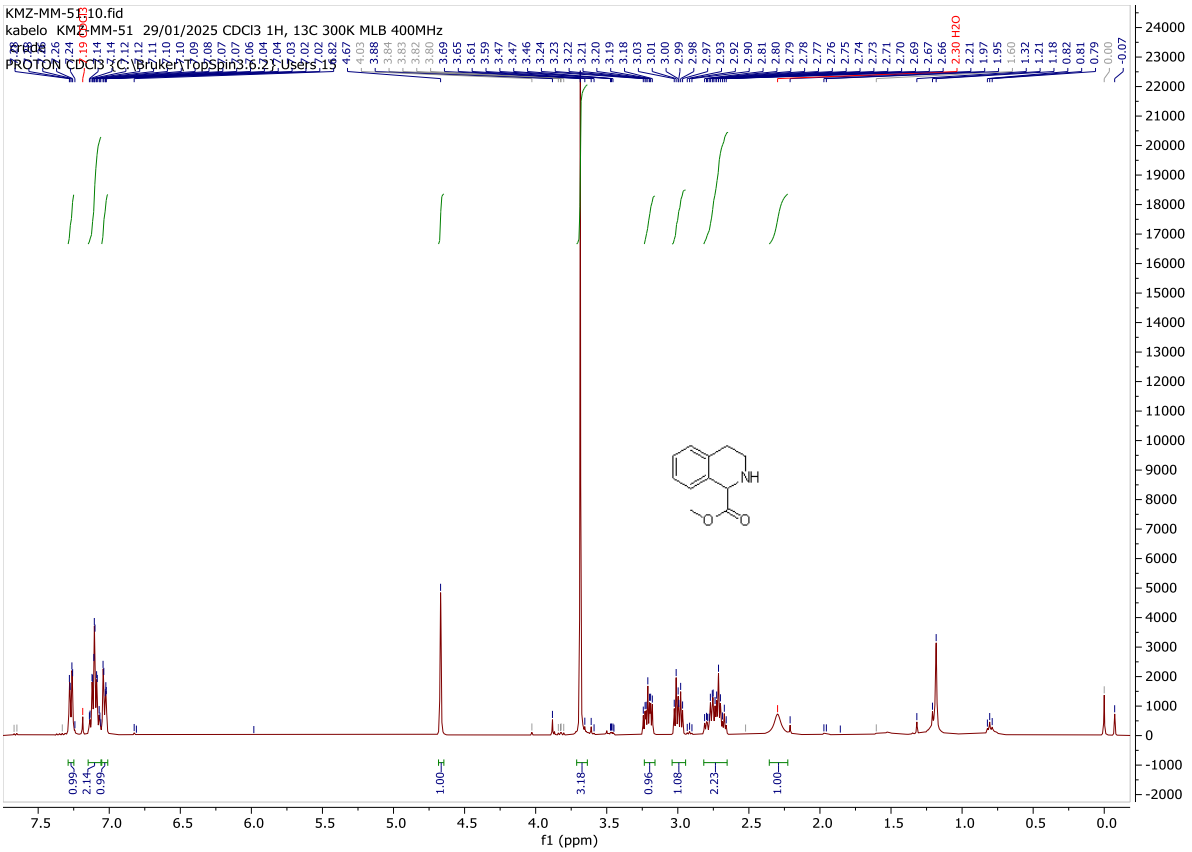

Figure 37: ^{1}H NMR spectrum of **71**.

As anticipated, the 4 aromatic proton signals appeared as a doublet at 7.39 ppm, integrating for one proton and a multiplet at 7.20 ppm, integrating for three protons. The proton attached to the stereogenic centre appeared at 5.33 ppm. The two -CH_2- proton signals attached to the carbon atoms between the phenyl group and the nitrogen atom appeared at 3.47 ppm and 2.97 ppm as multiplets, integrating for two protons each. The methyl ester protons appeared at 3.71 ppm as a singlet and integrating for 3 protons. The ^{13}C spectrum was similar to that observed for the reaction detailed in Scheme 79, since they are the same compounds. Again, HPLC-MS (m/z) revealed that the theoretical molecular mass of 192.1025 g/mol ($C_{11}H_{13}NO_2$) for **71** matched to that obtained experimentally, which was 192.1023 $[M + H]^+$, as shown in Fig. 38

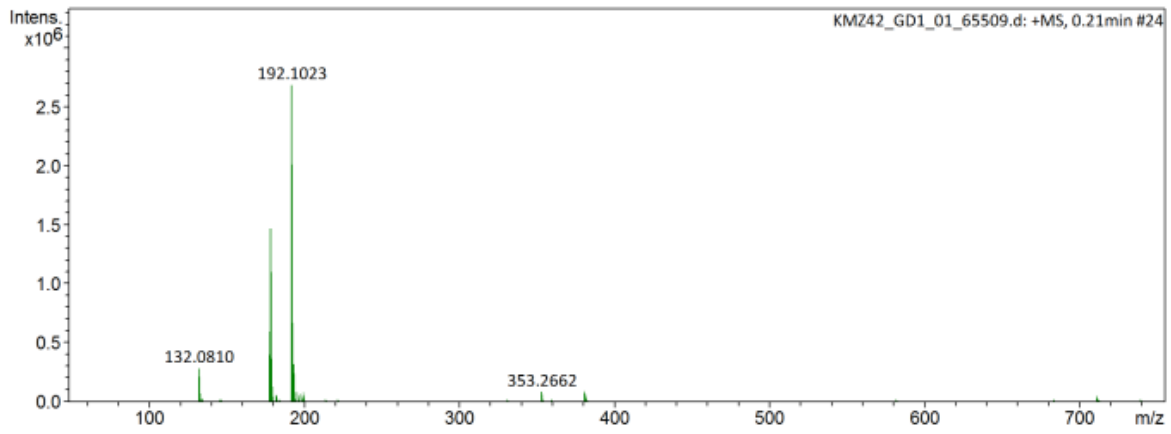

Figure 38: HPLC-MS (m/z) spectrum of compound **71.**

The purpose of preparing the PZQ intermediates **71** and **72** was pivotal for the enzymatic reactions that would follow in the next section. Retrospectively, the preparation of the said intermediates proved to be a challenging endeavour, where we saw that the preparation **72** returned meagre yields, whilst the preparation of **71** involved more steps when compared to **72**. The preparation of **71**, albeit in many steps, returned appreciable yields and enabled us to attempt the enzymatic reactions discussed in the next section.

2.2 Enzymatic reactions

Thus far, an in-depth discussion on the synthetic strategies used to make PZQ intermediates has been provided. Equally important, is the discussion on enzymatic reactions, given that the entire basis of the project hinged on the use of enzymes to effect chemical transformations that historically relied on classical chemistry.[38,78] The synthetic strategies explored in section **2.1** were chosen for their suitability in the preparation of intermediates that would be amenable to enzyme reactions. Discussed herein, are interesting findings that have been uncovered.

2.2.1 Enzymatic hydrolysis of PZQ intermediates

The chemical reactions that led to the desired PZQ intermediates, particularly **2.1.1**, **2.1.2**, and **2.1.5** availed the intermediates in poor to moderate yields in a range of 50-100 mg. Nonetheless, there was enough material to make a meaningful attempt at understanding the interaction of the enzymes and the intermediates. Prior to the study of the reactions of the enzymes and substrates in question, a test reaction was set up to ascertain if the enzymes are still active since they tend to lose activity over time. Mathebula *et al.*[142] conducted an extensive study on the enzymatic kinetic resolution of Morita-Baylis-Hillman (MBH) derivatives using various lipases. They were able to show that several lipase preparations showed a remarkable prowess

in the hydrolysis of MBH derivatives to give products with excellent enantiomeric excess values.

2.2.1.1 Preparation of Lipase enzymes test substrate

To test the activity of the enzymes we had at our disposal, we first had to synthesise the test substrate. The ideal test substrate was informed by the successful hydrolysis of esters prepared by Mathebula *et al.*[142] One such ester, 1-(4-bromophenyl)-2-cyanoallyl acetate **117**, was shown to be particularly amenable to hydrolysis. Additionally, this substrate was resolved in the least amount of time when contrasted with similar analogues, resulting in excellent enantiomeric excess of the now resolved secondary alcohol. These experimental findings made it ideal for this study to use **117** as the test substrate. The synthesis of **117** is a two-step reaction that seeks to prepare the MBH adduct from 4-bromobenzaldehye **113** and acrylonitrile **114**, whose product **115** is reacted with acetic anhydride **116** (Scheme 78).

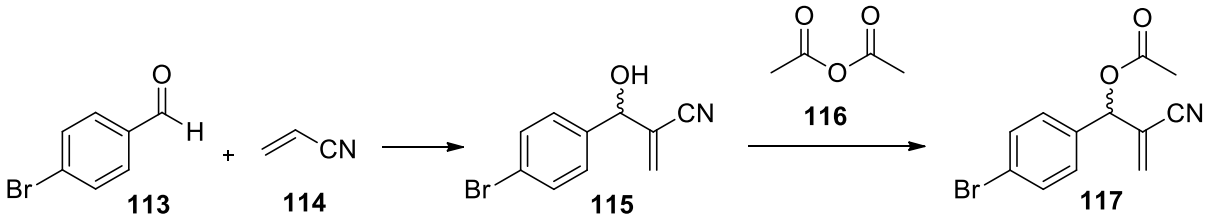

Scheme 78: Two step synthesis of lipase enzyme test substrate.

The MBH adduct **115**, was prepared from a solvent-less reaction of 4-bromobenzaldehyde **113** and acrylonitrile **114** in the presence of DABCO, as shown in Scheme 79. ^{1}H and ^{13}C NMR spectroscopic analysis of compound **115** pointed to a successful synthesis, yielding the MBH adduct **115** in 70 %. Looking at the ^{1}H NMR spectrum, the four aromatic protons appeared as two doublets, integrating for two protons each at 7.53 ppm and 7.27 ppm.

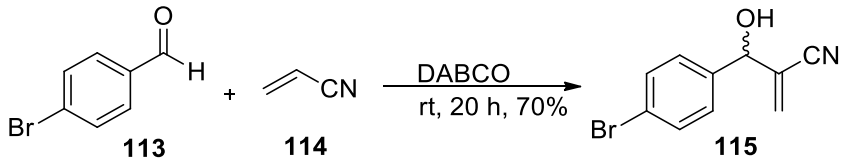

Scheme 79: Morita-Baylis-Hillman reaction.

This was followed by 2 alkene protons appearing as two singlets at 6.11 ppm and 6.04 ppm. The proton attached to the stereogenic carbon appeared at 5.27 ppm and the -OH proton appeared as a broad peak at 2.65 ppm. From the ^{13}C NMR spectrum, 6 aromatic carbon signals appeared between 138.1 ppm and 123.6 ppm. The alkene carbons appeared at 130.2 ppm and

125.9 ppm. The nitrile carbon signal appeared at 116.7 ppm. Lastly, the stereogenic centre carbon signal appeared at 73.6 ppm. These signals were similar to those reported by Mathebula and co-workers;[142] their 4 aromatic protons appeared at 7.55-7.50 ppm and 7.29-7.23 ppm as multiplets. The alkene doublets appeared at 6.10 ppm and 6.03 ppm. The proton attached to the stereogenic carbon appeared at 5.26 ppm and the hydroxyl proton appeared at 2.81 ppm. For the carbon NMR spectrum the aromatic signals were in a range of 138.1-122.9 ppm, along with the two alkene carbons. The nitrile carbon appeared at 116.6 ppm and the stereogenic centre carbon signal appeared at 73.5 ppm.

The MBH acetate **117** was obtained from the reaction of the MBH adduct **115** and acetic anhydride **116** in the presence of DMAP and triethylamine in 2-methyltetrahydrofuran. The reaction was left to stir at room temperature for an hour and isolated to give **117** in 81 % as shown in Scheme 80.

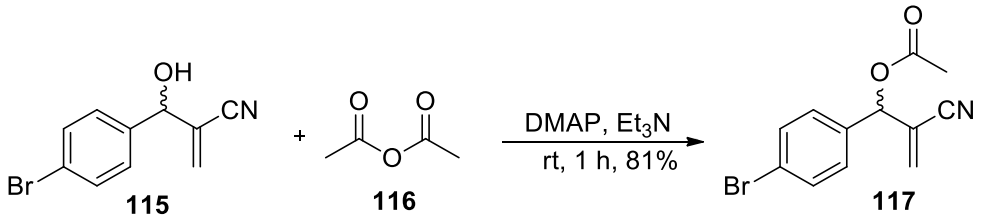

Scheme 80: Synthesis of MBH acetate **117**.

The ^{1}H NMR spectrum obtained from compound **117** was similar to that of **115**, only with the disappearance of the hydroxyl proton and the appearance of the -CH_3 peak at 2.18 ppm. The aromatic protons appeared as two doublets at 7.55 ppm and 7.28 ppm, both integrating for 2 protons. The alkene singlets appeared at 6.28 ppm and 6.10 ppm, both integrating for one proton each. The proton attached to the stereogenic centre carbon appeared at 6.02 ppm and the -CH_3 protons appeared at 2.18 ppm.

For the ^{13}C NMR spectrum, the carbonyl carbon appeared at 169.2 ppm. The aromatic signals were in a range of 134.7 ppm to 122.6 ppm. The two alkene carbon signals appeared at 132.4 ppm and 123.5. The nitrile carbon appeared at 115.9 ppm and the stereogenic carbon signal appeared at 73.8 ppm. Lastly, the -CH_3 protons appeared at 20.9 ppm. Similar proton and carbon NMR signals were obtained by Mathebula *et al*;[142] the aromatic protons appeared as doublets at 7.54 ppm and 7.28 ppm, both integrating for 2 protons each. The proton attached to the stereogenic centre appeared at 6.328 ppm, and the two alkene protons appeared at 6.10 ppm and 6.03 ppm as singlets, integrating for one proton each. Lastly, the methyl protons

appeared at 2.18 ppm, appearing as a singlet and integrating for 3 protons. For the carbon signals, the carbonyl carbon signals appeared at 169.0 ppm, followed by the 6 aromatic carbon signals in the range of 132.2-122.6 ppm along with the two alkene protons. The nitrile carbon appeared at 115.8 ppm and the stereogenic centre carbon appeared at 73.6 ppm. Lastly, the methyl group carbon attached to the carbonyl carbon appeared at 20.8 ppm.

2.2.1.2 Lipase enzyme activity test reaction

The experimental data pointed to the successful synthesis of the MBH acetate **117**, which was then used to test whether the enzymes were still active. Due to the availability of the substrate **117** prepared, only 3 enzymes were tested for activity; *Pseudomonas cepacea* lipase (PCL) (I), *Candida antarctica* A (CAL A) (II), and Novozyme 435 (III) were lipases chosen for the hydrolysis of the MBH acetate **117** (Scheme 81).

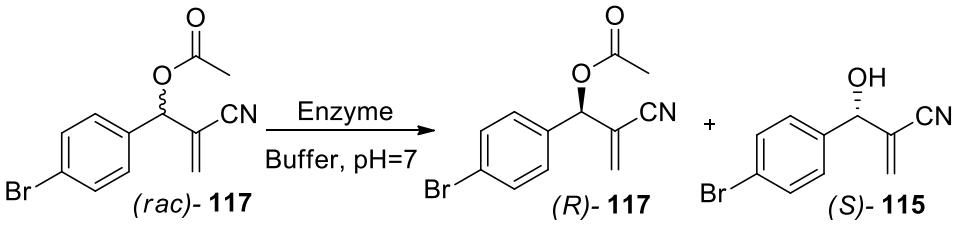

Scheme 81: Enzymatic kinetic resolution of **117.**

For the hydrolysis reactions, two small scale reactions, one containing the enzyme and substrate in a phosphate buffer of pH = 7 and one without the enzyme as a control reaction were set up and incubated at 28 °C. This was done for all three enzyme reactions. Using TLC to follow the reactions, all enzymes exhibited activity over 48 hours. This observation was seen when the control reaction was spotted on the TLC plate against the reaction that contained the enzyme. Over 48 hours, the control reaction did not show any change, however, the reactions with the enzyme showed two spots on the TLC plate. This indicated that the chosen enzymes were catalysing the hydrolysis of **117**. One additional observation made was that Novozyme 435 (III) started exhibiting the hydrolysis of **117** in the first 24 hours of the reaction, which is not surprising given the fact that Novozyme 435 is a robust lipase enzyme.[143]

Now that it had been established that the enzymes were still active, we were one step closer to subjecting the PZQ intermediates prepared in this study to enzymatic hydrolysis reaction conditions reported by Mathebula and co-workers. Prior to setting up the enzyme reactions, a literature review on enzyme work was done and this revealed that Paal *et al*[47] have done extensive work on enzymatic kinetic resolution of tetrahydroisoquinoline derivatives, and so it

was crucial to ascertain whether there could be some valuable lessons learned from this earlier work.

2.2.1.3 PZQ intermediates enzymatic kinetic resolution

The work done by Paal and co-workers involved the enzymatic kinetic and dynamic kinetic resolution of 1,2,3,4-tetrahydroisoquinoline-1-carboxylic acid **77**. Because they used the same starting material as us (**77**), their findings were particularly relevant. They were trying to obtain an amide analogue **118** of compound **72** enantioselectively using lipase CAL-B as the enzyme of choice. To their amazement, the aminolysis reaction generated a product they were not expecting; instead of the amide **118**, a hydrolysis product (*R*)-**77** was obtained (Scheme 82).

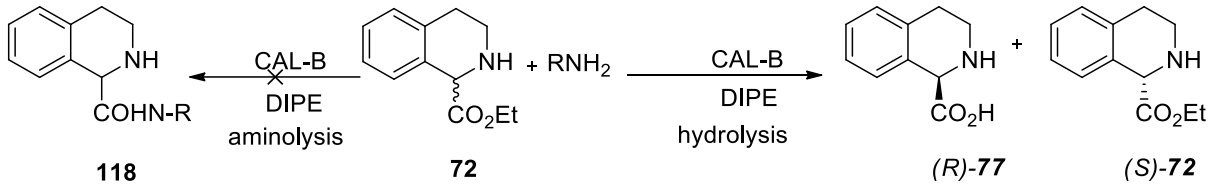

Scheme 82: Enzymatic kinetic resolution of (±) **72**, where R=Bu or Bz.

It is understood that the CAL-B (Novozyme 435) enzyme preparation, in its immobilized form, has considerable amounts of water adsorbed onto it. Under these conditions, the CAL-B enzyme makes use of the adsorbed water to hydrolyze the carboxylic acid ester moiety. Further analysis of the reaction media revealed to them that the hydrolysis reaction proceeded slowly, showing rates of ≤ 5% in 24 h, however, they observed no signs of a competing aminolysis reaction. Seeing that these conditions yielded the enantiopure acid (*R*)-**77** in a shorter period, albeit still in small quantities, the next obvious step was the optimization of the hydrolysis reaction.

During the optimization reaction of the kinetic resolution of **72**, Paal and co-workers went on to report insightful observations that became critical for us to avoid. One important observation made was that the use of basic compounds led to the racemization of the less reactive enantiomer, thus reducing the enantiomeric ratios (*E*) over time. The enantiomeric ratio (*E*) is a measure of the enantioselective properties of an enzyme, which represents how well an enzyme resolves a chiral compound.[144] It is a representation of the intrinsic selectivity of the enzyme, which speaks to uniqueness of its catalytic abilities. In simple terms, a large enantiomeric ratio means an enzyme can catalyze the resolution of one enantiomer over the other in a racemic mixture, selectively. Another parameter that is used when speaking about asymmetric catalysis is enantiomeric excess (*ee*), which speaks to how efficient the

enantioselective reaction is under the influence of the enzyme in question.[145] This parameter, expressed in percentages, tells us how much of one enantiomer exists in solution over the other enantiomer.

Paal and co-workers observed that, in the presence of benzylamine, the enantiomeric ratios (E) were observed to decrease from 35 at 52% conversion after 16 h of reaction time to 23 at 55% conversion after 40 h of reaction time. The effect of basicity on the racemization was also seen when the compound was left to stand over time; the drop in *ee* of *(S)*-**72** with time even in the absence of CAL-B pointed to the self-racemization of the resolved starting material, which alluded to the basic nature of the compound itself. Thus, for a fully optimized kinetic resolution reaction of **72**, basic reagents should be avoided. No racemisation of the resolved carboxylic acid product **77** was observed.

The work done by Paal and co-workers was particularly useful to us, in that it provided information about reaction conditions that were unlikely to yield the desired results. For example, they found that the use of CAL-A enzyme adsorbed on Celite and sucrose, led to extremely slow conversion, even at an elevated temperature of 47 °C. Additionally, using basic conditions led to racemization.

Both Mathebula *et al* and Paal *et al.* provided some invaluable insights that assisted us in setting up the enzyme reactions for PZQ intermediates prepared in this study. Between the two methods used by these researchers, the method used by Mathebula and co-workers proved to be much simpler and easier to execute.

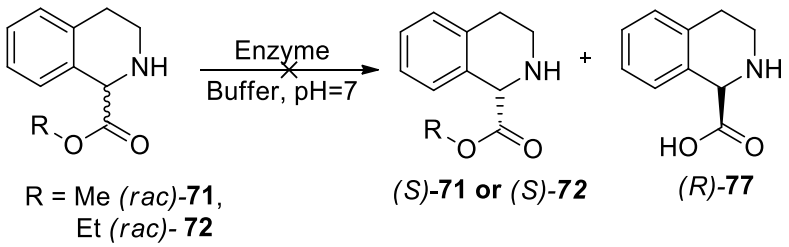

Scheme 83: Attempted enzymatic hydrolysis of PZQ intermediates **71** and **72**.

In Eppendorf tubes, 8 mg of enzyme in a phosphate buffer (0.1M pH = 7, 950 µl) was mixed separately with substrates **71** and **72** (8 mg) dissolved in 50 µl of acetone (Scheme 83). The control reactions were also set up in the same manner, but without enzymes. The resulting mixtures were incubated for 48 hours at 28 °C. This was done for the following enzymes: *Pseudomonas cepacea* lipase (PCL) (I), *Candida antarctica* A (CAL A) (II), and Novozyme

435 (III). Regular monitoring of the enzyme reactions using TLC plates did not point to any hydrolysis taking place. To improve the solubility of some of the enzyme reactions, substrate *(rac)*-**71** was introduced into the buffer as a hydrochloride salt, allowing better dissolution into the aqueous nature of the buffer, and thus removing the need for using acetone, however, no hydrolysis was observed using this approach either.

We then moved on to test other esters that we had prepared and this revealed some interesting results. For example, subjecting compound **112** to the same enzymatic reaction conditions using all three enzymes as shown in Scheme 84 did not lead to any hydrolysis of the substrate. This observation is consistent with what other researchers have reported, that lipase enzymes generally are unable to resolve compounds with bulky groups next to the site of resolution.[146]

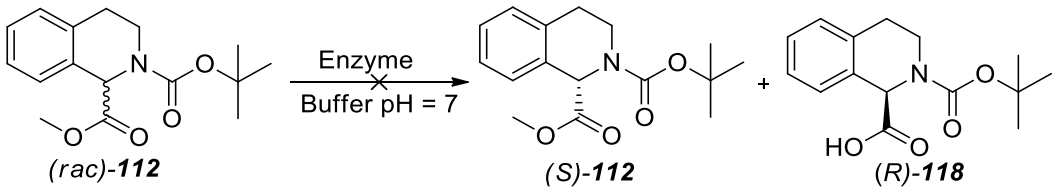

Scheme 84: Unsuccessful EKR of bulky compound **112.**

One last attempt was made to see if any of the enzymes would be able to hydrolyse aromatic isoquinoline compound **97** to its carboxylic acid **78** analogue (Scheme 85). The enzyme tested was Novozyme 435, owing to its demonstrated success of hydrolysis in other studies of similar compounds. TLC analysis revealed that there was some hydrolysis taking place in the first 24 hours of the reaction. It is important to mention that the control reaction was also monitored using TLC analysis, which revealed that no hydrolysis had taken place in the first 48 hours.

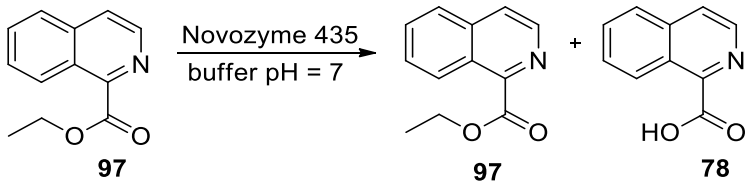

Scheme 85: Successful enzymatic hydrolysis of ester **97** to its carboxylic acid analogue **78**.

The promising result observed for the lipase-catalysed hydrolysis of isoquinoline derivative **97** at small scale led to the decision to scale up the reaction and isolate the products. The reaction was scaled up to 127 mg of the ester **97** and 127 mg of Novozyme 435 in a phosphate buffer of pH = 7. The resulting mixture was left to stir at 28 °C for 19 hours. The reaction mixture was extracted with ethyl acetate. Removing ethyl acetate under reduced pressure and spotting

the concentrated organic phase on a TLC plate revealed two distinct spots, presumably that of the unreacted ester and the newly formed carboxylic acid. The pH of the reaction mixture was then lowered to 5, in an attempt to protonate any carboxylic acid that may have remained in the aqueous phase. Indeed, reducing the pH to about 5 using 2M HCl and extracting the resulting aqueous phase with ethyl acetate yielded more carboxylic acid. For purification, a preparatory TLC plate was used to separate the ester and the newly formed carboxylic acid.

Running a ^{1}H NMR spectrum of the crude ester isolated from the enzyme reaction revealed the expected peaks as shown in Figure 39. The ester was not purified any further, to prevent material loss. The NMR spectrum shown in blue is the ester **97** prepared in section **2.1.3**.

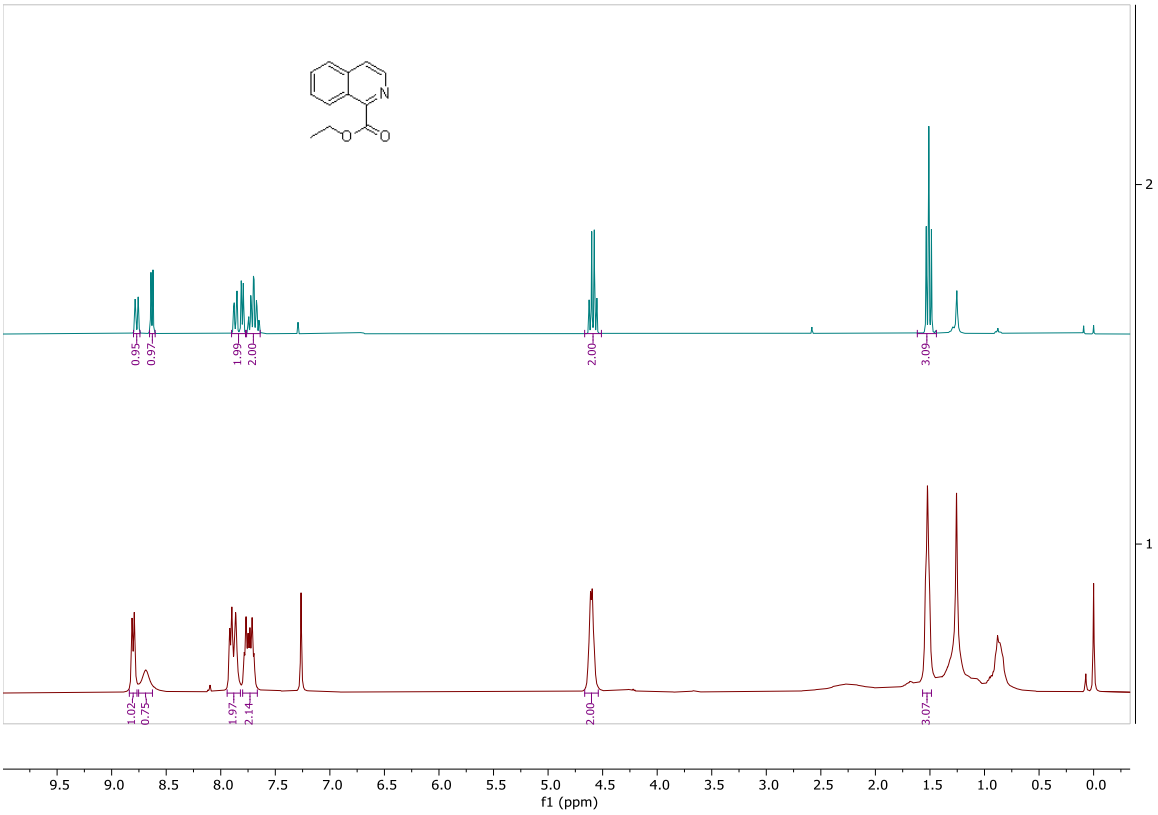

Figure 39: Stacked spectra of ester **97** prepared in section **2.1.3** (top) and ester isolated from enzyme reaction (bottom).

The spectrum in brown is the crude ester isolated from the enzyme reaction. From the stacked spectra shown in Figure 39, it is evident that these are the same compounds, albeit the one in brown is present in crude form and the resolution of the signals is not as good as that for the clean material.

NMR analysis of the carboxylic acid **78** obtained from the preparatory TLC plate revealed the expected result. This ^{1}H NMR spectrum was compared to that of a commercially obtained sample of **78**. Stacking the two spectra revealed that the hydrolysis reaction had indeed taken place and the second material recovered from the preparatory TLC plate was the carboxylic acid **78** (Figure 40).

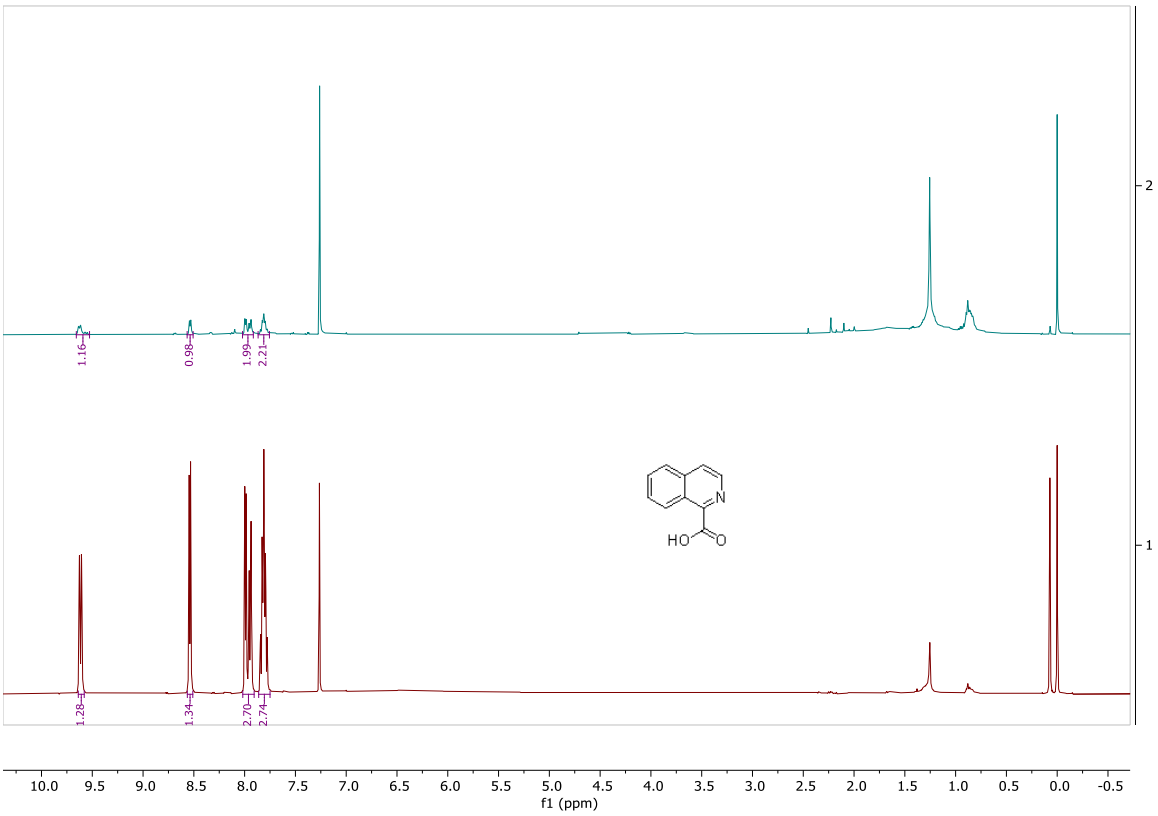

Figure 40: Stacked spectra of carboxylic acid **78** obtained commercially (bottom) and carboxylic acid **78** isolated from the enzyme reaction (top).

The ^{1}H NMR spectrum in brown is the spectrum of the carboxylic acid obtained commercially, while the one in blue was extracted from the enzyme reaction. Looking at the stacked spectra, it is evident that these two compounds are the same, and thus it can be concluded that there is sufficient evidence to believe that lipase enzymes can catalyse the hydrolysis of unsaturated isoquinoline derivatives.

It is important to mention that the hydrolysis of the ester **78** is not what was envisaged during the commencement of the project. Originally, we aimed to resolve partially saturated isoquinoline intermediates, particularly those presented in section **2.1.1**, **2.1.2**, and **2.1.5**. All the attempts to hydrolyse these compounds returned disappointing experimental results.

However, the observed hydrolysis of ester **97** is a welcomed results and inspires hope that investigating alternative reaction conditions and the use of other lipase enzyme preparations will ultimately lead to successful lipase-catalysed resolution of these compounds.

2.2.2 Biosynthesis of INH intermediate

The commercial success of Nitrile hydratase enzyme can be attributed to the problematic conversion of the nitrile functional group to its amide analogue using classical chemistry.[98,147] Prior to the use of biocatalysis for this conversion, this reaction was primarily facilitated by an acid or a base. The problem associated with the latter methods involved the uncontrollable conversion of the amide to a carboxylic acid analogue, which was often a fast reaction and thus hard to circumvent. To inhibit carboxylic acid formation, heterogeneous catalysis has been applied in these reactions, particularly metallic copper catalysts.[148] However, we decided to embark on a greener approach.

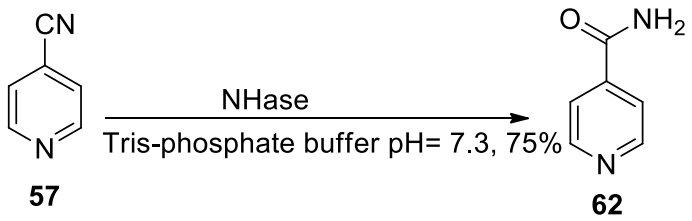

Scheme 86: Biocatalyic synthesis of INH intermediate **62**.

As already described in section **1.4.2**, the wide substrate scope of the nitrile hydratase enzyme, as demonstrated by Mashweu *et al,*[99] has led us to hypothesize that 4-cyanopyridine **57** would most likely be amenable to nitrile hydratase hydrolysis of the nitrile to the amide analogue. Indeed, this has been proven true by Cantarella *et al* when they converted 3-cyanopyridine **57** to nicotinic acid **62** using a NHase enzyme.[149] In our study, 50 mg of NHase enzyme and 50 mg of 4-cyanopyridine **57** dissolved in acetone were mixed in a 2 mL Eppendorf tube containing a Tris-phosphate buffer of pH = 7.3 (Scheme 86). The resulting mixture was then incubated at 30 °C for 3 hours and monitored using TLC chromatography. After 3 hours, the mixture was worked up with water and ethyl acetate, and the organic layer was removed under reduced pressure. The resulting mixture was purified by column chromatography using 90% ethyl acetate: 10% methanol and the percentage yield of the amide product **62** was worked up to be 75%.

To enhance our understanding of the NHase enzyme reaction, additional studies were conducted where we were interested in the optimal enzyme to substrate ratio for maximal

amide conversion in the least amount of time. From these studies, it became clear that the optimal conditions were when the mass ratio of substrate to enzyme did not exceed 6:1. For a rapid conversion, the best conditions would be a 1:1 ratio of substrate to enzyme as shown in Table 5 below.

Table 5: Performance of the enzyme activity relative to the substrate load

Substrate to enzyme ratio	Reaction Time (h)
1:1	3
6:1	24-48
12:1	>12 days

This reaction proved to be relatively facile, offering good yields and ease of reaction. The yield of 75% pointed to the polarity of the resulting amide **62**, which was relatively hard to leach from the stationary phase, as is seen by the use of a 90% EtOAc: 10% MeOH polar mobile phase. Nonetheless, the objective of using NHase to transform 4-cyanopyridine **57**, a relatively cheap reagent, to its amide analogue **62**, which is an intermediate to isoniazid **53**, was successful.

Chapter 3: Conclusions and future work

The project aimed to develop eco-friendly methods for the synthesis of known anti-schistosomal and anti-TB chemotherapies, particularly enantiopure praziquantel (*R*-PZQ) and isoniazid (INH), using enzyme catalysis. Pivotal to this was the successful synthesis of key intermediates for both compounds, which formed the starting point for biocatalysis reactions. The key intermediates of PZQ were synthesized according to five synthetic strategies.

The first synthetic strategy was chosen for its ability to yield diverse bioactive products in just one reaction step. This one-pot reaction, called the Ugi multicomponent reaction (UMCR) usually occurs between an amine, a carboxylic acid and an isocyanide. When the reaction was initially attempted, the experimental data did not point to the desired products. This was attributed to the failure of iodoxybenzoic acid (IBX) **86** to oxidize the amine **49** into its imine **75** analogue *in-situ*. Instead, success was achieved by synthesizing the imine **75** intermediate *ex-situ* using a bromosuccinimide (NBS) mediated oxidation of the amine **49**. The resulting imine **75** underwent the Ugi reaction with benzoic acid **73** and two different isocyanides **74a** and **74b** to yield cyclohexyl carboxamide **76a** and *tert*-butyl carboxamide **76b** in 78% and 83% yields respectively (Scheme 87).

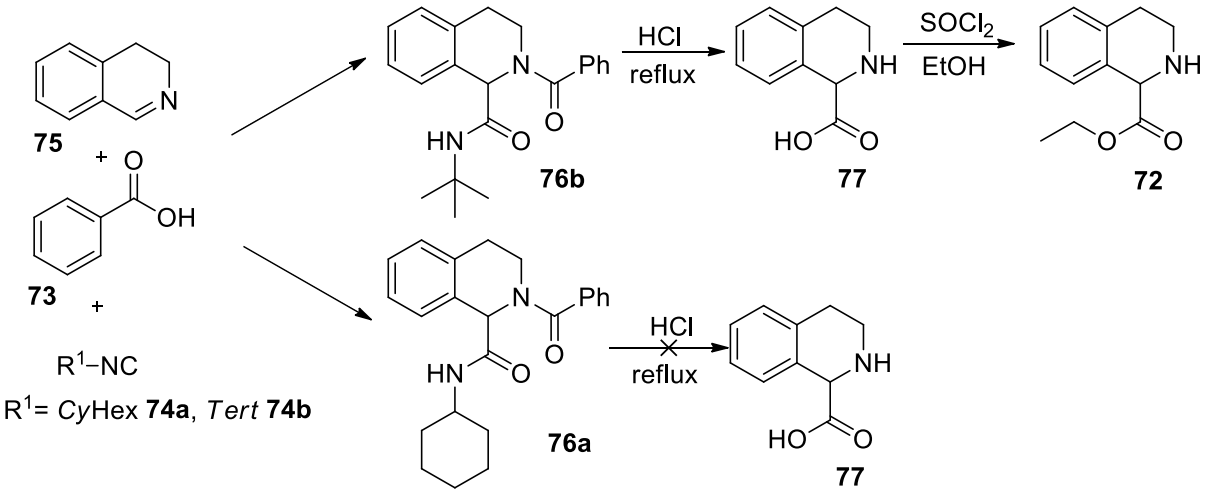

Scheme 87: Schematic summary of the first synthetic strategy.

The hydrolysis of the two carboxamides **76a** and **76b** was attempted using hydrochloric acid, which resulted in the successful conversion of the *tert*-butyl carboxamide **76b** to the desired tetrahydroisoquinoline-1-carboxylic acid **77** in 57% yield, while cyclohexyl carboxamide **76a** remained unchanged. We attributed this selectivity to the stability of the resulting ammonium ion that forms during hydrolysis, which is given additional stability by the *tert*-butyl group as

opposed to the cyclohexyl group. Subsequent to this was the esterification of the generated carboxylic acid **77** with thionyl chloride in ethanol. This reaction availed lower yields of the ethyl ester **72** due to the possible side reactions and the difficulty of transforming zwitterionic species.

To overcome the challenges encountered in the first approach, the second synthetic strategy sought to partially hydrogenate isoquinoline-1-carboxylic acid **78**, followed by the subsequent esterification reaction of the resulting tetrahydroisoquinoline-1-carboxylic acid **77**. In our second attempt, Pd/C was initially chosen as the catalyst of choice due to its versatility in hydrogenation reactions. However, the hydrogenation reaction did not yield the expected result, and this was likely due to the poisoning effect of nitrogen-containing compounds on Pd/C based catalysts. Pt(IV) oxide, otherwise referred to as Adams catalyst, showed promise, particularly because of its demonstrated ability to hydrogenate inert heterocyclic hydrocarbons, and its ubiquitous use in literature. The hydrogenation of isoquinoline-1-carboxylic acid using PtO_2 under hydrogen atmosphere yielded tetrahydroisoquinoline-1-carboxylic acid **77** in moderate yields of 53-61%. The optimisation studies revealed that the catalyst's weight percentage and reaction time had slight effects on the overall yield, with the data suggesting that to produce the hydrogenated product optimally, one would need 10-15% catalyst load and a reaction time of 18-24 hours. During work-up, challenges arose regarding the solubility of the tetrahydroisoquinoline product in methanol and water, leading to the loss of product during extraction. Despite these challenges, successful synthesis of the desired compound was confirmed through ^{1}H and ^{13}C NMR spectroscopy. The esterification reaction of the synthesized acid **77** using thionyl chloride in ethanol or the Steglich esterification method produced low yields of the desired ester product **72**. This discouraging result can be likened to that observed in the first synthetic approach (Scheme 88).

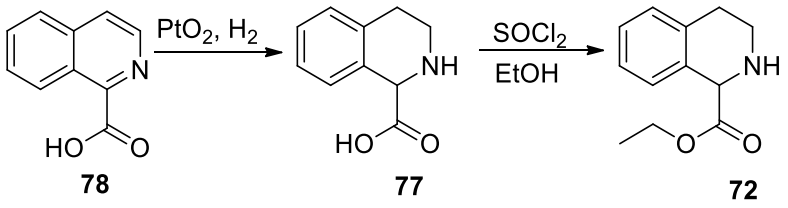

Scheme 88: Schematic summary of the second synthetic strategy.

The third strategy recognised challenges associated with esterifying tetrahydroisoquinoline-1-carboxylic acid **77** and sought to mask the free base moiety of the molecule in an effort to facilitate esterification. It was envisaged that starting with the esterification reaction of **78**, the

fully aromatic isoquinoline, would mask the effects of the amine, making it less likely to interfere with the esterification reaction. Indeed, the esterification of **78** was successfully achieved using thionyl chloride in absolute ethanol, yielding the desired ethyl ester **97** in 75% yield. However, attempts to hydrogenate **97** to obtain **72** were unsuccessful. Instead, hydrogenation occurred selectively at the phenyl ring, yielding undesired compound **98**, which was confirmed by NMR analysis. Despite variations in reaction conditions and catalysts (including PtO_2 and Rh/C), the desired hydrogenation product could not be obtained (Scheme 89).

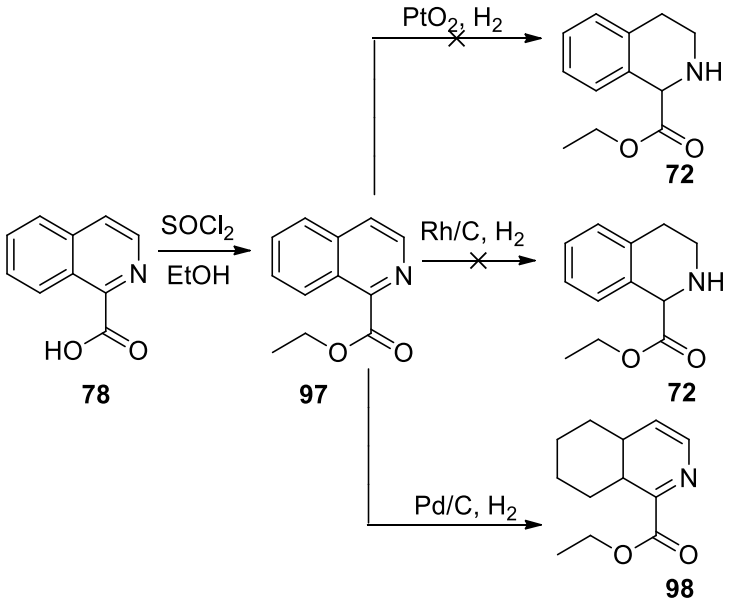

Scheme 89: Schematic summary of the third synthetic strategy.

Seeing that the first three synthetic approaches aimed at preparing the PZQ intermediate were problematic, with only a maximum of 17% yield of the desired ester **72** achieved in the first two strategies, and the third strategy encountering difficulties in the hydrogenation step, the project shifted towards alternative synthesis methods, with a particular interest in aromatic functinalisation chemistry. To prepare isoquinoline scaffolds using aromatic functionalisation chemistry, a number of eponymous reactions exist, however, the famous reactions for this transformation are the Pictet-Spengler reaction and the Bichler-Napieralski reaction. Initially, we attempted the Pictet-Spengler reaction to prepare the isoquinoline scaffold using 3-methoxyphenethylamine **99** and glyoxylic acid monohydrate **100** to yield the isoquinoline scaffold **101**. However, this reaction did not yield the desired product, even after attempting a demethylation step of 3-methoxyphenethylamine **99** to the corresponding hydroxylamine **102** to enhance reactivity. The Bischler-Napieralski method was then attempted, utilizing various

phenethylamines **79a-c** and oxalates **80a-b** to form the corresponding oxoacetates **81a-c**. While successful in forming the oxoacetates **81a-c**, the yields were low, ranging from 16% to 41%, and unexpected *bis*-amides **103**, **105** and **106** were formed as side products. From the cyclisation reactions of **81a** and **81b**, only **81b** was successful in cyclising, yielding the desired isoquinoline scaffold **108** in 50% yield. Finally, we attempted the hydrogenation of the Bischler-Napieralski product **108** that survived the multistep synthesis; however, we did not succeed in attaining the desired compound **108** (Scheme 90).

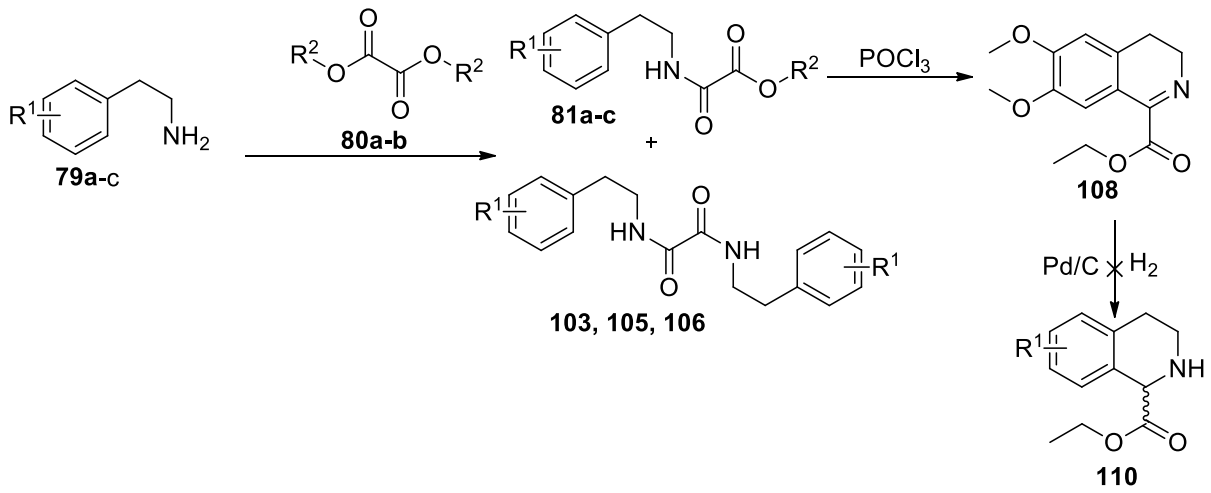

Scheme 90: Schematic summary of the fourth synthetic strategy.

The failures of the preceding strategies provided pockets of successes that, when assembled, gave rise to a meticulous approach to overcoming the challenges encountered in the preparation of the PZQ intermediates. In section **2.1.2** we learned that heterogeneous catalysis could be exploited to provide tetrahydroisoquinoline-1-carboxylic acid **77** in moderate yields of 53-61%. We later learned in section **2.1.3** that it easier to esterify the isoquinoline acid scaffold when the amine is masked, as was evidenced by the esterification of **78** to **97** in a good yield of 75%. The protection of the amine prior to the esterification seemed like the prudent method to adopt, and so the protection of the amine moiety of the partially hydrogenated isoquinoline acid **78** to give **77** was attempted using di-*tert*-butyl dicarbonate (Boc_2O). This reaction availed the protected product **111** in 89% yield, which was a step in the right direction. Subsequent to this was the esterification reaction, where conditions were chosen carefully so as not to deprotect the amine. A methylation reaction, over a classical esterification reaction would preserve the Boc protection and give an ester without risking the deprotection of the Boc group. The methylation of **111** using methyl iodide yielded methyl 1,2,3,4-tetrahydroisoquinoline-1-carboxylate **112** in 64% yield, indicating that the project was drawing closer to its objective of

preparing a PZQ intermediate. The successful installation of the ester meant the protection could now be removed from **120**, thus availing the highly desirable PZQ intermediate **71**. The Boc group was dislodged using trifluoroacetic acid in one reaction and hydrochloric acid in another, availing **71** in 65% and 69% respectively (Scheme 91). The success of these reactions was confirmed by proton NMR, carbon NMR and HPLC- MS.

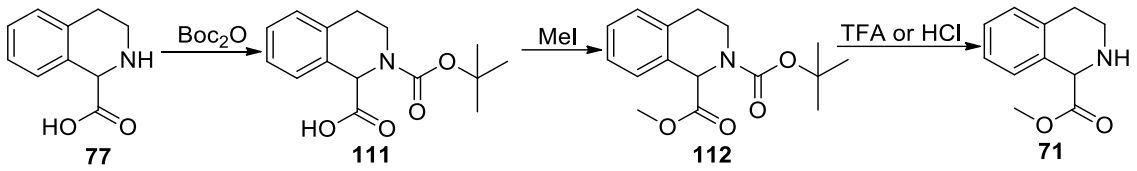

Scheme 91: Schematic summary of the fifth synthetic strategy.

The compounds prepared in sections **2.1.1**, **2.1.2**, and **2.1.5** were then subjected to enzymatic hydrolysis conditions. Prior to that, MBH acetate **117** was synthesised as a test substrate to test the activity of the enzymes that were used to catalyse the hydrolysis reactions (Scheme 92). The MBH adduct **115** was prepared by reacting 4-bromobenzaldehyde **113** and acrylonitrile **114** in the presence of DABCO. This was followed by the reaction of the resulting MBH adduct **115** with acetic anhydride **116** in the presence of triethylamine and DMAP.

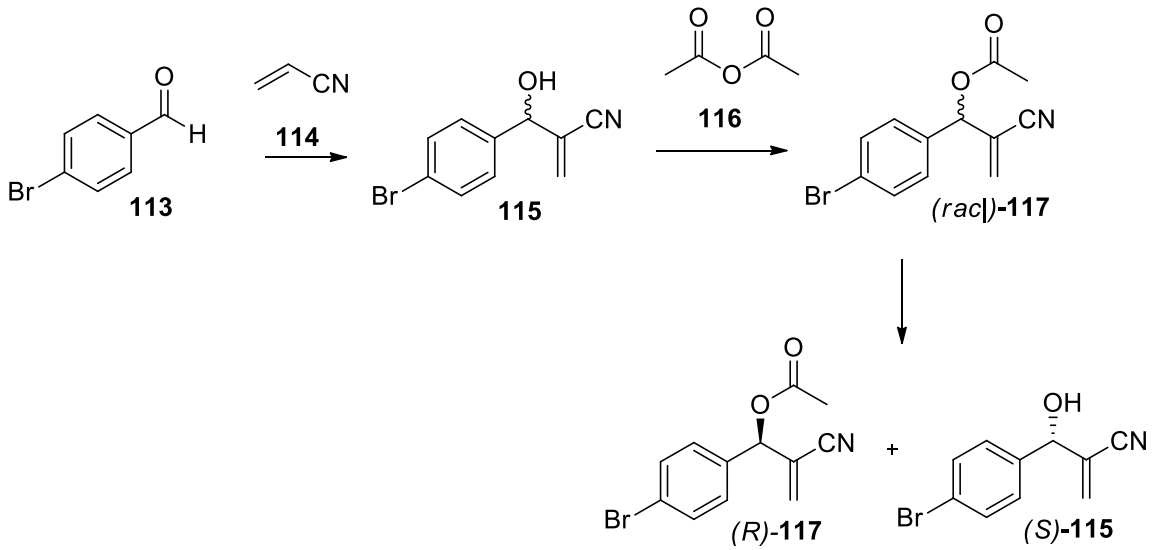

Scheme 92: Enzyme test substrate 2-step synthesis, followed by lipase catalysed hydrolysis.

Following the successful synthesis of the MBH acetate *(rac)*-**117**, three enzymes were tested for activity. These enzymes were *Pseudomonas cepacea* lipase (PCL) (I), *Candida antarctica* A (CAL A) (II), and Novozyme 435 (III). Following the enzyme reactions using TLC analysis and comparing them against their control reactions, all three enzymes showed activity. That is, the enzymes were catalysing the hydrolysis of the prepared MBH acetate *(rac)*- **117** to its

corresponding secondary alcohol **115**. An interesting observation made from the enzyme reactions was that the enzymes catalysed the hydrolysis reactions at varying speeds, where Novozyme 435 was far better at catalysing the hydrolysis reaction when contrasted with PCL and CAL-A.

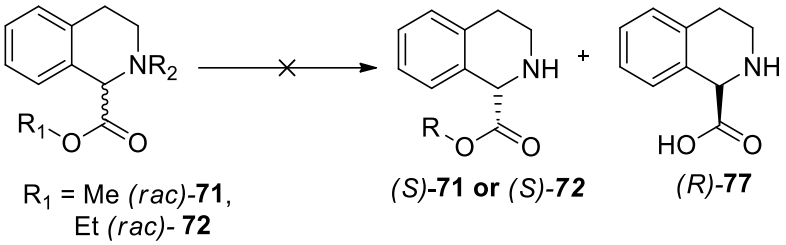

Scheme 93: Unsuccessful lipase-catalysed hydrolysis of PZQ intermediates **71** and **72**.

Following the confirmation of the activity of the three enzymes, the PZQ intermediates prepared (described in sections **2.1.1**, **2.1.2**, and **2.1.5**) were subjected to the same conditions as those of the test substrate (Scheme 93). Following the progress of the reaction over 48 hours using TLC analysis showed that there was no hydrolysis taking place. The TLC spots observed for each of the enzyme reactions on both PZQ intermediates **71** and **72** corresponded to the starting materials. These were the same as those observed from the control reactions.

An attempt was also made to hydrolyse **112** to its corresponding carboxylic acid (Scheme 94). The same conditions used for the test substrate were also used in this reaction. Following the reaction using TLC did not point to a successful hydrolysis of **112**. This was not an unexpected result since lipase enzymes are generally unable to resolve stereogenic centres that are next to bulky groups.

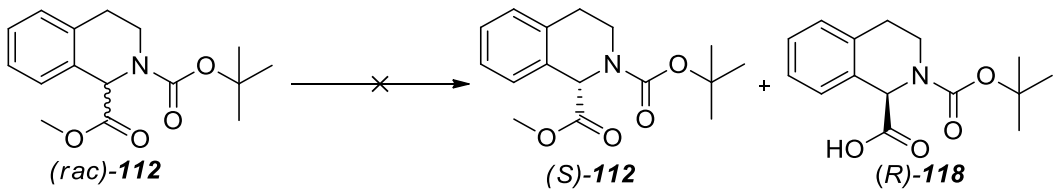

Scheme 94: Unsuccessful lipase-catalysed hydrolysis of PZQ intermediate **112**.

Looking at the work done in this study, there was one more PZQ intermediate that was prepared in section **2.1.3**, which could be tested for hydrolysis in the enzyme reactions. Compound **97**, which is an unsaturated version of a PZQ intermediate was then tested in the enzyme reaction. When a small-scale reaction was set up, using Novozyme 435, spotting the reaction material

on the TLC plate revealed that a hydrolysis reaction was taking place (Scheme 95). When the control reaction was also spotted on the TLC plate, only the starting material spot was observed. This meant that Novozyme 435 was catalysing the hydrolysis of the ester **97** to its corresponding carboxylic acid **78**.

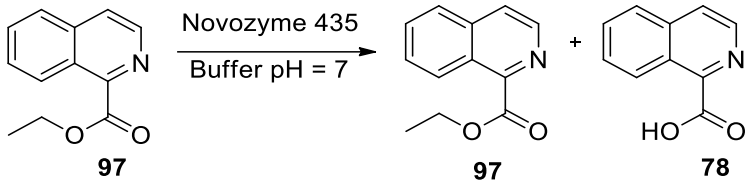

97 **97** **78**

Scheme 95: Successful enzymatic hydrolysis of ester **97** to its carboxylic acid analogue **78**.

The observation of one new spot with a lower R_f value compared to the spot of the starting material prompted us to scale up the reaction in an attempt to obtain sufficient material for isolation and analysis using NMR spectroscopy. Indeed, the scaled-up reaction provided enough material to run a crude proton NMR spectrum on both the ester **97** and the newly formed acid **78**, which then served as experimental evidence of hydrolysis. This was a promising result in that it provided evidence that, under the right conditions, PZQ intermediates are amenable to lipase-catalysed hydrolysis.

The synthesis of PZQ intermediates using various synthetic methods presented challenges, however, sufficient material was recovered and ultimately tested for enzyme hydrolysis. It is important to note that there is a need to investigate efficient ways to make intermediates of PZQ. One such method that could be explored in future is the use of flow chemistry, which has been recently reported to produce PZQ in excellent yield and purity.[150] To be specific, more focus should be given to the Bischler-Napieralski reaction; we have been able to demonstrate that it is possible to make the isoquinoline scaffolds using relatively cheap starting materials that were commercially available. There is also a need to investigate suitable conditions for enzyme reactions, particularly for the resolution of partially saturated isoquinoline analogues, which were not amenable to hydrolysis using the three enzymes tested in this study. A range of additional enzymes will need to be tested to identify those able to perform this transformation.

Chapter 4: Experimental procedures

4.1 General experimental procedures

All reagents were purchased from Sigma-Aldrich (Darmstadt, Germany) and were used without further purification. All solvents used for reactions and column chromatography were purified by distillation. THF and toluene were dried over sodium wire and distilled, with benzophenone as an indicator. CH_2Cl_2 and MeCN were distilled from calcium hydride. All other reagents and solvents for HPLC were obtained from commercial sources and used without further purification. Reactions were monitored using aluminium-backed Merck silica gel 60 F254 plates (Darmstadt, Germany). Purification of compounds by column chromatography was performed on normal silica gel (particle size 0.63–0.200 mm) or flash silica gel (particle size 0.040–0.063) purchased from Merck. ^{1}H and ^{13}C NMR spectra were recorded on either a Bruker AVANCE 300, 400 or 500 MHz spectrometer. Spectra were recorded in either deuterated chloroform, deuterated water, or deuterated methanol. The chemical shift values for all obtained spectra are reported in parts per million and referenced against TMS as an internal standard, which has a value of zero parts per million. Coupling constants are reported in Hertz. Small-scale enzymatic reactions were done on an Esco provocell TM microplate shaker. All melting points were obtained using a Stuart SMP10 melting point apparatus and are uncorrected. Infrared spectra were recorded on a Bruker Tensor 27 single channel infrared spectrometer.

4.1.1 Preparation of 3,4-dihydroisoquinoline (75)

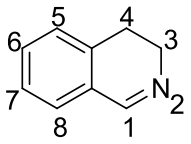

1,2,3,4-Tetrahydroisoquinoline (**49**) (2.503g, 18.97 mmol) was dissolved in CH_2Cl_2 (40 mL). NBS (3.714 g, 20.86 mmol, 1.1 equiv) was slowly added in portions over a period of 10 min and the reaction mixture was stirred for 30 min at room temperature. To this mixture 30% NaOH (12.65 ml, 5.0 equiv) was added, and the resulting biphasic mixture was stirred vigorously for 1 h. The organic layer was separated and washed with H_2O (25 ml) and 1 M HCl (25 mL). The acid extract was basified to pH = 10 with 1 M NaOH (55 mL) and the liberated oil was extracted with CH_2Cl_2 (2 × 100 mL). The organic portions were washed with sat. aq. NaCl (500 mL), dried over Na_2CO_3 and the volatile material removed *in vacuo*. The residue obtained was purified by flash column chromatography (CH_2Cl_2: MeOH 15:1)

furnishing compound **3,4-dihydroisoquinoline** (**75**) (1.820 g, 73%) as a yellow oil. R_f = 0.14 (CH_2Cl_2: MeOH 15:1). IR: (ν, cm^{-1}) 3019 (=C-H str.), 2935 (C-H str.), 1625 (C=N str.). ^1H NMR (400 MHz, $CDCl_3$) δ 8.34 (s, 1H, H-1), 7.36 (td, *J* = 7.1, 2.1 Hz, 1H, Ar-H), 7.33 – 7.28 (m, 2H, Ar-H), 7.16 (d, *J* = 7.3 Hz, 1H, Ar-H), 3.78 (td, *J* = 10.0, 2.2 Hz, 2H, H-3), 2.76 (t, *J* = 6.8 Hz, 2H, H-4). ^{13}C NMR (101 MHz, $CDCl_3$) δ 160.4 (C-1), 136.3 (Ar-C), 131.1 (Ar-C), 128.5 (Ar-C), 127.4 (Ar-C), 127.2 (Ar-C), 127.1 (Ar-C), 47.4 (C-3), 25.0 (C-2).

4.1.2 Preparation of 2-benzoyl-*N*-cyclohexyl-1,2,3,4-tetrahydroisoquinoline-1-carboxamide (76a)

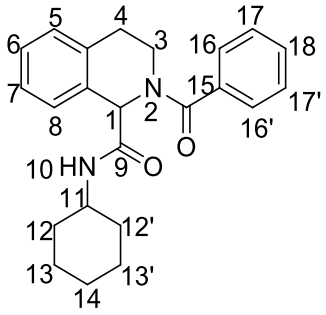

A solution of 3,4-dihydroisoquinoline (**75**) (329 mg, 2.50 mmol) and benzoic acid (**73**) (306 mg, 2.50 mmol) in abs. MeOH (15 mL) was stirred at room temperature for 30 min. Cyclohexyl isocyanide (**74a**) (273 mg, 2.50 mmol) was then added and the mixture was stirred at room temperature until complete consumption of the starting materials was indicated by TLC analysis (24-72 h). The solvent was removed by evaporation and the residue was purified by flash column chromatography (30% EtOAc: Hex). The oily product crystallized when dried under high vacuum to give **2-benzoyl-*N*-cyclohexyl-1,2,3,4-tetrahydroisoquinoline-1-carboxamide** (**76a**) (756 mg, 83%). Mp: 154-155 °C, lit[103] mp: 89 °C; IR: (ν, cm^{-1}) 3292 (NH str.), 2934 (C-H str.), 1650 (C=O), 1543 (NH bend). ^1H NMR (400 MHz, $CDCl_3$) δ 7.50 – 7.40 (m, 5H, Ar-H), 7.26 – 7.20 (m, 3H, Ar-H), 7.20 – 7.16 (m, 1H, Ar-H), 6.81 (d, *J* = 8.3 Hz, 1H, NH), 6.01 (s, 1H, H-1), 3.85 – 3.74 (m, 2H, H-3 & H-11 overlap), 3.67 (td, *J* = 12.3, 4.0 Hz, 1H, H-3), 3.06 – 2.94 (m, 1H, H-4), 2.93 – 2.78 (m, 1H, H-4), 1.91 (t, *J* = 14.9 Hz, 2H, CyHex), 1.74 – 1.65 (m, 2H, CyHex), 1.64 – 1.51 (m, 2H, CyHex), 1.45 – 1.31 (m, 2H, CyHex), 1.30 – 1.14 (m, 2H, CyHex). ^{13}C NMR (101 MHz, $CDCl_3$) δ 171.8 (C=O), 169.5 (C=O), 135.7 (Ar-C), 134.5 (Ar-C), 131.6 (Ar-C), 130.5 (Ar-C), 129.2 (Ar-C), 129.0 (Ar-C), 128.3 (Ar-C), 127.8 (Ar-C), 127.0 (Ar-C), 126.9 (Ar-C), 57.7 (C-1), 48.5 (CyHex-C), 43.8 (C-3), 33.2 (CyHex-C), 29.4 (C-4), 25.8 (CyHex-C), 24.9 (CyHex-C).

4.1.3 Preparation of 2-benzoyl-*N*-(*tert*-butyl)-1,2,3,4-tetrahydroisoquinoline-1-carboxamide (76b)

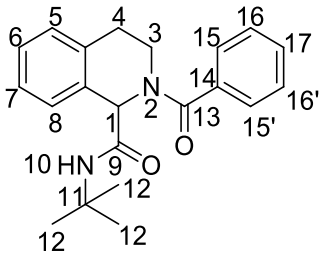

A solution of 3,4-dihydroisoquinoline (**75**) (328 mg, 2.50 mmol) and benzoic acid (**73**) (305. mg, 2.50 mmol) in abs. MeOH (15 mL) was stirred at room temperature for 30 min. *Tert*-butyl isocyanide (**74b**) (208 mg, 2.50 mmol) was then added and the mixture was stirred at room temperature until complete consumption of the starting materials was indicated by TLC analysis (24-72 h). The solvent was removed by evaporation and the residue was purified by flash column chromatography (50% EtOAc: Hex). The oily product crystallized when dried under high vacuum to give **2-benzoyl-*N*-(*tert*-butyl)-1,2,3,4-tetrahydroisoquinoline-1-carboxamide** (**76b**) (650 mg, 77%). Mp: 139-140 °C, lit[103] mp: 119 °C; IR: (ν, cm^{-1}), 3321 (NH str.), 2935 (C-H str.), 1656 (C=O), 1541 (N-H bend). ^{1}H NMR (400 MHz, $CDCl_3$) δ 7.45 (s, 5H, Ar-H), 7.26 – 7.20 (m, 3H, Ar-H), 7.20 – 7.15 (m, 1H, Ar-H), 6.73 (s, 1H, NH), 5.96 (s, 1H, H-1), 3.89 – 3.74 (m, 1H, H-3), 3.66 (td, *J* = 12.5, 4.0 Hz, 1H, H-3), 3.04 – 2.93 (m, 1H, H-2), 2.89 – 2.77 (m, 1H, H-2), 1.38 (s, 9H, H-12). ^{13}C NMR (101 MHz, $CDCl_3$) δ 171.5 (C=O), 169.5 (C=O), 135.4(Ar-C), 134.1 (Ar-C), 131.4 (Ar-C), 130.2 (Ar-C), 128.8 (Ar-C), 128.7 (Ar-C), 128.1 (Ar-C), 127.5 (Ar-C), 126.7 (Ar-C), 126.5 (Ar-C), 58.0 (C-1), 51.5 (C-11), 43.4 (C-3), 29.1 (C-4), 28.8 (C-12).

4.1.4 Preparation of 1,2,3,4-tetrahydroisoquinoline-1-carboxylic acid (77)

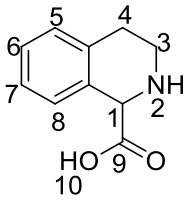

Method I

To compound **76b** (168 mg, 0.5 mmol) was added 10% HCl (5 mL), and the mixture was refluxed for 24 h. The excess aqueous HCl was removed *in vacuo* to give a brownish residue. The resulting residue was partitioned between water (10 mL) and ethyl acetate (10 mL). Water was removed from the aqueous extract *in vacuo* to give a beige solid. The resulting solid was

purified using column chromatography (50% MeOH: EtOAc) to give **1,2,3,4-tetrahydroisoquinoline-1-carboxylic acid** (**77**) (54.0 mg, 29%) as a white salt. Mp: 273-275 °C, lit[108] mp: 244-247 °C.

Method II

Isoquinoline-1-carboxylic acid (**78**) (1.008 g, 5.820 mmol) was dissolved in glacial acetic acid (33 mL) and PtO_2 (66.70 mg, 2.410 mmol) was added to the solution. The mixture was stirred under a H_2 atmosphere (7 bar) at 25 °C for 24 h. The catalyst was removed by filtration through a celite pad and rinsed with MeOH (10 mL) and acetic acid (10 mL). The filtrate was concentrated to dryness to give a light grey solid. The resulting solid was triturated using methanol and dried in an oven overnight. This yielded **1,2,3,4-tetrahydroisoquinoline-1-carboxylic acid** (**77**) as a white powder (625 mg, 61%). Mp: 254-255 °C, lit[120] mp: 269-271 °C.

IR: (ν, cm^{-1}) 3057 (=C-H str.), 2953 (C-H str.), 1606 (C=O). ^{1}H NMR (400 MHz, D_2O) δ 7.38 (d, *J* = 6.9 Hz, 1H, Ar-H), 7.28 – 7.18 (m, 2H, Ar-H), 7.15 (d, *J* = 6.9 Hz, 1H, Ar-H), 4.83 (s, 1H, H-1), 3.52 – 3.41 (m, 1H, H-4), 3.38 – 3.28 (m, 1H, H-4), 2.95 (t, *J* = 6.6 Hz, 2H, H-3). ^{13}C NMR (101 MHz, D_2O) δ 171.9 (C=O), 131.7 (Ar-C), 128.7 (Ar-C), 128.3 (Ar-C), 128.1 (Ar-C), 127.9 (Ar-C), 126.9 (Ar-C), 58.6 (C-1), 39.8 (C-3), 24.5 (C-4).

4.1.5 Preparation of ethyl 2-((3-methoxyphenethyl)amino)-2-oxoacetate (81a)

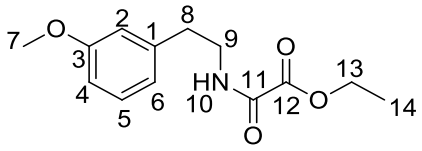

A mixture of 2-(3-methoxyphenyl)ethanamine (**79a**) (251 mg, 1.0 mmol) and diethyl oxalate (**80b**) (438 mg, 3.0 mmol) was stirred at 140 °C for 6 h. The ethanol formed and the excess diethyl oxalate were removed by distillation *in vacuo*, and the oily residue crystallized when treated with Et_2O, resulting in **ethyl 2-((3-methoxyphenethyl)amino)-2-oxoacetate (81a)**, as a crystalline product (82,3 mg, 33%). The crystals were collected by filtration, washed with Et_2O (10 mL), and used in the next step without further purification. Mp: 69-70 °C, lit mp: not reported. IR: (ν, cm^{-1}) 3339 (N-H str.), 2939(C-H str.), 1733 (C=O). ^{1}H NMR (400 MHz, $CDCl_3$) δ 7.20 – 7.14 (m, 1H), 6.73 (d, J = 2.0 Hz, 1H), 6.71 (d, J = 1.9 Hz, 1H), 6.67 (s, 1H), 4.26 (q, J = 7.1 Hz, 2H), 3.73 (s, 3H), 3.53 (q, J = 6.9 Hz, 2H), 2.77 (t, J = 7.1 Hz, 2H), 1.30 (t, J = 7.1 Hz, 3H). ^{13}C NMR (101 MHz, $CDCl_3$) δ 160.66 (C=O), 159.90 (C=O), 156.55 (Ar-C),

139.69 (Ar-C), 129.80 (Ar-C), 120.98 (Ar-C), 114.36 (Ar-C), 112.16(Ar-C), 63.22 (C-13), 55.21 (C-7), 40.90 (C-9), 35.28 (C-8), 13.98 (C-14).

4.1.6 Preparation of ethyl 2-((3,4-dimethoxyphenethyl)amino)-2-oxoacetate (81b)

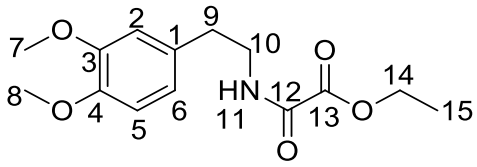

A mixture of 2-(3,4-dimethoxyphenyl)ethanamine (**79b**) (281 mg, 1.0 mmol) and diethyl oxalate (**80b**) (438 mg, 3.0 mmol) was stirred at 140 °C for 6 h. The ethanol formed and the excess diethyl oxalate were removed by distillation *in vacuo*, and the oily residue crystallized when treated with Et_2O, resulting in **ethyl 2-((3,4-dimethoxyphenethyl)amino)-2-oxoacetate** (**81b**), as a crystalline product (115 mg, 41%). The crystals were collected by filtration, washed with Et_2O (10 mL), and used in the next step without further purification. Mp: 69-70 °C, lit[136] mp: 68–70 °C). IR: (ν, cm^{-1}) 3290 (N-H str.), 2931(C-H str.), 1745 (C=O). ^{1}H NMR (500 MHz, $CDCl_3$) δ 7.13 (s, 1H, NH), 6.82 (d, *J* = 8.1 Hz, 1H, Ar-H), 6.77 – 6.70(m, 2H, Ar-H), 4.33 (q, *J* = 7.1 Hz, 2H, H-14), 3.88 (s, 3H, H-7 or H-8), 3.87 (s, 3H, H-7 or H-8), 3.59 (q, *J* = 6.8 Hz, 2H, H-10), 2.82 (t, *J* = 7.0 Hz, 2H, H-9), 1.38 (t, *J* = 7.1 Hz, 3H, H-15). ^{13}C NMR (126 MHz, $CDCl_3$) δ 160.7 (C=O), 156.5 (C=O), 149.2 (Ar-C), 147.9 (Ar-C), 130.6 (Ar-C), 120.6 (Ar-C), 111.9 (Ar-C), 111.5 (Ar-C), 63.2 (C-14), 56.0 & 55.9 (C-7 & C-8), 41.1 (C-10), 34.9 (C-9), 14.0 (C-15).

4.1.7 Preparation of ethyl 6,7-dimethoxy-3,4-dihydroisoquinoline-1-carboxylate (108)

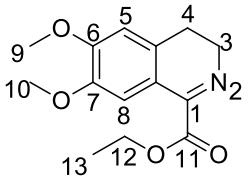

To a stirred solution of ethyl 2-((3,4-dimethoxyphenethyl)amino)-2-oxoacetate (**81b**), (281 mg, 1.0 mmol) in abs. acetonitrile (5 mL) under Ar gas, freshly distilled $POCl_3$ (843 mg, 5.5 mmol) was added. The resulting mixture was stirred at rt overnight and refluxed for 3.5 h, and then evaporated under reduced pressure. The oily residue was carefully dissolved in warm 96% ethanol (50 mL) and the resulting solution was added to a mixture of ice-cold water (200 mL) and EtOAc (150 mL). The biphasic mixture was made alkaline with conc. aq. NH_4OH solution under vigorous stirring and external cooling in an ice-water bath. The organic layer was separated, and the aqueous layer was extracted with EtOAc (2 × 150mL). The combined

organic extracts were dried (Na_2SO_4) and evaporated. The oily residue crystallized when treated with Et_2O to give **ethyl 6,7-dimethoxy-3,4-dihydroisoquinoline-1-carboxylate** (**108**) as a beige crystalline product (133 mg, 50%), which was collected by filtration, washed with Et_2O, and used in the next step without any further purification. Mp 75-76 °C, lit[136] mp: 76–78 °C. IR: (ν, cm^{-1}) 3085 (=C-H str.), 2942 (C-H str.), 1714 (C=O), 1616 (C=N). ^{1}H NMR (400 MHz, $CDCl_3$) δ 7.38 (s, 1H, Ar-H), 6.69 (s, 1H, Ar-H), 4.42 (q, *J* = 7.1 Hz, 2H, H-12), 3.92 (s, 3H, H-9 or H-10), 3.89 (s, 3H, H-9 or H-10), 3.88 – 3.83 (m, 2H, H-3), 2.73 – 2.67 (m, 2H, H-4), 1.43 (t, *J* = 7.1 Hz, 3H, H-13). ^{13}C NMR (101 MHz, $CDCl_3$) δ 164.9 (C=O), 158.6 (C=N), 151.6 (Ar-C), 147.4 (Ar-C), 131.7 (Ar-C), 119.0 (Ar-C), 110.3 (Ar-C), 110.1 (Ar-C), 61.9 (C-3), 56.1 (C-9 or C-10), 56.0 (C-9 or C-10), 47.7 (C-3), 25.2 (C-4), 14.2 (C-13).

4.1.8 Preparation of ethyl isoquinoline-1-carboxylate (97)

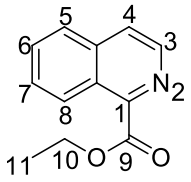

To a stirred solution of isoquinoline-1-carboxylic acid (**78**) (173 mg, 1.0 mmol) in abs. ethanol (1.5 mL) was added thionyl chloride (0.6 mL, 984 mg, 8.27 mmol) dropwise over 5 minutes. Then, the mixture was heated under reflux for 4 h. Ethanol was removed by distillation and saturated $NaHCO_3$ solution was added to adjust the pH to 7. The mixture was extracted with ethyl acetate (10 mL), and the organic layer was dried over anhydrous Na_2SO_4. Removal of the ethyl acetate by evaporation gave the ester **ethyl isoquinoline-1-carboxylate** (**97**) as a light-yellow oily compound (150 mg, 75%). R_f = 0.73 (EtOAc:Hex 1:1). IR: (ν, cm^{-1}) 3056 (=C-H str.), 2982 (C-H str.), 1716 (C=O). ^{1}H NMR (400 MHz, $CDCl_3$) δ 8.76 (d, *J* = 8.3 Hz, 1H, Py-H), 8.63 (s, 1H. Py-H), 7.85 (d, *J* = 8.1 Hz, 1H, Ar-H), 7.79 (d, *J* = 5.5 Hz, 1H, Ar-H), 7.75 – 7.63 (m, 2H, Ar-H), 4.58 (q, *J* = 1.7 Hz, 2H, H-10), 1.51 (t, *J* = 8.0 Hz, 3H, H-11). ^{13}C NMR (101 MHz, $CDCl_3$) δ 166.0 (C=O), 149.0 (C=N), 141.6 (Py-C), 136.9 (Ar-C), 130.5 (Ar-C), 128.6 (Ar-C), 127.1 (Py-C), 126.7 (Ar-C), 126.4 (Ar-C), 124.0 (Ar-C), 62.1 (C-10), 14.3 (C-11).

4.1.9 Preparation of ethyl 1,2,3,4-tetrahydroisoquinoline-1-carboxylate (72)

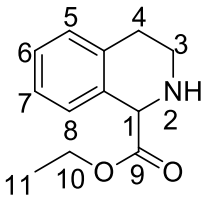

To absolute ethanol cooled to –10°C, $SOCl_2$ (0.32 mL, 2.27 mmol) was added dropwise under stirring whilst keeping the temperature at -10°C. Following the addition of $SOCl_2$, the reaction mixture was allowed to stir for 2 minutes, and 1,2,3,4-tetrahydroisoquinoline-1-carboxylic acid (**77**) (285 mg, 1.607 mmol) was added in one portion. The resulting mixture was allowed to warm to room temperature, stirred for an additional 3 hours and refluxed for 1 hour. The solvent was removed under reduced pressure and the resulting residue was extracted with EtOAc and saturated $NaHCO_3$ solution. The organic portions were basified to pH=14 with 1M NaOH and extracted with ethyl acetate (2 x 10 mL). The solvent was evaporated using a rotary evaporator followed by purification with column chromatography (EtOAc:Hex 1:1), affording **ethyl 1,2,3,4-tetrahydroisoquinoline-1-carboxylate (72)** as a brown dense oil (56.1 mg, 17%). R_f = 0.65 (EtOAc:Hex 1:1). IR: (ν, cm^{-1}): 2980-2903(C-H str), 1723(C=O str), 1619 (N-H str). ^1H NMR (400 MHz, $CDCl_3$) δ 7.36 (d, *J* = 8.5 Hz, 1H, Ar-H), 7.23 – 7.12 (m, 2H, Ar-H), 7.10 (d, *J* = 9.0 Hz, 1H, Ar-H), 4.72 (s, 1H, H-1), 4.31 – 4.14 (m, 2H, H-10), 3.37 – 3.25 (m, 1H, H-3), 3.12 – 3.01 (m, 1H, H-3), 2.90 – 2.72 (m, 2H, H-4), 2.14(s, 1H, N-H), 1.30 (t, *J* = 7.1 Hz, 3H, H-11). ^{13}C NMR (101 MHz, $CDCl_3$) δ 173.11 (C=O), 135.46 (Ar-C), 131.99 (Ar-C), 129.41 (Ar-C), 127.74 (Ar-C), 127.11 (Ar-C), 125.82 (Ar-C), 61.38 (C-1), 59.05 (C-10), 40.89 (C-3), 29.18 (C-4), 14.20 (C-11)

4.1.10 Preparation of 2-(*tert*-butoxycarbonyl)-1,2,3,4-tetrahydroisoquinoline-1-carboxylic acid (111)

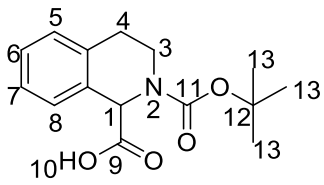

A mixture of l,2,3,4-tetrahydroisoquinoline-l-carboxylic acid (150mg, 0.85 mmol) (**77**), and CH_2Cl_2 were stirred at 0 °C. To that solution, di-*tert*-butyldicarbonate (185 mg, 0.85 mmol) and triethylamine (177 uL, 1.27 mmol) were added and the resulting mixture was allowed to

warm to room temperature while stirring overnight. An aqueous solution of HCl (1.0 M) was added until the pH reached 3.0. The mixture was extracted with EtOAc (3 X 25 mL) and the organic portions were washed with brine (10 mL) and dried over Mg_2SO_4 anhydrous. The solution was filtered and concentrated under reduced pressure to afford **2-(*tert*-butoxycarbonyl)-1,2,3,4-tetrahydroisoquinoline-1-carboxylic acid (111)** (210 mg, 89%) as a light brown low melting point solid. Mp 62-65 °C, lit mp: not reported. IR: (ν, cm^{-1}) 3466 (O-H str.), 2977 (C-H str.), 1807 (C=O). ^{1}H NMR (400 MHz, $CDCl_3$) δ 7.52 – 7.41 (m, 1H), 7.25 – 7.19 (m, 2H), 7.18 – 7.13 (m, 1H), 5.59-5.41 (m, 1H), 3.92 – 3.58 (m, 2H), 3.00 – 2.78 (m, 2H), 1.46 (m, 9H). ^{13}C NMR (101 MHz, $CDCl_3$) δ 177.16 (C=O), 175.98 (C'=O), 155.71(C=O),154.67 (C'=O), 135.85 (Ar-C), 135.47 (Ar-C'), 130.23 (Ar-C), 129.53(Ar-C'), 128.60 (Ar-C), 128.38 (Ar-C), 128.25 (Ar-C'), 128.02 (Ar-C), 126.63 (Ar-C), 81.94 (C-12), 81.07(C'-12), 58.51 (C-1), 57.58 (C'-1),), 40.97 (C-3), 39.80 (C'-3), 28.76 (C-4), 28.40 (C-13), 28.28 (C'-13). Restricted rotation of the Boc group caused a splitting of carbon signals, which we donated as C'.

4.1.11 Preparation of 2-*tert*-butyl 1-methyl 3,4-dihydroisoquinoline-1,2(1*H*)-dicarboxylate (112)

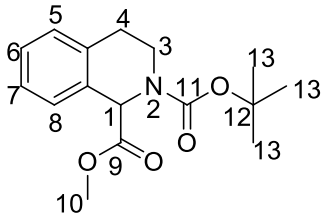

A mixture of 2-(tert-butyoxycarbonyl)-1,2,3,4-tetrahydroisoquinoline-1-carboxylic acid (**111**) (76.2 mg, 0.274 mmol), potassium carbonate (49.4 mg, 0.357 mmol), and iodomethane (58.3 mg, 0.411 mmol) were stirred in 3 mL of DMF at room temperature for 3 hours. The resulting mixture was diluted with ethyl acetate and washed with saturated $NaHCO_3$ and saturated NaCl. The organic portion was dried over Na_2SO_4 anhydrous, filtered, and concentrated under reduced pressure. The resulting residue was purified by column chromatography (30% Hex:EtOAc), furnishing **2-*tert*-butyl 1-methyl 3,4-dihydroisoquinoline-1,2(1*H*)-dicarboxylate (112)** a yellow oil (79.8 mg, 64%) R_f = 0,63 (30% EtOAc: Hex) IR: (ν, cm^{-1}) 2980 (=C-H str.), 2882 (C-H str.), 1740 (C=O), 1681(C=O). ^{1}H NMR (400 MHz, $CDCl_3$) δ 7.51 – 7.44 (m, 1H), 7.25 – 7.19 (m, 2H), 7.16 (s, 1H), 5.60 (s, 1H), 5.43 (s, 1H), 3.84 – 3.74 (m, 1H), 3.71 (s, 3H), 3.01 – 2.90 (m, 1H), 2.90 – 2.80 (m, 1H), 1.48 (d, J = 8.7 Hz, 8H). ^{13}C NMR (101 MHz, $CDCl_3$) δ 172.18 (C=O), 171.92 (C'=O), 155.35 (C=O), 154.75 (C'=O), 135.67 (Ar-C), 135.41 (Ar-C'), 130.90 (Ar-C), 130.14 (Ar-C'), 128.63(Ar-C), 128.32 (Ar-C),

128.20 (Ar-C'), 127.79 (Ar-C), 127.71 (Ar-C'), 126.52 (Ar-C), 80.68 (C-12), 80.48 (C'-12), 58.69 (C-1), 57.64 (C'-1), 52.48 (C-10), 52.33 (C'-10), 40.85 (C-3), 39.76 (C'-3), 28.85 (C-4), 28.75 (C'-4), 28.41 (C-13), 28.34 (C'-13)). Restricted rotation of the Boc group caused a splitting of carbon signals, which we donated as C'.

4.1.12 Preparation of methyl 1,2,3,4-tetrahydroisoquinoline-1-carboxylate (71)

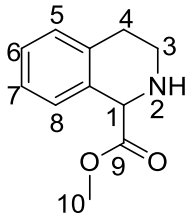

Method I

To a solution of 2-tert-butyl 1-methyl 3,4-dihydroisoquinoline-1,2(1*H*)-dicarboxylate (**112**) (200 mg, 0.721 mmol) in dioxane (10 mL), 4M HCl solution (10 mL) was added, and the resulting mixture was stirred overnight. The resulting mixture was concentrated under reduced pressure to afford **methyl 1,2,3,4-tetrahydroisoquinoline-1-carboxylate (71)** as a beige solid (94,7 mg, 69%). Mp 87-89 °C, lit mp: not reported. IR: (ν, cm^{-1}) 3260 (N-H str), 2935 (C-H str), 1731 (C=O str). HPLC-MS (m/z), calculated for $C_{11}H_{13}NO_2$: 191.01, found $[M + H]^+$: 192.1023.

Method II

To a solution of 2-tert-butyl 1-methyl 3,4-dihydroisoquinoline-1,2(1H)-dicarboxylate (**112**) (200 mg, 0.721 mmol) in chloroform (10 mL), trifluoroacetic acid (0,53 mL, 0,69 mmol) was added, and the resulting mixture was stirred overnight. The resulting mixture was concentrated under reduced pressure to afford **methyl 1,2,3,4-tetrahydroisoquinoline-1-carboxylate (71)** as a beige solid (89.3 mg, 65%). Mp 68-72 °C, lit mp: not reported. IR: (ν, cm^{-1}) 3431-3389 (N-H str), 2934-2910 (C-H str), 1749 (C=O str). HPLC-MS (m/z), calculated for $C_{11}H_{13}NO_2$: 191.01, found $[M + H]^+$: 192.1025. ^{1}H NMR (400 MHz, D_2O) δ 7.55 (d, J = 7.8 Hz, 1H, Ar-H), 7.45 – 7.34 (m, 2H, Ar-H), 7.32 (d, J = 7.5 Hz, 1H, Ar-H), 5.49 (s, 1H, H-1), 3.88 (s, 3H, H-10), 3.74 – 3.57 (m, 2H, H-3), 3.19 – 3.08 (m, 2H, H-4). ^{13}C NMR (101 MHz, D_2O) δ 168.44 (C=O), 131.77 (Ar-C), 129.29 (Ar-C), 129.16 (Ar-C), 128.21 (Ar-C), 127.14 (Ar-C), 124.94 (Ar-C), 56.10 (C-1), 54.07 (C-10), 39.85 (C-3), 24.20 (C-4).

4.1.13 Preparation of ethyl 5,6,7,8-tetrahydroisoquinoline-1-carboxylate (98)

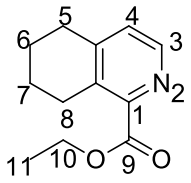

Ethyl isoquinoline-1-carboxylate (**97**) (330 mg, 1.60 mmol) was dissolved in glacial acetic acid (12 mL) and Pd/C (3.3 mg) was added to the solution. The mixture was stirred under a H_2 atmosphere (7 bar) at 25 °C for 24 h. The catalyst was removed by filtration through a celite pad and rinsed with MeOH (10 mL) and acetic acid (10 mL) to give **ethyl 5,6,7,8-tetrahydroisoquinoline-1-carboxylate (98)** in trace amounts. ^{1}H NMR (400 MHz, $CDCl_3$) δ 8.36 (d, *J* = 4.9 Hz, 1H), 7.11 (d, *J* = 4.9 Hz, 1H), 4.44 (q, *J* = 7.2 Hz, 2H), 3.01 (s, 2H), 2.81 (s, 2H), 1.81 (m, 4H), 1.43 (t, *J* = 7.1 Hz, 3H). ^{13}C NMR (126 MHz, $CDCl_3$) δ 166.7 (C=O), 148.4 (Ar-H), 148.1 (Ar-H), 145.8 (Ar-H), 133.9 (Ar-H), 126.5 (Ar-H), 61.5 (C-10), 29.6 (C-7 or C-8), 26.0 (C-7 or C-8), 22.6 (C-5 or C-8), 21.7 (C-5 or C-8), 14.3 (C-11).

4.1.14 Preparation of N^1, N^2-*bis*(3-methoxyphenethyl)oxalamide (105)

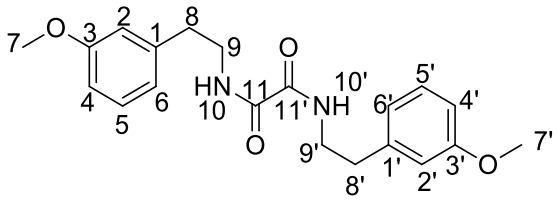

A mixture of 2-(3-methoxyphenyl)ethanamine (**79a**) (251 mg, 1.0 mmol) and diethyl oxalate (**80b**) (438 mg, 3.0 mmol) was stirred at 140°C for 6 h. The ethanol formed and the excess diethyl oxalate were removed by distillation *in vacuo*, and the oily residue was purified by flash column chromatography (30% EtOAc: Hex). The oily product crystallized when dried under high vacuum. The crystals were collected by filtration, washed with Et_2O (10 mL), to give ***N*^{1}, *N*^{2}-*bis*(3-methoxyphenethyl)oxalamide (105)** (81 mg, 22%). ^{1}H NMR (400 MHz, $CDCl_3$) δ 7.51 (t, *J* = 6.0 Hz, 2H, N-H/H'), 7.23 (t, *J* = 7.8 Hz, 2H, Ar-H/H'), 6.79 (d, *J* = 7.9 Hz, 4H, Ar-H/H'), 6.74 (s, 2H, Ar-H/H'), 3.80 (s, 6H, H-7/7'), 3.56 (q, *J* = 6.9 Hz, 4H, H-9/9'), 2.83 (t, *J* = 7.2 Hz, 4H, H-8/8'). ^{13}C NMR (101 MHz, $CDCl_3$) δ 159.9 (C=O C-11&C-11'), 159.7 (Ar-H/H'), 139.7 (Ar-H/H'), 129.8 (Ar-H/H'), 121.0 (Ar-H/H'), 114.5 (Ar-H/H'), 112.1 (Ar-H/H'), 55.2 (C-7/7'), 40.8 (C -9/9'), 35.5 (C-8/8').

4.1.15 Preparation of N^1, N^2-*bis*(3,4-dimethoxyphenethyl)oxalamide (106)

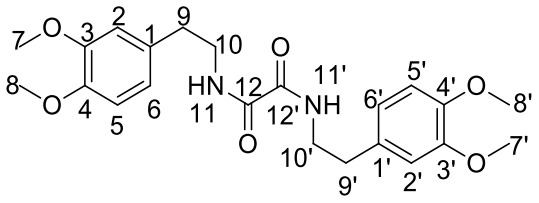

A mixture of 2-(3,4-dimethoxyphenyl)ethanamine (79b) (281 mg, 1.0 mmol) and diethyl oxalate (80b) (438 mg, 3.0 mmol) was stirred at 140°C for 6 h. The ethanol formed and the excess diethyl oxalate were removed by distillation *in vacuo*, and the oily residue was purified by flash column chromatography (30% EtOAc: Hex). The oily product crystallized when treated with Et_2O, resulting in ***N*^{1}, *N*^{2}-*bis*(3,4-dimethoxyphenethyl)oxalamide (106)** (49.2 mg 8.5 %.) ^{1}H NMR (400 MHz, $CDCl_3$) δ 7.42 (t, *J* = 6.6 Hz, 2H, N-H/H'), 6.75 (d, *J* = 8.1 Hz, 2H, Ar-H/H'), 6.69 – 6.61 (m, 4H, Ar-H), 3.81 (s, 6H, H-7 or H-8/H-7' or H-8'), 3.80 (s, 6H, H-7 or H-8/H-7' or H-8') 3.48 (q, *J* = 6.9 Hz, 4H, H-10/H-10'), 2.73 (t, *J* = 7.1 Hz, 4H, H-9/H-9'). ^{13}C NMR (101 MHz, $CDCl_3$) δ 159.7 (C=O, C-12/C-12'), 149.1 (Ar-H/H'), 147.9 (Ar-H/H'), 130.6 (Ar-H/H'), 120.6 (Ar-H/H'), 111.8 (Ar-H/H'), 111.4 (Ar-H/H'), 55.9 (C-7 or C-8/ C-7' or C-8'), 55.9 (C-7 or C-8/ C-7' or C-8'), 41.0 (C-10/ C-10'), 35.1 (C-9/C-9').

4.1.16 Preparation of N^1, N^2-*bis*(4-methoxyphenethyl)oxalamide (103)

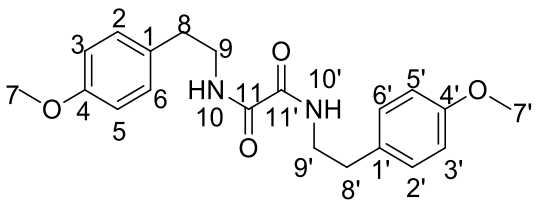

A mixture of 2-(4-methoxyphenyl)ethanamine (**79c**) (251 mg, 1.0 mmol) and dimethyl oxalate (**80a**) (438 mg, 3.0 mmol) was stirred at 140°C for 6 h. The ethanol formed and the excess diethyl oxalate were removed by distillation *in vacuo*, and the oily residue was purified by flash column chromatography (30% EtOAc: Hex). The oily product crystallized when dried under high vacuum. The crystals were collected by filtration, washed with Et_2O (10 mL), to give ***N*^{1}, *N*^{2}-*bis*(4-methoxyphenethyl)oxalamide (103)** (13.7 mg, 5.5 %). ^{1}H NMR (400 MHz, $CDCl_3$) δ 7.46 (s, 2H, N-H/H'), 7.11 (d, *J* = 8.3 Hz, 4H, Ar-H), 6.85 (d, *J* = 8.3 Hz, 4H, Ar-H), 3.79 (s, 6H, H-7/7'), 3.53 (q, *J* = 6.8 Hz, 4H, H-9/9'), 2.79 (t, *J* = 7.1 Hz, 4H, H-8/8').

4.1.17 Preparation of Iodoxybenzoic acid (86)

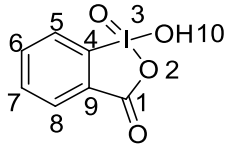

A slow addition of potassium bromate (2.00 g, 12.0 mmol) was added to a rapidly stirred sulphuric acid mixture (2 M, 45 mL) containing 2-iodobenzoic acid (2 g, 8.06 mmol). The reaction temperature of the resulting mixture was maintained below 55°C until the addition of potassium bromate was complete. The reaction mixture was then to 65°C for 3 h. The flask was then cooled to 0°C and the resulting solid was filtered and washed with water (1000 mL) and ethanol (2 x 50 mL) to obtain **iodoxybenzoic acid (86)** (1.039g, 65 %). ^{1}H NMR (400 MHz, DMSO) δ 8.14 (d, *J* = 7.9 Hz, 1H), 8.01 (q, *J* = 7.5 Hz, 2H), 7.84 (t, *J* = 7.3 Hz, 1H).

4.1.18 Preparation of methyl 2-((4-methoxyphenethyl)amino)-2-oxoacetate (81c)

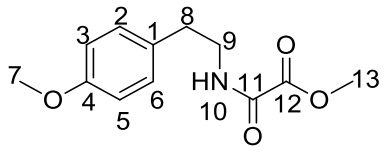

Dimethyl oxalate (**80a**) (1.063 g, 9.0 mmol) was dissolved in DMF (10 mL) and stirred for 5 min at room temperature. 2-(4-Methoxyphenyl)ethanamine (**79c**) (0.454 g, 3.0 mmol) was added to the mixture and the resulting mixture was heated to 160 °C for 6 h. The ethanol formed and the excess diethyl oxalate were removed by distillation *in vacuo*, and the oily residue was purified by flash column chromatography (30% EtOAc: Hex). The oily product crystallised when dried under high vacuum. The crystals were collected by filtration, washed with Et_2O (10 mL), and dried under high vacuum to give **methyl 2-((4-methoxyphenethyl)amino)-2-oxoacetate (81c)** as a brownish solid (115 mg, 16.19%). ^{1}H NMR (400 MHz, $CDCl_3$) δ 7.23 (d, *J* = 7.9 Hz, 1H), 7.14 (s, 1H), 6.79 (d, *J* = 7.6 Hz, 2H), 6.74 (t, *J* = 2.0 Hz, 1H), 3.89 (s, 3H), 3.81 (s, 3H), 3.62 (q, *J* = 6.8 Hz, 2H), 2.85 (t, *J* = 7.0 Hz, 2H). ^{13}C NMR (101 MHz, $CDCl_3$) δ 161.2 (C=O), 159.9 (C=O), 156.2 (Ar-C), 139.6 (Ar-C), 129.8 (Ar-C), 121.0 (Ar-C), 114.4 (Ar-C), 112.2 (Ar-C), 55.2 (C-13), 53.7 (C-7), 40.9 (C-9), 35.3 (C-8).

4.1.19 Preparation of 3-(2-aminoethyl)phenol (102)

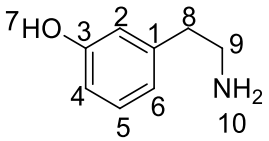

To a solution of 2-(3-methoxyphenyl)ethylamine (**99**) (300 mg, 1.98 mmol) in dry DCM (10 mL) under argon at –78 °C, boron tribromide in hexane (1 M; 5 mL) was added. The mixture was slowly warmed to room temperature and stirred for 20 h. The reaction was subsequently

cooled to –78°C and water (50 mL) added dropwise. The aqueous layer was washed with dichloromethane (3 × 50 mL). The organic layer was dried and removed under reduced pressure. The resulting oily residue was purified using column chromatography (100% MeOH) to obtain **3-(2-aminoethyl)phenol (102)** in trace amounts. ^{1}H NMR (400 MHz, MeOD) δ 7.18 (t, *J* = 7.8 Hz, 1H, Ar-H), 6.80 – 6.69 (m, 3H, Ar-H), 3.19 (t, *J* = 7.8 Hz, 2H, H-9), 2.93 (t, *J* = 7.8 Hz, 2H, H-8).

4.1.20 Preparation of Pyridine-4-carboxamide (62)

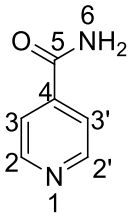

4-Pyridinecarbonitrile (20 mg, 0.19 mmol) was dissolved in acetone (0.2 mL). The resulting mixture was dissolved in tris-phosphate buffer (1.8 mL) of pH = 7.3. To the resulting mixture, NHAse enzyme (20 mg) was added and the resulting mixture was incubated at 30 ℃ for 24 h. After 24 h, the reaction mixture was washed with water and extracted with ethyl acetate. The organic layer was dried over anhydrous $MgSO_4$. The organic solvent was removed under reduced pressure the residue was purified using flash chromatography (10% MeOH: 90% EtOAC) to afford **pyridine-4-carboxamide (62)** as a white solid (17.3 mg, 75%). ^{1}H NMR (400 MHz, $CDCl_3$) δ 8.78 (d, *J* = 6.0 Hz, 2H, H-3/3'), 7.64 (d, *J* = 6.0 Hz, 2H, H-2/2'), 6.17 (s, 1H, H-6), 5.87 (s, 1H, H-6). ^{13}C NMR (101 MHz, $CDCl_3$) δ 167.2 (C=O), 150.7 (C-3/3'), 140.4 (C-4), 121.0 (C-2/2').

4.1.21 Preparation of 2-((4-bromophenyl)(hydroxy)methyl)acrylonitrile (115)

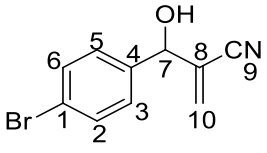

4-Bromobenzaldehyde (1.5 eq) and DABCO (1 eq.) were dissolved in excess acrylonitrile (10 mL) in a 50 mL round bottom flask and stirred at room temperature for 20 hours. After completion of the reaction, ethyl acetate (30 mL) and water (30 mL) were added to the reaction mixture. The aqueous layer was separated from the organic layer and the aqueous layer was washed two more times with ethyl acetate. The organic portions were dried over anhydrous

$MgSO_4$ and purified by column chromatography (30 % ethyl acetate/hexane) using normal silica gel. The reaction products were then concentrated under reduced pressure to afford **2-((4-bromophenyl)(hydroxy)methyl)acrylonitrile (115)** as a yellow oil (250.3 mg, 70%). ^{1}H NMR (400 MHz, $CDCl_3$) δ 7.53 (d, *J* = 8.4 Hz, 2H, H2 & H6), 7.27 (d, *J* = 8.4 Hz, 2H, H3 & H5), 6.11 (s, 1H, H10a), 6.04 (s, 1H, H10b), 5.27 (s, 1H, H7), 2.65 (s, 1H, OH). ^{13}C NMR (101 MHz, $CDCl_3$) δ 138.1 (C4), 132.1(C2 & C6), 130.2 (C10), 128.2 (C3 & C5), 125.9 (C8), 123.1 (C1), 116.7 (C9), 73.6 (C7).

4.1.22 Preparation of 1-(4-bromophenyl)-2-cyanoallyl acetate (117)

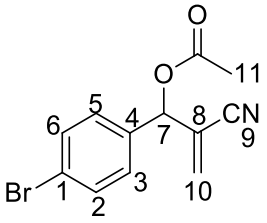

2-((4-Bromophenyl)(hydroxy)methyl)acrylonitrile (115) (1 eq.) was stirred in 2-methyltetrahydrofuran (20 mL) for 5 minutes. Acetic anhydride (1.2 eq.), triethylamine (1.2 eq.), and DMAP (1 mol%) were added to the solution. The resulting mixture was stirred at room temperature for 1 hour. The organic layer was washed with an aqueous saturated solution of $NaHCO_3$ (2 x 25 mL) and then dried over anhydrous MgSO4, concentrated *in vacuo* and purified by column chromatography (30% ethyl acetate/hexane) to afford **1-(4-bromophenyl)-2-cyanoallyl acetate (117)** (113.7 mg, 81%). ^{1}H NMR (300 MHz, $CDCl_3$) δ 7.55 (d, *J* = 8.6 Hz, 2H, H2 & H6), 7.28 (d, *J* = 8.5 Hz, 2H, H3 & H5), 6.28 (s, 1H, H10a), 6.10 (s, 1H, H10b), 6.02 (s, 1H, H7), 2.18 (s, 3H, H11). ^{13}C NMR (101 MHz, $CDCl_3$) δ 169.2 (C=O), 134.7 (C4), 132.2 (C10), 132.2 (C2 & C6), 128.6 (C3 & C5), 123.5 (C8), 122.8 (C1), 115.9 (C9), 73.77 (C7), 20.89 (C11).

4.1.23 General method for enzymatic hydrolysis reactions

To a mixture of enzyme (8 mg) in phosphate buffer (0.1 M, pH=7, 950 μL) in an Eppendorf tube was added substrate (8 mg) dissolved in acetone (50 μL). A blank reaction, where there was no added enzyme an Eppendorf tube, was also set as a control reaction in an Eppendorf tube. Both reactions were monitored using TLC, and when hydrolysis was observed a preparatory TLC was used for purification and isolation.

References

[1] N. Feasey, M. Wansbrough-Jones, D. C. W. Mabey, A. W. Solomon, *Br Med Bull* **2010**, *93*, 179–200.

[2] D. Cioli, L. Pica-Mattoccia, A. Basso, A. Guidi, *Mol Biochem Parasitol* **2014**, *195*, 23–29.

[3] World Health Organization, *Weekly Epidemiological Record= Relevé épidémiologique hebdomadaire* **2019**, *94*, 601–612.

[4] J. Utzinger, E. K. N'Goran, C. R. Caffrey, J. Keiser, *Acta Trop* **2011**, *120*, 121–137.

[5] T. Elbaz, G. Esmat, *J Adv Res* **2013**, *4*, 445–452.

[6] C. H. King, *N Engl J Med* **2009**, *360*, 106–109.

[7] E. Meltzer, E. Schwartz, *Curr Infect Dis Rep* **2013**, *15*, 211–215.

[8] P. J. Hotez, A. Fenwick, L. Savioli, D. H. Molyneux, *The Lancet* **2009**, *373*, 1570–1575.

[9] D. G. Colley, A. L. Bustinduy, W. E. Secor, C. H. King, *The Lancet* **2014**, *383*, 2253–2264.

[10] M. D. French, D. Evans, F. M. Fleming, W. E. Secor, N. K. Biritwum, S. J. Brooker, A. Bustinduy, A. Gouvras, N. Kabatereine, C. H. King, M. Rebollo Polo, J. Reinhard-Rupp, D. Rollinson, L. A. Tchuem Tchuenté, J. Utzinger, J. Waltz, Y. Zhang, *PLoS Negl Trop Dis* **2018**, *12*, 1–6.

[11] C. H. King, *Acta Trop* **2010**, *113*, 95–104.

[12] A. P. Mewabo, R. S. Moyou, L. E. Kouemeni, J. Y. Ngogang, L. Kaptue, E. Tambo, *Infect Dis Poverty* **2017**, *6*, 1–8.

[13] P. J. Hotez, *PLoS Negl Trop Dis* **2014**, *8*, 1–3.

[14] World Health Organization, *WHO GUIDELINE on Control and Elimination of Human Schistosomiasis*, **2022**.

[15] World Health Organization, *Weekly Epidemiological Record* **2018**, *93*, 681–692.

[16] M. Livingston, P. Pillay, S. G. Zulu, L. Sandvik, J. D. Kvalsvig, S. Gagai, H. N. Galappaththi-Arachchige, E. Kleppa, P. Ndhlovu, B. Vennervald, S. G. Gundersen, M. Taylor, E. F. Kjetland, *Am J Trop Med Hyg* **2021**, *104*, 2055–2064.

[17] K. Magaisa, M. Taylor, E. F. Kjetland, P. J. Naidoo, *S Afr J Sci* **2015**, *111*, 1–6.

[18] P. J. Hotez, *Microbes Infect* **2015**, *17*, 539–541.

[19] N. Shrestha, *J Chitwan Med Coll* **2021**, *11*, 1–3.

[20] T. S. Champion, S. Connelly, C. J. Smith, P. H. L. Lamberton, *WIREs Water* **2021**, *8*, 1–13.

[21] F. D. Chevalier, W. Le Clec'h, N. Eng, A. R. Rugel, R. R. de Assis, G. Oliveira, S. P. Holloway, X. Cao, P. J. Hart, P. T. LoVerde, T. J. C. Anderson, *Int J Parasitol* **2016**, *46*, 417–424.

[22] P. Mäder, G. A. Rennar, A. M. P. Ventura, C. G. Grevelding, M. Schlitzer, *Chem Med Chem* **2018**, *13*, 2374–2389.

[23] S. D. Melman, M. L. Steinauer, C. Cunningham, L. S. Kubatko, I. N. Mwangi, N. B. Wynn, M. W. Mutuku, D. M. S. Karanja, D. G. Colley, C. L. Black, W. E. Secor, G. M. Mkoji, E. S. Loker, *PLoS Negl Trop Dis* **2009**, *3*, 1–10.

[24] S. Botros, H. Sayed, N. Amer, M. El-Ghannam, J. L. Bennett, T. A. Day, *Int J Parasitol* **2005**, *35*, 787–791.

[25] R. A. Wilson, *Parasitology* **2020**, *147*, 507–515.

[26] World Health Organization, *Weekly Epidemiological Record= Relevé épidémiologique hebdomadaire* **2015**, *90*, 25–32.

[27] J. R. Stothard, J. C. Sousa-Figueiredo, M. Betson, A. Bustinduy, J. Reinhard-Rupp, *Trends Parasitol* **2013**, *29*, 197–205.

[28] J. F. Friedman, R. M. Olveda, M. H. Mirochnick, A. L. Bustinduy, A. M. Elliott, *Bull World Health Organ* **2018**, *96*, 59–65.

[29] P. Olliaro, P. Delgado-Romero, J. Keiser, *J Antimicrob Chemother* **2014**, *69*, 863–870.

[30] M. Woelfle, J. P. Seerden, J. de Gooijer, K. Pouwer, P. Olliaro, M. H. Todd, *PLoS Negl Trop Dis* **2011**, *5*, 1–7.

[31] A. Danso, A. Sake, J. De Vlas, A. Danso-Appiah, S. J. De Vlas, *Trends Parasitol* **2002**, *18*, 1–5.

[32] O. P. Aula, D. P. McManus, M. K. Jones, C. A. Gordon, *Trop Med Infect Dis* **2021**, *6*, 1–40.

[33] H. C. Kariuki, H. Madsen, J. H. Ouma, A. E. Butterworth, D. W. Dunne, M. Booth, G. Kimani, J. K. Mwatha, E. Muchiri, B. J. Vennervald, *Parasit Vectors* **2013**, *6*, 1–11.

[34] A. Monkiedje, A. C. Anderson, A. J. Englande, *Environ Toxicol Water Qual* **1991**, *6*, 405–413.

[35] M. Guzman, A. Rugel, R. S. Tarpley, X. Cao, S. F. McHardy, P. T. LoVerde, A. B. Taylor, *Mol Biochem Parasitol* **2020**, *236*, 111257.

[36] A. Rugel, R. S. Tarpley, A. Lopez, T. Menard, M. A. Guzman, A. B. Taylor, X. Cao, D. Kovalskyy, F. D. Chevalier, T. J. C. Anderson, P. J. Hart, P. T. Loverde, S. F. McHardy, *ACS Med Chem Lett* **2018**, *9*, 967–973.

[37] P. Roszkowski, J. K. Maurin, Z. Czarnocki, *Tetrahedron Asymmetry* **2006**, *17*, 1415–1419.

[38] F. Yustr, Y. Pallas, H. Barrios, B. Ortiz, R. Sanchez-Ohregcin, *J Heterocycl Chem* **1986**, *23*, 1–2.

[39] M. Qian, *Method for Preparing (R)-Praziquantel*, **2015**, US 20140370555 A1.

[40] Z. Xu, L. Li, Z. Shen, *Water Res* **2005**, *39*, 2189–2195.

[41] H. Liu, S. William, E. Herdtweck, S. Botros, A. Dömling, *Chem Biol Drug Des* **2012**, *79*, 470–477.

[42] A. Dömling, K. Khoury, *Chem Med Chem* **2010**, *5*, 1420–1434.

[43] J. H. Kim, Y. S. Lee, H. Park, C. Sup, Rim, *Tetrahedron* **1998**, *54*, 7395–7400.

[44] S. A. L. Laurent, J. Boissier, F. Coslédan, H. Gornitzka, A. Robert, B. Meunier, *Eur Journal of Organic Chemistry* **2008**, *2008*, 895–913.

[45] M. E. Pyne, V. J. J. Martin, *Curr Opin Green Sustain Chem* **2022**, *33*, 1–9.

[46] M. Naoi, W. Maruyama, P. Dostert, K. Kohda, T. Kaiya, *Neurosci Lett* **1996**, *212*, 183–186.

[47] T. A. Paál, E. Forró, A. Liljeblad, L. T. Kanerva, F. Fülöp, *Tetrahedron Asymmetry* **2007**, *18*, 1428–1433.

[48] C. G. Neochoritis, T. Zhao, A. Dömling, *Chem Rev* **2019**, *119*, 1970–2042.

[49] M. A. Fouad, H. Abdel-Hamid, M. S. Ayoup, *RSC Adv* **2020**, *10*, 42644–42681.

[50] H. G. O. Alvim, E. N. Da Silva Júnior, B. A. D. Neto, *RSC Adv* **2014**, *4*, 54282–54299.

[51] M. Lee, N. J. Vosburg, E. A. Shimizu, M. A. Rentería-Gómez, R. Gámez-Montaño, D. A. Vosburg, *J Chem Educ* **2022**, *99*, 2399–2402.

[52] A. Hegedüs, Z. Hell, A. Potor, *Catal Commun* **2006**, *7*, 1022–1024.

[53] A. Dömling, W. Wang, K. Wang, *Chem Rev* **2012**, *112*, 3083–3135.

[54] D. W. Fitzgerald, T. R. Sterling, D. W. Haas, *Mandell, Douglas, and Bennett's Principles and Practice of Infectious Diseases (Eighth Edition)* **2015**, 2985–3021.

[55] J. L. Flynn, J. Chan, *Annu Rev Immunol* **2001**, *19*, 93.

[56] WHO, *https://www.who.int/publications/i/item/9789240037021* **2021**, 31–41.

[57] B. C. de Jong, M. Antonio, S. Gagneux, *PLoS Negl Trop Dis* **2010**, *4*, 1–9.

[58] J. D. Ernst, G. Trevejo-Nuñez, N. Banaiee, *J Clin Invest* **2007**, *117*, 1738–1745.

[59] I. Law, K. Floyd, E. A. B. Abukaraig, K. K. Addo, I. Adetifa, Z. Alebachew, R. Banda, A. Bashorun, E. Bloss, F. A. Bonsu, *Trop Med Int Health* **2020**, *25*, 1308–1327.

[60] S. A. Stats, *Statistical Release* **2018**, 1–159.

[61] J. Bruchfeld, M. Correia-Neves, G. Källenius, *Cold Spring Harb Perspect Med* **2015**, *5*, 1–16.

[62] R. Kurth, W. H. Haas, *Ann Rheum Dis* **2002**, *61*, ii59–ii61.

[63] M. Laurenzi, A. Ginsberg, M. Spigelman, *Infectious Disorders-Drug Targets* **2007**, *7*, 105–119.

[64] H. C. J. Van Rensburg, *Hum Resour Health* **2014**, *12*, 1–16.

[65] C. Bateman, *S Afr J CH* **2012**, *6*, 100–101.

[66] A. Oliver, E. Mossialos, *J Epidemiol Community Health (1978)* **2004**, *58*, 655–658.

[67] J. Den Van Boogaard, G. S. Kibiki, E. R. Kisanga, M. J. Boeree, R. E. Aarnoutse, *Antimicrob Agents Chemother* **2009**, *53*, 849–862.

[68] E. African, B. M. R. Councils, *The Lancet* **1974**, *304*, 237–240.

[69] J. Johnson, A. Kagal, R. Bharadwaj, *Indian J. Chest Dis. Allied Sci.* **2003**, *45*, 105–109.

[70] J. A. Singh, R. Upshur, N. Padayatchi, *PLoS Med* **2007**, *4*, 20–25.

[71] M. Klopper, R. M. Warren, C. Hayes, N. C. G. van Pittius, E. M. Streicher, B. Müller, F. A. Sirgel, M. Chabula-Nxiweni, E. Hoosain, G. Coetzee, P. D. van Helden, T. C. Victor, A. P. Trollip, *Emerg Infect Dis* **2013**, *19*, 449–455.

[72] E. M. Streicher, B. Müller, V. Chihota, C. Mlambo, M. Tait, M. Pillay, A. Trollip, K. G. P. Hoek, F. A. Sirgel, N. C. Gey van Pittius, P. D. van Helden, T. C. Victor, R. M. Warren, *Infect Genet Evol* **2012**, *12*, 686–694.

[73] R. Van Crevel, T. H. M. Ottenhoff, J. W. M. Van der Meer, *Clin Microbiol Rev* **2002**, *15*, 294–309.

[74] L. Luies, I. du Preez, *Clin Microbiol Rev* **2020**, *33*, e00036-20.

[75] B. B. Rewari, A. Kumar, P. P. Mandal, A. K. Puri, *Expert Rev Respir Med* **2021**, *15*, 911–930.

[76] G. Poce, M. Cocozza, S. Consalvi, M. Biava, *Eur J Med Chem* **2014**, *86*, 335–351.

[77] A. D. Calver, A. A. Falmer, M. Murray, O. J. Strauss, E. M. Streicher, M. Hanekom, T. Liversage, M. Masibi, P. D. van Helden, R. M. Warren, T. C. Victor, W. Vaal Hospital, S. A. Africa Calver, A. Falmer, O. Strauss, E. Streicher, M. Hanekom, P. van Helden, R. Warren, T. Victor, *Emerg Infect Dis* **2010**, *16*, 264–271.

[78] H. B. Rode, D. M. Lade, R. Grée, P. S. Mainkar, S. Chandrasekhar, *Org Biomol Chem* **2019**, *17*, 5428–5459.

[79] P. Flowers, K. Theopold, *[ETextbook] Chemistry-2e*, OpenStax, **2019**.

[80] G. M. Anderson, *Thermodynamics of Natural Systems*, Cambridge University Press, **2005**.

[81] A. Illanes, *Principles and applications. Editorial Springer-Verlag New York Inc., United States* **2008**, 1–56.

[82] T. Deligeorgiev, N. Gadjev, A. Vasilev, S. Kaloyanova, J. J. Vaquero, J. Alvarez-Builla, *Mini-Rev Org Chem* **2010**, *7*, 44–53.

[83] P. Forzatti, L. Lietti, *Catal Today* **1999**, *52*, 165–181.

[84] Y. Avissar, J. Choi, J. DeSaix, V. Jurukovski, R. Wise, C. Rye, **2013**.

[85] G. Torrelo, U. Hanefeld, F. Hollmann, *Catal Letters* **2015**, *145*, 309–345.

[86] E. L. Bell, W. Finnigan, S. P. France, A. P. Green, M. A. Hayes, L. J. Hepworth, S. L. Lovelock, H. Niikura, S. Osuna, E. Romero, K. S. Ryan, N. J. Turner, S. L. Flitsch, *Nat Rev Methods Primers* **2021**, *1*, 1–21.

[87] R. León, P. Fernandes, H. M. Pinheiro, J. M. S. Cabral, *Enzyme Microb Technol* **1998**, *23*, 1–18.

[88] T. Ishige, K. Honda, S. Shimizu, *Curr Opin Chem Biol* **2005**, *9*, 174–180.

[89] M. A. Huffman, A. Fryszkowska, O. Alvizo, M. Borra-Garske, K. R. Campos, K. A. Canada, P. N. Devine, D. Duan, J. H. Forstater, S. T. Grosser, *Science (1979)* **2019**, *366*, 1255–1259.

[90] K.-E. Jaeger, T. Eggert, *Curr Opin Chem Biol* **2002**, *13*, 390–397.

[91] R. T. Manfred, *Curr Opin Chem Biol* **2002**, *6*, 145–150.

[92] J. Błaszczyk, P. Kiełbasiński, *Crystals (Basel)* **2020**, *10*, 3–9.

[93] A. Hietanen, K. Lundell, L. T. Kanerva, A. Liljeblad, *Arkivoc* **2012**, *2012*, 60–74.

[94] R. Sánchez, H. Luna, H. I. Pérez, N. Manjarrez, A. Solís, *Tetrahedron Asymmetry* **2001**, *12*, 1399–1401.

[95] S. Katayama, N. Ae, R. Nagata, *Tetrahedron Asymmetry* **1998**, *9*, 4295–4299.

[96] P. K. Mascharak, *Coord Chem Rev* **2002**, *225*, 201–214.

[97] W. Huang, J. Jia, J. Cummings, M. Nelson, G. Schneider, Y. Lindqvist, *Structure* **1997**, *5*, 691–699.

[98] Y. Hideaki, K. Michihiko, *Biosci Biotechnol Biochem* **1996**, *60*, 1391–1400.

[99] A. R. Mashweu, V. P. Chhiba-Govindjee, M. L. Bode, D. Brady, *Molecules* **2020**, *25*, 1–15.

[100] G. D. Yadav, S. S. Joshi, P. S. Lathi, *Enzyme Microb Technol* **2005**, *36*, 217–222.

[101] J. Clayden, N. Greeves, S. Warren, *Organic Chemistry*, Oxford University Press, New York, **2012**.

[102] D. Insuasty, J. Castillo, D. Becerra, H. Rojas, R. Abonia, *Molecules* **2020**, *25*, 1–75.

[103] T. Ngouansavanh, J. Zhu, *Angew Chem* **2007**, *119*, 5877–5880.

[104] A. Duschek, S. F. Kirsch, *Angew Chem Int Ed* **2011**, *50*, 1524–1552.

[105] J. Shi, G. Manolikakes, C.-H. Yeh, C. A. Guerrero, R. A. Shenvi, H. Shigehisa, P. S. Baran, *J Am Chem Soc* **2011**, *133*, 8014–8027.

[106] E. Li, M. Wang, Z. Wang, W. Yu, J. Chang, *Tetrahedron* **2018**, *74*, 4613–4618.

[107] M. Peña-Lõpez, H. Neumann, M. Beller, *Chem Cat Chem* **2015**, *7*, 865–871.

[108] I. Schuster, A. Sztojkov-Ivanov, L. Lázár, F. Fülöp, *Lett Org Chem* **2007**, *4*, 102–108.

[109] C. O'Connor, *Quarterly Reviews, Chemical Society* **1970**, *24*, 553–564.

[110] J. F. Sebastian, *J Chem Educ* **1971**, *48*, 97.

[111] T. A. Paál, E. Forró, A. Liljeblad, L. T. Kanerva, F. Fülöp, *Tetrahedron Asymmetry* **2007**, *18*, 1428–1433.

[112] C. H. Su, *Appl Energy* **2013**, *104*, 503–509.

[113] E. Forró, R. Megyesi, T. A. Paál, F. Fülöp, *Tetrahedron Asymmetry* **2016**, *27*, 1213–1216.

[114] S. M. Lu, Y. Q. Wang, X. W. Han, Y. G. Zhou, *Angew Chem Int Ed* **2006**, *45*, 2260–2263.

[115] D. S. Wang, Q. A. Chen, S. M. Lu, Y. G. Zhou, *Chem Rev* **2012**, *112*, 2557–2590.

[116] A. Mori, Y. Miyakawa, E. Ohashi, T. Haga, T. Maegawa, H. Sajiki, *Org Lett* **2006**, *8*, 3279–3281.

[117] C. W. Scheeren, J. B. Domingos, G. Machado, J. Dupont, *J Phys Chem C* **2008**, *112*, 16463–16469.

[118] D. R. Perkins, M. R. V. Finlay, J. W. M. Nissik, P. A. Raubo, P. D. Smith, A. Bailey, *1,3,4-Thiadiazole Compounds and Their Uses in Treating Cancer*, **2017**, US 2017/0333429 A1.

[119] J. Adams, Y.-T. Ma, R. Stein, M. Baevsky, L. Grenier, L. Plamondon, *Boronic Ester and Acid Compounds, Synthesis and Uses*, **2000**, 6,083,903.

[120] B. Ho, A. M. Crider, J. P. Stables, *Eur J Med Chem* **2001**, *36*, 265–286.

[121] P. Rylander, *Catalytic Hydrogenation over Platinum Metals*, Elsevier, **2012**.

[122] C. W. Keenan, B. W. Gieseman, H. A. Smith, *J Am Chem Soc* **1954**, *76*, 229–232.

[123] N. Ikemoto, D. M. Tellers, S. D. Dreher, J. Liu, A. Huang, N. R. Rivera, E. Njolito, Y. Hsiao, J. C. McWilliams, J. M. Williams, J. D. Armstrong, Y. Sun, D. J. Mathre, E. J. J. Grabowski, R. D. Tillyer, *J Am Chem Soc* **2004**, *126*, 3048–3049.

[124] B. Neises, W. Steglich, *Angew Chem Int Ed Engl* **1978**, *17*, 522–524.

[125] R. A. Al-Horani, U. R. Desai, *Tetrahedron* **2012**, *68*, 2027–2040.

[126] S. Kotha, D. Deodhar, P. Khedkar, *Org Biomol Chem* **2014**, *12*, 9054–9091.

[127] M. J. Fisher, L. S. Kuklish, P. R. Manninen, M. A. Schiffer, A. M. Warshawsky, J. S. York, *Phenoxyethyl Cyclic Amine Derivatives and Their Activity as EP4 Receptor Modulators*, **2017**, US 9,776,964 B2.

[128] J. W. Xie, Z. Bin Yao, X. C. Wang, J. Zhang, *Tetrahedron* **2019**, *75*, 3788–3792.

[129] S. Platte, M. Korff, L. Imberg, I. Balicioglu, C. Erbacher, J. M. Will, C. G. Daniliuc, U. Karst, D. V Kalinin, *Chem Med Chem* **2021**, *16*, 3672–3690.

[130] D. L. Boger, J. S. Panek, *J Am Chem Soc* **1985**, *107*, 5745–5754.

[131] S. Klutchko, C. J. Blankley, R. W. Fleming, M. Hinkley, A. E. Werner, I. Nordin, A. Holmes, M. L. Hoeñe, D. M. Cohen, A. D. Essenburg, H. R. Kaplan, *J. Med. Chem* **1986**, *29*, 1953–1961.

[132] I. Fleming, *Pericyclic Reactions*, Oxford University Press, USA, **2015**.

[133] K. A. Wayne, L. M. J. Howard, S. N. James, C. R. Arvela, *Am Chem Soc* **1984**, *27*, 1321–1325.

[134] T. Pesnot, M. C. Gershater, J. M. Ward, H. C. Hailes, *Adv Synth Catal* **2012**, *354*, 2997–3008.

[135] J. Zhao, B. R. Lichman, J. M. Ward, H. C. Hailes, *Chem Comm* **2018**, *54*, 1323–1326.

[136] Z. Zalán, T. A. Martinek, L. Lázár, R. Sillanpää, F. Fülöp, *Tetrahedron* **2006**, *62*, 2883–2891.

[137] B. Ho, A. M. Crider, J. P. Stables, *Eur J Med Chem* **2001**, *36*, 265–286.

[138] S. D. Kuduk, R. K. Chang, C. N. Marco, *Quinolizidinone 1M Receptor Positive Allosteric Modulators*, **2009**, WO 2009/117283 A2.

[139] T. You, S.-H. Zeng, J. Fan, L. Wu, F. Kang, Y. Liu, C.-M. Che, *Chem Comm* **2021**, *57*, 10711–10714.

[140] P. G. M. Wuts, T. W. Greene, *Greene's Protective Groups in Organic Synthesis*, John Wiley & Sons, New Jersey, **2006**.

[141] G. Han, M. Tamaki, V. J. Hruby, *J Pept Res* **2001**, *58*, 338–341.

[142] N. P. Mathebula, R. A. Sheldon, M. L. Bode, *Chem Bio Chem* **2022**, *23*, 1–6.

[143] R. Kumar, V. K. Maikhuri, D. Mathur, M. Kumar, N. Singh, A. K. Prasad, *Biocatal Biotransformation* **2024**, *42*, 19–33.

[144] A. J. J. Straathop, J. A. Jongejan, *Enzyme Microb Technol* **1997**, *21*, 1–13.

[145] D. Leung, S. O. Kang, E. V. Anslyn, *Chem Soc Rev* **2012**, *41*, 448–479.

[146] S. Hari Krishna, N. G. Karanth, *Catal Rev Sci Eng* **2002**, *44*, 499–591.

[147] T. Nagasawa, H. Shimizu, H. Yamada, *Appl Microbiol Biotechnol* **1993**, *40*, 189–195.

[148] A. W. Parkins, *Platin Met Rev* **1996**, *40*, 169–174.

[149] L. Cantarella, A. Gallifuoco, A. Malandra, L. Martínková, A. Spera, M. Cantarella, *Enzyme Microb Technol* **2011**, *48*, 345–350.

[150] M. S. Phull, S. S. Jadav, C. S. Bohara, R. Gundla, P. S. Mainkar, *SynOpen* **2023**, *7*, 362–370.

Appendix: ^{1}H and ^{13}C NMR spectral data for a select number of compounds

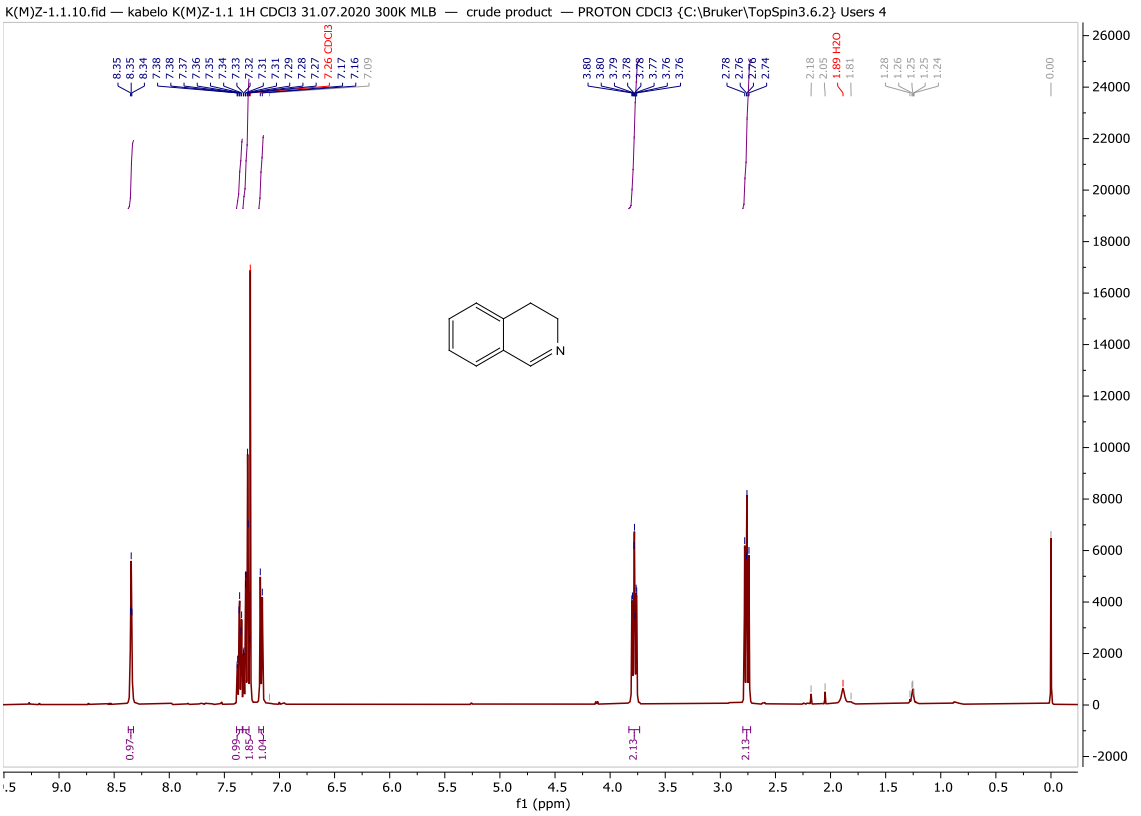

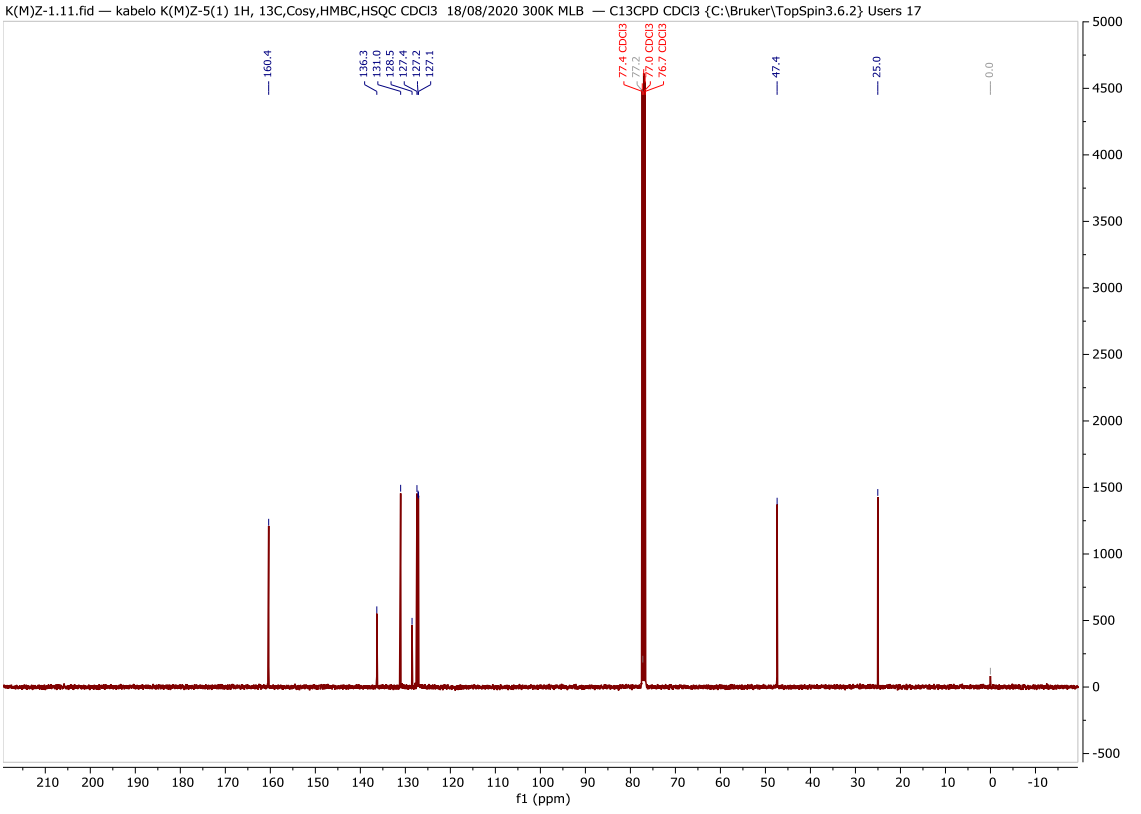

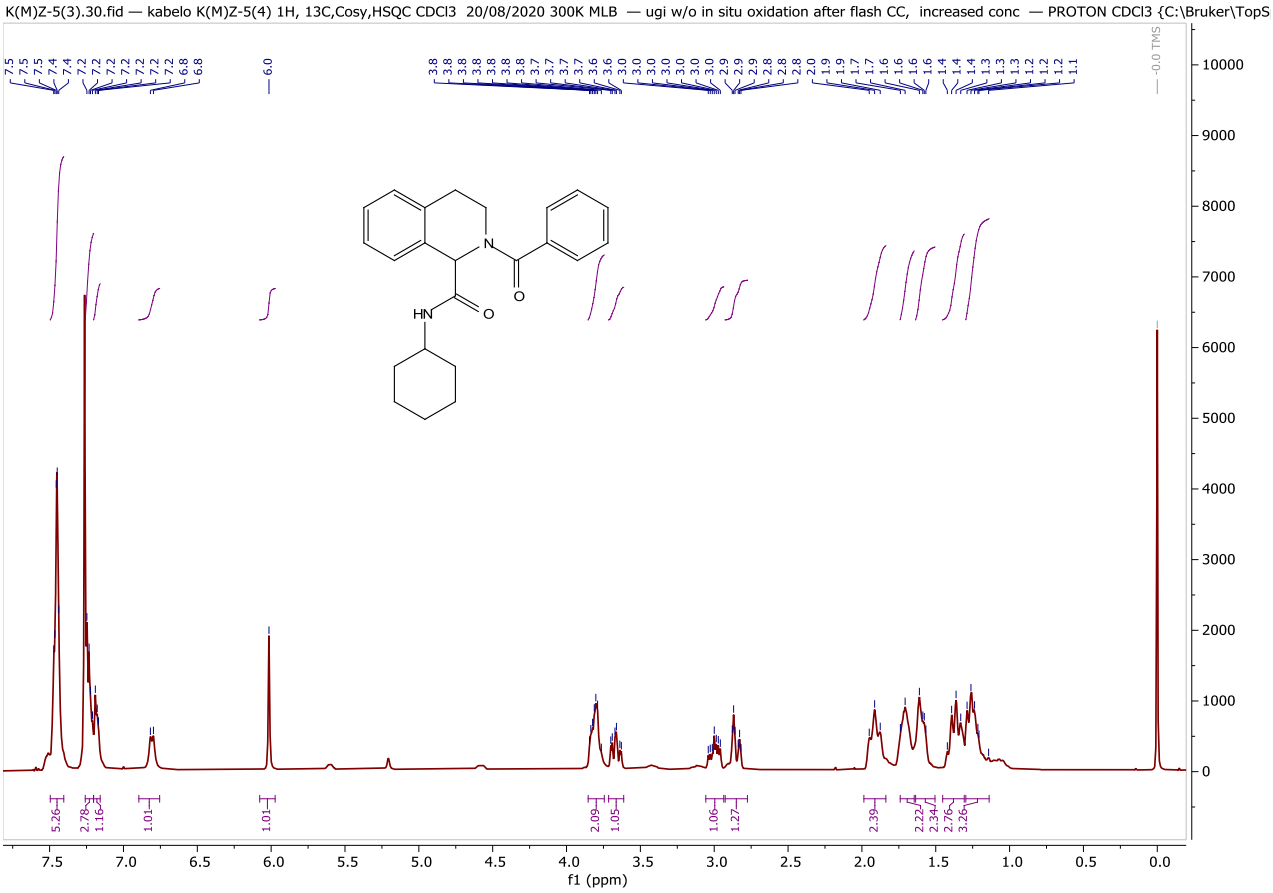
K(M)Z-5(3).30.fid — kabelo K(M)Z-5(4) 1H, 13C,Cosy,HSQC CDCl3 20/08/2020 300K MLB — ugi w/o in situ oxidation after flash CC, increased conc — PROTON CDCl3 {C:\Bruker\TopS
f1 (ppm)

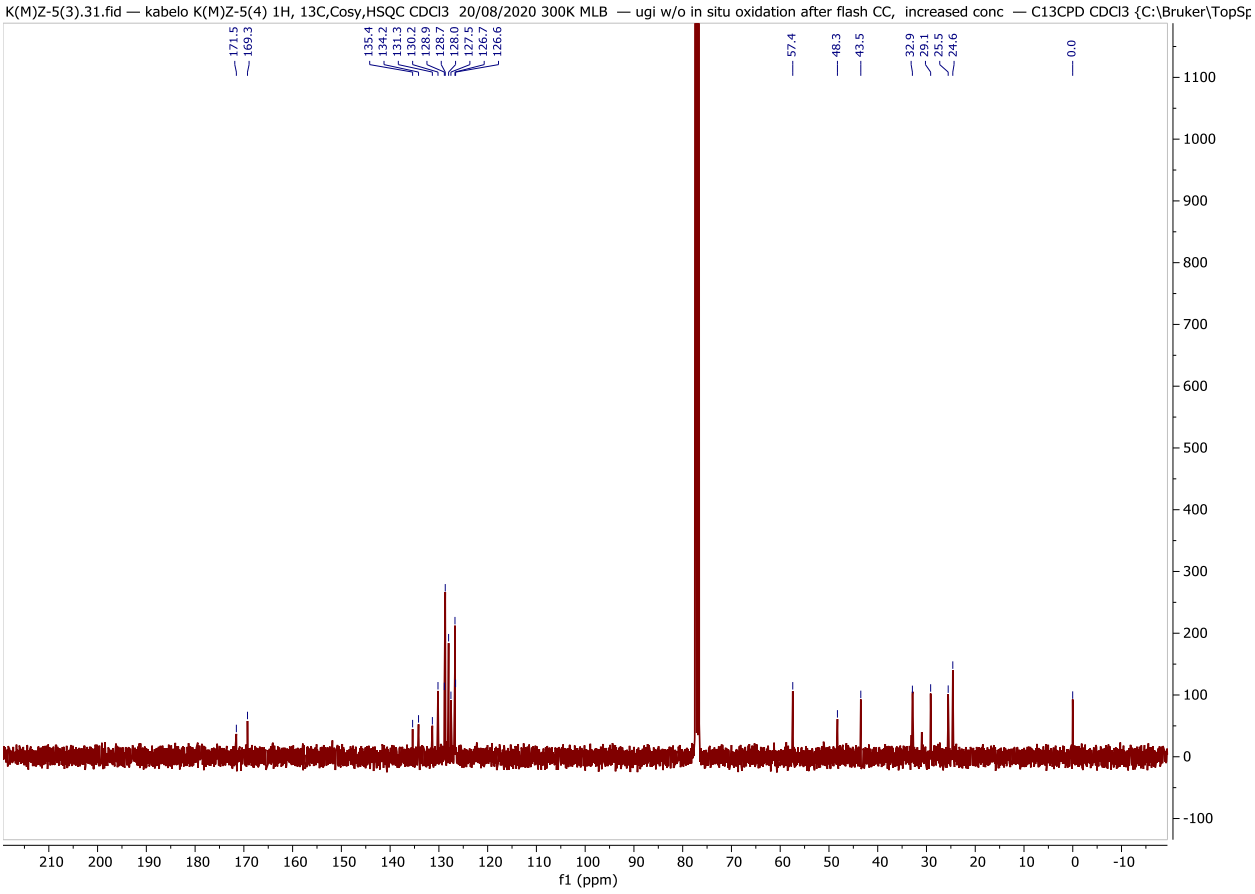
K(M)Z-5(3).31.fid — kabelo K(M)Z-5(4) 1H, 13C,Cosy,HSQC CDCl3 20/08/2020 300K MLB — ugi w/o in situ oxidation after flash CC, increased conc — C13CPD CDCl3 {C:\Bruker\TopSp
f1 (ppm)

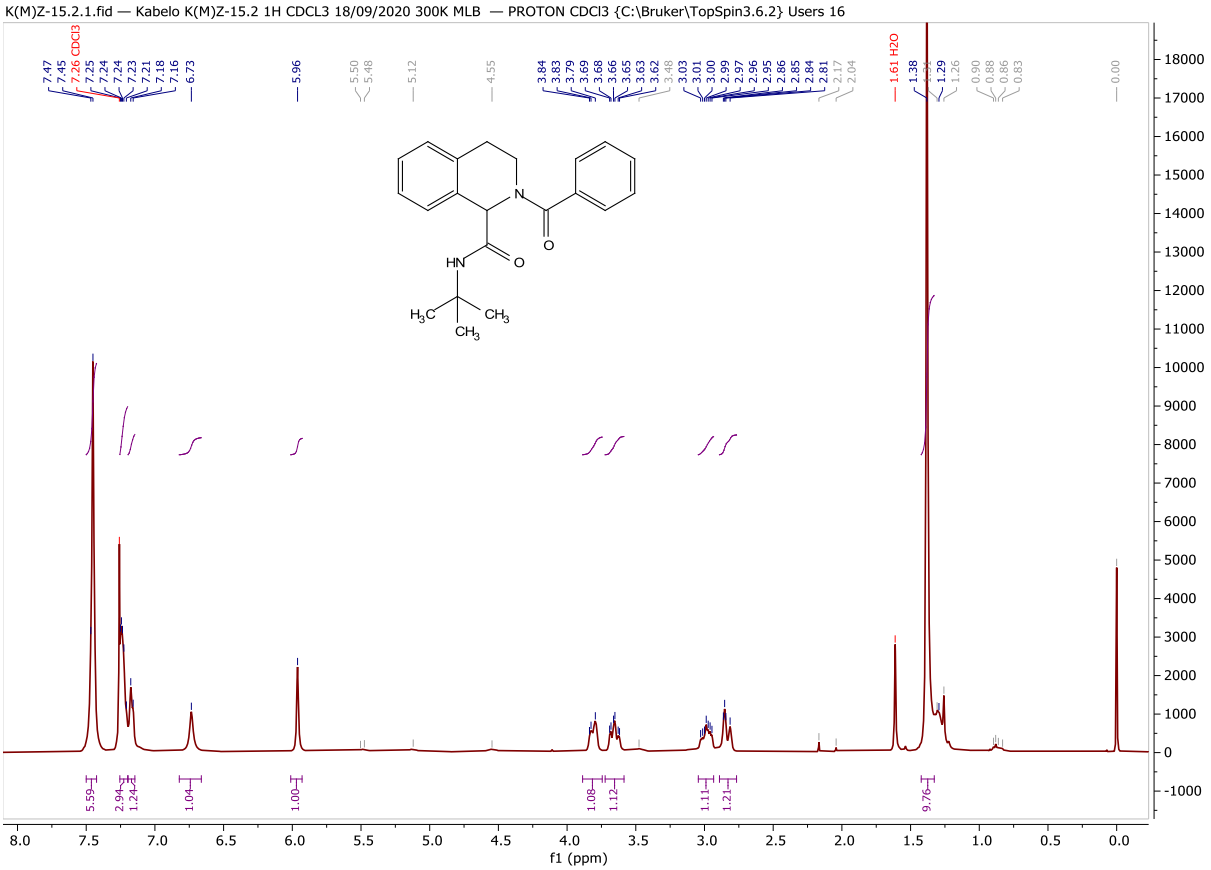
K(M)Z-15.2.1.fid — Kabelo K(M)Z-15.2 1H CDCL3 18/09/2020 300K MLB — PROTON CDCl3 {C:\Bruker\TopSpin3.6.2} Users 16
7.47
7.45
7.26 CDCl3
7.25
7.24
7.24
7.23
7.21
7.18
7.16
6.73
5.96
5.50
5.48
5.12
4.55
3.84
3.83
3.79
3.69
3.68
3.66
3.65
3.63
3.62
3.48
3.03
3.01
3.00
2.99
2.97
2.96
2.95
2.86
2.85
2.84
2.81
2.17
2.04
1.61 H2O
1.38
1.29
1.26
0.90
0.88
0.86
0.83
0.00
HN
O
N
O
H3C
CH3
CH3
5.59
2.94
1.24
1.04
1.00
1.08
1.12
1.11
1.21
9.76
f1 (ppm)

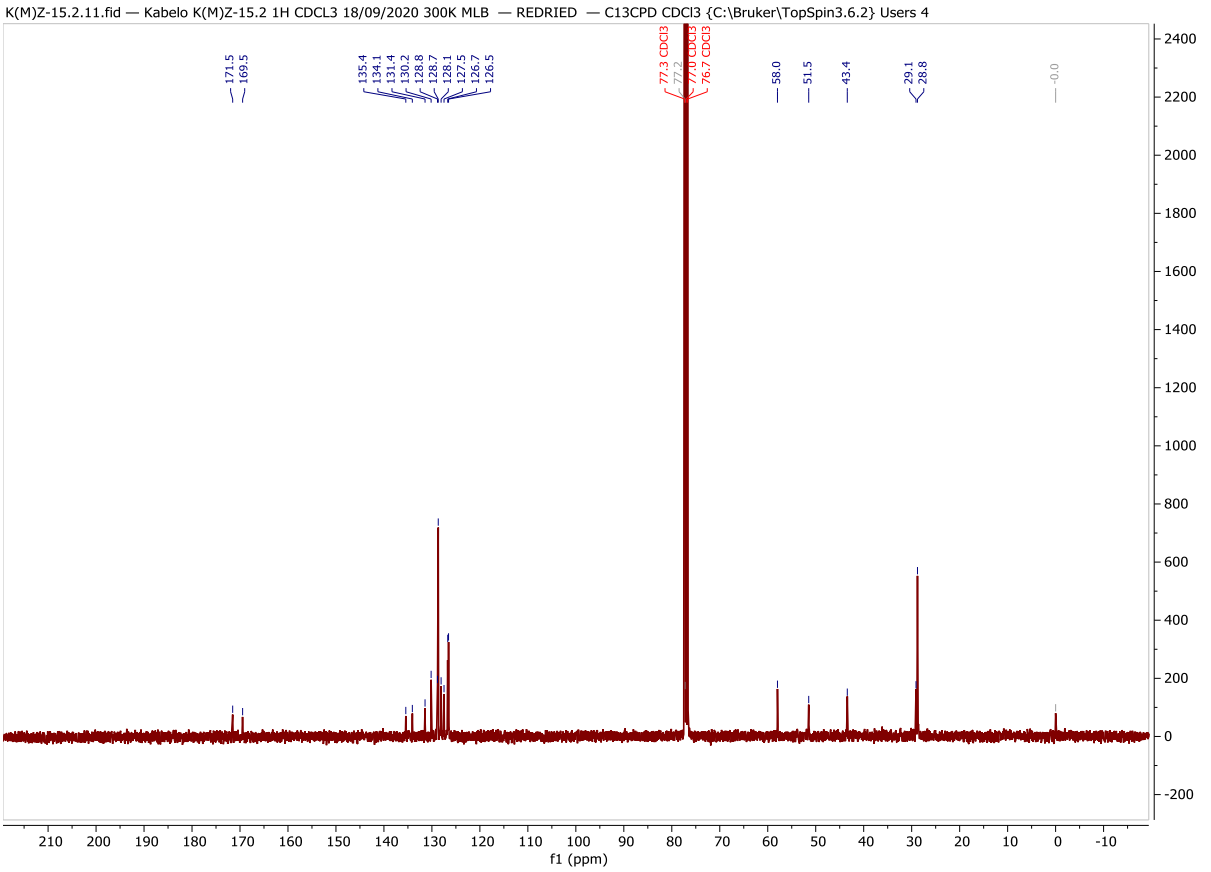
K(M)Z-15.2.11.fid — Kabelo K(M)Z-15.2 1H CDCL3 18/09/2020 300K MLB — REDRIED — C13CPD CDCl3 {C:\Bruker\TopSpin3.6.2} Users 4
171.5
169.5
135.4
134.1
131.4
130.2
128.8
128.7
128.1
127.5
126.7
126.5
77.3 CDCl3
77.0 CDCl3
76.7 CDCl3
58.0
51.5
43.4
29.1
28.8
-0.0
f1 (ppm)

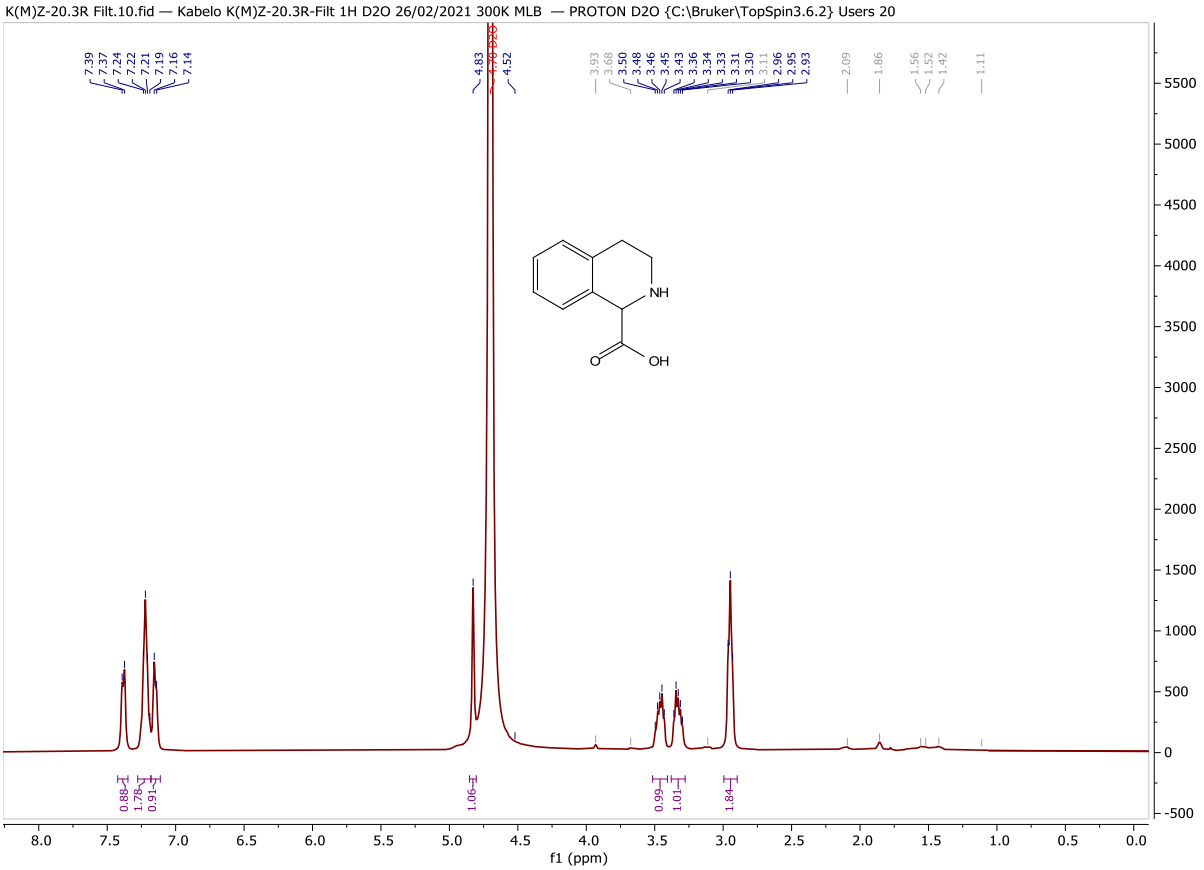
K(M)Z-20.3R Filt.10.fid — Kabelo K(M)Z-20.3R-Filt 1H D2O 26/02/2021 300K MLB — PROTON D2O {C:\Bruker\TopSpin3.6.2} Users 20
7.39
7.37
7.24
7.22
7.21
7.19
7.16
7.14
4.83
4.52
3.93
3.68
3.50
3.48
3.46
3.45
3.43
3.36
3.34
3.33
3.31
3.30
3.11
2.96
2.95
2.93
2.09
1.86
1.56
1.52
1.42
1.11
NH
O
OH
0.88
1.78
0.91
1.06
0.99
1.01
1.84
f1 (ppm)

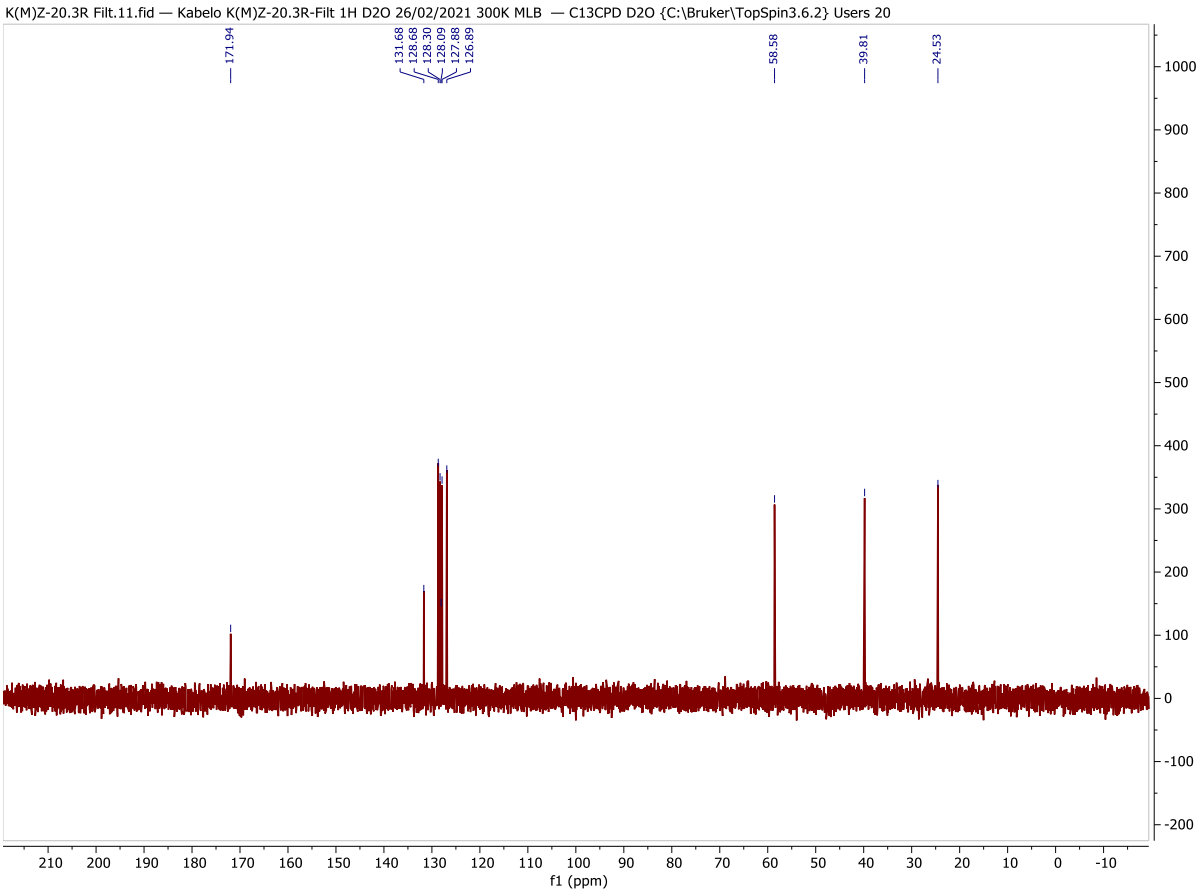
K(M)Z-20.3R Filt.11.fid — Kabelo K(M)Z-20.3R-Filt 1H D2O 26/02/2021 300K MLB — C13CPD D2O {C:\Bruker\TopSpin3.6.2} Users 20
171.94
131.68
128.68
128.30
128.09
127.88
126.89
58.58
39.81
24.53
f1 (ppm)

KMZ-MM-3-Reclmn-REDRY.10.fid — Kabelo KMZ-MM-3-Reclmn-REDRY CDCl3 11/05/22 1H, MLB 400MHz — PROTON CDCl3 {C:\Bruker\TopSpin3.6.2} Users 19

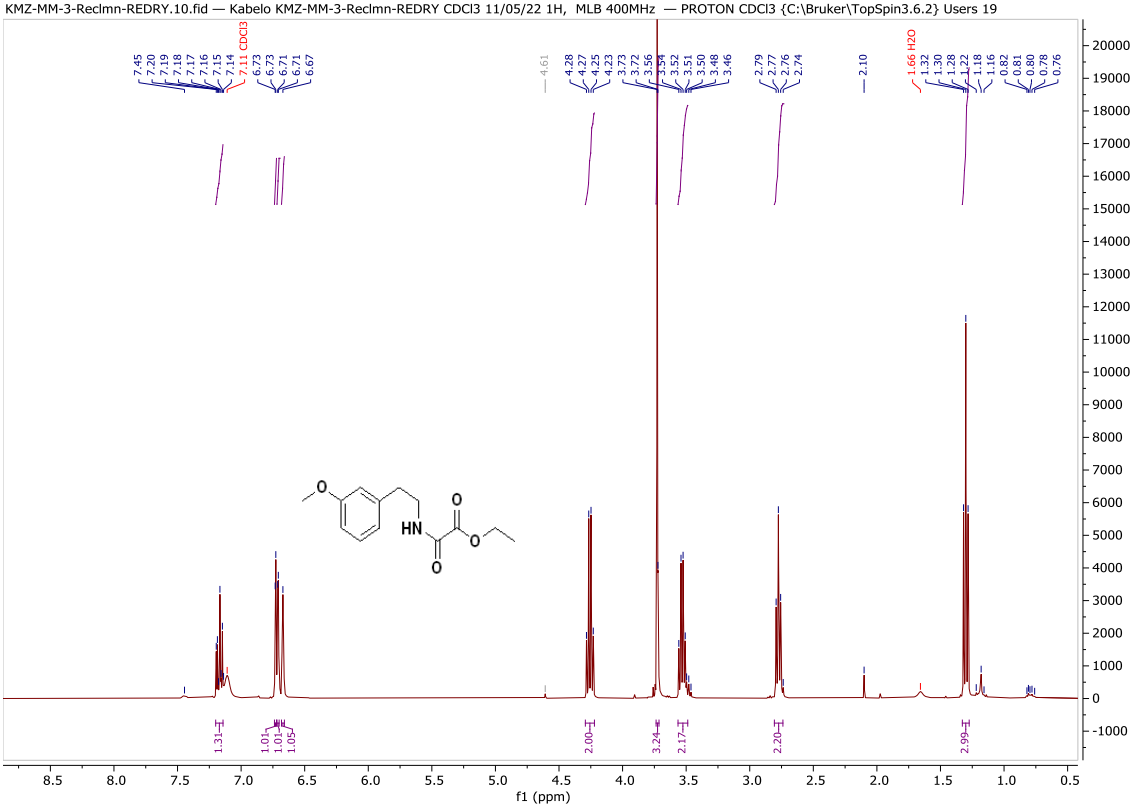

KMZ-MM-3-Reclmn.11.fid — Kabelo KMZ-MM-3-Reclmn CDCl3 10/05/22 1H MLB 400MHz — C13CPD CDCl3 {C:\Bruker\TopSpin3.6.2} Users 15

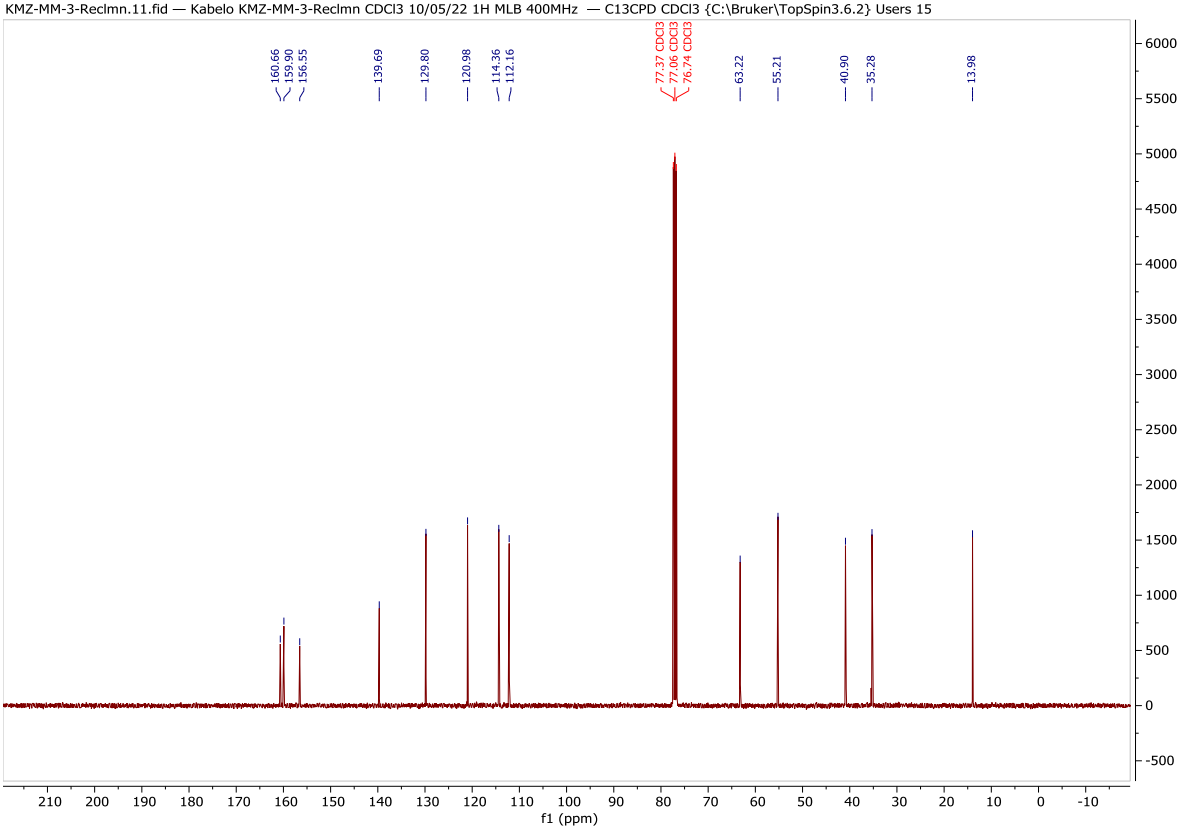

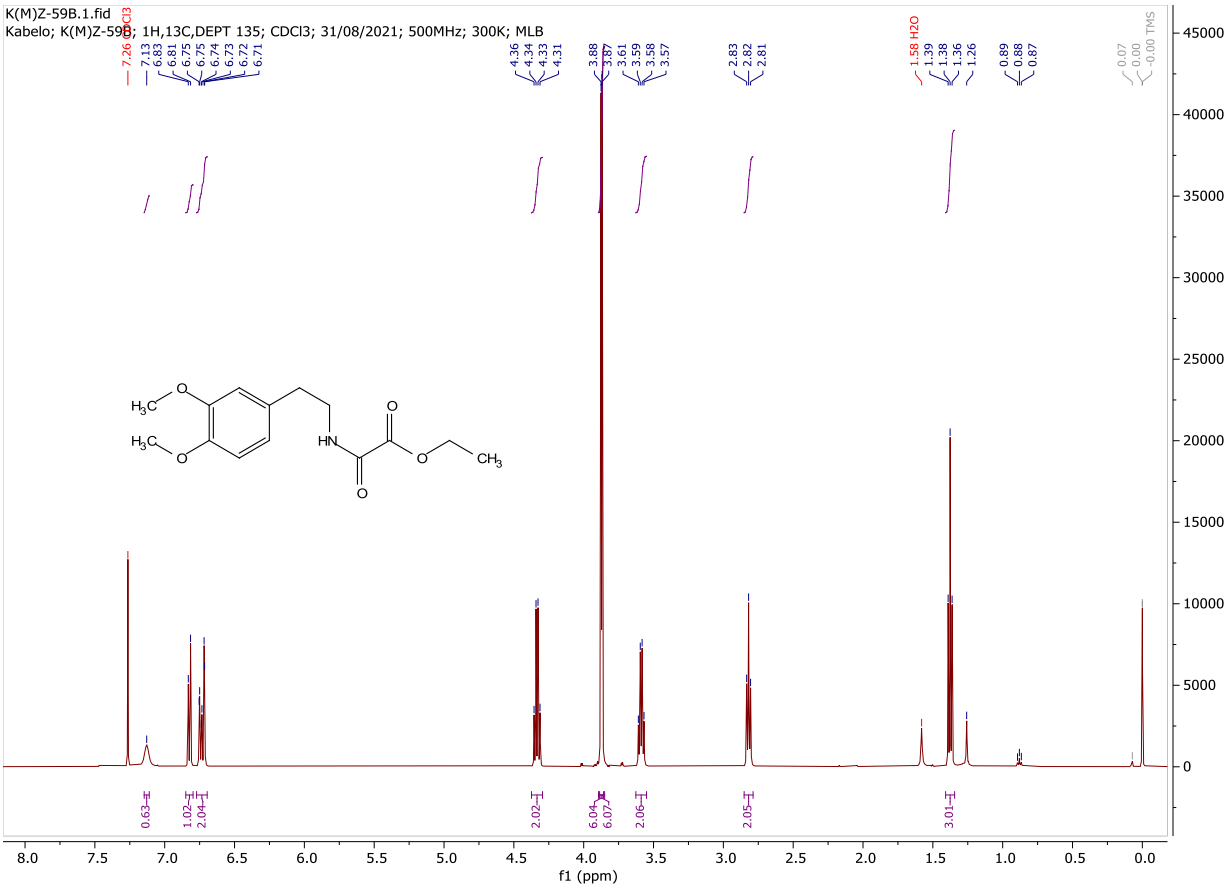
K(M)Z-59B.1.fid
Kabelo; K(M)Z-59B; 1H,13C,DEPT 135; CDCl3; 31/08/2021; 500MHz; 300K; MLB
7.26 CDCl3
7.13
6.83
6.81
6.75
6.75
6.74
6.73
6.72
6.71
4.36
4.34
4.33
4.31
3.88
3.87
3.61
3.59
3.58
3.57
2.83
2.82
2.81
1.58 H2O
1.39
1.38
1.36
1.26
0.89
0.88
0.87
0.07
0.00
-0.00 TMS
0.63
1.02
2.04
2.02
6.04
6.07
2.06
2.05
3.01
f1 (ppm)

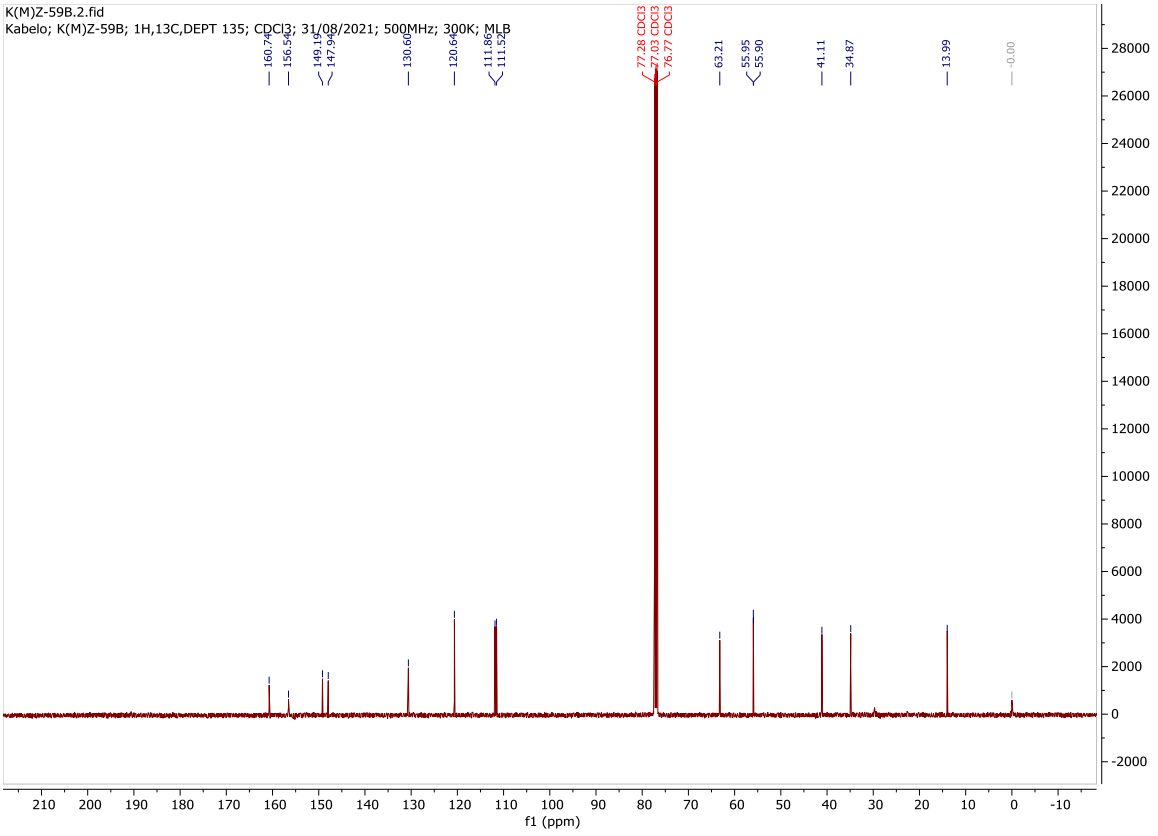
K(M)Z-59B.2.fid
Kabelo; K(M)Z-59B; 1H,13C,DEPT 135; CDCl3; 31/08/2021; 500MHz; 300K; MLB
160.74
156.54
149.19
147.94
130.60
120.64
111.86
111.52
77.28 CDCl3
77.03 CDCl3
76.77 CDCl3
63.21
55.95
55.90
41.11
34.87
13.99
-0.00
f1 (ppm)

KMZ-MM-15.10.fid — kabelo KMZ-MM-15 CDCl3 17/01/2022 1H MLB 400NMR — PROTON CDCl3 {C:\Bruker\TopSpin3.6.2} Users 5

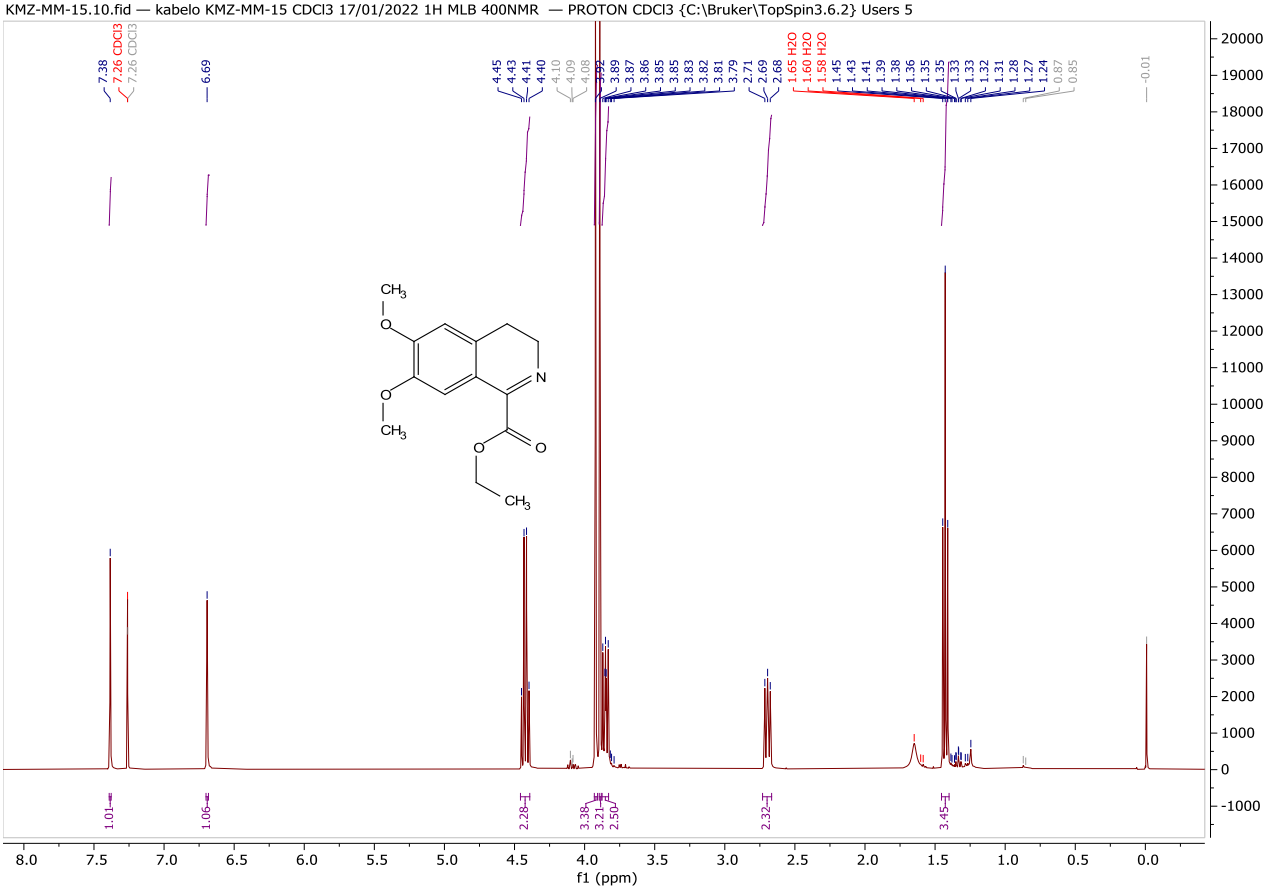

KMZ-MM-15.11.fid — kabelo KMZ-MM-15 CDCl3 17/01/2022 1H MLB 400NMR — C13CPD CDCl3 {C:\Bruker\TopSpin3.6.2} Users 5

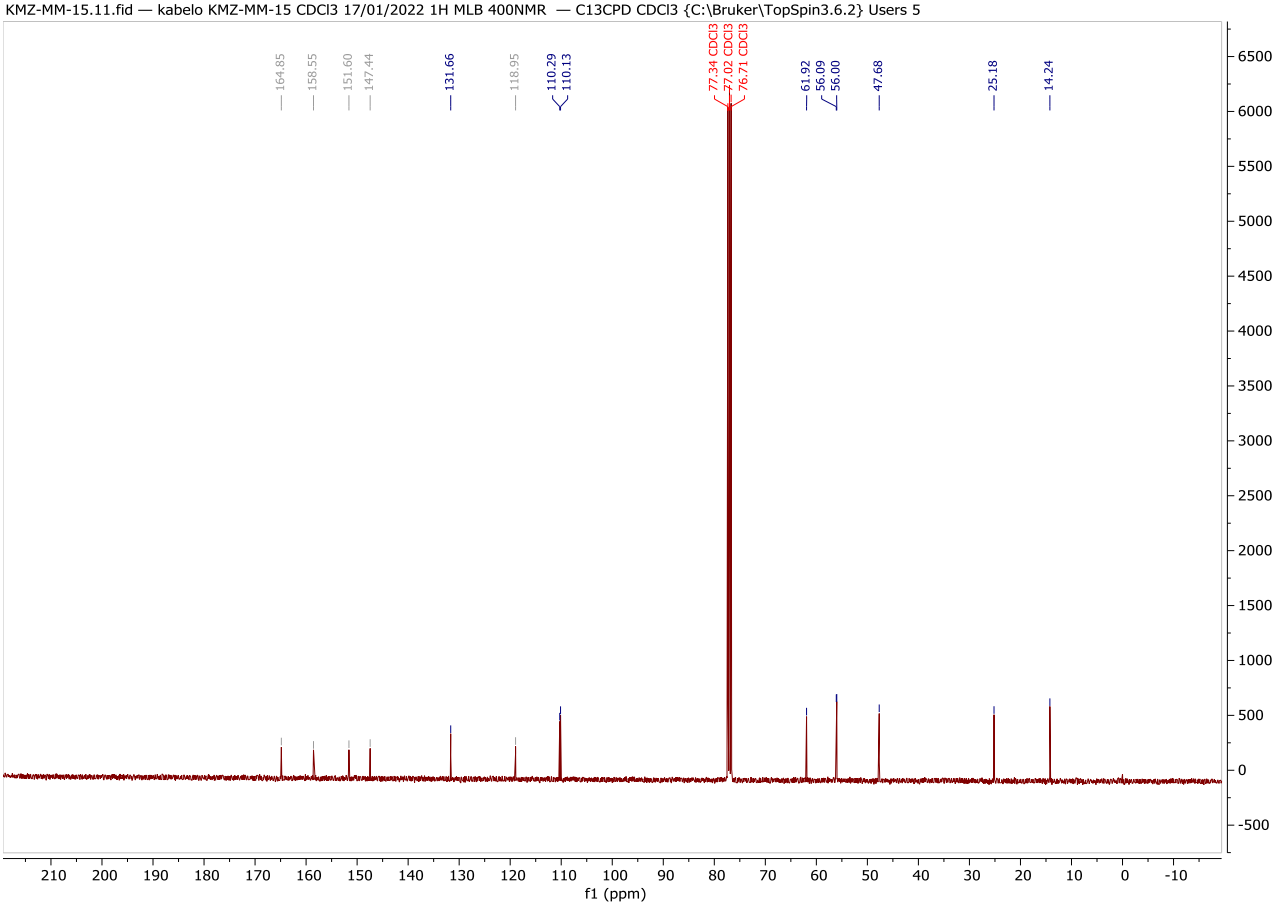

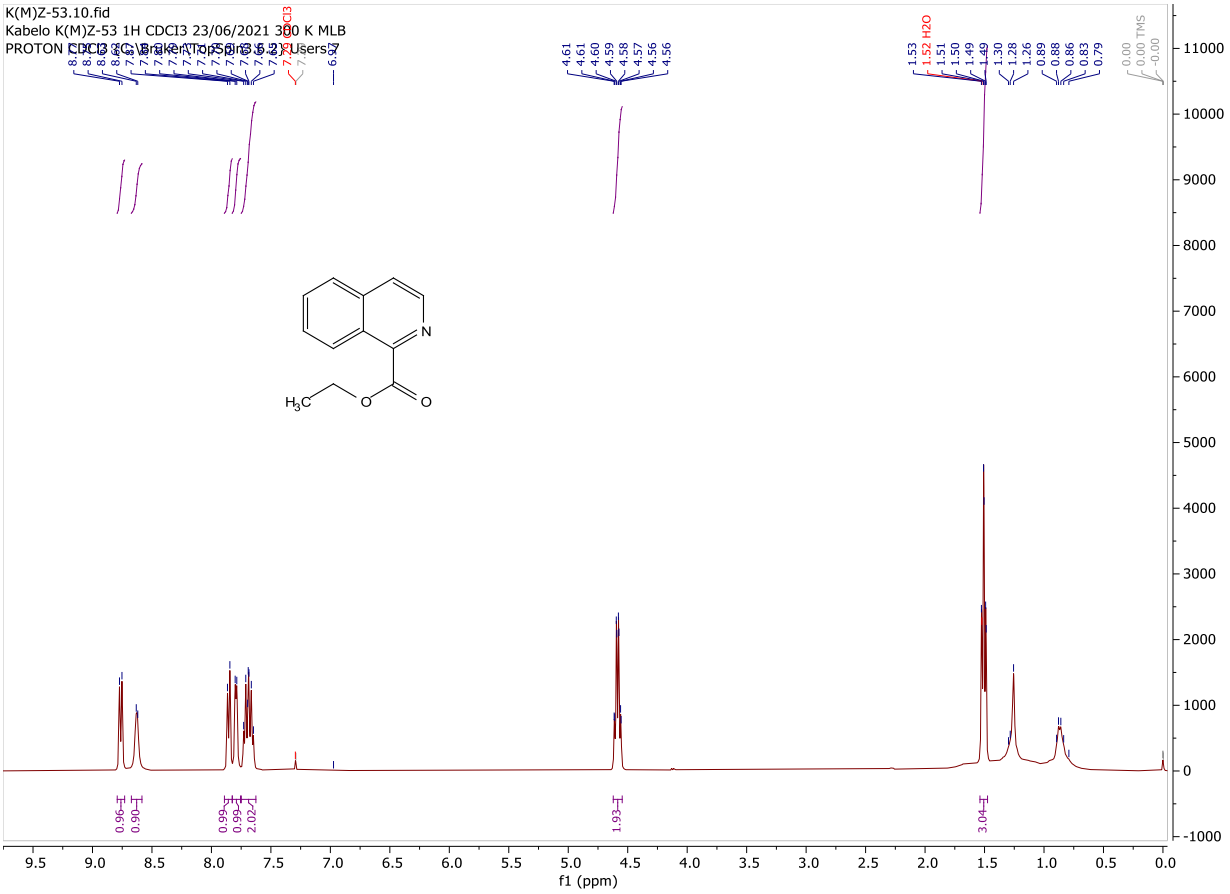
K(M)Z-53.10.fid
Kabelo K(M)Z-53 1H CDCl3 23/06/2021 300 K MLB
PROTON CDCl3 {C:\Bruker\TopSpin3.6.2} Users 7
f1 (ppm)

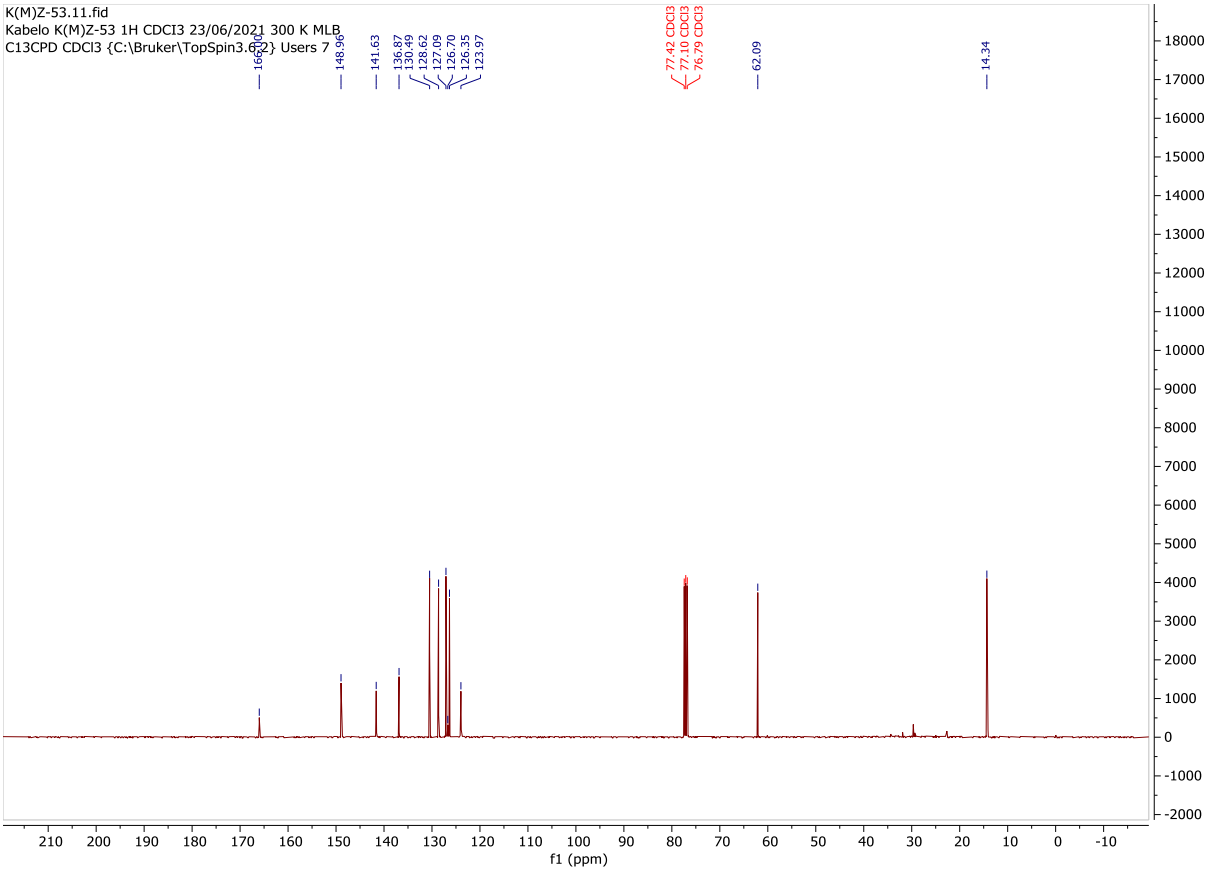
K(M)Z-53.11.fid
Kabelo K(M)Z-53 1H CDCl3 23/06/2021 300 K MLB
C13CPD CDCl3 {C:\Bruker\TopSpin3.6.2} Users 7
f1 (ppm)

Ethyl 1,2,3,4-tetrahydroisoquinoline-1-carboxylate, CDCl3, 1H, 300K, 400MHz

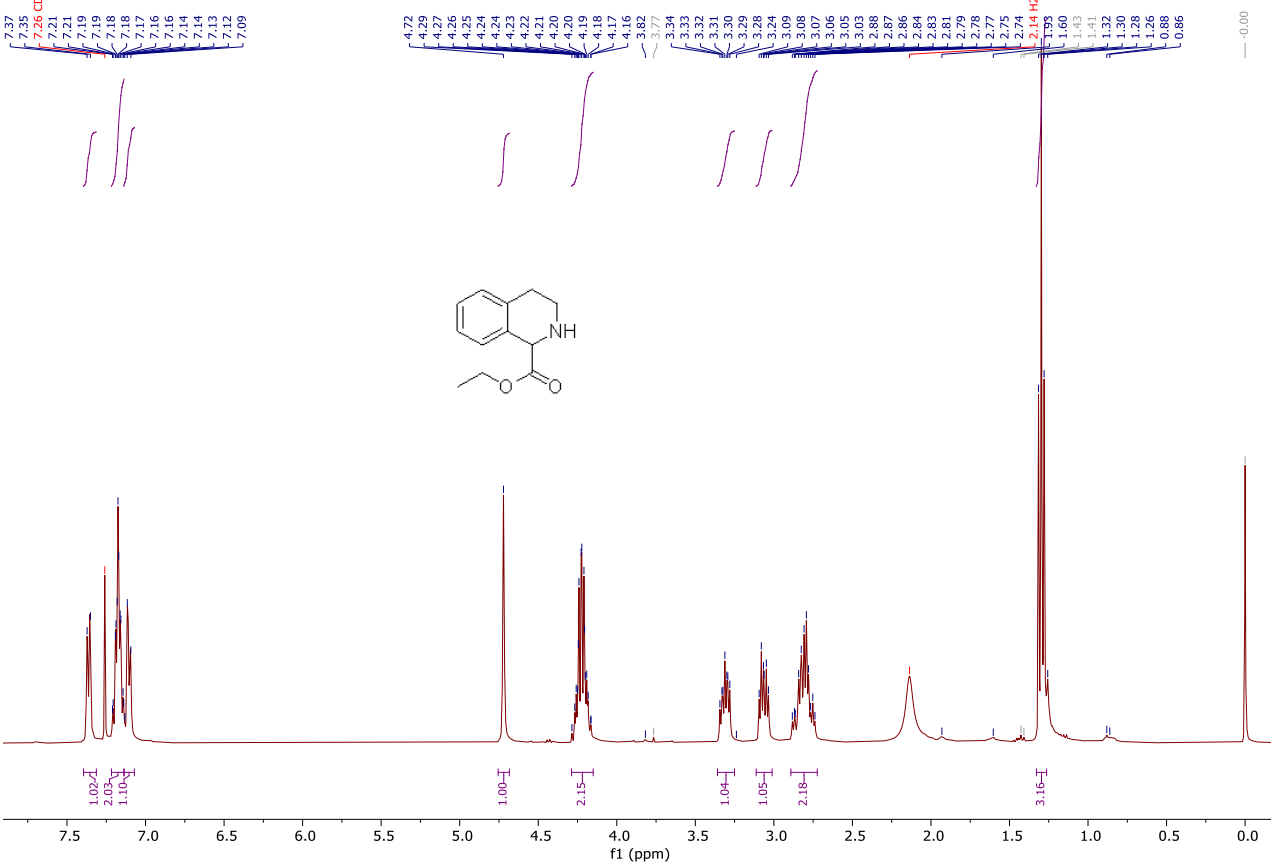

Ethyl 1,2,3,4-tetrahydroisoquinoline-1-carboxylate, CDCl3, 13C, 300K, 400MHz

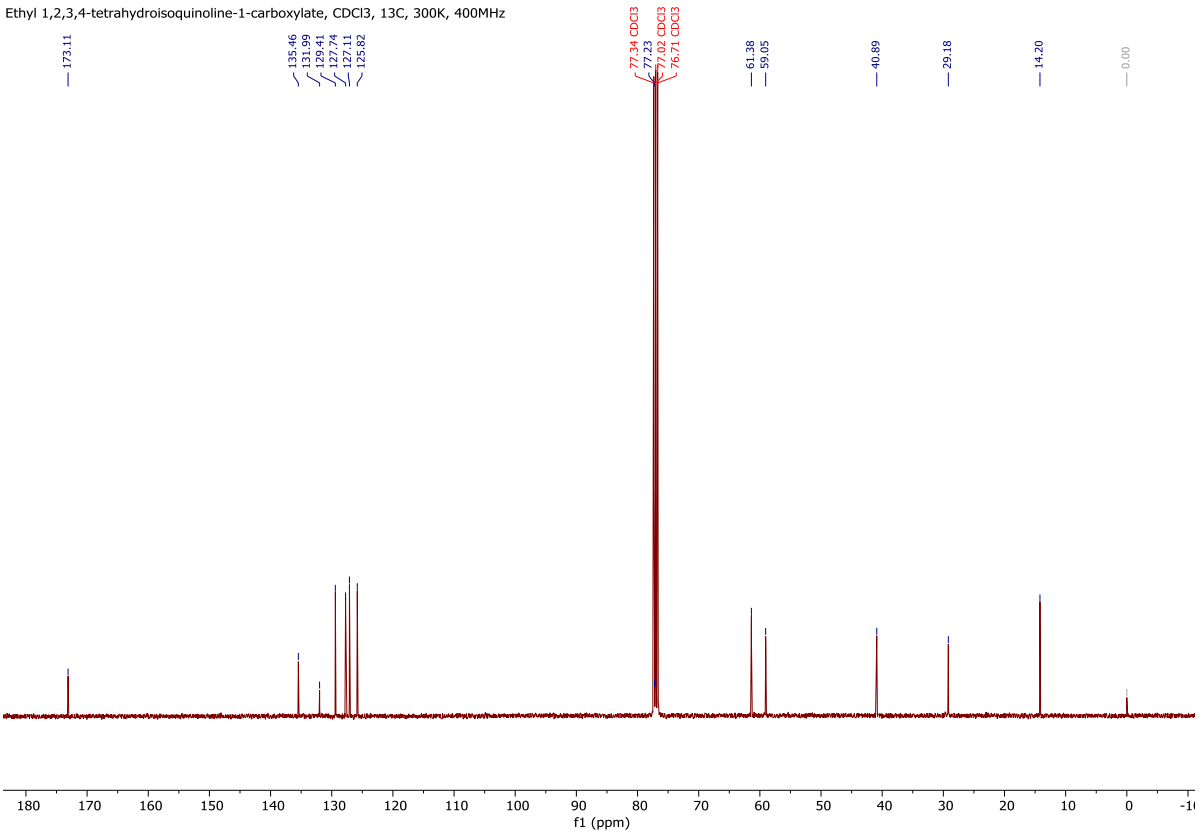

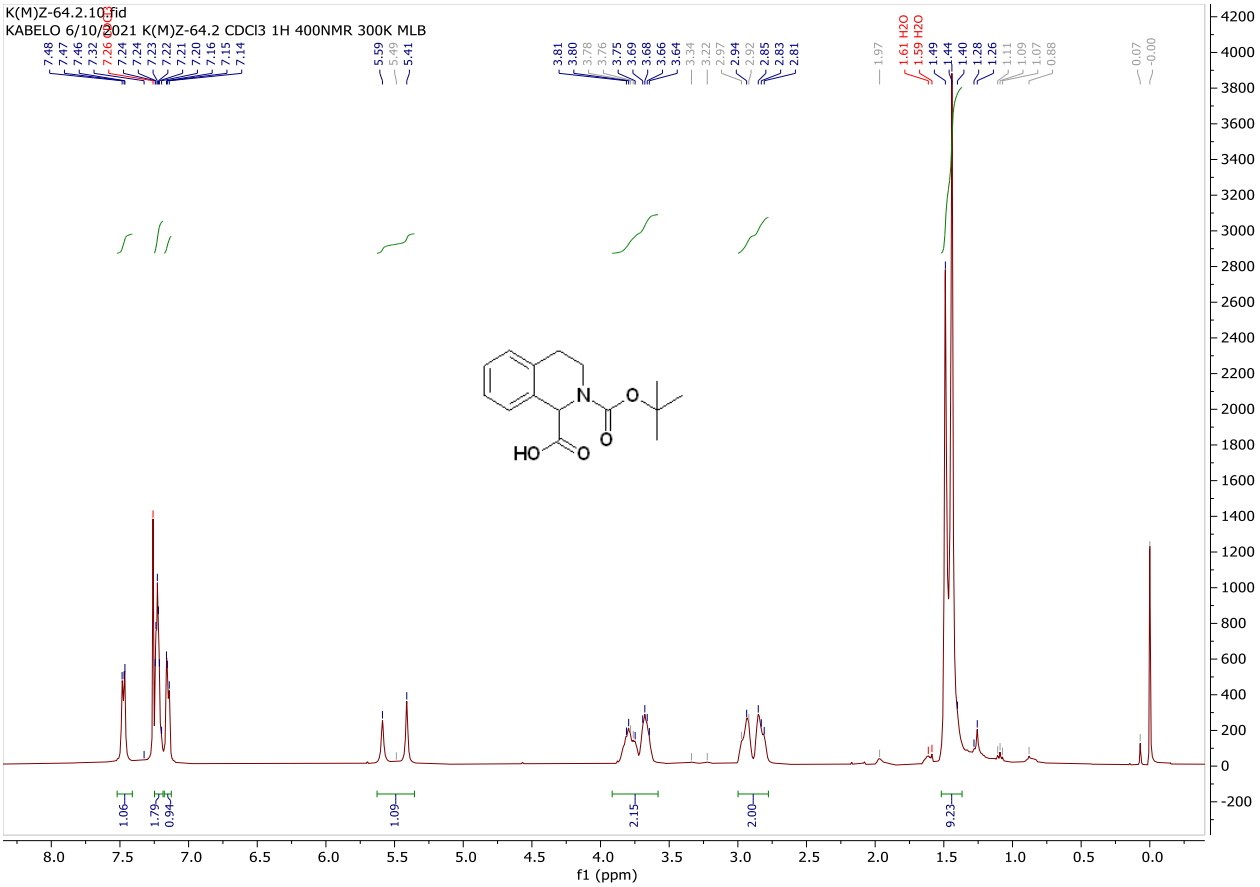
K(M)Z-64.2.10.fid
KABELO 6/10/2021 K(M)Z-64.2 CDCl3 1H 400NMR 300K MLB
7.48 7.47 7.46 7.32 7.26 CDCl3 7.24 7.24 7.23 7.22 7.21 7.20 7.16 7.15 7.14
5.59 5.49 5.41
3.81 3.80 3.78 3.76 3.75 3.69 3.68 3.66 3.64 3.34 3.22 2.97 2.94 2.92 2.85 2.83 2.81
1.97
1.61 H2O 1.59 H2O 1.49 1.44 1.40 1.28 1.26 1.11 1.09 1.07 0.88
0.07 -0.00
N
O
O
HO
O
1.06 1.79 0.94 1.09 2.15 2.00 9.23
f1 (ppm)

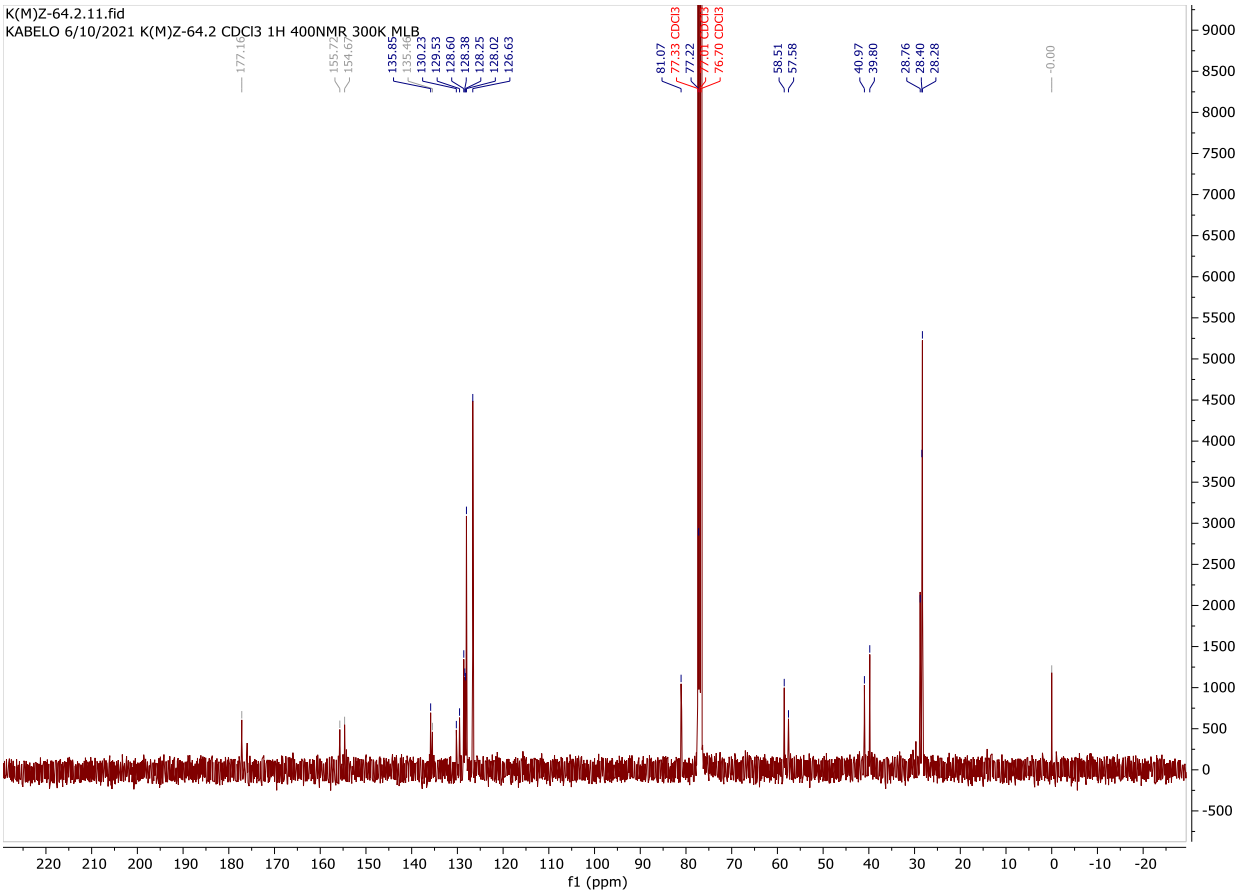
K(M)Z-64.2.11.fid
KABELO 6/10/2021 K(M)Z-64.2 CDCl3 1H 400NMR 300K MLB
177.16
155.72
154.67
135.85
135.46
130.23
129.53
128.60
128.38
128.25
128.02
126.63
81.07
77.33 CDCl3
77.22
77.01 CDCl3
76.70 CDCl3
58.51
57.58
40.97
39.80
28.76
28.40
28.28
-0.00
f1 (ppm)

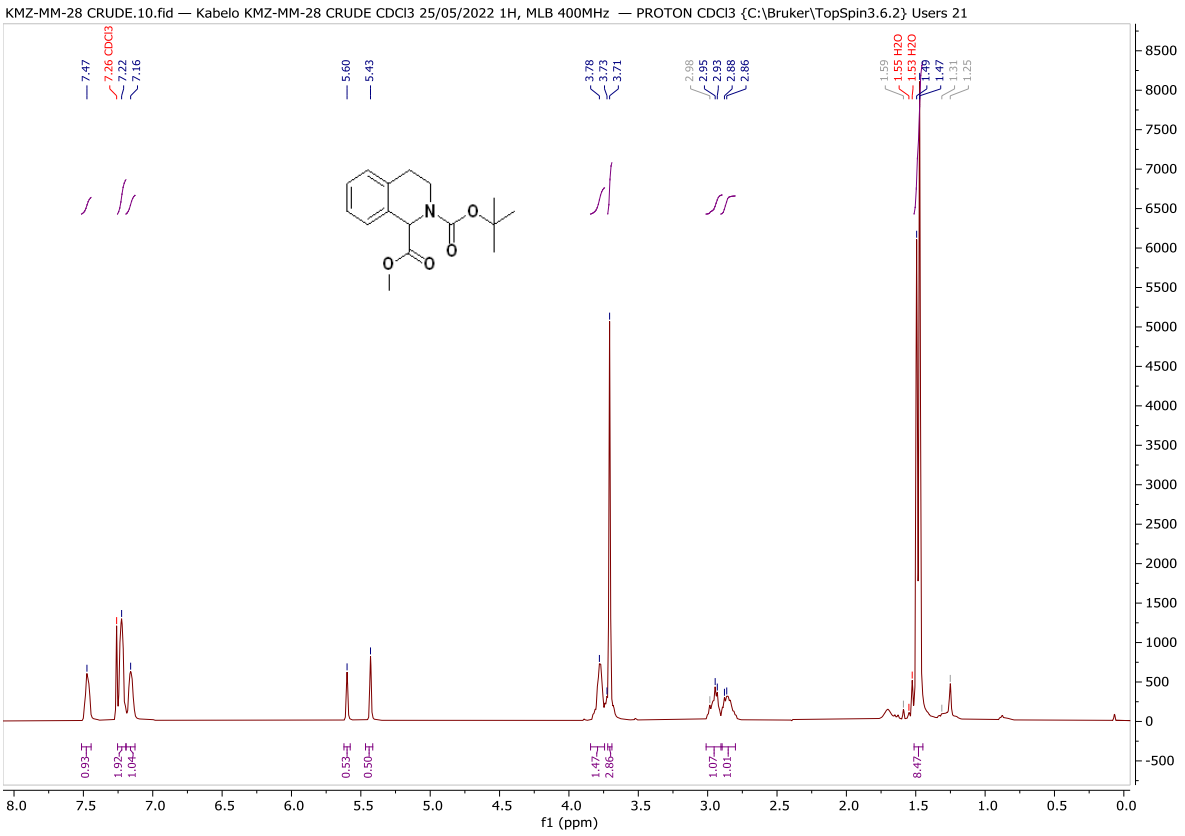
KMZ-MM-28 CRUDE.10.fid — Kabelo KMZ-MM-28 CRUDE CDCl3 25/05/2022 1H, MLB 400MHz — PROTON CDCl3 {C:\Bruker\TopSpin3.6.2} Users 21
7.47
7.26 CDCl3
7.22
7.16
5.60
5.43
3.78
3.73
3.71
2.98
2.95
2.93
2.88
2.86
1.59
1.55 H2O
1.53 H2O
1.47
1.31
1.25
0.93
1.92
1.04
0.53
0.50
1.47
2.86
1.07
1.01
8.47
f1 (ppm)

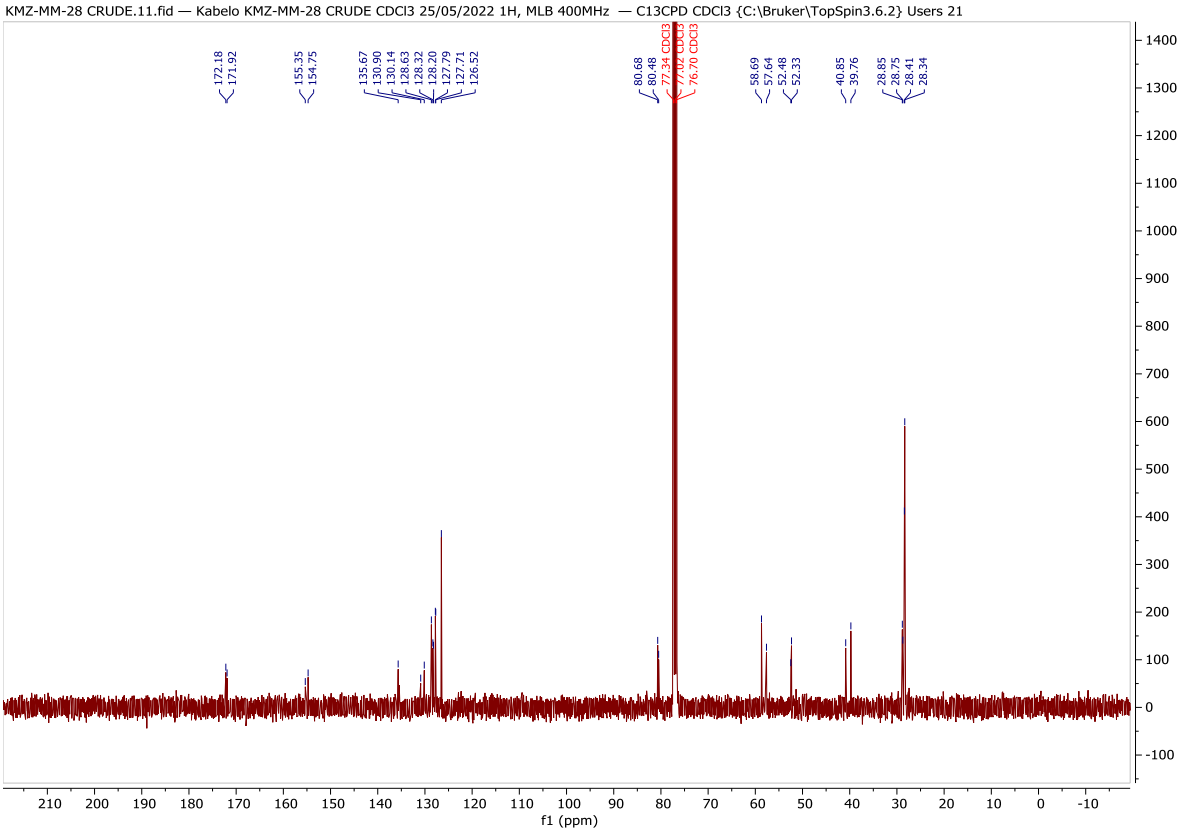
KMZ-MM-28 CRUDE.11.fid — Kabelo KMZ-MM-28 CRUDE CDCl3 25/05/2022 1H, MLB 400MHz — C13CPD CDCl3 {C:\Bruker\TopSpin3.6.2} Users 21
f1 (ppm)

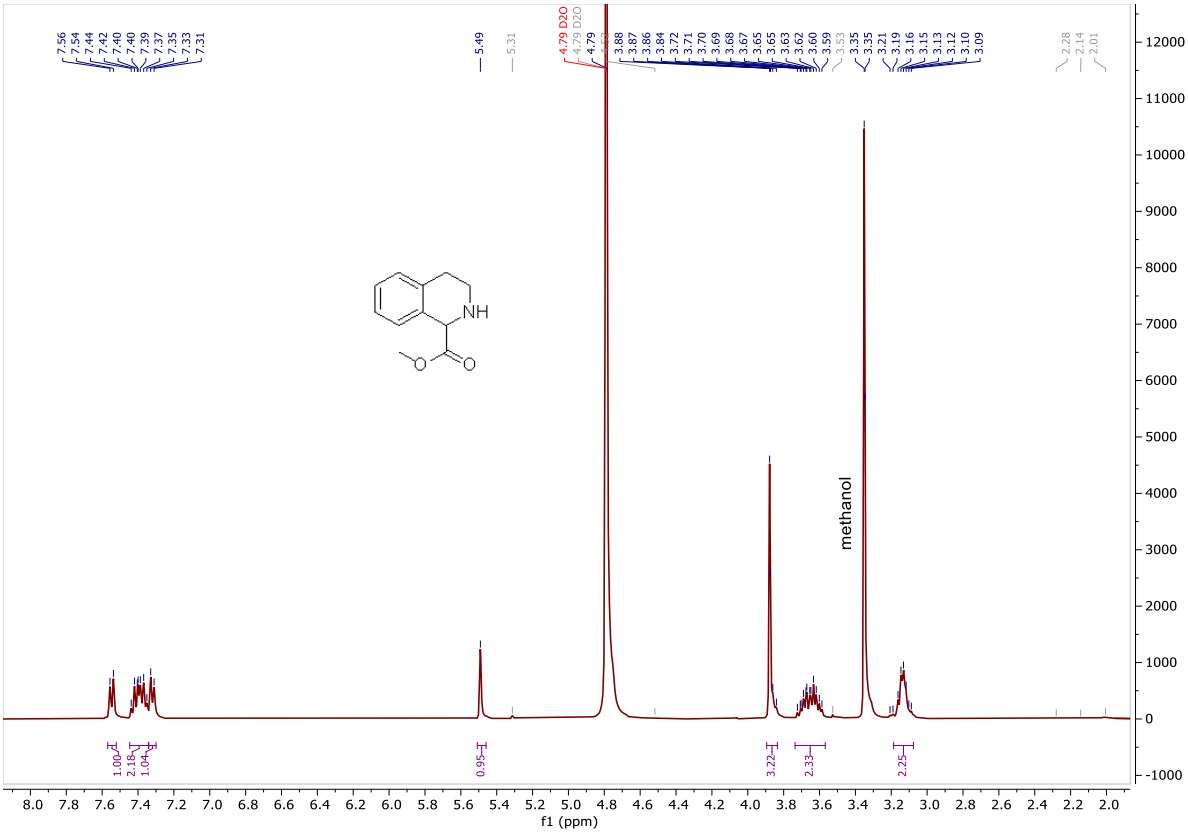
methanol
f1 (ppm)

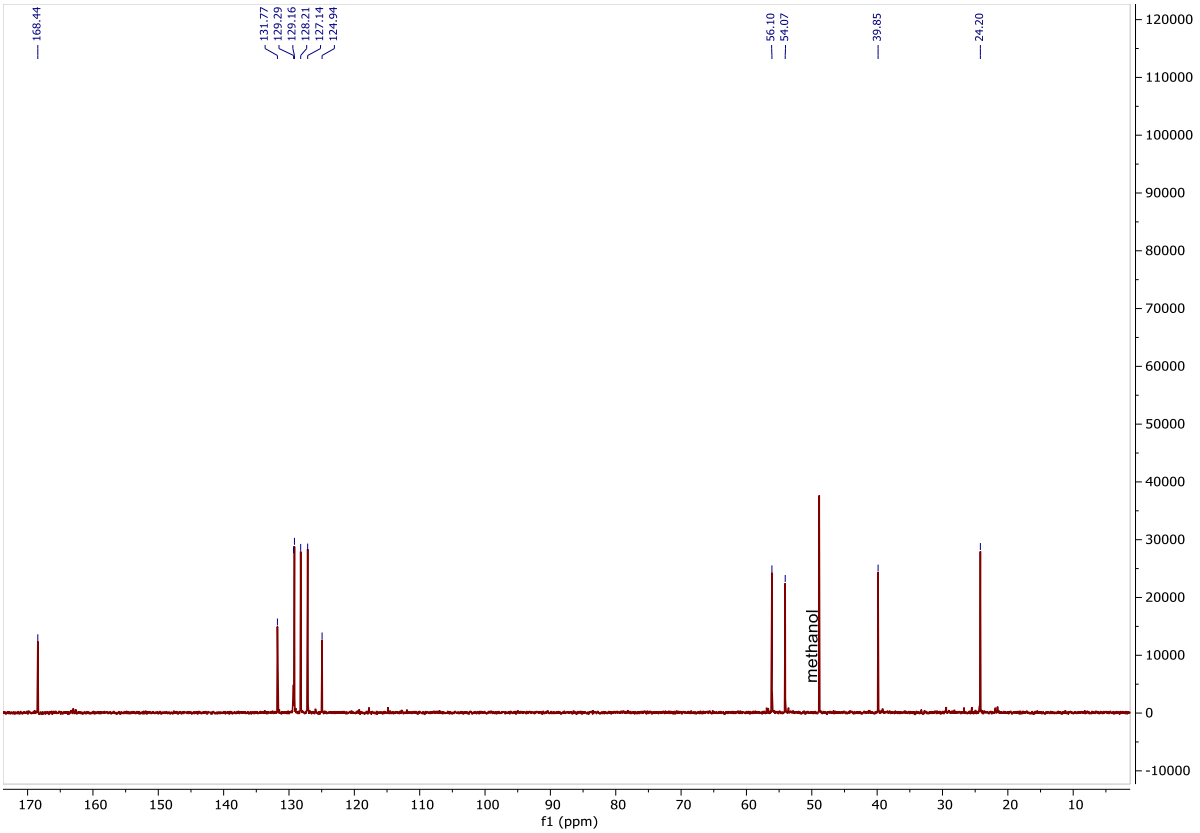
168.44
131.77
129.29
129.16
128.21
127.14
124.94
56.10
54.07
39.85
24.20
methanol
f1 (ppm)

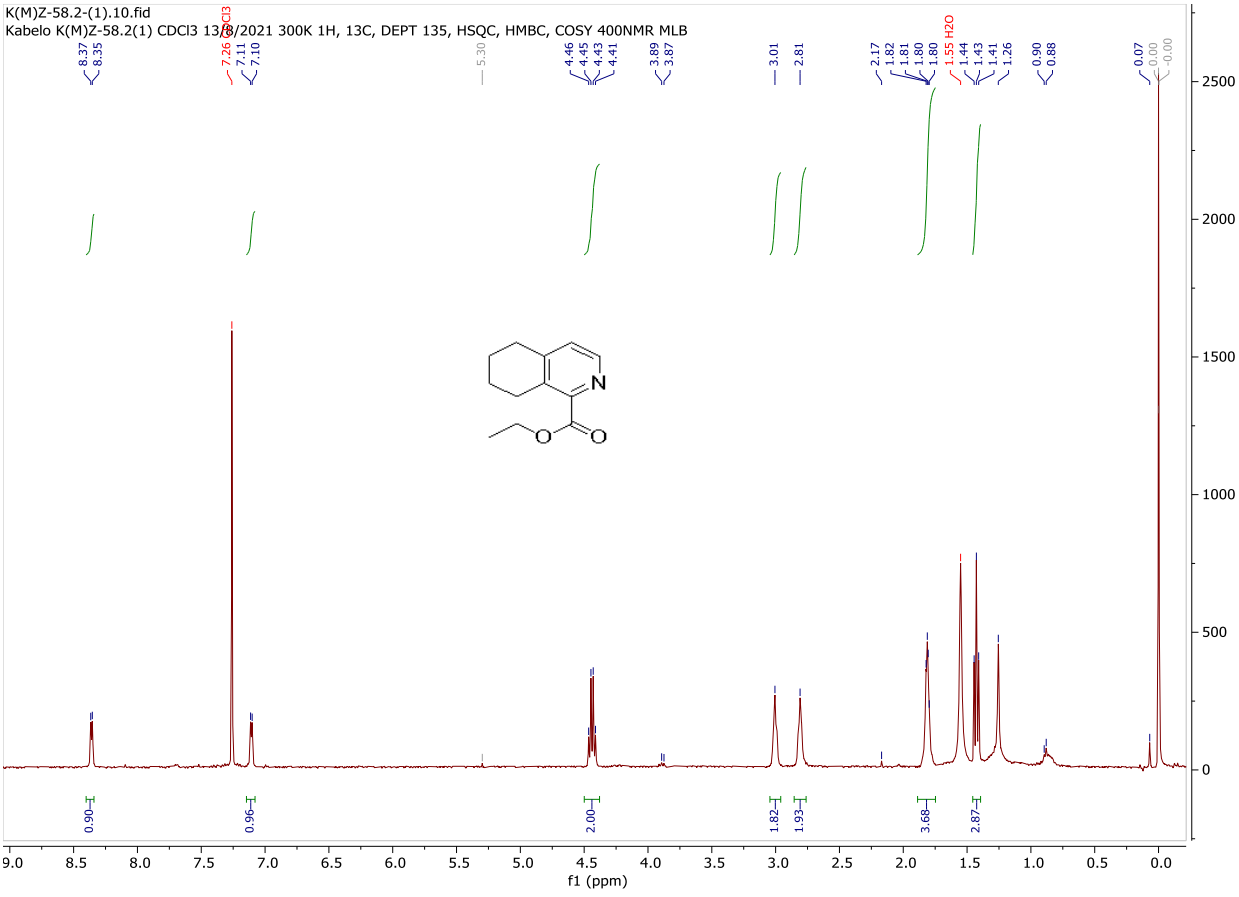
K(M)Z-58.2-(1).10.fid
Kabelo K(M)Z-58.2(1) CDCl3 13/8/2021 300K 1H, 13C, DEPT 135, HSQC, HMBC, COSY 400NMR MLB
8.37
8.35
7.26 CDCl3
7.11
7.10
5.30
4.46
4.45
4.43
4.41
3.89
3.87
3.01
2.81
2.17
1.82
1.81
1.80
1.55 H2O
1.44
1.43
1.41
1.26
0.90
0.88
0.07
0.00
-0.00
N
O
O
0.90
0.96
2.00
1.82
1.93
3.68
2.87
f1 (ppm)

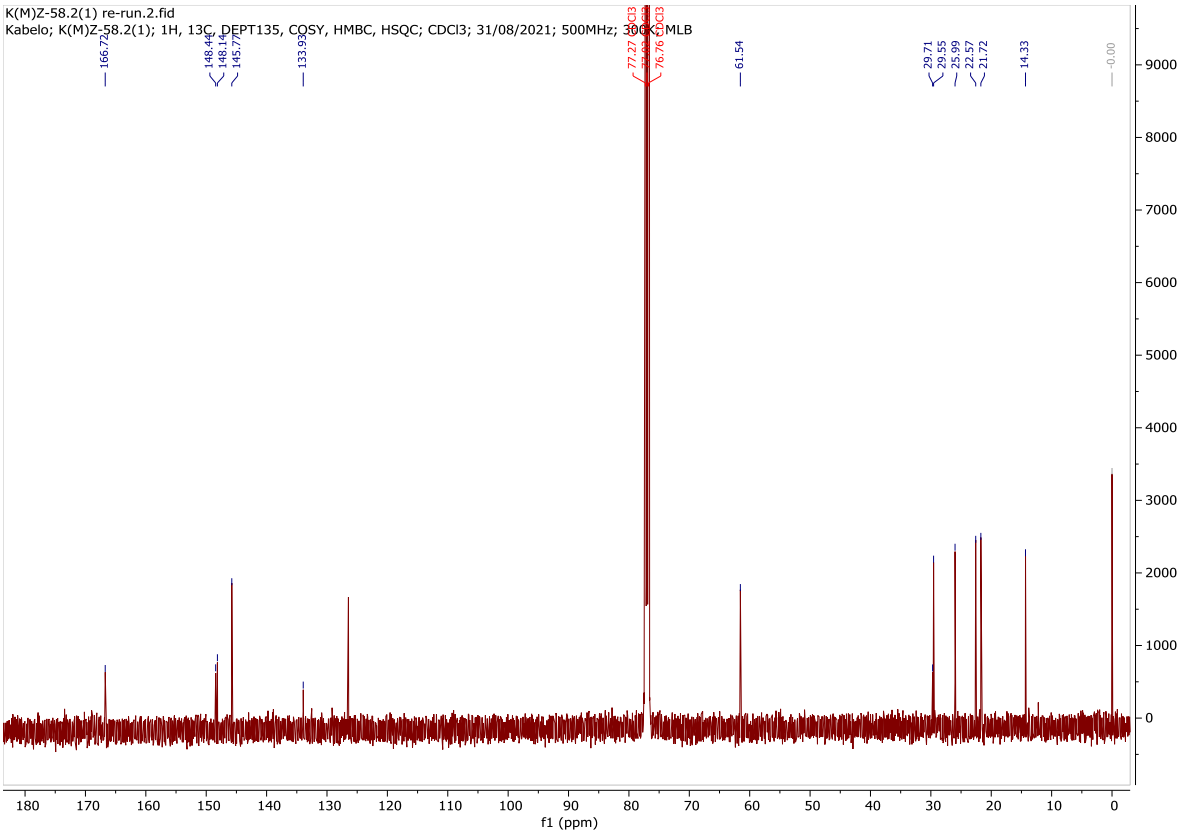
K(M)Z-58.2(1) re-run.2.fid
Kabelo; K(M)Z-58.2(1); 1H, 13C, DEPT135, COSY, HMBC, HSQC; CDCl3; 31/08/2021; 500MHz; 300K; MLB
166.72
148.44
148.14
145.77
133.93
77.27 CDCl3
76.76 CDCl3
61.54
29.71
29.55
25.99
22.57
21.72
14.33
-0.00
f1 (ppm)

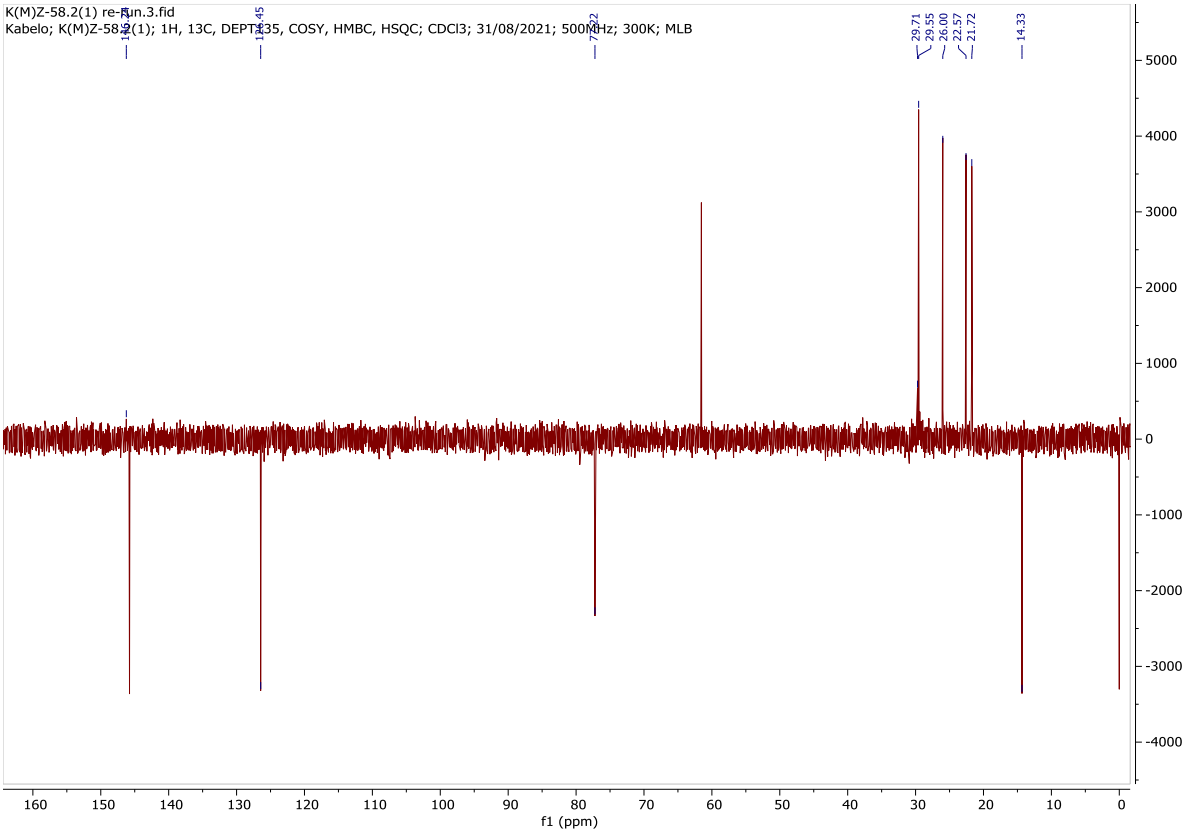
K(M)Z-58.2(1) re-run.3.fid
Kabelo; K(M)Z-58.2(1); 1H, 13C, DEPT135, COSY, HMBC, HSQC; CDCl3; 31/08/2021; 500MHz; 300K; MLB
148.45
77.22
29.71
29.55
26.00
22.57
21.72
14.33
f1 (ppm)

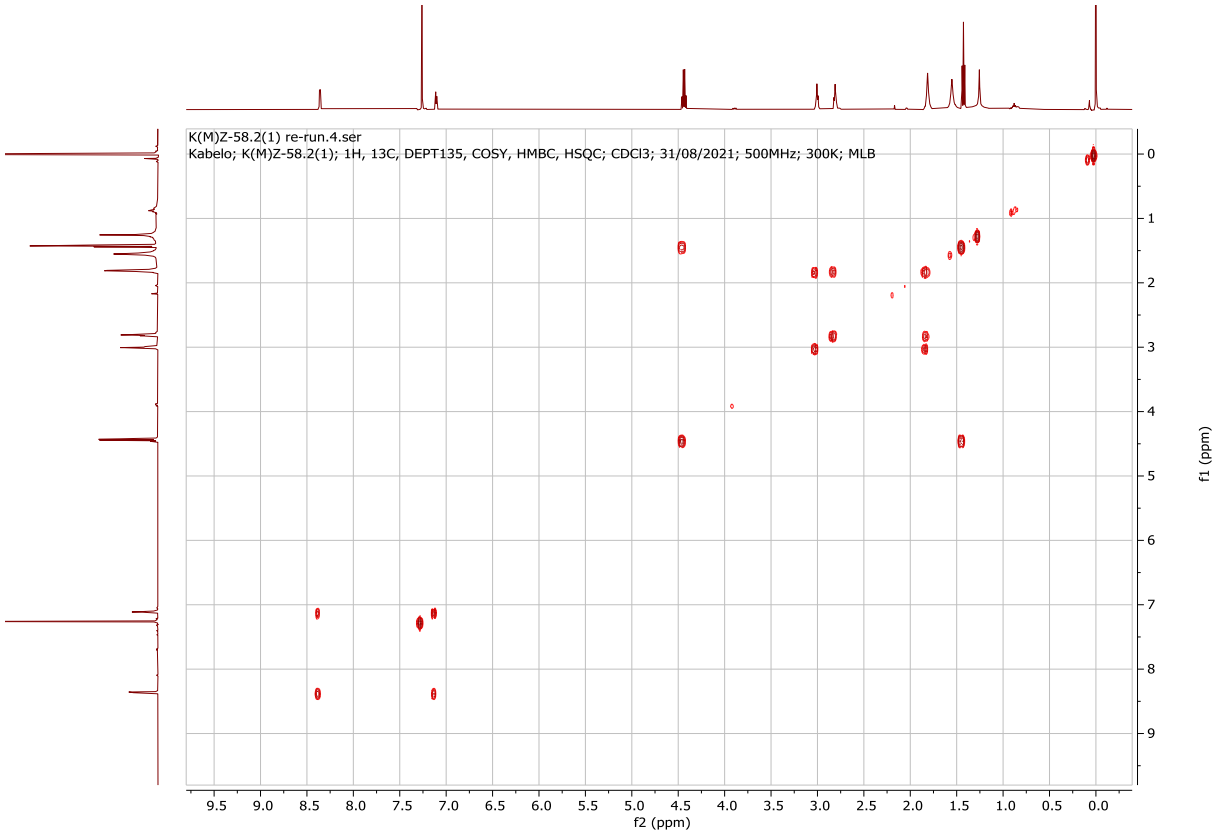
K(M)Z-58.2(1) re-run.4.ser
Kabelo; K(M)Z-58.2(1); 1H, 13C, DEPT135, COSY, HMBC, HSQC; CDCl3; 31/08/2021; 500MHz; 300K; MLB
f2 (ppm)
f1 (ppm)

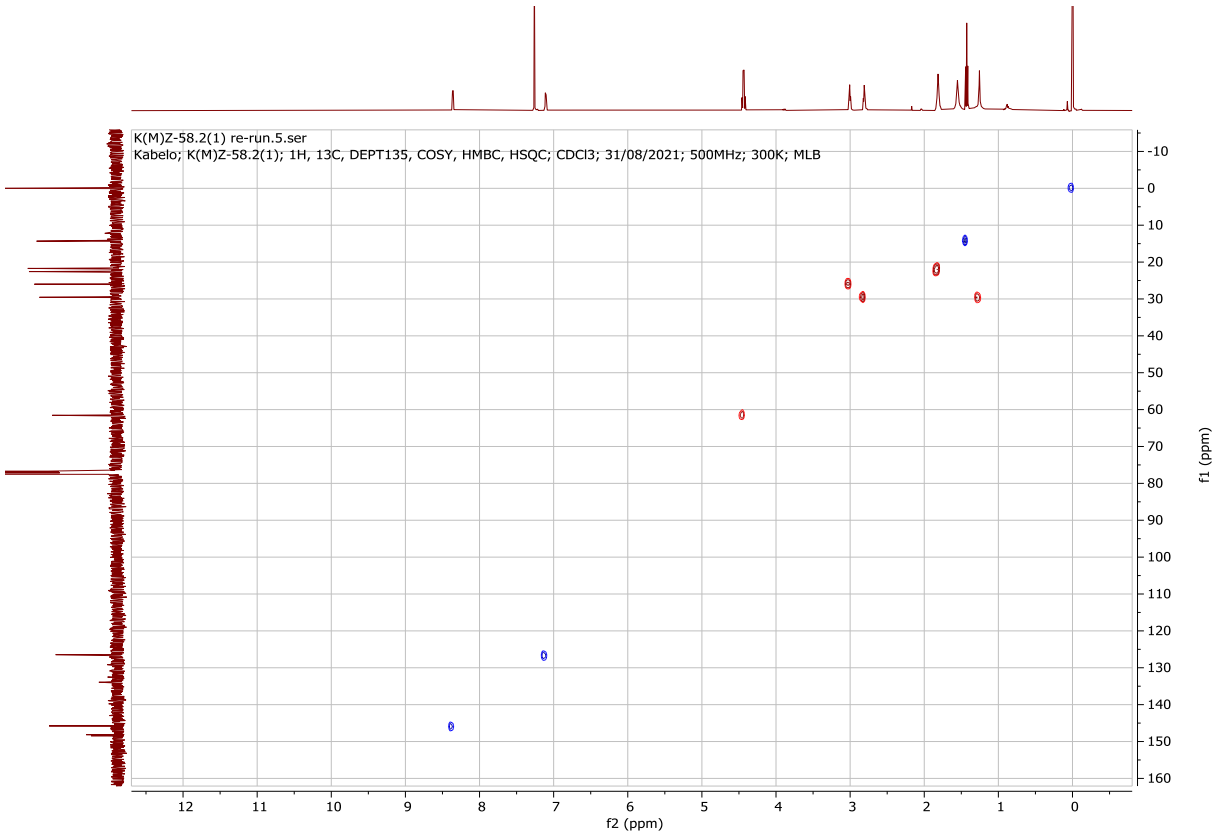
K(M)Z-58.2(1) re-run.5.ser
Kabelo; K(M)Z-58.2(1); 1H, 13C, DEPT135, COSY, HMBC, HSQC; CDCl3; 31/08/2021; 500MHz; 300K; MLB
f2 (ppm)
f1 (ppm)

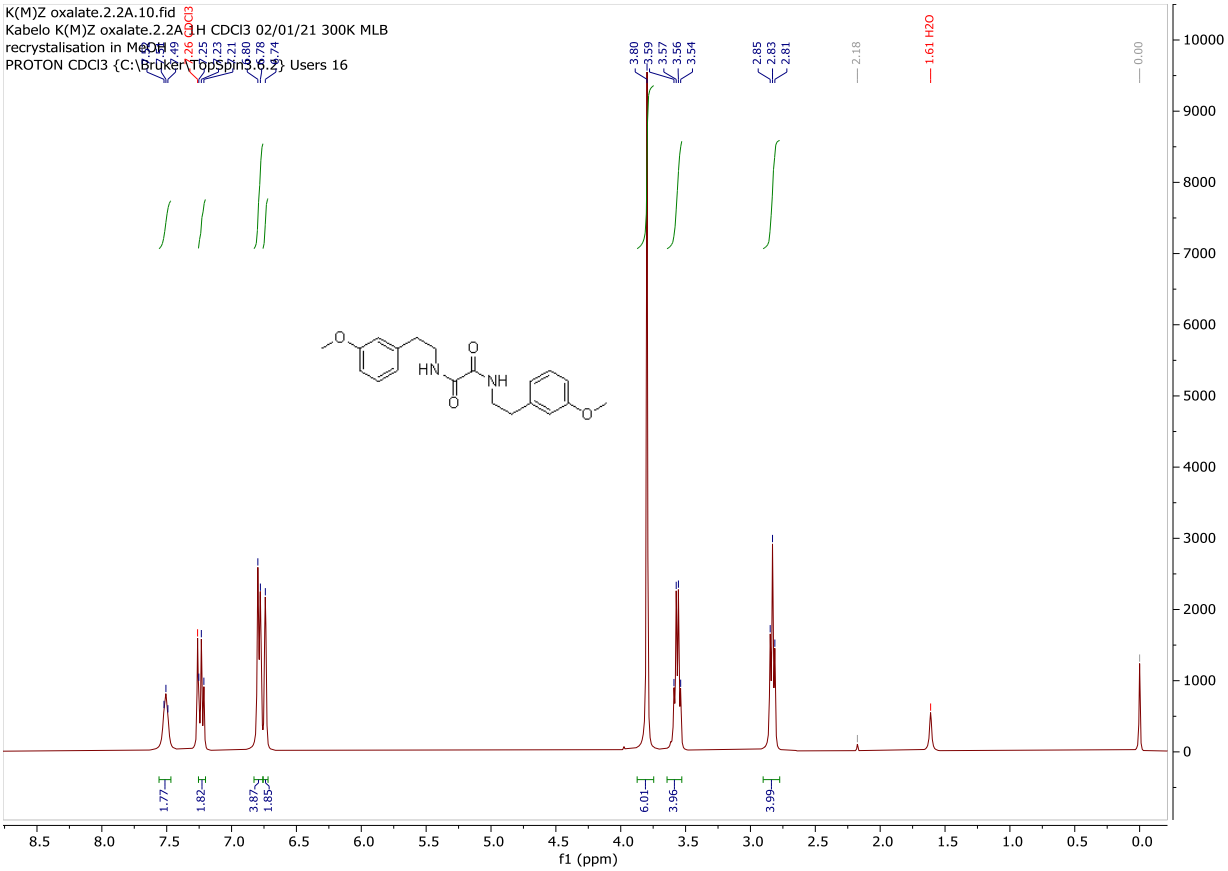
K(M)Z oxalate.2.2A.10.fid
Kabelo K(M)Z oxalate.2.2A 1H CDCl3 02/01/21 300K MLB
recrystalisation in MeOH
PROTON CDCl3 {C:\Bruker\TopSpin3.6.2} Users 16
7.49
7.26 CDCl3
7.25
7.23
7.21
6.80
6.78
6.74
3.80
3.59
3.57
3.56
3.54
2.85
2.83
2.81
2.18
1.61 H2O
0.00
HN
NH
O
O
O
O
1.77
1.82
3.87
1.85
6.01
3.96
3.99
f1 (ppm)

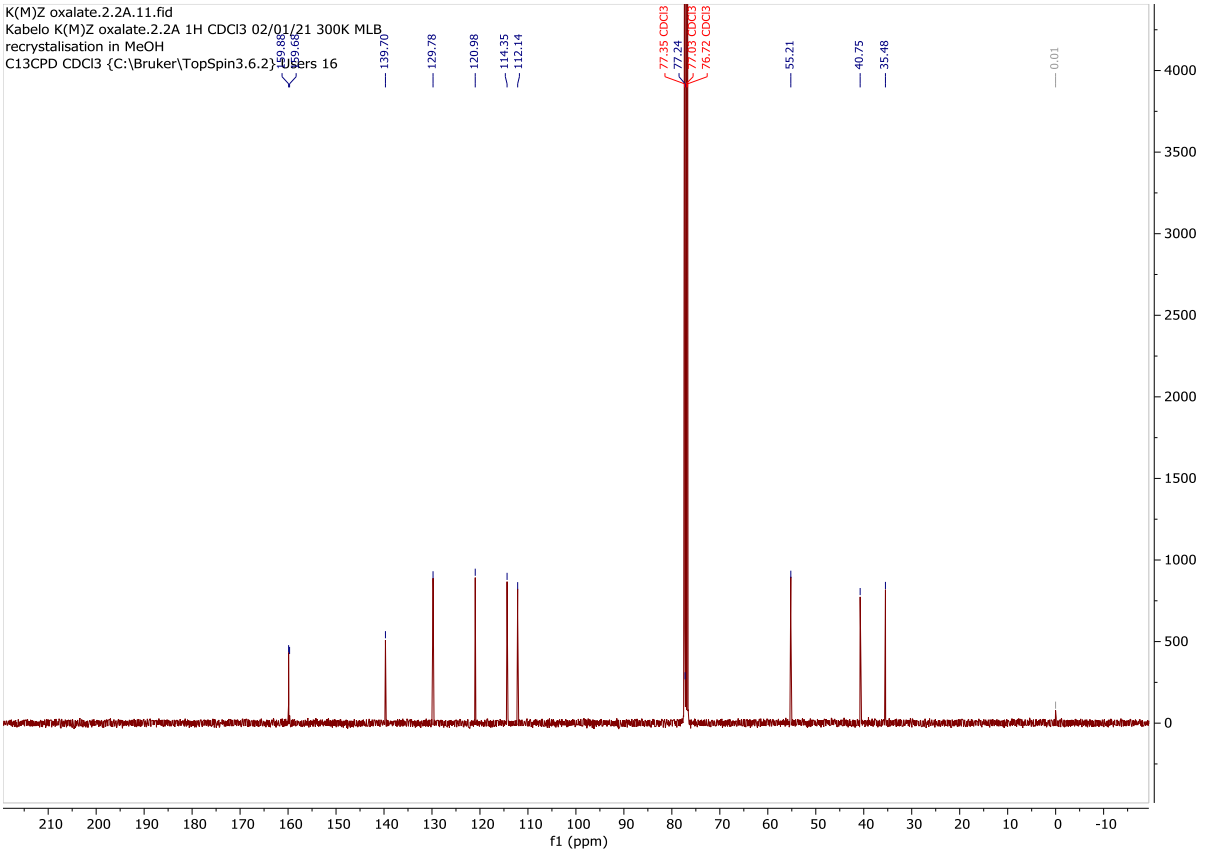
K(M)Z oxalate.2.2A.11.fid
Kabelo K(M)Z oxalate.2.2A 1H CDCl3 02/01/21 300K MLB
recrystalisation in MeOH
C13CPD CDCl3 {C:\Bruker\TopSpin3.6.2} Users 16
159.88
159.68
139.70
129.78
120.98
114.35
112.14
77.35 CDCl3
77.24
77.03 CDCl3
76.72 CDCl3
55.21
40.75
35.48
0.01
f1 (ppm)

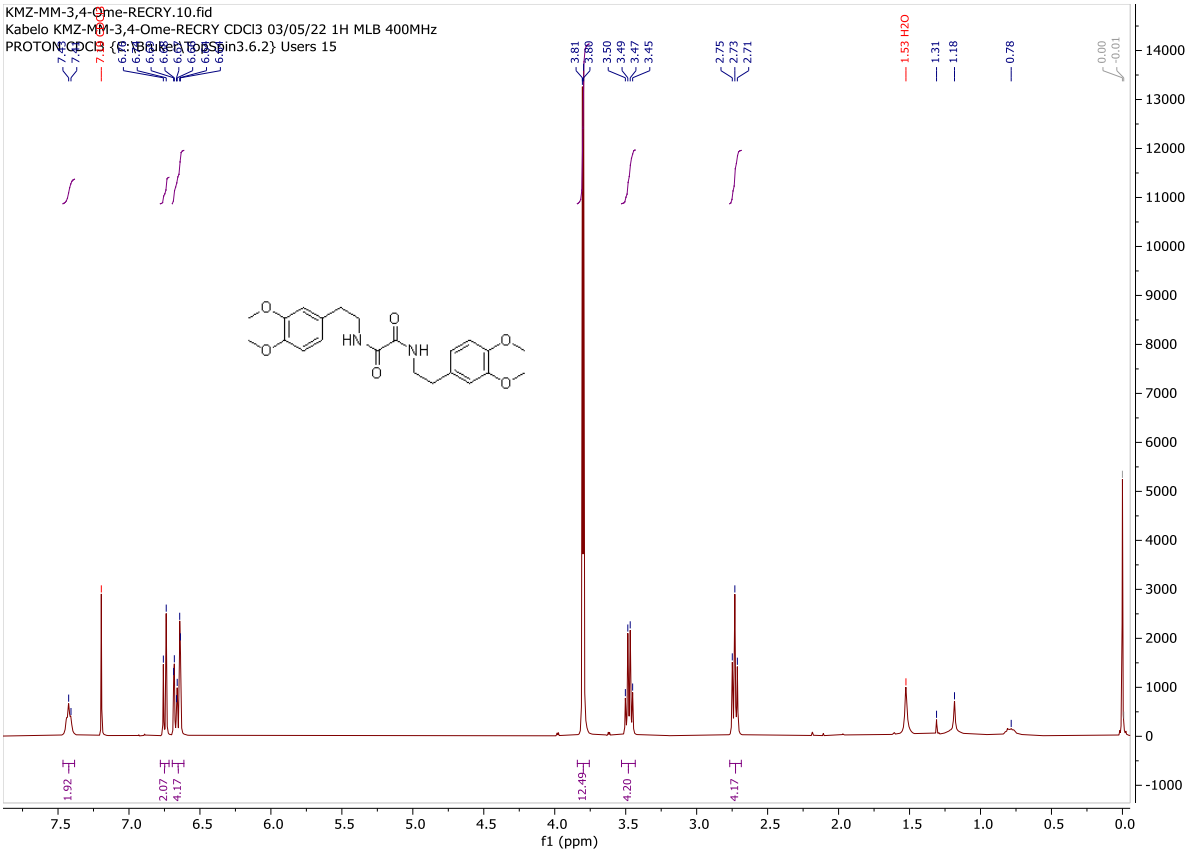
KMZ-MM-3,4-Ome-RECRY.10.fid
Kabelo KMZ-MM-3,4-Ome-RECRY CDCl3 03/05/22 1H MLB 400MHz
PROTON CDCl3 {C:\Bruker\TopSpin3.6.2} Users 15
7.26 CHCl3
1.53 H2O
1.31
1.18
0.78
3.81
3.80
3.50
3.49
3.47
3.45
2.75
2.73
2.71
1.92
2.07
4.17
12.49
4.20
4.17
f1 (ppm)

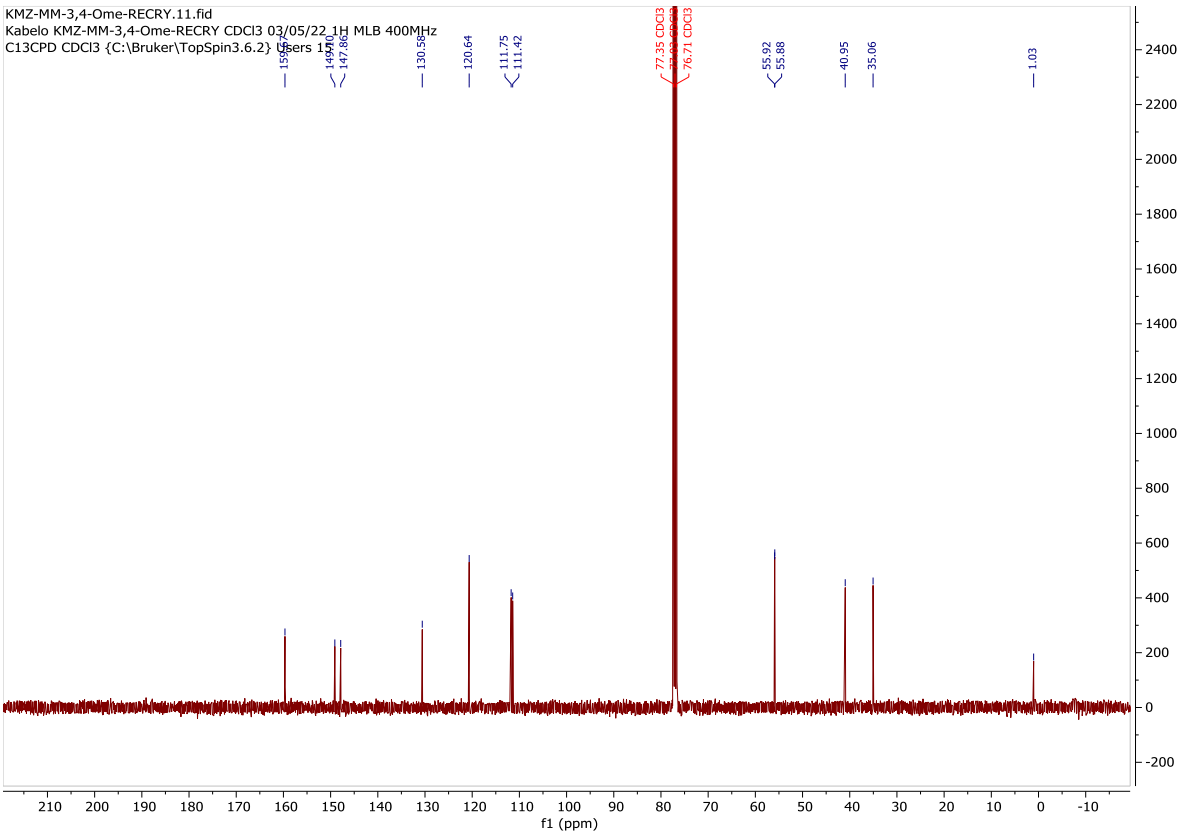
KMZ-MM-3,4-Ome-RECRY.11.fid
Kabelo KMZ-MM-3,4-Ome-RECRY CDCl3 03/05/22 1H MLB 400MHz
C13CPD CDCl3 {C:\Bruker\TopSpin3.6.2} Users 15
159.92
149.01
147.86
130.58
120.64
111.75
111.42
77.35 CDCl3
76.71 CDCl3
55.92
55.88
40.95
35.06
1.03
f1 (ppm)

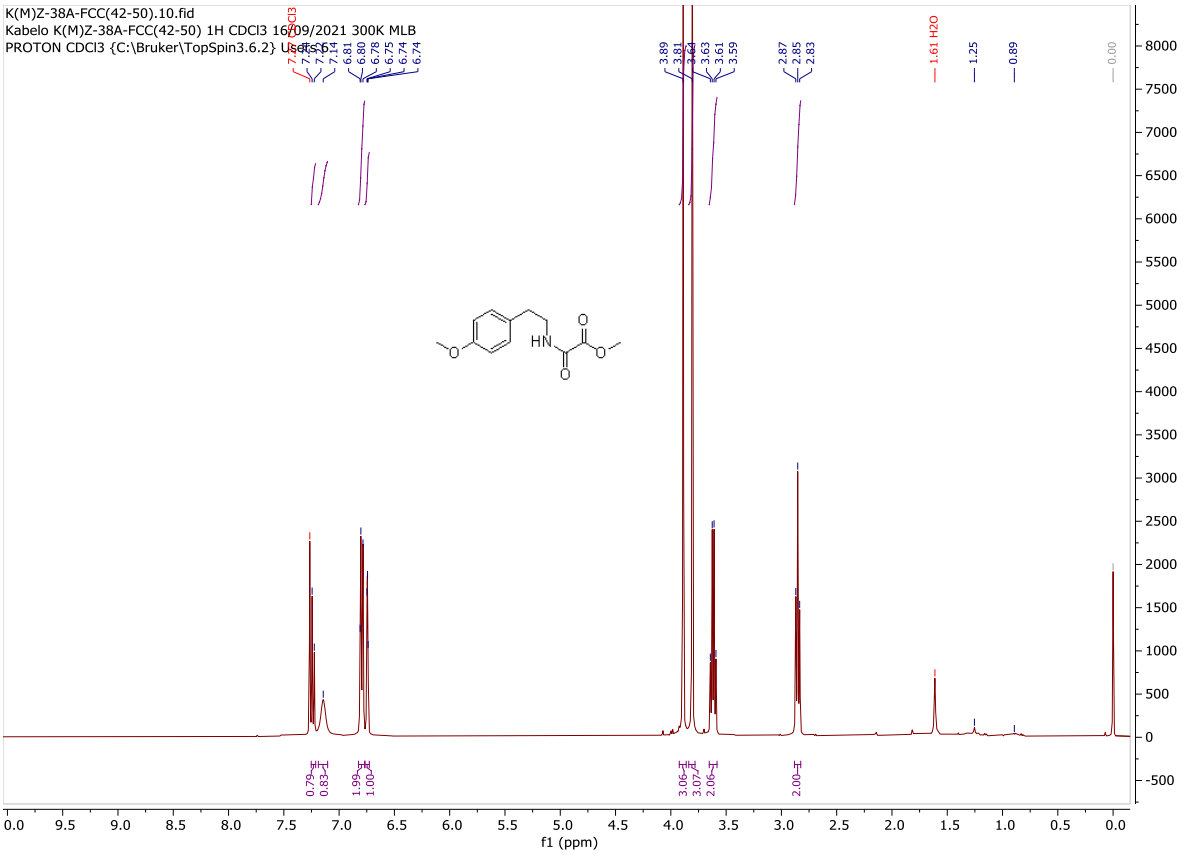
K(M)Z-38A-FCC(42-50).10.fid
Kabelo K(M)Z-38A-FCC(42-50) 1H CDCl3 16/09/2021 300K MLB
PROTON CDCl3 {C:\Bruker\TopSpin3.6.2} Users
7.26 CDCl3
7.28
7.27
7.16
7.14
6.81
6.80
6.78
6.75
6.74
6.74
3.89
3.81
3.64
3.63
3.61
3.59
2.87
2.85
2.83
1.61 H2O
1.25
0.89
0.00
HN
O
O
O
O
0.79
0.83
1.99
1.00
3.06
3.07
2.06
2.00
f1 (ppm)

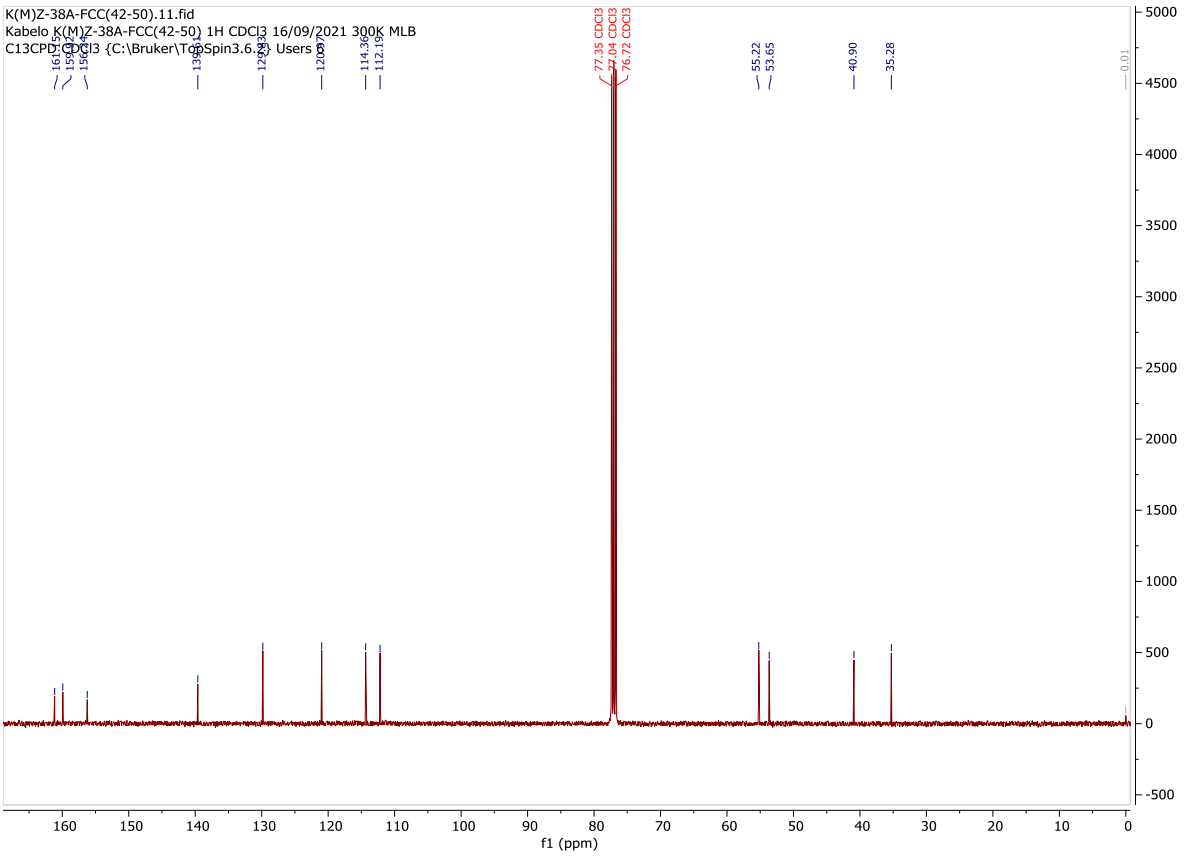
K(M)Z-38A-FCC(42-50).11.fid
Kabelo K(M)Z-38A-FCC(42-50) 1H CDCl3 16/09/2021 300K MLB
C13CPD CDCl3 {C:\Bruker\TopSpin3.6.2} Users
161.15
159.27
156.46
139.14
129.73
120.67
114.36
112.19
77.35 CDCl3
77.04 CDCl3
76.72 CDCl3
55.22
53.65
40.90
35.28
0.01
f1 (ppm)

K(M)Z-30B.10.fid — Kabelo K(M)Z-30B 1H CDCl3 19-02-2020 301K MLB — PROTON CDCl3 {C:\Bruker\TopSpin3.6.2} Users 13

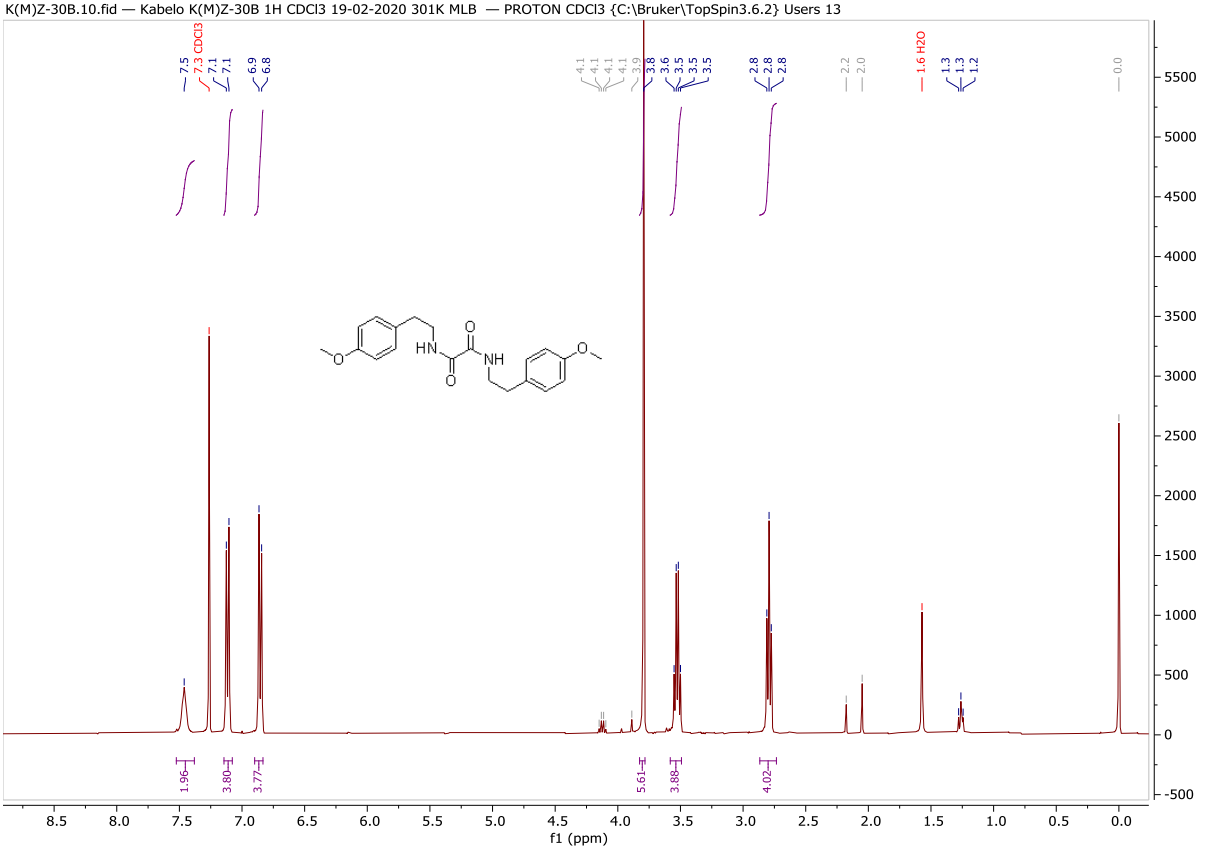

K(M)z-3.1.10.fid — kabelo K(M)Z-3.1 1H DMSO 05.08.2020 300K MLB — iodoxybenzoic acid in dmso — PROTON DMSO {C:\Bruker\TopSpin3.6.2} Users 20

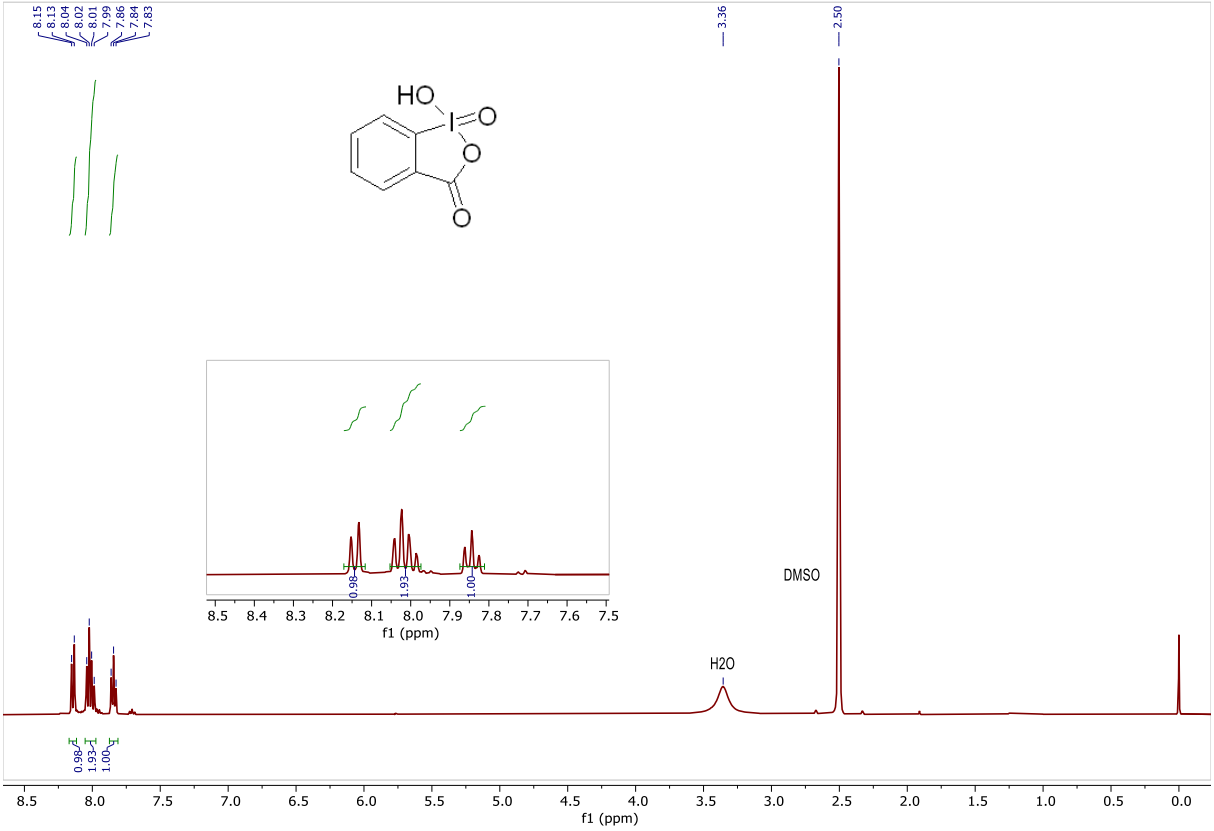

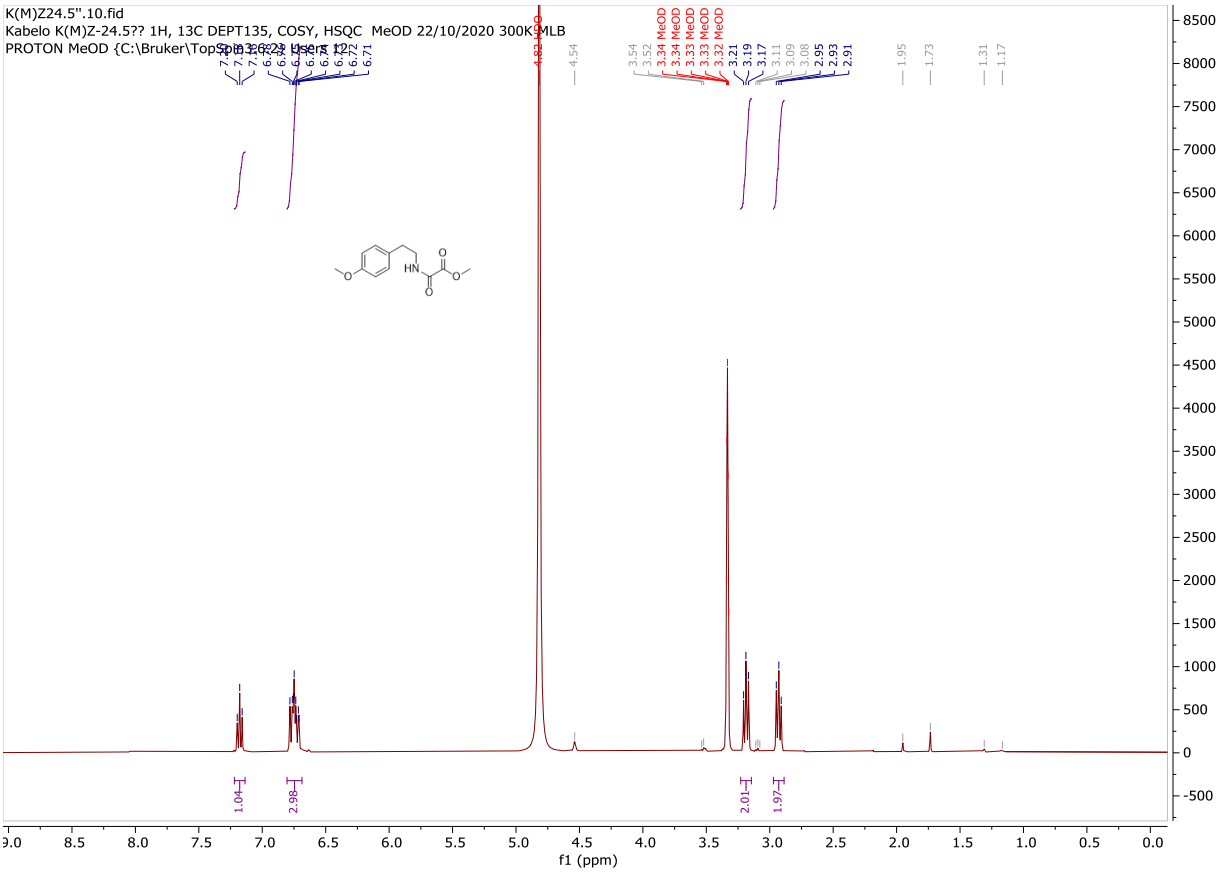
K(M)Z24.5''.10.fid
Kabelo K(M)Z-24.5?? 1H, 13C DEPT135, COSY, HSQC MeOD 22/10/2020 300K MLB
PROTON MeOD {C:\Bruker\TopSpin3.6.2} Users 12
f1 (ppm)

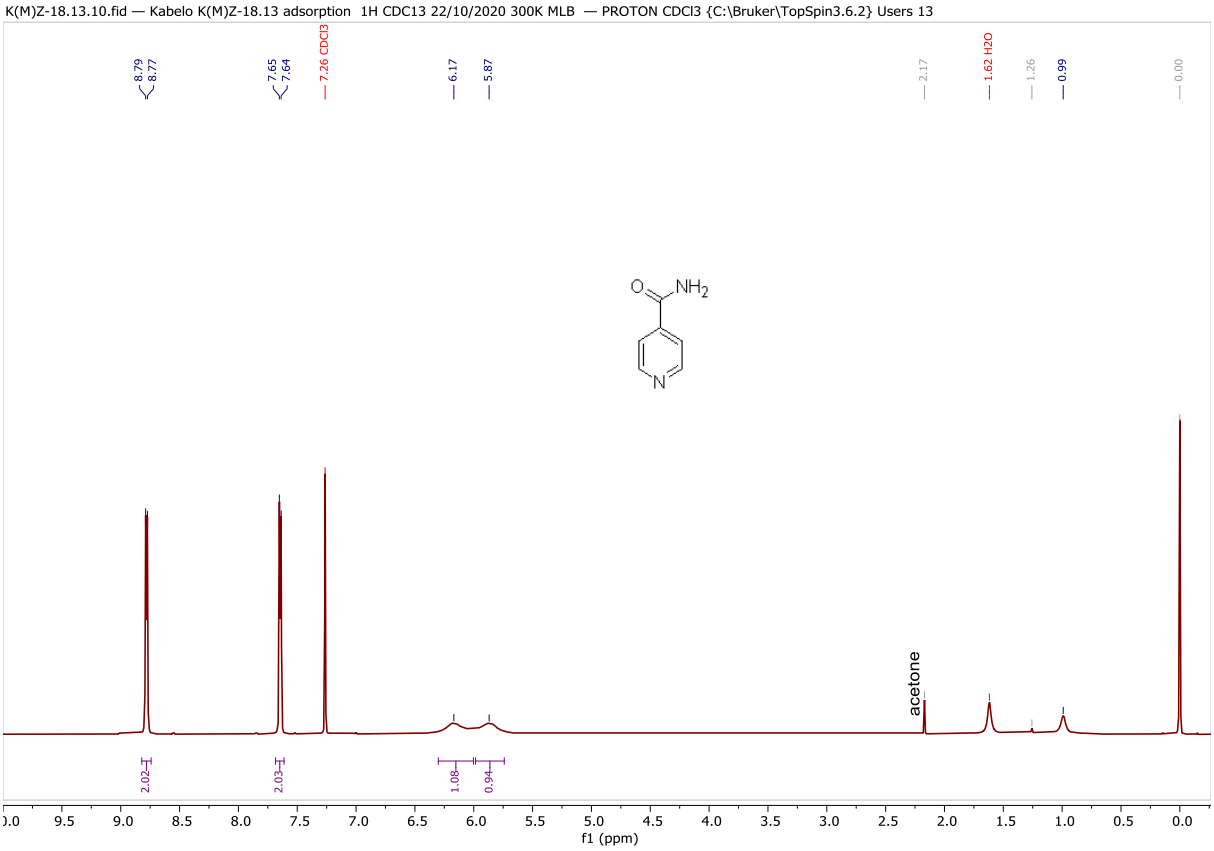
K(M)Z-18.13.10.fid — Kabelo K(M)Z-18.13 adsorption 1H CDC13 22/10/2020 300K MLB — PROTON CDCl3 {C:\Bruker\TopSpin3.6.2} Users 13
7.26 CDCl3
1.62 H2O
acetone
f1 (ppm)

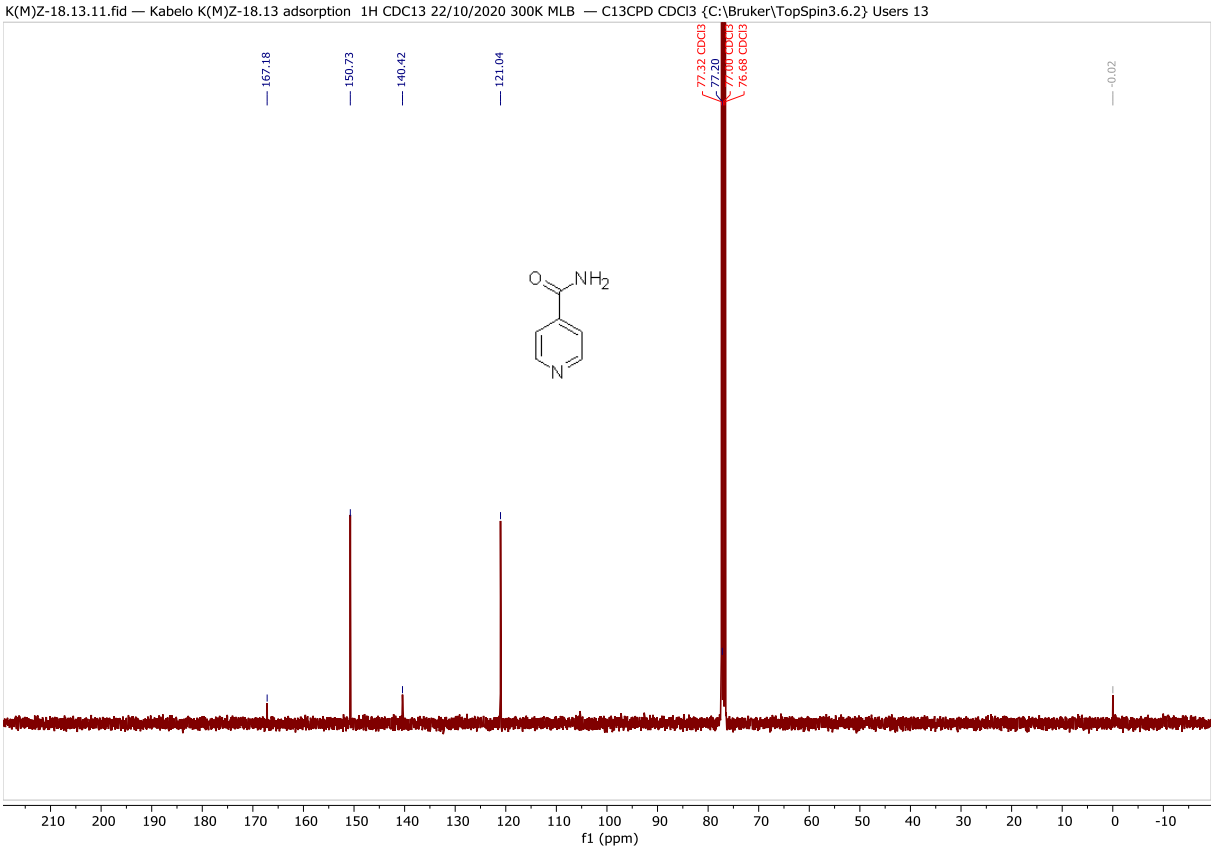
K(M)Z-18.13.11.fid — Kabelo K(M)Z-18.13 adsorption 1H CDC13 22/10/2020 300K MLB — C13CPD CDCl3 {C:\Bruker\TopSpin3.6.2} Users 13
167.18
150.73
140.42
121.04
77.32 CDCl3
77.20
77.00 CDCl3
76.68 CDCl3
-0.02
O
NH2
N
f1 (ppm)

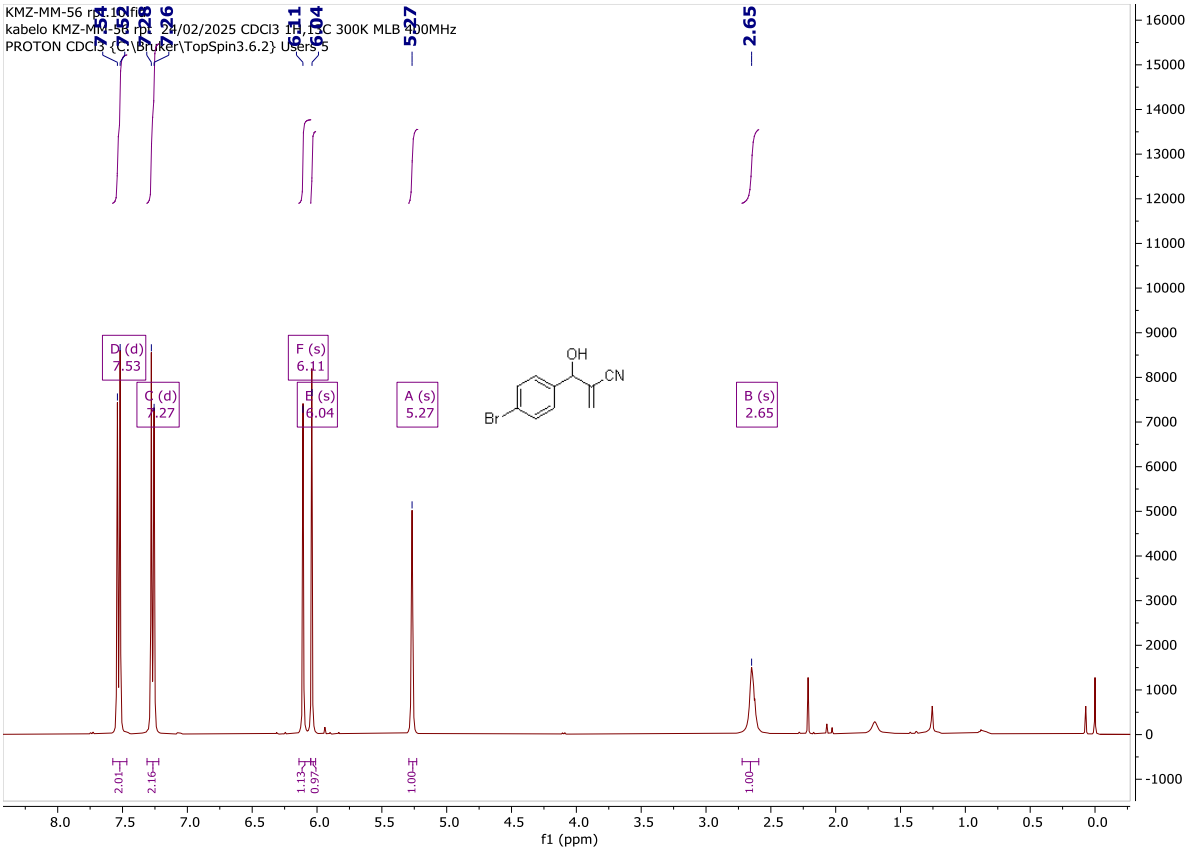
KMZ-MM-56 rpt.10.fid
kabelo KMZ-MM-56 rpt 28/02/2025 CDCl3 1H 1C 300K MLB 400MHz
PROTON CDCl3 {C:\Bruker\TopSpin3.6.2} Users 5
7.53
7.28
7.26
6.11
6.04
5.27
2.65
D (d) 7.53
C (d) 7.27
F (s) 6.11
E (s) 6.04
A (s) 5.27
B (s) 2.65
OH
CN
Br
2.01
2.16
1.13
0.97
1.00
1.00
f1 (ppm)

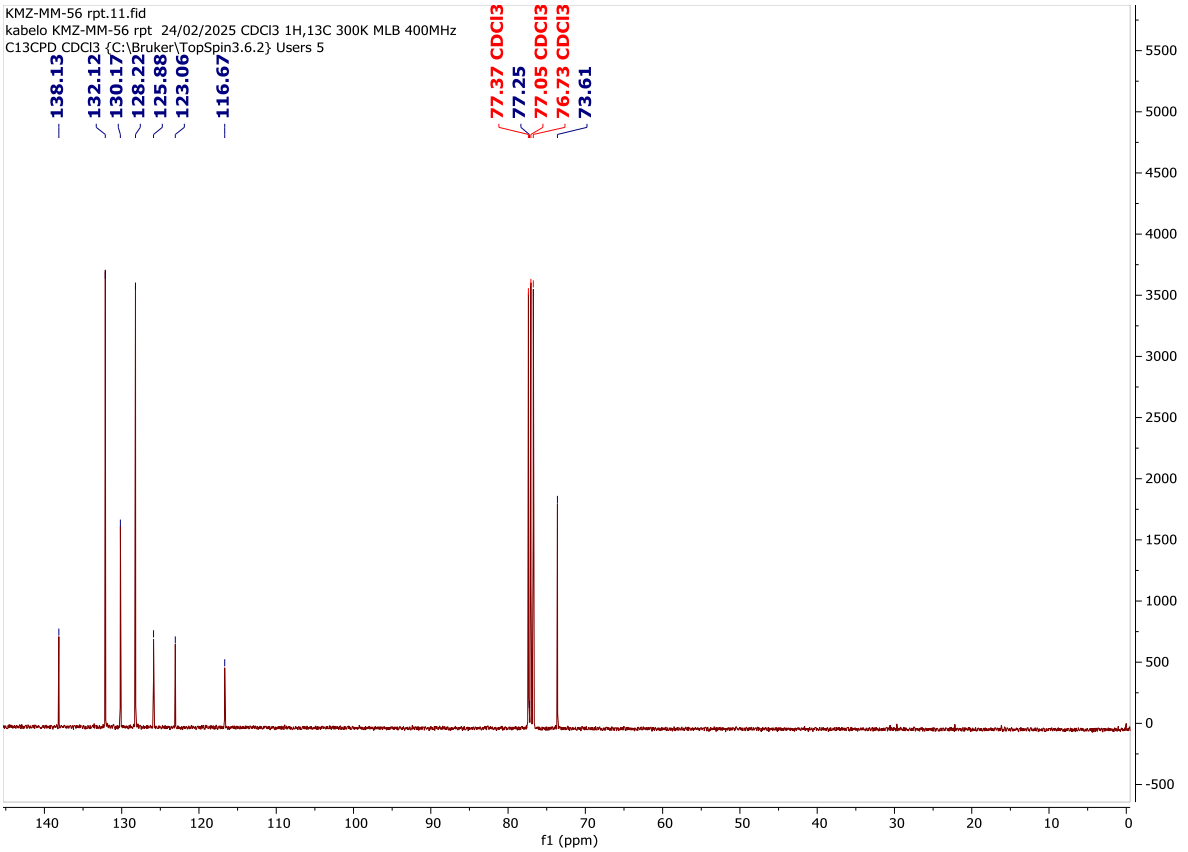
KMZ-MM-56 rpt.11.fid
kabelo KMZ-MM-56 rpt 24/02/2025 CDCl3 1H,13C 300K MLB 400MHz
C13CPD CDCl3 {C:\Bruker\TopSpin3.6.2} Users 5
138.13
132.12
130.17
128.22
125.88
123.06
116.67
77.37 CDCl3
77.25
77.05 CDCl3
76.73 CDCl3
73.61
f1 (ppm)

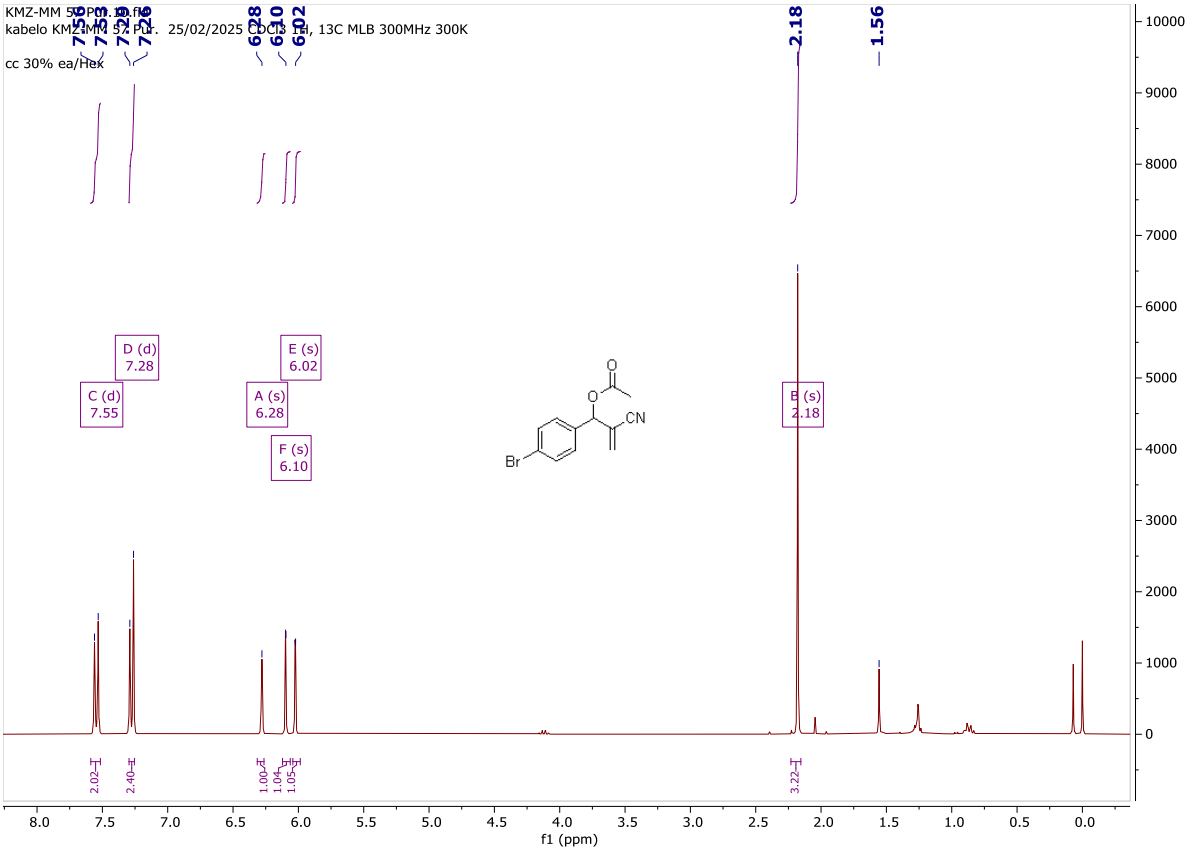
kabelo KMZ-MM 56 Pur. 25/02/2025 CDCl3 1H, 13C MLB 300MHz 300K
cc 30% ea/Hex
7.55
7.28
7.26
6.28
6.10
6.02
2.18
1.56
D (d)
7.28
C (d)
7.55
E (s)
6.02
A (s)
6.28
F (s)
6.10
B (s)
2.18
O
O
CN
Br
2.02
2.40
1.00
1.04
1.05
3.22
f1 (ppm)

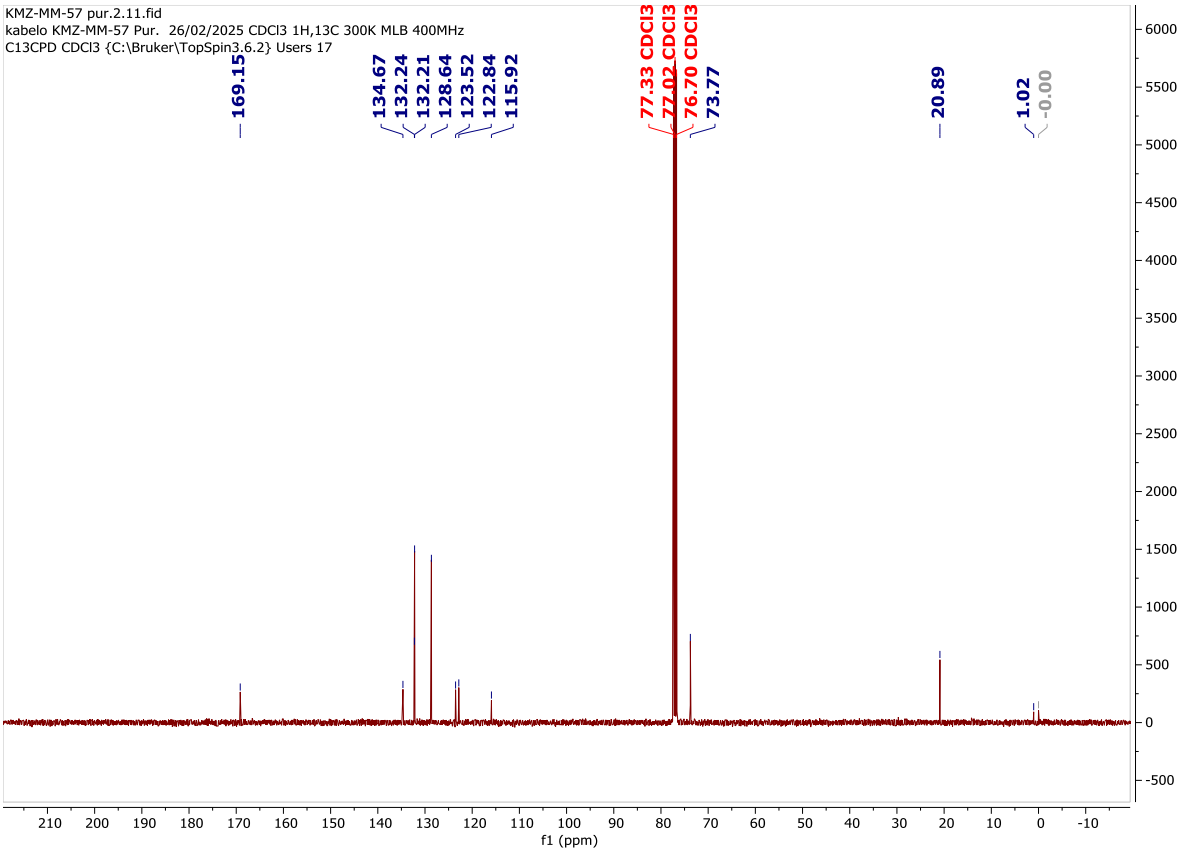
KMZ-MM-57 pur.2.11.fid
kabelo KMZ-MM-57 Pur. 26/02/2025 CDCl3 1H,13C 300K MLB 400MHz
C13CPD CDCl3 {C:\Bruker\TopSpin3.6.2} Users 17
169.15
134.67
132.24
132.21
128.64
123.52
122.84
115.92
77.33 CDCl3
77.02 CDCl3
76.70 CDCl3
73.77
20.89
1.02
-0.00
f1 (ppm)